Journal of Immunology Research

Immunotherapy of Liver Diseases

Lead Guest Editor: Dechun Feng
Guest Editors: YinYing Lu, Xiaoni Kong, and Feng Li

Immunotherapy of Liver Diseases

Journal of Immunology Research

Immunotherapy of Liver Diseases

Lead Guest Editor: Dechun Feng
Guest Editors: YinYing Lu, Xiaoni Kong, and Feng Li

Editorial Board

Contents

Hindawi
Journal of Immunology Research
Volume 2019, Article ID 9343505, 3 pages
https://doi.org/10.1155/2019/9343505

Editorial

Immunotherapy of Liver Diseases

Dechun Feng,[1] **YinYing Lu**,[2] **Xiaoni Kong**,[3] **and Feng Li**[4]

[1]*Laboratory of Liver Diseases, National Institute on Alcohol Abuse and Alcoholism, National Institutes of Health, Bethesda, MD, USA*
[2]*Comprehensive Liver Cancer Center, Beijing 302 Hospital, Beijing, China*
[3]*Department of Liver Surgery, Renji Hospital, School of Medicine, Shanghai Jiao Tong University, Shanghai, China*
[4]*Department of Molecular and Cellular Biology, Baylor College of Medicine, Houston, TX, USA*

Correspondence should be addressed to Dechun Feng; dechun.feng@nih.gov

Received 9 June 2019; Accepted 14 June 2019; Published 21 August 2019

As an immunological organ, the liver played critical roles against invading pathogens. Many immune cells such as Kupffer cells, natural killer (NK) cells, and NKT cells were located in the liver under normal physiological condition. Under pathological condition, such as acute or chronic liver injury, more immune cells migrated into the liver. These cells may act as friends to clear damaged hepatocytes, promote liver repair, improve the resolution of liver fibrosis, and eliminate liver cancer cells. They may also play bad roles in the liver, such as further damaging hepatocytes, promoting hepatic stellate cell activation and live fibrosis, and facilitating tumor growth. So, how to understand the detailed regulation mechanisms in liver immune cells and how to target immune cells in the liver to improve the therapy of liver diseases are a challenging problem in the liver study field.

In this special issue, we have invited a few Research Articles and Reviews that address such issues.

In the paper titled "Elevated Serum IgG Levels Positively Correlated with IL-27 May Indicate Poor Outcome in Patients with HBV-Related Acute-On-Chronic Liver Failure," the authors studied the correlation of serum immunoglobulins including IgG, IgA, and IgM and interleukin-27 (IL-27) in patients with HBV-related acute-on-chronic liver failure (HBV-ACLF). They compared HBV-ACLF patients with chronic hepatitis B (CHB) patients as well as normal control. They found that serum immunoglobulins were preferentially elevated in HBV-ACLF patients. In addition, serum IgG levels were positively correlated with IL-27. This study may be helpful for predicting prognosis in HBV-ACLF patients.

In the paper titled "Immunoregulatory Effect of Koumine on Nonalcoholic Fatty Liver Disease Rats," the authors studied the effects of koumine, the main and active ingredient isolated from *Gelsemium elegans*, on a rat nonalcoholic fatty liver disease (NAFLD) model. They showed that Koumine could significantly reduce improved liver injury in NAFLD rats. Koumine treatment also decreased the percentages of Th1 and Th17 cells and increased Th2 and Treg cells in the liver.

In the paper titled "Overexpression of Tumor Necrosis Factor-Like Ligand 1 A in Myeloid Cells Aggravates Liver Fibrosis in Mice," the authors studied how myeloid cell derived TNF-like ligand 1 aberrance (TL1A) contributed to the development of liver fibrosis. They found that overexpression of TL1A in myeloid cells accelerated the necrosis and apoptosis of hepatocytes and promoted activation of hepatic stellate cells (HSCs). Moreover, TL1A overexpression in macrophages promoted secretion of platelet-derived growth factor-BB (PDGF-BB), tumor necrosis factor-α (TNF-α), and interleukin-1β (IL-1β) which further activated HSCs and deteriorated liver fibrosis.

In the paper titled "Immunomodulatory Effects of Combination Therapy with Bushen Formula plus Entecavir for Chronic Hepatitis B Patients," the authors evaluated the beneficial effects of the traditional Chinese medicine Bushen formula (BSF) in combination of plus entecavir (ETV) in naïve chronic hepatitis B (CHB) patients and that in CHB patients with partial virological response to ETV. They found that the combination therapy with BSF plus ETV increased Th1 and DC frequencies and decreased Treg frequency in

naïve CHB patients. In CHB patients with partial virological response to ETV, the combination therapy downregulated PD-L1 levels on DCs and the frequency of Treg. The modulation of the immune system in these patients with BSF was related to HBsAg decline.

In the paper titled "The Crosstalk between Fat Homeostasis and Liver Regional Immunity in NAFLD," the authors reviewed how liver nonparenchymal cell, adipocytes, and hepatocytes crosstalk with each other in the development of NAFLD and NASH. They also summarized how ncRNAs (including miRNAs and lncRNAs) participated in the pathological process of NAFLD by changing body fat homeostasis.

In the paper titled "Alda-1 Ameliorates Liver Ischemia-Reperfusion Injury by Activating Aldehyde Dehydrogenase 2 and Enhancing Autophagy in Mice," the authors investigated the novel role of acetaldehyde metabolizing enzyme ALDH2 in ischemia-reperfusion injury (IRI). Pretreatment of ALDH2 activator Alda-1 protects mice from IRI. Detailed mechanism study revealed that Alda-1 treatment could activate AMPK and autophagy which was very helpful to remove damaged organelles and protected hepatocyte from necrosis and apoptosis. These findings collectively indicate that Alda-1-mediated ALDH2 activation could be a promising strategy to improve liver IRI by clearance of reactive aldehydes and enhancement of autophagy.

In the paper titled "Total HLA Class I Antigen Loss with the Downregulation of Antigen-Processing Machinery Components in Two Newly Established Sarcomatoid Hepatocellular Carcinoma Cell Lines," the authors studied HLA class I antigen abnormalities in sarcomatoid hepatocellular carcinoma (sHCC). They analyzed the growth characteristics and HLA class I antigen status of four sHCC cell lines. Cell lines with nondetectable surface HLA class I antigen expression, intracellular β2-microglobulin (β2m) and marked HLA class I heavy chain, and selective antigen-processing machinery (APM) components showed enhanced growth ability. These findings may have implications for a proper design of T cell immunotherapy for the treatment of sHCC patients.

In the paper titled "Mesenchymal Stem Cells Ameliorate Hepatic Ischemia/Reperfusion Injury via Inhibition of Neutrophil Recruitment" that studied the protective effects of mesenchymal stem cells (MSCs) in a rat liver ischemia/reperfusion injury (IRI) model" the authors showed that treatment with MSCs protected rat against hepatic IRI and attenuated hepatic neutrophil infiltration. The protective effects may be attributed to the decreased expression of CXCR2 on the surface of neutrophils and reduced CXCL2 production in macrophages. MSCs can significantly ameliorate hepatic IRI predominantly through its inhibitory effect on hepatic neutrophil migration and infiltration.

In the paper titled "RIPK3-Mediated Necroptosis and Neutrophil Infiltration Are Associated with Poor Prognosis in Patients with Alcoholic Cirrhosis," the authors explored the immunomodulatory effects of mesenchymal stem cells (MSCs) on liver IRI. They showed that treatment with MSCs protected rat against hepatic IRI, with significantly decreased liver damage and hepatic neutrophil infiltration. The mechanisms can be attributed to reduced CXCR2 expression on neutrophils and diminished CXCL2 production in macrophages.

In the paper titled "Enhanced Regeneration and Hepatoprotective Effects of Interleukin 22 Fusion Protein on a Predamaged Liver Undergoing Partial Hepatectomy," the authors studied whether the RIPK3 level is correlated with neutrophil infiltration or poor prognosis in alcoholic cirrhotic patients. They analyzed 20 samples from alcoholic cirrhotic patients 5 normal liver samples. The results showed that the MPO and RIPK3 levels in the liver were positively related to the Ishak score. The RIPK3 was also significantly and positively related to the Knodell score. The study suggested that RIPK3-mediated necroptosis and neutrophil-mediated alcoholic liver inflammatory response are highly correlated with poor prognosis in patients with end-stage alcoholic cirrhosis.

The tenth paper discussed the beneficial role of interleukin 22 (IL-22) in liver regeneration deficiency in chronic liver disease patients and liver IRI after surgery. They found that IL-22 treatment prior to IRI effectively reduced liver damage through decreased liver injury and improved liver histology. IL-22 can also promote liver regeneration in mice with predamaged livers following PHx. IL-22 may be considered as a promising therapeutic agent to improve liver regeneration deficiency and liver IRI in patients.

In the paper titled "Complement System as a Target for Therapies to Control Liver Regeneration/Damage in Acute Liver Failure Induced by Viral Hepatitis," the authors evaluated the role of complement components in acute liver failure (ALF) caused by viral hepatitis. They found low levels of C3a in plasma samples with high frequency of C3a, C5a, and C5b/9 deposition in liver parenchyma. The data suggested that the complement system may be involved in liver dysfunction in viral-induced acute liver failure.

In the paper titled "Natural Killer Cells in Liver Disease and Hepatocellular Carcinoma and the NK Cell-Based Immunotherapy," the authors reviewed the NK cell phenotypic and functional changes in liver diseases. They discussed the role of NK cells in chronic viral hepatitis, alcoholic liver diseases, nonalcoholic fatty liver disease (NAFLD)/NASH, and hepatocellular carcinoma (HCC). In the review, NK cell-based immunotherapy for cancer was also discussed.

In the paper titled "Construction and Characterization of Adenovirus Vectors Encoding Aspartate-β-Hydroxylase to Preliminary Application in Immunotherapy of Hepatocellular Carcinoma," the authors described a DC vaccine targeting aspartate-β-hydroxylase (AAH), a tumor-associated cell surface protein. They tested the antitumor effect of the vaccine in HepG2 cells and found significantly enhanced lysis effect of cytotoxic T lymphocytes (CTLs) in the vaccine group. The approach can be considered as a potential candidate for DC-based immunotherapy of HCC.

In the paper titled "The Imbalance between Foxp3+Tregs and Th1/Th17/Th22 Cells in Patients with Newly Diagnosed Autoimmune Hepatitis," the authors studied the numbers of Foxp3+Tregs and Th1-Th17-Th22 cells newly diagnosed autoimmune hepatitis (AIH) patients. They showed that active AIH patients had significantly decreased numbers of Foxp3+Tregs and increased numbers of Th1/Th17/Th22

cells. Also, the serum levels of IL-17A and IL-22 were correlated positively with liver injury. The findings demonstrated that an imbalance between Tregs and Th1-Th17-Th22 cells might contribute to the pathogenic process of AIH.

Conflicts of Interest

We all do not have any conflict of interest to report.

Dechun Feng
YinYing Lu
Xiaoni Kong
Feng Li

Hindawi
Journal of Immunology Research
Volume 2019, Article ID 1538439, 10 pages
https://doi.org/10.1155/2019/1538439

Research Article

Elevated Serum IgG Levels Positively Correlated with IL-27 May Indicate Poor Outcome in Patients with HBV-Related Acute-On-Chronic Liver Failure

Geng-lin Zhang[1,2] **Qi-yi Zhao**[1,2] **Chan Xie**[1,2] **Liang Peng**[1,2] **Ting Zhang**[3] **and Zhi-liang Gao**[1,2,4]

[1]*Department of Infectious Diseases, The Third Affiliated Hospital of Sun-Yat-sen University, Guangzhou 510630, China*
[2]*Guangdong Provincial Key Laboratory of Liver Disease, The Third Affiliated Hospital of Sun-Yat-sen University, Guangzhou 510630, China*
[3]*Department of Ultrasound, The Third Affiliated Hospital of Sun-Yat-sen University, Guangzhou 510630, China*
[4]*Key Laboratory of Tropical Disease Control (Sun-Yat-sen University), Ministry of Education, Guangzhou 510630, China*

Correspondence should be addressed to Ting Zhang; 13631427814@163.com and Zhi-liang Gao; zhilianggao@21cn.com

Received 28 June 2018; Revised 11 October 2018; Accepted 21 April 2019; Published 6 May 2019

Guest Editor: Feng Li

Background and Aims. Serum immunoglobulins are frequently increased in patients with chronic liver disease, but little is known about the role of serum immunoglobulins and their correlations with interleukin-27 (IL-27) in patients with HBV-related acute-on-chronic liver failure (HBV-ACLF). This study was aimed at determining the role of serum immunoglobulin (IgG, IgA, and IgM) levels and their associations with IL-27 in noncirrhotic patients with HBV-ACLF. *Methods*. Samples were assessed from thirty patients with HBV-ACLF, twenty-four chronic hepatitis B (CHB) subjects, and eighteen normal controls. Disease severity of HBV-ACLF was evaluated. Serum IL-27 levels were examined by enzyme-linked immunosorbent assay. Immunoglobulin levels were assessed using immunoturbidimetric assay. Correlations between immunoglobulin levels and IL-27 were analyzed. Receiver operating characteristic (ROC) curves were used to predict the 3-month mortality. *Results*. 25 (83.3%) HBV-ACLF patients had elevated serum IgG levels (>1 ULN), 14 (46.7%) patients had elevated IgA, and 15 (50%) had raised IgM. IgG, IgA, and IgM levels were higher in HBV-ACLF patients than in CHB patients and normal controls. Moreover, IgG, IgA, and IgM levels were positively correlated with Tbil levels but negatively correlated with prothrombin time activity (PTA) levels. Additionally, IgG levels were significantly increased in nonsurviving patients than in surviving HBV-ACLF patients ($P = 0.007$) and positively correlated with MELD score ($r = 0.401$, $P = 0.028$). Also, IgG levels were positively correlated with IL-27 levels in HBV-ACLF patients ($r = 0.398$, $P = 0.029$). Furthermore, ROC curve showed that IgG levels could predict the 3-month mortality in HBV-ACLF patients (the area under the ROC curve: 0.752, $P = 0.005$). *Conclusions*. Our findings demonstrated that serum immunoglobulins were preferentially elevated in HBV-ACLF patients. IgG levels were positively correlated with IL-27 and may predict prognosis in HBV-ACLF patients.

1. Introduction

Acute-on-chronic liver failure (ACLF) is a dramatic clinical syndrome characterized by the sudden loss of hepatic cells leading to multiorgan failure in patients with preexisting chronic liver diseases [1]. The leading cause of ACLF in China is chronic HBV infection, while it is often a result of alcoholic cirrhosis in western countries [2]. An unclear pathogenesis of HBV-ACLF and the lack of effective treatment options result in an extremely high mortality rate. Substantial evidence indicates that immunity-mediated inflammation plays an essential role in HBV-ACLF. Particularly, different

arms of the innate and adaptive immune cells make critical contributions to the development and progression of HBV-ACLF [3, 4].

Classically referred as core part of humoral immunity, immunoglobulins have been shown to play key roles in several types of liver diseases. Serum immunoglobulins are frequently elevated in chronic liver disease and cirrhotic patients [5, 6]. In addition, characteristic patterns of elevation in serum immunoglobulins are observed in specific liver diseases such as raised immunoglobulin G (IgG) in autoimmune hepatitis, raised immunoglobulin A (IgA) in alcoholic liver disease, and raised immunoglobulin M (IgM) in primary biliary cholangitis (PBC), which can be applied to aid diagnosis in clinical practice [7–10]. These pieces of evidence strongly link immunoglobulins with immune-mediated liver injury. However, less information has been available about the role of immunoglobulins in patients with HBV-ACLF.

Interleukin-27 (IL-27) is a relatively new cytokine that belongs to the IL-12 family. IL-27 is a heterodimeric cytokine composed of the Epstein-Barr virus-induced gene 3 (EBI3) and IL-27p28, which engages a receptor composed of gp130 and IL-27Ra that activates the JAK-STAT and MAPK signaling pathways [11]. IL-27 has both proinflammatory and anti-inflammatory properties that act on various types of cells depending on the context [11, 12]. Most studies mainly focus the effects of IL-27 on T cells. Also, IL-27 has been evidenced to regulate the expression of immunoglobulins by B cells. Several recent reports showed that IL-27 can induce the production of IgG1 by B cells and support antibody-driven autoimmune disease [13–15]. However, another report revealed that IL-27 can directly inhibit the growth of leukemic B cells [16]. To date, less is known about the correlations between IL-27 levels and the expression of immunoglobulins in patients with HBV-ACLF.

An important report enrolling patients with HBV-associated acute liver failure (HBV-ALF) clearly revealed that massive accumulation of plasma cells secreting IgG and IgM was found in the liver tissue [17]. In view of the similar pathogenic mechanisms between HBV-ALF and HBV-ACLF, we hypothesized that serum immunoglobulins could be elevated in patients with HBV-ACLF and that higher levels may indicate the unfavorable outcome. Therefore, in the present study, our aim was to determine the role of serum immunoglobulin levels (IgG, IgA, and IgM) and their correlations with IL-27 in noncirrhotic patients with HBV-ACLF.

2. Patients and Methods

2.1. Study Design and Patients. This study used clinical data and serum samples from our prospective study investigating the pathogenesis of HBV-ACLF patients. Briefly, thirty HBV-ACLF patients admitted to our department between June 2009 and May 2010 were enrolled. The inclusion criterion was based on the published works and clinical practice guideline. Adult noncirrhotic patients with HBV-ACLF who were willing to participate and consented to the study were enrolled based on previously described inclusion criteria [18, 19]. The exclusion criteria were the following: (1) evidence of other liver diseases including autoimmune liver diseases (autoimmune hepatitis and PBC), Wilson's disease, or cancer; (2) coinfection with other hepatitis virus or HIV virus; (3) treatment with artificial liver support or immunomodulatory drugs; (4) history of alcohol or drug abuse; and (5) records of renal, cardiovascular, pulmonary, or rheumatic diseases and pregnant women. Cirrhosis was clinically diagnosed when a small and nodular liver was found on imaging tests before enrollment [20]. Each patient was treated with supportive internal treatment. All HBV-ACLF patients were followed up at least 6 months. The clinical outcome was recorded as surviving or nonsurviving. Twenty-four chronic hepatitis B (CHB) patients and eighteen normal controls (NC) from our hospital during the same period were recruited as controls. CHB was diagnosed based on previously described criteria [18, 19]. Clinical assessment was performed at admission prior to therapy. Peripheral blood was collected at admission; serum was separated and stored at -80°C until being analyzed. The study was conducted in accordance with the Declaration of Helsinki, and the protocol was assessed and approved by our hospital's ethics committee. Written informed consent was obtained from each participant before the study.

2.2. Analysis of the Expression of IgG, IgA, and IgM. Human IgG, IgA, and IgM quantitation kits were purchased from Roche Diagnostics (Indianapolis, IN, USA). Serum concentrations of IgG, IgA, and IgM were analyzed using immunoturbidimetric assay through an autoanalyzer (TBA-30FR Toshiba, Tokyo, Japan) according to the manufacturer's guidelines. All values were compared to the normal ranges which were reported as 8-16 g/L for IgG, 0.7-3.3 g/L for IgA, and 0.5-2.2 g/L for IgM.

2.3. Analysis of IL-27 Levels by Enzyme-Linked Immunosorbent Assay. Serum IL-27 concentrations were quantified by sandwich enzyme-linked immunosorbent assay (ELISA) using commercial kits (BioLegend, San Diego, CA, USA) according to the manufacturer's protocol. Serum IL-27 levels were quantified by using standard samples with known cytokine concentrations provided by the manufacturer and expressed as pg/mL. The detection sensitivity was 11 pg/mL.

2.4. Virological Assessment and Liver Biochemical Assays. Serum HBV markers, including hepatitis B s antigen (HBsAg), hepatitis B e antigen (HBeAg), hepatitis B e antibody (HBeAb), and hepatitis B c antibody (HBcAb), were determined using the Elecsys system (Hoffmann-La Roche, Basel, Switzerland). HBV-DNA levels were quantitated by Real-Time Quantitative PCR using the ABI7300 (Applied Biosystems, Foster City, CA, USA). The limit of detection of HBV-DNA was 100 IU/mL. Liver biochemical assays were quantitated using an autoanalyzer (TBA-30FR Toshiba, Tokyo, Japan). Prothrombin time activity (PTA) was measured using an automatic hemostasis/thrombosis analyzer (STA Compact, Holliston, MA, USA).

2.5. Assessment of Complications and Disease Severity. Complete medical histories, physical examinations, and laboratory parameters were assessed for all HBV-ACLF

patients. Complications (including spontaneous bacterial peritonitis, hepatic encephalopathy, hepatorenal syndrome, and upper gastrointestinal bleeding) were closely monitored and diagnosed based on our previously described standards [21]. Model for end-stage liver disease (MELD) score and MELD-Na score were used to assess disease severity and calculated as previously described [22]. If the sodium value was below 125 mmol/L, it was set to 125 mmol/L, and if the value was above 140 mmol/L, it was adjusted to 140 mmol/L. Moreover, the recently developed Chronic Liver Failure Consortium (CLIF-C) ACLF score for classification and prognostic assessment of ACLF patients was also applied to evaluate the disease severity [23]. CLIF-C ACLF score was calculated as follows: $\text{CLIF} - \text{C ACLF} = 10 \times [0.33 \times \text{CLIF} - \text{OFs} + 0.04 \times \text{Age} + 0.63 \times \ln(\text{WBC count}) - 2]$.

2.6. Statistical Analysis. Data were analyzed using SPSS version 20.0 software (IBM Corporation, Armonk, NY, USA) and expressed as frequencies, medians, and ranges or as means ± standard errors. Differences in variables were analyzed using ANOVA and Student's t-tests (for normally distributed data) or Kruskal-Wallis and Mann-Whitney U tests (for nonnormally distributed data). Categorical data were analyzed using the Chi-square test and Fisher's exact test. Correlation analysis was evaluated by the Pearson or Spearman test. Receiver operating characteristic (ROC) curves were used to predict the 3-month mortality. Comparisons of ROC curves were performed using the DeLong test. A two-sided $P < 0.05$ was considered statistically significant.

3. Results

3.1. Characteristics of Patients. The characteristics of HBV-ACLF, CHB, and normal controls are presented in Table 1. No significant differences existed among the three groups for the age ($P = 0.073$) or gender ratio ($P = 0.718$). Moreover, no statistically significant difference was found between the CHB and HBV-ACLF groups with respect to the presence of HBeAg ($P = 0.061$).

3.2. Serum Levels of IgG, IgA, and IgM Increased in HBV-ACLF Patients Independently of the Presence of HBeAg. IgG, IgA, and IgM levels in serum samples from HBV-infected patients and uninfected controls were assessed using commercial kits. Overall, there were more patients with serum elevated immunoglobulins levels (defined as >1 time the upper limit of normal, >1 ULN) in the HBV-ACLF group when compared with the CHB group for elevated IgG levels (83.3% vs. 54.2%, $P = 0.034$), for elevated IgA levels (46.7% vs. 25%, $P = 0.156$), and for elevated IgM levels (50% vs. 8.3%, $P = 0.001$). Moreover, serum IgG levels were significantly increased in patients with HBV-ACLF (mean 21.21 g/L) when compared with CHB subjects (median 16.83 g/L, $P = 0.002$) and normal controls (mean 11.44 g/L, $P < 0.001$; Figure 1(a)). Also, serum IgA levels were significantly increased in patients with HBV-ACLF (mean 3.15 g/L) than in CHB subjects (mean 2.50 g/L, $P = 0.042$) and normal controls (mean 2.27 g/L, $P = 0.001$; Figure 1(a)). Moreover, serum IgM levels were significantly increased in patients with HBV-ACLF (median 2.19 g/L) when compared with CHB subjects (median 1.38 g/L, $P < 0.001$) and normal controls (median 0.92 g/L, $P < 0.001$; Figure 1(a)). We then determined the correlations between HBeAg presence and immunoglobulin levels. In the CHB group, no significant differences existed in IgG, IgA, or IgM levels between HBeAg-positive ($n = 16$) and HBeAg-negative patients ($n = 8$) ($P = 0.337$, $P = 0.890$, and $P = 0.503$, resp.; Figure 1(b)). Also, no significant differences existed in IgG, IgA, or IgM levels between HBeAg-positive HBV-ACLF patients ($n = 12$) and patients with HBeAg-negative HBV-ACLF ($n = 18$) ($P = 0.776$, $P = 0.634$, and $P = 0.755$, resp.; Figure 1(c)).

3.3. Increased Serum IgG, IgA, and IgM Levels Were Closely Associated with Liver Injury in HBV-Infected Patients. We subsequently analyzed the correlations between IgG, IgA, and IgM levels and serum total bilirubin (Tbil), plasma PTA, serum albumin, serum globulin, serum ALT, serum AST levels, and serum HBV-DNA loads in CHB and HBV-ACLF patients. Interestingly, serum Tbil levels were positively correlated with IgG, IgA, and IgM levels ($r = 0.387$, $P = 0.004$; $r = 0.372$, $P = 0.006$; and $r = 0.515$, $P < 0.001$, resp.; Figure 2(a)), while plasma PTA levels were negatively correlated with IgG, IgA, and IgM levels ($r = -0.482$, $P < 0.001$; $r = -0.258$, $P = 0.059$; and $r = -0.557$, $P < 0.001$, resp.; Figure 2(b)) in these HBV-infected subjects. In addition, serum albumin levels were negatively correlated with IgG, IgA, and IgM levels ($r = -0.539$, $P < 0.001$; $r = -0.266$, $P = 0.052$; and $r = -0.485$, $P < 0.001$, resp.; Figure 2(c)). Serum globulin levels were positively correlated with IgG and IgA levels ($r = 0.300$, $P = 0.027$ and $r = 0.350$, $P = 0.010$; Figure 2(d)). However, no significant correlations existed between IgG, IgA, or IgM levels and ALT levels, AST levels, or HBV-DNA levels in these HBV-infected patients (all $P > 0.05$). These findings suggest that increased serum IgG, IgA, and IgM levels were closely associated with liver injury in HBV-infected patients.

3.4. IgG Levels Were Closely Associated with Clinical Outcome in HBV-ACLF Patients. We stratified patients into three stages according to the natural history of HBV-ACLF [24, 25], the ascent stage ($n = 5$), the plateau stage ($n = 13$), and the descent stage ($n = 12$). Interestingly, IgG levels were significantly lower in patients at the descent stage (17.04 ± 1.35 g/L) than in patients at the ascent stage (23.11 ± 1.96 g/L, $P = 0.022$) and in patients at the plateau stage (24.33 ± 1.32 g/L, $P = 0.001$). However, no significant differences existed in IgA or IgM levels among HBV-ACLF patients at different stages (Figure 3(a)). During the follow-up period, eighteen HBV-ACLF patients survived, while twelve patients died. Then, we examined the correlations between clinical outcome and expression of IgG, IgA, and IgM. Serum IgG levels were significantly higher in nonsurviving HBV-ACLF patients (24.51 ± 1.51 g/L, $n = 12$) than in surviving patients (19.02 ± 1.18 g/L, $n = 18$, $P = 0.007$; Figure 3(b)). Also, we noticed that serum IgM levels were slightly higher in nonsurviving HBV-ACLF patients (median 2.48 g/L) than in surviving HBV-ACLF patients (median 2.07 g/L, $P = 0.079$; Figure 3(b)). However, there was no

Table 1: Clinical characteristics of the participants enrolled in the study.

Groups	NC ($n = 18$)	CHB ($n = 24$)	HBV-ACLF ($n = 30$)
Gender (male)	17	24	29
Age (years)	36.33 ± 2.84	36.92 ± 1.50	42.97 ± 2.44
ALT (U/L)	22.67 ± 2.18	186.5 (34-2424)	187.5 (27-2879)
AST (U/L)	23.39 ± 1.75	211.5 (56-2646)	163 (66-1859)
Tbil (μmol/L)	N.D.	186.9 (39.1-826.2)	489.6 (204.5-1157.0)
PTA (%)	N.D.	85 (46-126)	34 (14-40)
Albumin (g/L)	N.D.	40.2 (35.4-50.7)	33.53 ± 0.92
Globulin (g/L)	N.D.	29.9 (22.8-43.9)	30.22 ± 1.03
HBV-DNA ($\log_{10}$IU/mL)	N.D.	5.33 ± 0.24	4.59 ± 0.25
Complication	0	0	22
SBP	0	0	19
Hepatic encephalopathy	0	0	11
Hepatorenal syndrome	0	0	2
UGB	0	0	1
MELD score	N.D.	N.D.	27.37 ± 0.89
MELD-Na score	N.D.	N.D.	28.24 ± 0.84
CLIF-C ACLF score	N.D.	N.D.	42.20 ± 1.15
IgG (g/L)	11.44 ± 0.44	16.83 (8.86-30.76)	21.21 ± 1.04
Elevated IgG (>1 ULN)	0	13	25
IgA (g/L)	2.27 ± 0.14	2.50 ± 0.24	3.15 ± 0.21
Elevated IgA (>1 ULN)	0	6	14
IgM (g/L)	0.92 (0.54-1.75)	1.38 (0.75-3.47)	2.19 (1.09-5.41)
Elevated IgM (>1 ULN)	0	2	15
HBsAg positive	0	24	30
HBsAb positive	18	0	0
HbeAg positive	0	16	12

Data are shown as means ± standard errors or medians and ranges. ACLF: acute-on-chronic liver failure; CHB: chronic hepatitis B; NC: normal control; ALT: alanine aminotransferase; AST: aspartate aminotransferase; Tbil: total bilirubin; PTA: prothrombin time activity; SBP: spontaneous bacterial peritonitis; UGB: upper gastrointestinal bleeding; MELD: model for end-stage liver disease; CLIF-C: Chronic Liver Failure Consortium; IgG: immunoglobulin G; IgA: immunoglobulin A; IgM: immunoglobulin M; ULN: upper limit of normal; N.D: not determined.

significant difference in IgA levels between nonsurviving HBV-ACLF patients (3.26 ± 0.30 g/L) and those surviving (3.08 ± 0.29 g/L, $P = 0.674$; Figure 3(b)). MELD score, MELD-Na score, and CLIF-C ACLF score are widely applied to assess disease severity in HBV-ACLF. In this study, these parameters were calculated as described at admission. The results were 27.37 ± 0.89, 28.24 ± 0.84, and 42.20 ± 1.15 for MELD score, MELD-Na score, and CLIF-C ACLF score, respectively. Next, the correlations between immunoglobulin levels (IgG, IgA, and IgM) and these parameters were determined by Pearson analysis. Interestingly, positive correlations were found between IgG levels and MELD score ($r = 0.401$, $P = 0.028$), between IgA levels and CLIF-C ACLF score ($r = 0.396$, $P = 0.030$; Figure 3(c)). And a positive correlation trend was found between IgG levels and MELD-Na score ($r = 0.351$, $P = 0.057$; Figure 3(c)). However, no significant correlations existed between IgM levels and these scores in HBV-ACLF patients (all $P > 0.05$).

3.5. IL-27 Levels Were Positively Correlated with Immunoglobulins in HBV-Infected Patients. IL-27 has been evidenced to regulate the production of immunoglobulin by B cells. In this study, serum IL-27 levels were significantly higher in HBV-ACLF patients (634.58 ± 40.21 pg/mL) than in the CHB group (441.25 ± 28.87 pg/mL, $P < 0.001$) and the NC group (277.14 ± 23.96 pg/mL, $P < 0.001$). Next, the correlations between IL-27 levels and immunoglobulin levels were examined by Spearman or Pearson analysis. Interestingly, IgG levels were positively correlated with IL-27 levels ($r = 0.398$, $P = 0.029$), and a positive correlation trend was found between IgM levels and IL-27 levels ($r = 0.344$, $P = 0.062$; Figure 4(a)) in HBV-ACLF patients. Furthermore, positive correlations were found between IL-27 levels and IgG levels ($r = 0.392$, $P = 0.003$), IgA levels ($r = 0.362$, $P = 0.007$), and IgM levels ($r = 0.507$, $P < 0.001$; Figure 4(b)) in HBV-infected patients. These results indicate that IL-27 may induce the production of immunoglobulins in HBV-infected patients.

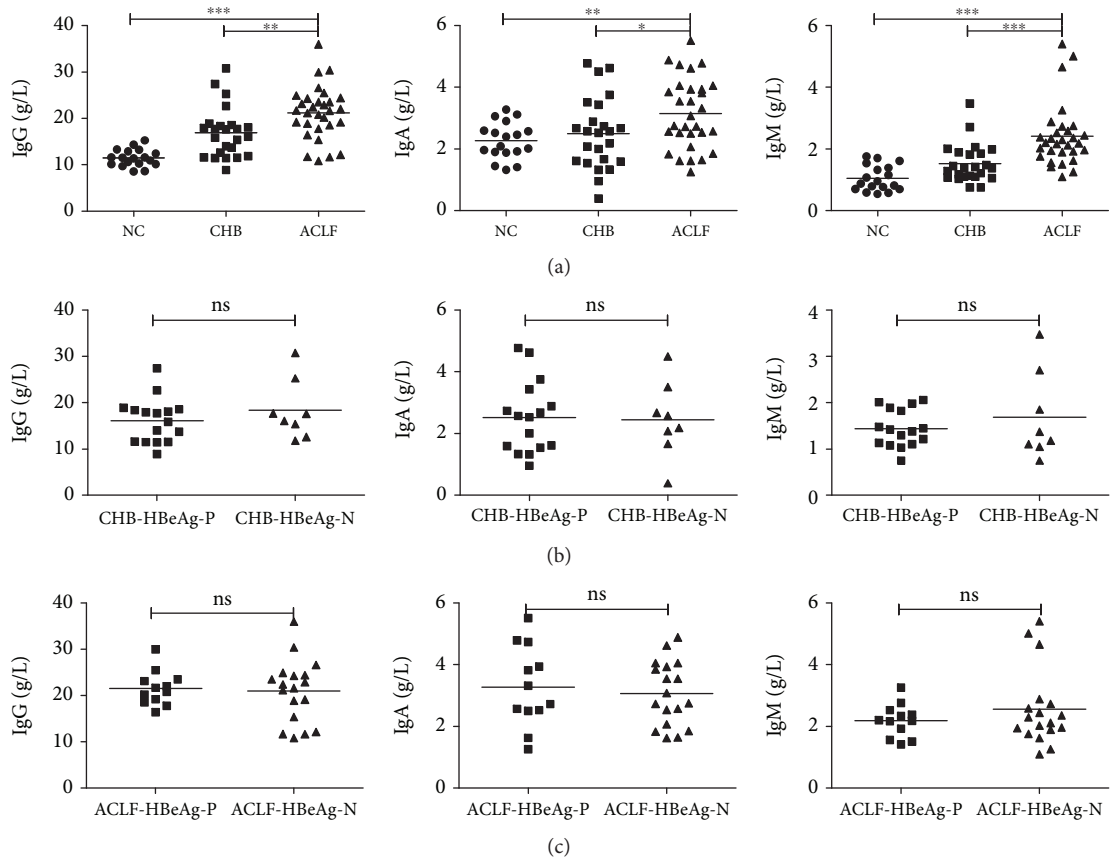

Figure 1: IgG, IgA, and IgM levels were significantly higher in HBV-ACLF patients independently of HBeAg presence. Pooled data indicated the levels of IgG, IgA, and IgM in each group, where the lines indicated the mean or median. (a) Serum IgG, IgA, and IgM levels were significantly higher in HBV-ACLF patients than in the CHB group and the NC group. No significant differences existed between patients with HBeAg positive and those with HBeAg negative, neither in the CHB group (b) nor in the HBV-ACLF group (c). ACLF: acute-on-chronic liver failure; CHB: chronic hepatitis B; NC: normal control; HBeAg-P: HBeAg-positive; HBeAg-N: HBeAg-negative; $*P < 0.05$; $**P < 0.01$; $***P < 0.001$; ns: not significant.

3.6. Higher IgG Levels May Predict Poor Prognosis in HBV-ACLF Patients. The 3-month mortality rate is a widely accepted indicator for the long-term prognosis of HBV-ACLF patients [23, 24]. In the current study, twelve HBV-ACLF patients died in the first three months, while eighteen patients survived during the follow-up period. Thus, the 3-month mortality rate was 40%. Finally, IgG levels were assessed to predict the 3-month mortality of HBV-ACLF patients and compared with IL-27 levels and disease severity scores (MELD, MELD-Na, and CLIF-C ACLF) by ROC curves (Figure 5, Table 2). The area under the ROC curve (AUC) for IgG levels was 0.752 (95% confidence interval: 0.562-0.891, $P = 0.005$). Interestingly, no significant differences existed between AUC values obtained using IgG levels and those obtained with IL-27 levels (0.824, $P = 0.531$), MELD score (0.870, $P = 0.320$), MELD-Na score (0.854, $P = 0.433$), or CLIF-C ACLF score (0.671, $P = 0.536$), indicating that IgG levels may have prognostic value equivalent to these parameters.

4. Discussion

To date, less information has been available on the role of serum immunoglobulins and their correlations with IL-27 in patients with HBV-ACLF. This study shows that there were more patients with elevated immunoglobulin levels in the HBV-ACLF group than in the CHB group; and immunoglobulin (IgG, IgA, and IgM) levels were positively linked with liver injury. In addition, IgG levels were positively associated with MELD score ($r = 0.401$, $P = 0.028$) and may predict the 3-month mortality using ROC curves (AUC = 0.752, $P = 0.005$) in patients with HBV-ACLF. Furthermore, this study demonstrates that IgG levels were positively correlated with the expression of IL-27 in patients with HBV-ACLF ($r = 0.398$, $P = 0.029$), indicating that IL-27 may participate in the production of IgG.

Previous studies have shown that specific elevations of serum immunoglobulin are found in several types of liver disease, such as autoimmune hepatitis (elevated IgG), PBC (elevated IgM), and alcoholic liver disease and nonalcoholic fatty liver disease (elevated IgA) [7–10, 26]. However, little is known about how serum immunoglobulin levels are altered in patients with HBV-ACLF. In the present study, 83.3% HBV-ACLF patients had an elevated IgG (>1 ULN), whereas 46.7% patients had an elevated IgA (>1 ULN) and 50% patients had an elevated IgM (>1 ULN). These data indicate a polyclonal increase of immunoglobulins, which may be

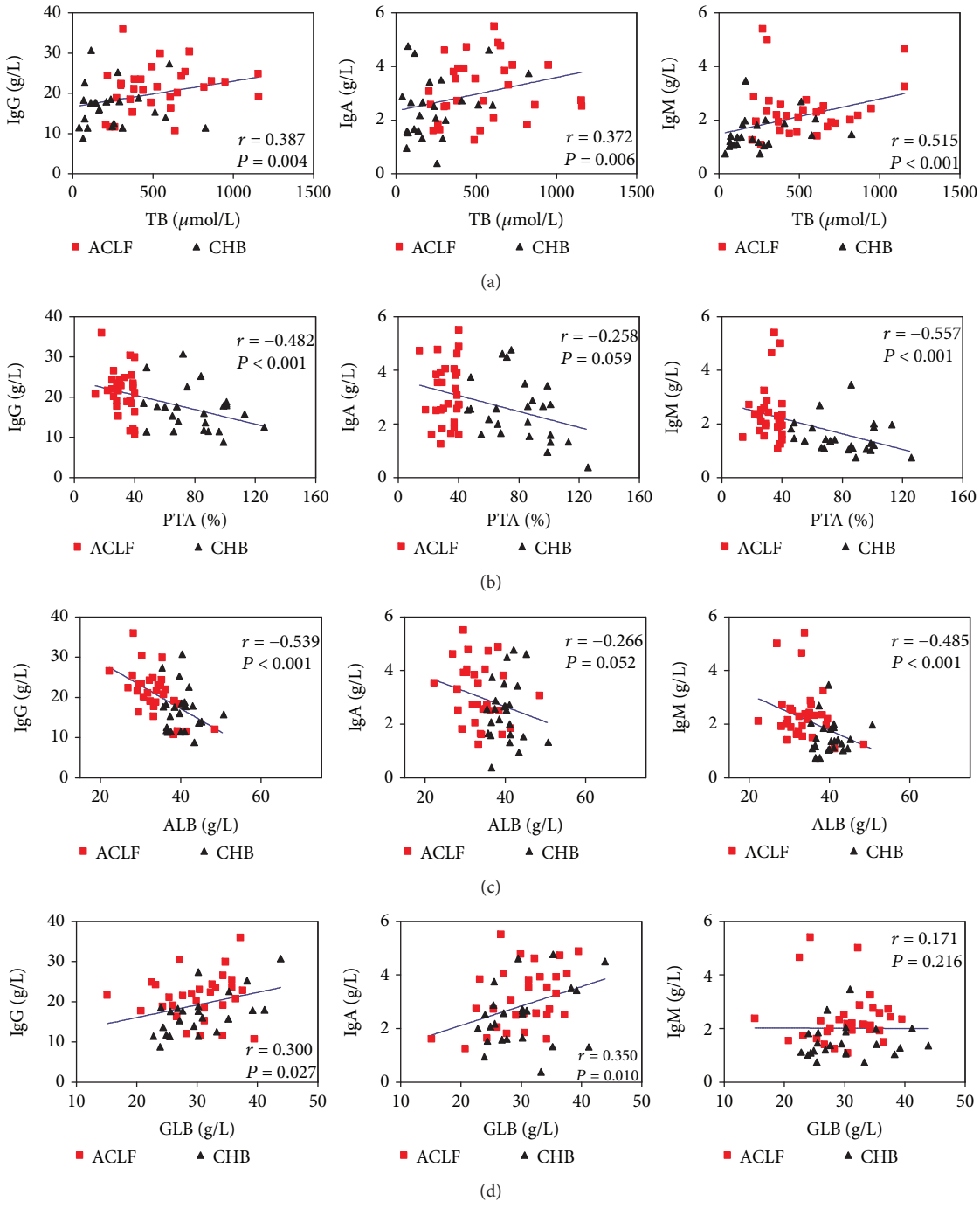

Figure 2: Elevated serum IgG, IgA, and IgM may contribute to liver injury. Serum IgG, IgA, and IgM levels were positively correlated with serum total bilirubin (TB) levels (a) but negatively associated with plasma prothrombin time activity (PTA) levels (b) and serum albumin (ALB) levels (c). In addition, positive correlations were found between immunoglobulin (IgG and IgA) and serum globulin (GLB) levels (d) in HBV-infected patients. Solid line: linear growth trend; *r*: correlation coefficient. *P* values are shown.

a characteristic of patients with HBV-ACLF. Therefore, when investigating patients with suspected liver disease, the finding of a polyclonal increase of immunoglobulins should prompt clinicians to consider HBV-ACLF as a diagnosis when there is no evidence of autoimmune liver diseases and no history of excessive alcohol consumption.

T lymphocytes have been evidenced to play an essential role in the pathogenesis of HBV-ACLF [27]. However, studies on B lymphocytes are limited. Also, the role of the immunoglobulins in HBV-ACLF patients is poorly understood. A recent study using liver tissue showed that B lymphocyte-mediated responses were highly active during the immune

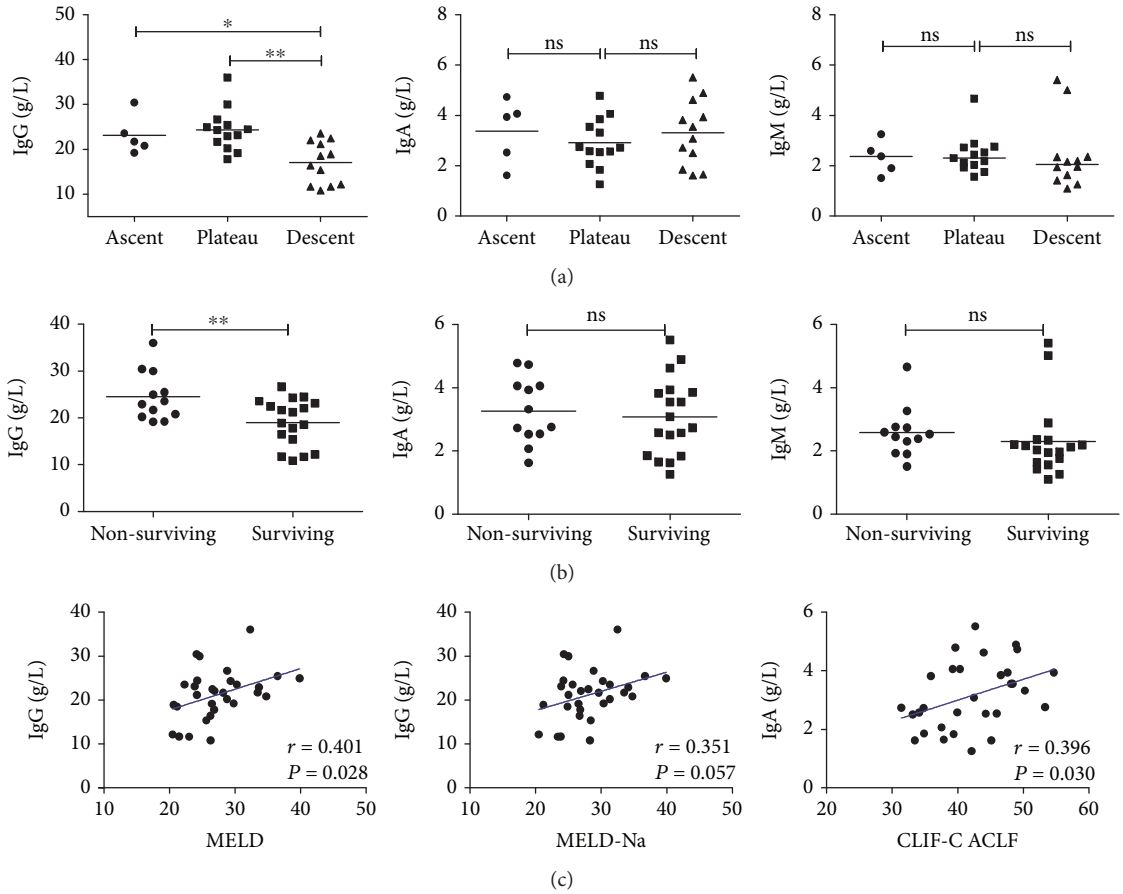

Figure 3: IgG levels were closely associated with disease severity in HBV-ACLF patients. (a) IgG levels were significantly lower in HBV-ACLF patients at the descent stage than patients at the ascent stage ($P = 0.022$) and patients at the plateau stage ($P = 0.001$). However, no significant differences existed in IgA or IgM levels among HBV-ACLF patients at different stages. (b) Serum IgG levels were significantly higher in nonsurviving HBV-ACLF patients than in surviving patients ($P = 0.007$). Also, we noticed that serum IgM levels were slightly higher in nonsurviving HBV-ACLF patients than in surviving patients ($P = 0.079$). (c) Positive correlations were found between IgG levels and MELD score, between IgA levels and CLIF-C ACLF score. And a positive correlation trend was found between IgG levels and MELD-Na score. $*P < 0.05$; $**P < 0.01$; ns: not significant; solid line: linear growth trend; r: correlation coefficient.

tolerance and immune active phases of patients with chronic hepatitis B [28]. Moreover, an overwhelming B cell response was seen, and massive production of immunoglobulin by plasma cells was found to be deposited in the liver parenchyma in patients with HBV-associated acute liver failure [17]. These studies led us to hypothesize that immunoglobulins produced by B cells may contribute to liver injury in HBV-ACLF. There are several lines of evidence to support this notion. Firstly, we demonstrate that HBV-ACLF patients had higher serum IgG, IgA, and IgM levels compared to CHB patients and normal controls. In addition, serum IgG, IgA, and IgM levels in HBV-infected patients were positively associated with serum Tbil levels but negatively correlated with PTA levels and ALB levels, which are often served as markers of liver injury [29]. Moreover, IgG levels were positively correlated with MELD score, which is an important indicator of disease severity in HBV-ACLF. And, IgG levels were significantly higher in nonsurviving HBV-ACLF patients than in surviving patients. Furthermore, the ROC curve analysis showed that IgG levels accurately predicted the 3-month mortality in patients with HBV-ACLF (AUC = 0.752, $P = 0.005$). These results suggest that IgG plays an important role in the pathogenesis of HBV-ACLF, and higher levels of IgG may predict poor prognosis.

Cytokines serving as mediators of immune responses play an essential role in the mechanism of immune-mediated diseases. IL-27, a heterodimeric cytokine comprising the IL-27p28 and EBI3 subunits, is a member of the IL-6/IL-12 family of cytokines and can exert proinflammatory and anti-inflammatory effects during immune responses [11, 12]. B cells express the complete IL-27R, which can be detected on human naïve B cells, memory B cells, and resting plasma cells [30]. More importantly, IL-27 has been evidenced to support antibody-driven autoimmune diseases through both direct and indirect effects on B cells [14, 15, 31], whereas another report revealed that IL-27 can directly inhibit the growth of leukemic B cells [16]. To date, less is known about the role of IL-27 on the expression of immunoglobulins in patients with HBV-ACLF. To our knowledge, the current study is the first

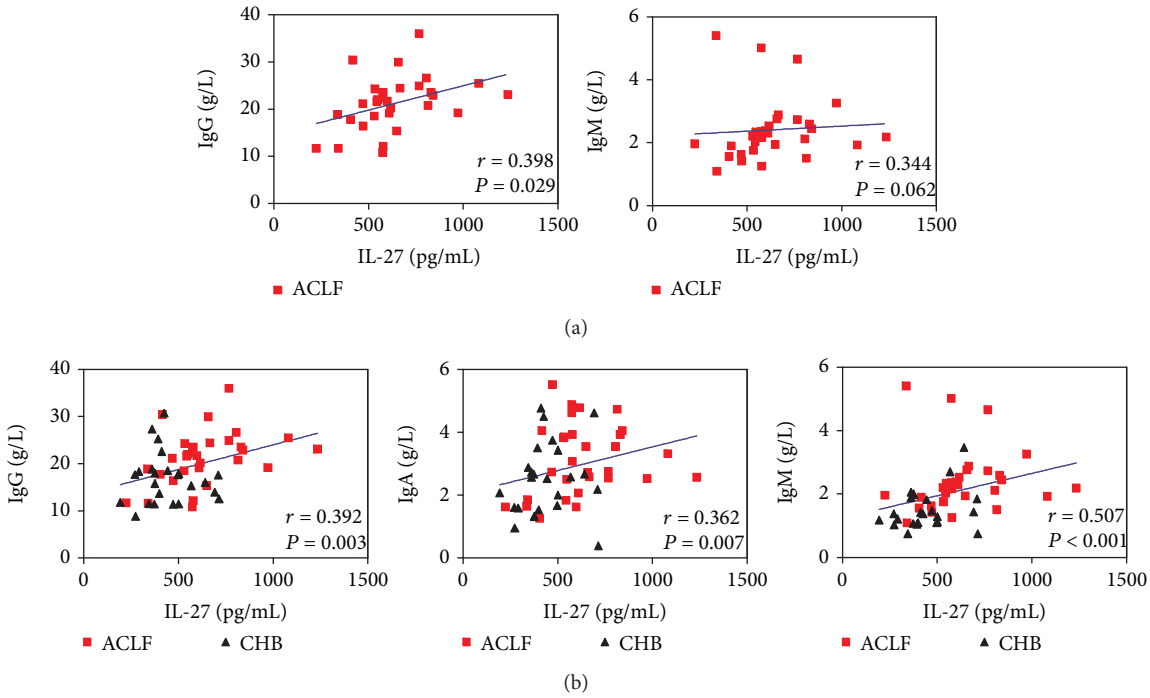

Figure 4: IL-27 levels were positively correlated with the expression of immunoglobulins. (a) IgG levels were found to be positively correlated with IL-27 levels; and a positive correlation trend was found between IgM levels and IL-27 levels in HBV-ACLF patients. (b) Positive correlations were found between IL-27 levels and serum immunoglobulin levels (IgG, IgA, and IgM) in HBV-infected patients. Solid line: linear growth trend; r: correlation coefficient. P values are shown.

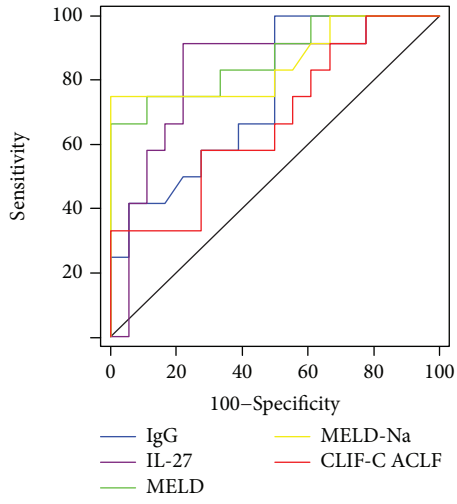

Figure 5: Accuracy of IgG levels was compared to other parameters in predicting the 3-month mortality of HBV-ACLF patients. The area under the ROC curve (AUC) for IgG levels was 0.752 (95% confidence interval: 0.562-0.891, $P = 0.005$). Interestingly, no significant differences existed between AUC values obtained using IgG levels and those obtained with IL-27 levels (0.824, $P = 0.531$), MELD score (0.870, $P = 0.320$), MELD-Na score (0.854, $P = 0.433$), or CLIF-C ACLF score (0.671, $P = 0.536$) in HBV-ACLF patients.

one to examine the correlations between IL-27 expression and immunoglobulins in HBV-ACLF. In accordance with our previous report [18], IL-27 levels were found to be significantly increased in HBV-ACLF patients than in the CHB group and the NC group in the present study. Next, we demonstrated that immunoglobulins were positively correlated with serum IL-27 levels in HBV-infected patients (Figure 4). More importantly, IgG levels were positively associated with IL-27 levels ($r = 0.398$, $P = 0.029$), and a positive trend between IgM levels and IL-27 levels ($r = 0.344$, $P = 0.062$) was found in patients with HBV-ACLF. Collectively, these data indicate that the preferential elevated immunoglobulins were closely linked with IL-27 levels. IL-27 may participate in the production of IgG in HBV-ACLF, but the exact mechanism should be intensely explored and further studies are required.

This study has several limitations. The intrahepatic expressions of immunoglobulins were not determined in patients with HBV-ACLF due to the poor coagulation, which is considered to be a contraindication for liver biopsy. Also, further studies are necessary to investigate the direct effects of IL-27 on the production of immunoglobulins by B lymphocytes in patients with HBV-ACLF. Moreover, this study was retrospective with a limited sample size; consequently, the results should be further validated in larger studies.

In summary, our findings demonstrate that a polyclonal increase of immunoglobulins existed and was closely linked with liver injury in patients with HBV-ACLF. Furthermore, immunoglobulin levels were positively correlated with IL-27 levels, suggesting that IL-27 may help induce the expression of immunoglobulins. In addition, higher IgG levels could predict poor prognosis in HBV-ACLF. Therefore, along with other clinical features and biochemical

Table 2: Comparisons of the area under the ROC curves (AUCs) estimated for each parameter.

Parameters	IL-27 (g/L)	IgG (g/L)	MELD	MELD-Na	CLIF-C ACLF
AUC	0.824 (0.642-0.938)	0.752 (0.562-0.891)	0.870 (0.697-0.964)	0.854 (0.678-0.956)	0.671 (0.477-0.831)
P value vs. IgG	0.531	-	0.320	0.433	0.536

Data in parentheses are 95% confidence interval. IgG: immunoglobulin G; MELD: model for end-stage liver disease; CLIF-C: Chronic Liver Failure Consortium; AUC: area under the ROC curve.

results, assessment of serum IgG levels could help physicians identify higher-risk HBV-ACLF patients earlier.

Abbreviations

ACLF: Acute-on-chronic liver failure
CHB: Chronic hepatitis B
NC: Normal control
HBV: Hepatitis B virus
Tbil: Total bilirubin
PTA: Prothrombin time activity
MELD: Model for end-stage liver disease
CLIF-C: Chronic Liver Failure Consortium
IgG: Immunoglobulin G
IgA: Immunoglobulin A
IgM: Immunoglobulin M
IL-27: Interleukin-27
ULN: Upper limit of normal.

Data Availability

The data used or analyzed during the current study are available from the first author (Geng-lin Zhang) on reasonable request.

Conflicts of Interest

The authors report no conflicts of interest in this work.

Authors' Contributions

Geng-lin Zhang and Qi-yi Zhao contributed equally to this work.

Acknowledgments

This study was supported by grants from the National Science and Technology Major Project (2018ZX10302204-002), National Natural Science Foundation of China (81672701), Guangdong Province Medical Research (A2017048), and Guangzhou Science and Technology Project (201508020118 and 2014Y2-00544).

References

[1] W. Bernal, R. Jalan, A. Quaglia, K. Simpson, J. Wendon, and A. Burroughs, "Acute-on-chronic liver failure," *The Lancet*, vol. 386, no. 10003, pp. 1576–1587, 2015.

[2] F. S. Wang and Z. Zhang, "Liver: how can acute-on-chronic liver failure be accurately identified?," *Nature Reviews Gastroenterology & Hepatology*, vol. 10, no. 7, pp. 390-391, 2013.

[3] W. K. Seto, C. L. Lai, and M. F. Yuen, "Acute-on-chronic liver failure in chronic hepatitis B," *Journal of Gastroenterology and Hepatology*, vol. 27, no. 4, pp. 662–669, 2012.

[4] R. Jalan, P. Gines, J. C. Olson et al., "Acute-on chronic liver failure," *Journal of Hepatology*, vol. 57, no. 6, pp. 1336–1348, 2012.

[5] D. Moskophidis, J. Löhler, and F. Lehmann-Grube, "Antiviral antibody-producing cells in parenchymatous organs during persistent virus infection," *Journal of Experimental Medicine*, vol. 165, no. 3, pp. 705–719, 1987.

[6] N. Sipeki, P. Antal-Szalmas, P. L. Lakatos, and M. Papp, "Immune dysfunction in cirrhosis," *World Journal of Gastroenterology*, vol. 20, no. 10, pp. 2564–2577, 2014.

[7] G. Husby, S. Skrede, J. P. Blomhoff, C. D. Jacobsen, K. Berg, and E. Gjone, "Serum immunoglobulins and organ non-specific antibodies in diseases of the liver," *Scandinavian Journal of Gastroenterology*, vol. 12, no. 3, pp. 297–304, 1977.

[8] D. M. Martin, D. H. Vroon, and S. M. Nasrallah, "Value of serum immunoglobulins in the diagnosis of liver disease," *Liver*, vol. 4, no. 3, pp. 214–218, 1984.

[9] H. Iturriaga, T. Pereda, A. Estévez, and G. Ugarte, "Serum immunoglobulin A changes in alcoholic patients," *Annals of Clinical Research*, vol. 9, no. 1, pp. 39–43, 1977.

[10] A. van de Wiel, J. van Hattum, H. J. Schuurman, and L. Kater, "Immunoglobulin A in the diagnosis of alcoholic liver disease," *Gastroenterology*, vol. 94, no. 2, pp. 457–462, 1988.

[11] C. A. Hunter and R. Kastelein, "Interleukin-27: balancing protective and pathological immunity," *Immunity*, vol. 37, no. 6, pp. 960–969, 2012.

[12] Y. Iwasaki, K. Fujio, T. Okamura, and K. Yamamoto, "Interleukin-27 in T cell immunity," *International Journal of Molecular Sciences*, vol. 16, no. 2, pp. 2851–2863, 2015.

[13] A. Boumendjel, L. Tawk, W. Malefijt Rde, V. Boulay, H. Yssel, and J. Pène, "IL-27 induces the production of IgG1 by human B cells," *European Cytokine Network*, vol. 17, no. 4, pp. 281–289, 2006.

[14] F. Qiu, L. Song, N. Yang, and X. Li, "Glucocorticoid down-regulates expression of IL-12 family cytokines in systemic lupus erythematosus patients," *Lupus*, vol. 22, no. 10, pp. 1011–1016, 2013.

[15] L. P. Xia, B. F. Li, H. Shen, and J. Lu, "Interleukin-27 and interleukin-23 in patients with systemic lupus erythematosus: possible role in lupus nephritis," *Scandinavian Journal of Rheumatology*, vol. 44, no. 3, pp. 200–205, 2015.

[16] S. Canale, C. Cocco, C. Frasson et al., "Interleukin-27 inhibits pediatric B-acute lymphoblastic leukemia cell spreading in a preclinical model," *Leukemia*, vol. 25, no. 12, pp. 1815–1824, 2011.

[17] P. Farci, G. Diaz, Z. Chen et al., "B cell gene signature with massive intrahepatic production of antibodies to hepatitis B core antigen in hepatitis B virus-associated acute liver failure,"

Proceedings of the National Academy of Sciences of the United States of America, vol. 107, no. 19, pp. 8766–8771, 2010.

[18] G. L. Zhang, D. Y. Xie, Y. N. Ye et al., "High level of IL-27 positively correlated with Th17 cells may indicate liver injury in patients infected with HBV," *Liver International*, vol. 34, no. 2, pp. 266–273, 2014.

[19] G. L. Zhang, D. Y. Xie, B. L. Lin et al., "Imbalance of interleukin-17-producing CD4 T cells/regulatory T cells axis occurs in remission stage of patients with hepatitis B virus-related acute-on-chronic liver failure," *Journal of Gastroenterology and Hepatology*, vol. 28, no. 3, pp. 513–521, 2013.

[20] L. Peng, D. Y. Xie, B. L. Lin et al., "Autologous bone marrow mesenchymal stem cell transplantation in liver failure patients caused by hepatitis B: short-term and long-term outcomes," *Hepatology*, vol. 54, no. 3, pp. 820–828, 2011.

[21] G. L. Zhang, T. Zhang, Q. Y. Zhao, C. S. Lin, and Z. L. Gao, "Th17 cells over 5.9% at admission indicate poor prognosis in patients with HBV-related acute-on-chronic liver failure," *Medicine*, vol. 97, no. 40, article e12656, 2018.

[22] W. R. Kim, S. W. Biggins, W. K. Kremers et al., "Hyponatremia and mortality among patients on the liver-transplant waiting list," *The New England Journal of Medicine*, vol. 359, no. 10, pp. 1018–1026, 2008.

[23] R. Jalan, F. Saliba, M. Pavesi et al., "Development and validation of a prognostic score to predict mortality in patients with acute-on-chronic liver failure," *Journal of Hepatology*, vol. 61, no. 5, pp. 1038–1047, 2014.

[24] S. K. Sarin and A. Choudhury, "Acute-on-chronic liver failure: terminology, mechanisms and management," *Nature Reviews Gastroenterology & Hepatology*, vol. 13, no. 3, pp. 131–149, 2016.

[25] Y. B. Zheng, Z. L. Huang, Z. B. Wu et al., "Dynamic changes of clinical features that predict the prognosis of acute-on-chronic hepatitis B liver failure: a retrospective cohort study," *International Journal of Medical Sciences*, vol. 10, no. 12, pp. 1658–1664, 2013.

[26] S. McPherson, E. Henderson, A. D. Burt, C. P. Day, and Q. M. Anstee, "Serum immunoglobulin levels predict fibrosis in patients with non-alcoholic fatty liver disease," *Journal of Hepatology*, vol. 60, no. 5, pp. 1055–1062, 2014.

[27] R. Moreau, "The pathogenesis of ACLF: the inflammatory response and immune function," *Seminars in Liver Disease*, vol. 36, no. 02, pp. 133–140, 2016.

[28] T. Vanwolleghem, J. Hou, G. van Oord et al., "Re-evaluation of hepatitis B virus clinical phases by systems biology identifies unappreciated roles for the innate immune response and B cells," *Hepatology*, vol. 62, no. 1, pp. 87–100, 2015.

[29] B. Rehermann and M. Nascimbeni, "Immunology of hepatitis B virus and hepatitis C virus infection," *Nature Reviews Immunology*, vol. 5, no. 3, pp. 215–229, 2005.

[30] C. Cocco, F. Morandi, and I. Airoldi, "Interleukin-27 and interleukin-23 modulate human plasmacell functions," *Journal of Leukocyte Biology*, vol. 89, no. 5, pp. 729–734, 2011.

[31] D. Vijayan, N. Mohd Redzwan, D. T. Avery et al., "IL-27 directly enhances germinal center B cell activity and potentiates lupus in *Sanroque* mice," *The Journal of Immunology*, vol. 197, no. 8, pp. 3008–3017, 2016.

Hindawi
Journal of Immunology Research
Volume 2019, Article ID 8325102, 9 pages
https://doi.org/10.1155/2019/8325102

Research Article

Immunoregulatory Effect of Koumine on Nonalcoholic Fatty Liver Disease Rats

Rongcai Yue,[1] Guilin Jin,[1] Shanshan Wei,[2] Huihui Huang,[1] Li Su,[3] Chenxi Zhang,[3] Ying Xu,[1] Jian Yang,[1] Ming Liu,[1] Zhiyong Chu,[2] and Changxi Yu[1]

[1]*School of Pharmacy, Fujian Medical University, Fuzhou, 350122 Fujian, China*
[2]*Naval Medical Research Institute, Second Military Medical University, Shanghai 200433, China*
[3]*School of Pharmacy, Second Military Medical University, Shanghai 200433, China*

Correspondence should be addressed to Zhiyong Chu; zhiyongchuleader@163.com and Changxi Yu; changxiyu@mail.fjmu.edu.cn

Received 29 June 2018; Revised 13 November 2018; Accepted 3 December 2018; Published 17 February 2019

Guest Editor: Xiaoni Kong

Nonalcoholic fatty liver disease (NAFLD) is the most common and important chronic liver disease all over the world. In the present study, we found that koumine, the main and active ingredient isolated from *Gelsemium elegans*, has the potential therapeutic effect on NAFLD rats by immunomodulatory activity. Koumine could significantly reduce the level of TG, TC, LDL-C, ALT, and AST in the serum of NAFLD rats and increase the level of HDL-C, reduce the liver index, and improve the adipose-like lesions of liver cells in NAFLD rats. Furthermore, treatment with koumine inhibited the severity of NAFLD. In addition, koumine-treated rats significantly increased the proportion of $CD4^+/CD8^+$ T cells and also decreased the percentages of Th1 and Th17 cells and increased Th2 and Treg cells in the liver. Moreover, koumine reduced the production and mRNA expression of proinflammatory cytokines *in vivo*. This result showed that koumine could effectively modulate different subtypes of helper T cells and prevent NAFLD. The present study revealed the novel immunomodulatory activity of koumine and highlighted the importance to further investigate the effects of koumine on hepatic manifestation of the metabolic syndrome.

1. Introduction

Nonalcoholic fatty liver disease (NAFLD) is the most common and important chronic liver disease all over the world [1, 2]. NAFLD is clinically divided into two forms: simple fatty liver (SFL) and nonalcoholic steatohepatitis (NASH), with NASH accounting for approximately half of all NAFLD cases. The probability of developing cirrhosis is 0.6%-3.0% in patients with SFL for 10-20 years and as high as a quarter in patients with NASH for 10-15 years. Approximately 1% of cirrhosis cases develop hepatocellular carcinoma each year [3–5]. Consequently, NAFLD represents a spectrum of disease ranging from hepatocellular steatosis through steatohepatitis to fibrosis and irreversible cirrhosis [6–8]. Although NAFL may occur in nonobese patients, most cases of NAFL are associated with obesity, type 2 diabetes mellitus, and hyperlipidaemia [9–11] and are accompanied by cardiovascular risk [12]. The prevalence of NAFLD has risen rapidly in parallel with the dramatic rise in obesity and diabetes, especially in the prevalence of obesity increases in adults and children [13, 14]. NAFLD is now recognized to represent the hepatic manifestation of the metabolic syndrome and is rapidly becoming one of the leading causes of liver disease in Western countries and China [15, 16]. The current medical treatment for NAFLD includes antioxidants, antiatherosclerotic drugs, hydroxymethylglutaryl coenzyme A reductase inhibitor, and angiotensin-II receptor antagonist [17–19]. However, since there is currently no specific treatment for NAFLD, it encourages the search for complementary and alternative treatments, such as medicinal medicine.

Over the course of more than 2000 years, traditional Chinese medicine has identified and utilized many herbs for the treatment of various diseases. Herbal drugs obtained from the plant source are relatively safe and less expensive and possess good tolerability even at higher doses without severe side effects, which may have a profound impact on

the treatment of NAFLD. Koumine (Figure 1(a)), an indole alkaloid isolated from *Gelsemium elegans*, has shown diverse pharmacological activities including antitumor, anti-inflammatory, and immunomodulatory activities [20, 21]. We recently reported the anti-inflammatory and immunoregulatory effect of koumine in a rheumatoid arthritis model [22–24] with a high-efficiency and low-toxicity feature, and next mechanism study found that koumine has the potential activated T cell regulation activity. Therefore, more immunomodulatory effects of koumine deserve further study.

The dysregulation of immune cells plays an important role in NAFLD, and several liver nonparenchymal cells including Kupffer cells, natural killer cells, and T lymphocytes are involved in the immune response of NAFLD morbidity process [25]. A longer adaptation process to injury and healing involves other cell types such as hepatocytes, hepatic stellate cells, and endothelial cells in addition to immune cells. Currently, effective treatment for NAFLD remains limited. In the present study, we investigated the therapeutic effect and mechanism of koumine on NAFLD. The result showed that koumine can effectively inhibit the development of NAFLD, decrease the clinical symptoms and inflammation, and reduce the infiltration of $CD4^+$ T cells and activation in the liver. The present study will be very helpful for developing novel and effective strategies for NAFLD treatment.

2. Material and Methods

2.1. Rats. Male Sprague-Dawley rats (170-200 g) were purchased from Shanghai SLAC Laboratory Animal Co. Ltd. (Shanghai, China). All rats were housed in specific pathogen-free conditions (22°C, a 12 h light/dark cycle with the light cycle from 6:00 to 18:00 and the dark cycle from 18:00 to 6:00) with *ad libitum* access to standard laboratory chow. All animal experiments were approved by the ethics committee at Fujian Medical University (no. 2017-021), and the study was conducted in accordance with the guidelines published in the NIH Guide for the Care and Use of Laboratory Animals.

2.2. Drugs. Koumine (PubChem CID: 91895267; purity > 98.5%, HPLC; Figure 1(a)) was isolated from *Gelsemium elegans* Benth. via pH-zone-refining countercurrent chromatography, which has been described in our previous study (Su et al., 2011). Koumine was intraperitoneally injected at a dose of 1.4 mg/kg, 0.28 mg/kg, and 0.056 mg/kg dissolved in sterile physiological saline (0.9% NaCl).

2.3. Induction of NAFLD. After 1 week of adaptive feeding, 50 male SD rats were randomly divided into the control group (10) and the model group (40 rats). The control group was fed with ordinary feed, and the model group was fed a high-fat diet (cholesterol 1%, bile salt 0.1%, lard 10%, egg yolk powder and whole milk powder 5%, and the rest for ordinary feed). At the end of the sixteenth week, each group was given intraperitoneal injection of koumine or equal volume of saline once a day for two weeks. At the end of the eighteenth week, blood was collected from the abdominal aorta after anesthesia, and serum and liver tissue samples were collected.

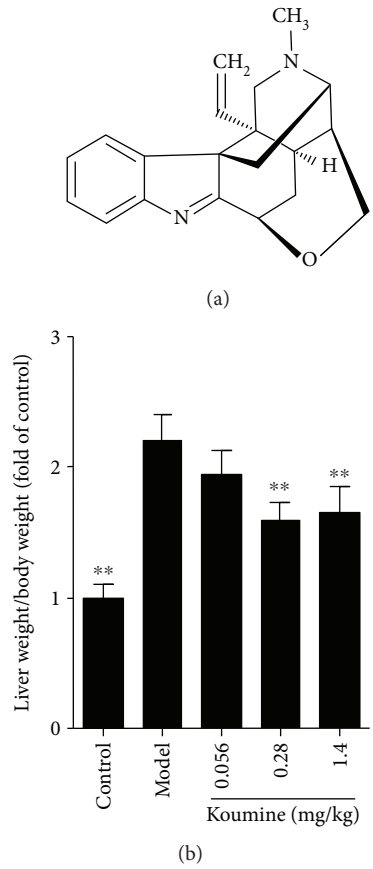

Figure 1: Chemical structures of koumine (a) and the effect of koumine on the liver index of NAFLD rats induced by fat diet. $^{**}p < 0.01$ versus the model group.

2.4. Histopathology. Rats were anesthetized to obtain the liver tissue; the samples with 4% paraformaldehyde were perfused and fixed overnight. After routine operation, paraffin-embedded 5 μm sections of the liver tissue were cut for HE staining and observed under the microscope (Olympus, Tokyo, Japan). Each histological sample was evaluated for the NAFLD activity score (NAS) as previously described [26].

2.5. Liver Index Measure. The liver was taken, cleaned with normal saline, dried with filter paper, and weighed. The liver index was calculated as liver weight compared to body mass.

2.6. Colorimetric Assay. The contents of serum total cholesterol (TC), triglyceride (TG), high-density lipoprotein (HDL), low-density lipoprotein (LDL), aspartate aminotransferase (AST), alanine aminotransferase (ALT), hepatic malondialdehyde (MDA), and nicotinamide adenine dinucleotide (NAD) were measured according to the kit instructions (Nanjing Jiancheng Bioengineering Institute).

2.7. Measurement of Cytokine Production. Serum and liver were collected to assay for cytokine levels. Serum was

Table 1: The specific primers used for amplification.

Gene	Forward 5′-3′	Reverse 5′-3′
TNF-α	CACCACCATCAAGGACTCAA	GAGACAGAGGCAACCTGACC
IL-6	TTCTTGGGACTGATGCTG	CTGGCTTTGTCTTTCTTGTT
IL-10	GGAAGAGAAACCAGGGAGAT	GCAGACAAACAATACACCATTC
IL-1β	GCCCATCCTCTGTGACTCAT	AGGCCACAGGTATTTTGTCG
GAPDH	AGTGGCAAAGTGGAGATT	GTGGAGTCATACTGGAACA

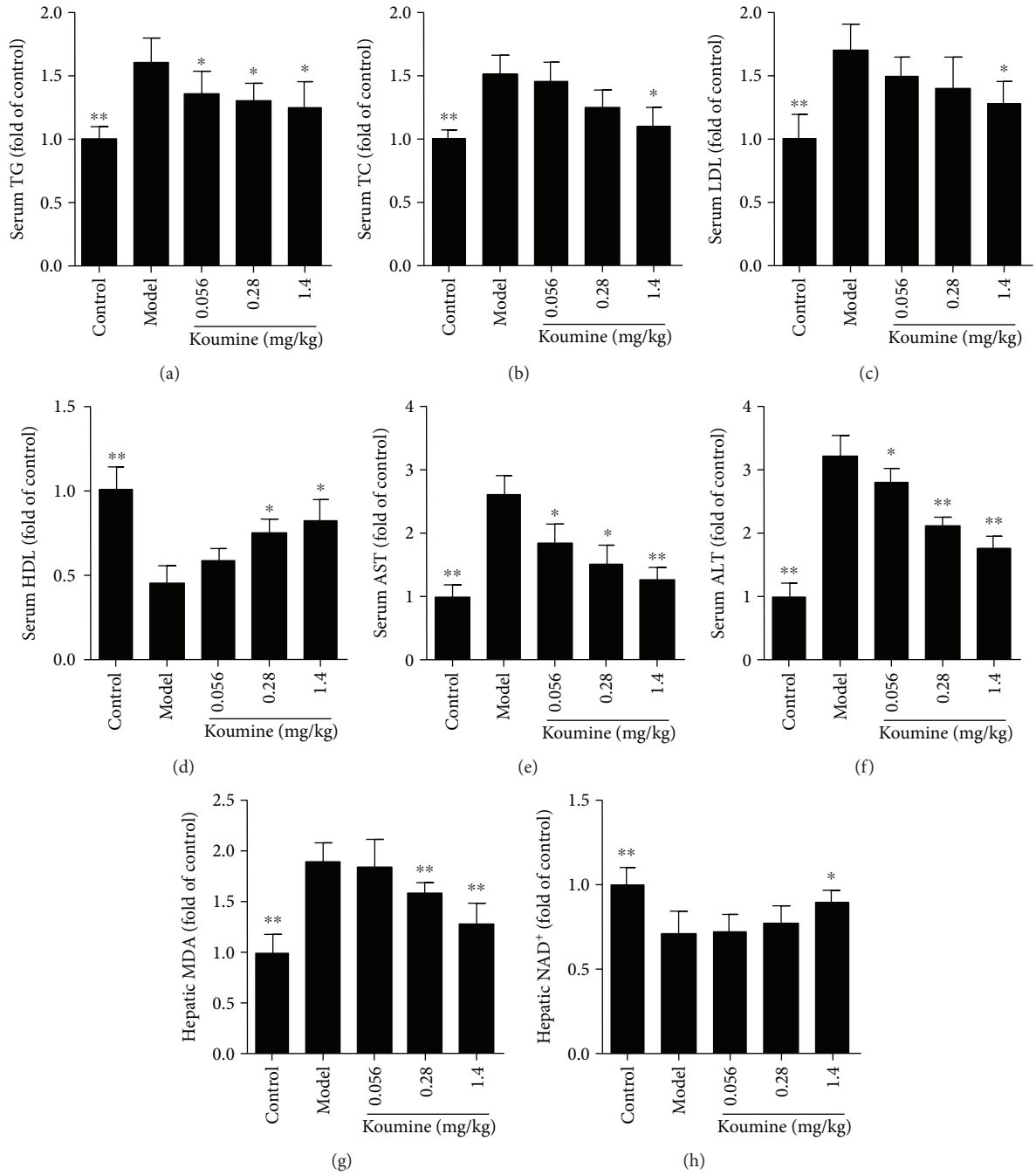

Figure 2: Effect of koumine on serological indexes of NAFLD rats induced by fat diet. TG: total cholesterol; TG: triglyceride; HDL: high-density lipoprotein; LDL: low-density lipoprotein; AST: aspartate aminotransferase; ALT: alanine aminotransferase; hepatic malondialdehyde (MDA) and nicotinamide adenine dinucleotide (NAD). $^{*}p < 0.05$ and $^{**}p < 0.01$, compared with the model group.

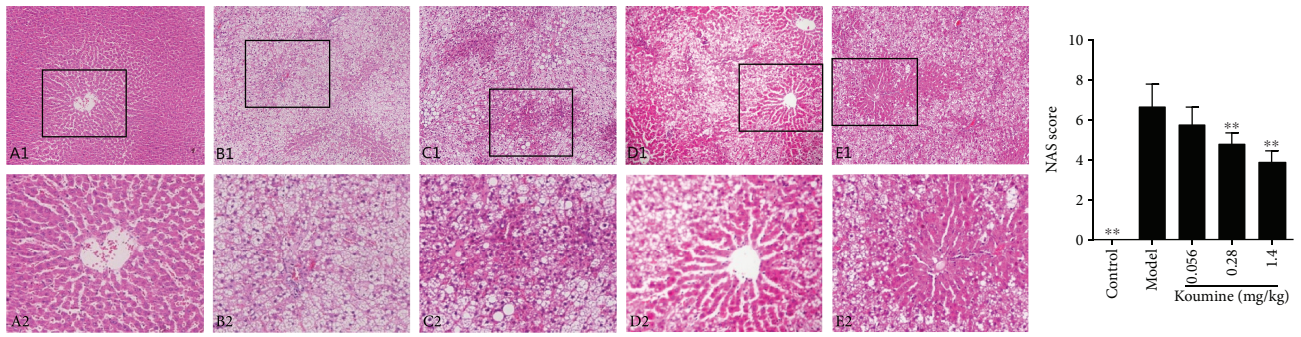

Figure 3: Effect of koumine on the pathomorphology of liver tissue induced by fat diet in NAFLD rats. A1-E1 represent the control group, model group, 0.056 mg/kg koumine-treated group, 0.28 mg/kg koumine-treated group, and 1.4 mg/kg koumine-treated group, respectively (×100 magnification); A2-E2 represent the same group with ×200 magnification. $^{**}p < 0.01$ compared with the model group.

analyzed by a LEGENDplex™ kit (BioLegend, San Diego, CA) according to the manufacturer's protocol. Liver homogenate (10%, *w*/*v*) was prepared by homogenizing the liver tissue in PBS, and supernatants were harvested and analyzed for ELISA (eBioscience, San Diego, CA) according to the manufacturer's protocol.

2.8. Quantitative Real-Time PCR. Total RNA was isolated from the liver using RNAiso Plus (Takara) according to the manufacturer's protocol. One microgram total RNA was reverse transcribed to first-strand cDNA, which was performed with PrimeScript™ RT Master Mix (Takara), and then expression levels of mRNA were quantified by real-time PCR using SYBR Premix Ex Taq™ (Takara). The PCR program included 1 cycle of 95°C for 30 s and 40 cycles of 95°C for 5 s and 60°C for 30 s. The specific primers used for amplification were shown in Table 1. The results were expressed by calculating the $2^{-\Delta\Delta CT}$ values and the housekeeping gene is GAPDH.

2.9. Flow Cytometry Analysis. The liver tissue was shredded, grinded by 200-mesh screen mesh, and filtered to a 50 ml centrifuge tube. To isolate mouse T cells, hepatocytes were prepared and other cells depleted using a mouse pan T cell isolation kit (Miltenyi Biotec) according to the manufacturer's instructions. For surface staining, the livers were collected and washed with PBS once, then incubated for 30 min with fluorochrome-conjugated antibodies as follows: PE-CD3, FITC-CD4, and PC5.5-CD8 (eBioscience). For intracellular staining, liver cells were stimulated with 100 ng/ml PMA (Sigma), 750 ng/ml ionomycin (Sigma), and 2 μM monensin (BD Biosciences) for 5 h. The livers were collected and incubated with anti-CD4, then fixed, permeabilized, and stained with Mouse Th1/Th2/Th17 Phenotyping Cocktail (BD Biosciences) and FITC-Foxp3 (eBioscience). Flow cytometry analyses were performed on FACSCalibur (BD).

2.10. Statistical Analysis. The data were analyzed by GraphPad Prism software (GraphPad Software Inc., San Diego, CA). All quantitative data were expressed as mean ± SEM as indicated. The comparison between the two groups was analyzed by unpaired Student's *t*-test, and multiple comparisons were compared by one-way ANOVA followed by Dunnett's test. Statistical significance was established at $p < 0.05$.

3. Results

3.1. Koumine Protects the Rats from NAFLD. NAFLD is recognized to represent the hepatic manifestation of the metabolic syndrome. We asked whether administration of koumine could affect the disease progression of NAFLD. Compared with the control group, the liver index of the rats in the model group increased significantly. Koumine treatment at the doses of 0.28 and 1.4 mg/kg significantly decreased the liver index of the control group compared with that of the model group (Figure 1(b)). Furthermore, we investigated the effects of koumine on serological indexes of NAFLD rats induced by fat diet. TG, TC, LDL, ALT, AST, and MDA in the model rats were significantly increased, and the content of HDL and NAD was significantly decreased compared with the control group. The level of TG, TC, LDL, ALT, AST, and MDA in the koumine-treated rats was significantly lower than that in the model group. The content of HDL in serum and NAD in the liver of rats was higher than that in the model group and increased in a dose-dependent manner (Figure 2). Moreover, the effect of koumine on the histopathological morphology of the liver was investigated in NAFLD rats induced by fat diet. In the control group, the liver surface was smooth and the hepatic lobule structure was clear. There were no hepatocyte swelling, fatty lesions, and inflammatory cell infiltration in the portal area. In the model group, the surface of the rat liver was roughened by the yellow soil. The volume of the liver increased obviously, and the hepatocytes showed fatty degeneration with necrosis and inflammatory cell infiltration. After koumine treatment, different degrees of improvement were observed and the proportion of nonfat liver cells increased significantly (Figure 3).

3.2. Koumine Suppresses Proinflammatory Cytokine Production and Expression in NAFLD Rats. We next investigated the effect of koumine on serum levels of cytokines by multifactor detection of flow cytometry. Koumine administration significantly decreased the proinflammatory

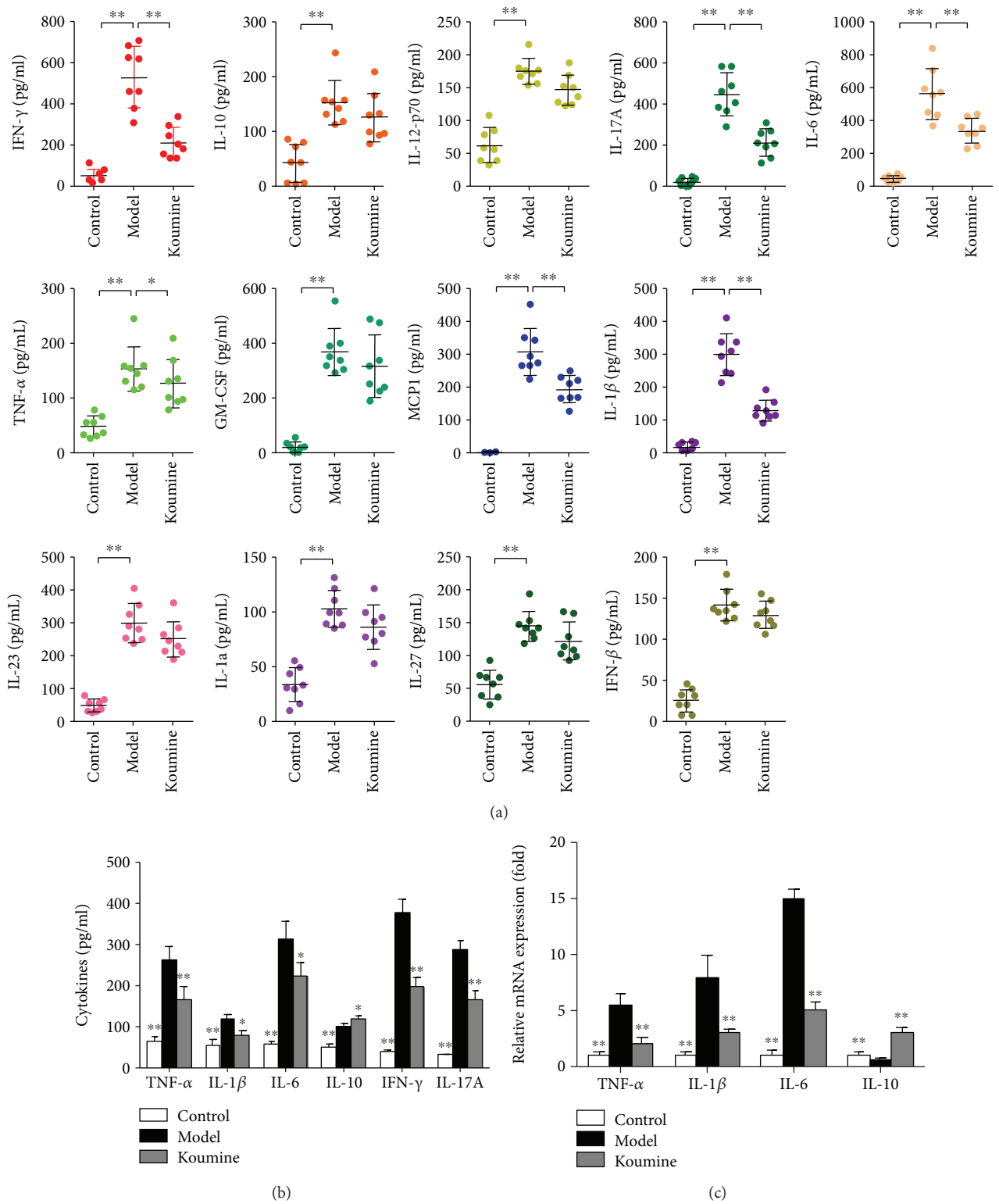

Figure 4: Koumine reduces the production and mRNA expression of cytokines in activated T cells. (a) Model and 1.4 mg/kg koumine-treated rats were sacrificed to obtain the serum and measured for the cytokines by multifactor detection of flow cytometry. (b) The livers were isolated from model and koumine-treated rats, and after being homogenized, the supernatants were harvested to measure the cytokine production by ELISA. (c) The livers were isolated from model and koumine-treated rats, and mRNA expression of selected genes were measured by real-time PCR. Data are means ± SEM ($n = 3$). $^{*}p < 0.05$ and $^{**}p < 0.01$ versus model. Data presented are representative of three independent experiments.

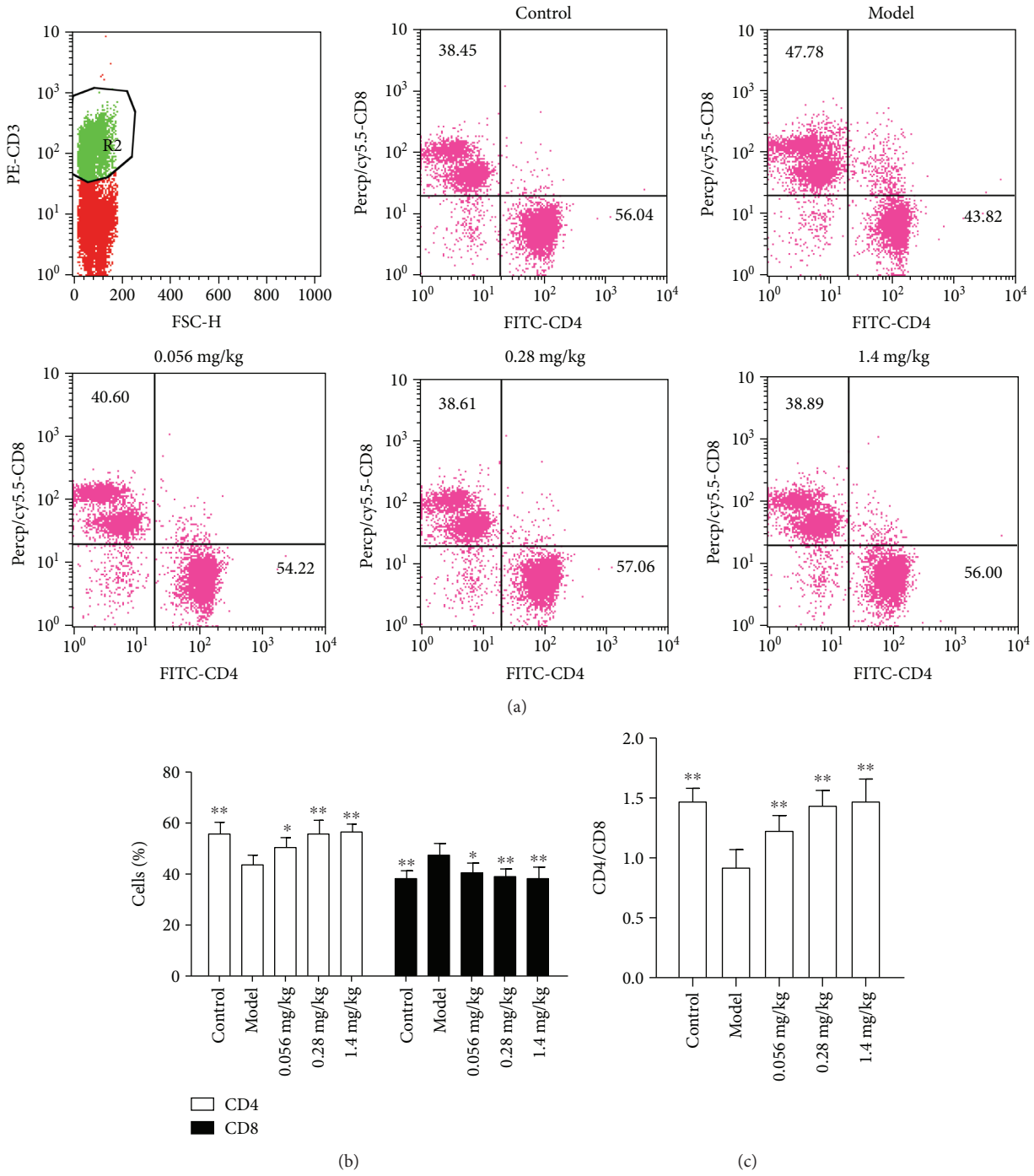

Figure 5: Koumine reduces the number of total leukocytes and $CD4^+$ T cells infiltrated in the liver. The livers were isolated from model and koumine-treated rats. (a) Cells were analyzed for expression of CD4, CD8, and CD3 by flow cytometry. (b) The percentages of cells that are positive to these antigens were represented. $^*p < 0.05$ and $^{**}p < 0.01$ versus model.

cytokines IFN-γ, IL-17A, TNF-α, IL-6, MCP1, and IL-1β levels in serum, while cytokines IL-10, IL-12, GMCSF, IL-23, IL-1α, IL-27, and IFN-β levels had a weakening trend (Figure 4(a)). Due to the noticeably preventive effect of koumine on NAFLD, we wondered whether koumine can suppress the inflammatory response. The liver isolated from model and koumine-treated rats were homogenized, and the supernatants were collected to analyze the production of proinflammatory cytokines. Compared with the model group, treatment with koumine significantly reduced the production of IL-6, IL-1β, IFN-γ, IL-17A, and TNF-α, while increasing the anti-inflammatory cytokine IL-10 level (Figure 4(b)). Subsequently, we investigated the effect of koumine on the mRNA expression of proinflammatory cytokines in the liver of different groups. The mRNA expression of IL-6, IL-1β, and TNF-α was also decreased

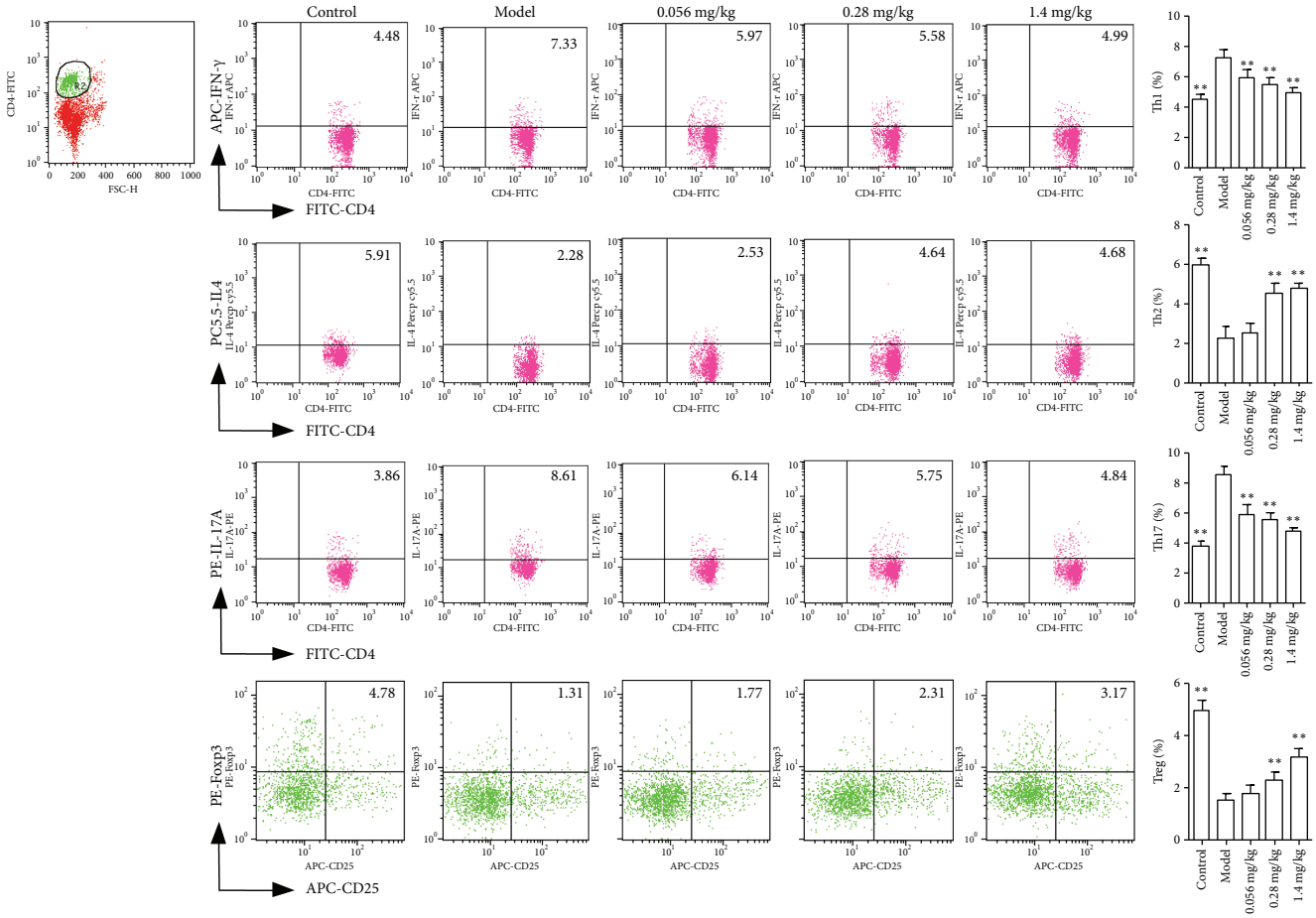

Figure 6: Koumine suppresses the differentiation of Th1 and Th17 cells while enhances Th2 and Treg cells. Cells were analyzed for the percentages of Th1, Th2, Th17, and Treg cells in the CD4 subsets by flow cytometry. $^{**}p < 0.01$ versus the model group.

while the anti-inflammatory cytokine IL-10 level was increased by koumine treatment (Figure 4(c)).

3.3. Koumine Increases CD4$^+$ Cell Proportion in Liver Lymphocytes. The livers were isolated from model and koumine-treated rats at the end of disease. Cells were stained with anti-CD3, anti-CD4, and anti-CD8 to analyze the infiltration of total leukocytes, CD4$^+$ T, and CD8$^+$ T cells by flow cytometry. Compared with the model group, koumine can significantly increase CD4$^+$ and decrease CD8$^+$ cell percentage in liver lymphocytes (Figure 5).

3.4. Koumine Inhibits Th1 and Th17 while Promoting Th2 and Treg in Liver Lymphocytes. As we all know, activated T cells can be differentiated into a variety of subtypes, including Th1, Th2, Th17, and Treg cells, and the imbalance of subtype differentiation is closely related to the progress of disease. To account for the abovementioned results, koumine significantly increased the number of CD4$^+$ T cells infiltrated into the liver, so it is necessary to investigate the effect of koumine on the subtypes of CD4$^+$ T cells. First of all, liver monocytes isolated from naive, NAFLD, and koumine-treated rats were analyzed for the Th1 (CD4$^+$IFN-γ^+), Th2 (CD4$^+$IL-4$^+$), Th17 (CD4$^+$IL-17$^+$), and Treg (CD4$^+$Foxp3$^+$) cell populations by flow cytometry. Compared with naive rats, the NAFLD rats showed a significantly increased number of Th1 and Th17 and decreased Th2 and Treg, while koumine could reverse the trends in contrast to the model group (Figure 6).

4. Discussion

The liver is recognized as an immunological organ playing critical roles in fighting invading pathogens. It hosts hepatocytes and nonparenchymal cells. The nonparenchymal cells include large populations of immune cells such as lymphocytes which have complex interactions with each other and with the hepatocytes, making the liver an important organ bridging innate immunity and adaptive immunity. The dysregulation of immune cells in the liver is involved in almost all types of liver diseases, such as NAFLD [25, 27]. Currently, effective treatment for inflammatory liver diseases such as NAFLD remains limited [28, 29]. An improved understanding of the inflammatory processes responsible for the progression of liver diseases will be very helpful in developing novel and effective strategies for NAFLD treatment [30]. In the present study, treatment with koumine effectively inhibited the development of NAFLD and reduced the serum proinflammatory cytokine levels. Koumine-treated rats displayed less leukocytes and CD4$^+$

T cells aggregated in the liver. With regard to $CD4^+$ T cells, we demonstrated that koumine decreased the percentages of $CD4^+IFN\text{-}\gamma^+$ and $CD4^+IL\text{-}17^+$ cells in the liver. Furthermore, koumine reduced the production and mRNA expression of proinflammatory cytokines *in vivo*.

The pathogenesis of NAFLD is not clear. It is thought that the pathogenesis of NAFLD is related to immunity and inflammation. $CD4^+$ T cells play a crucial role in metabolic syndrome. The diverse functions of $CD4^+$ T cells depend on their multiple subtypes. Activated $CD4^+$ T cells can be differentiated into at least Th1, Th2, Th17, and Treg. Among them, Th1 and Th17 cells always play a pathogenic role, yet Th2 cells display an antagonistic function to Th1 and Treg cells undertake the responsibility of regulating the immune responses [31, 32]. To mention the pathogenesis of NAFLD, the effector cells promote the activated $CD4^+$ T cell differentiation into more Th1 and Th17 subtypes and less Th2 and Treg subtypes; subsequently, Th1 and Th17 cells migrate across the liver [33]. As demonstrated above, we comprehended that the effect of koumine may be targeted on $CD4^+$ T cells; thus, we isolated the liver from naive, model, and koumine-treated rats to further investigate the effect of koumine on the differentiation of $CD4^+$ T cells. The result showed that koumine-treated rats presented decreasing trends for the percentages of Th1 and Th17 cells and increasing Th2 and Treg cells compared to model rats. So we demonstrated that koumine ameliorated NAFLD through modulating the proportion of different subtypes of helper T cells. Otherwise, we future investigated the related cytokines that participate in controlling the differentiation of $CD4^+$ T cells. The present experiments showed that koumine could inhibit the immune response and the secretion of Th1- and Th17-type cytokines in $CD4^+$ T lymphocytes, increase the level of Th2 type cytokines, and regulate the cytokine network, suggesting that koumine has immunosuppressive and anti-inflammatory effects, and the anti-NAFLD effect of koumine may also be mediated by its immunomodulatory action.

NAFLD is a chronic inflammatory process, with a number of proinflammatory cytokines released by activated immune cells in the peripheral immune organs [34]. Previous studies have shown that inflammatory cytokines such as TNF-α, IL-6, and IL-1β are predominantly detected in NAFLD mice [35]. TNFR1 signaling is considerable in the development of demyelination and contributes to the limitation of T cell responses during immune-mediated CNS disease [36]. The high level of IL-6 mRNA expression in the peripheral immune organs correlates with the progression of NAFLD. IL-6 and TNF-α are also the important cytokines secreted by Th17 and Th1 cells [37]. We observed that koumine suppresses the production of IL-6, IL-1β, and TNF-α along with their expression of mRNA levels in the liver, indicating that koumine prevents the onset of NAFLD also through the inhibition of proinflammatory cytokines in the peripheral immune organs.

In summary, our study demonstrates that koumine ameliorates NAFLD with an appropriate tolerance. Koumine further reduced the Th1 and Th17 cells and increased Th2 and Treg cells *in vivo*. Furthermore, koumine also reduces the production of related cytokines in the liver, indicating that it ameliorates NAFLD mainly through modulating the proportion of different subtypes of helper T cells and weakens the immune responses. However, this study is far from enough to explain the effect of koumine, and further investigations should be performed to elucidate the penetrating mechanisms that koumine acts and discover the possible effects on other metabolic diseases.

Data Availability

The data used to support the findings of this study are available from the corresponding author upon request.

Conflicts of Interest

The authors have declared that no competing interests exist.

Authors' Contributions

Rongcai Yue, Guilin Jin, and Shanshan Wei contributed equally to this work.

Acknowledgments

This work was supported by the National Natural Science Foundation of China (no. 81773716), the Joint Funds for the Innovation of Science and Technology, Fujian Province (no. 2016Y9058), the Special Support Funds for the Science And Technology Innovation Leader, Fujian Province (no. 2016B017), and the Natural Science Foundation of Fujian (2018J01845).

References

[1] G. Targher and C. D. Byrne, "Non-alcoholic fatty liver disease: an emerging driving force in chronic kidney disease," *Nature Reviews Nephrology*, vol. 13, no. 5, pp. 297–310, 2017.

[2] A. Alisi, A. E. Feldstein, A. Villani, M. Raponi, and V. Nobili, "Pediatric nonalcoholic fatty liver disease: a multidisciplinary approach," *Nature Reviews Gastroenterology & Hepatology*, vol. 9, no. 3, pp. 152–161, 2012.

[3] A. Lonardo, S. Ballestri, G. Marchesini, P. Angulo, and P. Loria, "Nonalcoholic fatty liver disease: a precursor of the metabolic syndrome," *Digestive and Liver Disease*, vol. 47, no. 3, pp. 181–190, 2015.

[4] European Association for the Study of the Liver (EASL), European Association for the Study of Diabetes (EASD), and European Association for the Study of Obesity (EASO), "EASL-EASD-EASO clinical practice guidelines for the management of non-alcoholic fatty liver disease," *Obesity Facts*, vol. 9, no. 2, pp. 65–90, 2016.

[5] C. D. Byrne and G. Targher, "EASL–EASD–EASO clinical practice guidelines for the management of non-alcoholic fatty liver disease: is universal screening appropriate?," *Journal of Hepatology*, vol. 59, no. 6, pp. 1141–1144, 2016.

[6] H. Yki-Järvinen, "Diagnosis of non-alcoholic fatty liver disease (NAFLD)," *Diabetologia*, vol. 59, no. 6, pp. 1104–1111, 2016.

[7] A. Asgharpour, S. C. Cazanave, T. Pacana et al., "A diet-induced animal model of non-alcoholic fatty liver disease

and hepatocellular cancer," *Journal of Hepatology*, vol. 65, no. 3, pp. 579–588, 2016.

[8] M. Afonso, P. Rodrigues, A. Simão, and R. Castro, "Circulating microRNAs as potential biomarkers in non-alcoholic fatty liver disease and hepatocellular carcinoma," *Journal of Clinical Medicine*, vol. 5, no. 3, p. 30, 2016.

[9] L. A. Adams, Q. M. Anstee, H. Tilg, and G. Targher, "Non-alcoholic fatty liver disease and its relationship with cardiovascular disease and other extrahepatic diseases," *Gut*, vol. 66, no. 6, pp. 1138–1153, 2017.

[10] G. Targher, A. Lonardo, and C. D. Byrne, "Nonalcoholic fatty liver disease and chronic vascular complications of diabetes mellitus," *Nature Reviews Endocrinology*, vol. 14, 2018.

[11] S. Wu, F. Wu, Y. Ding, J. Hou, J. Bi, and Z. Zhang, "Association of non-alcoholic fatty liver disease with major adverse cardiovascular events: a systematic review and meta-analysis," *Scientific Reports*, vol. 6, no. 1, article 33386, 2016.

[12] S. M. Francque, D. van der Graaff, and W. J. Kwanten, "Non-alcoholic fatty liver disease and cardiovascular risk: pathophysiological mechanisms and implications," *Journal of Hepatology*, vol. 65, no. 2, pp. 425–443, 2016.

[13] B. W. Smith and L. A. Adams, "Nonalcoholic fatty liver disease and diabetes mellitus: pathogenesis and treatment," *Nature Reviews Endocrinology*, vol. 7, no. 8, pp. 456–465, 2011.

[14] A. J. Engstler, T. Aumiller, C. Degen et al., "Insulin resistance alters hepatic ethanol metabolism: studies in mice and children with non-alcoholic fatty liver disease," *Gut*, vol. 65, no. 9, pp. 1564–1571, 2016.

[15] L. J. Carbone, P. W. Angus, and N. D. Yeomans, "Incretin-based therapies for the treatment of non-alcoholic fatty liver disease: a systematic review and meta-analysis," *Journal of Gastroenterology and Hepatology*, vol. 31, no. 1, pp. 23–31, 2016.

[16] G. Targher, C. D. Byrne, A. Lonardo, G. Zoppini, and C. Barbui, "Non-alcoholic fatty liver disease and risk of incident cardiovascular disease: a meta-analysis," *Journal of Hepatology*, vol. 65, no. 3, pp. 589–600, 2016.

[17] F. Salomone, J. Godos, and S. Zelber-Sagi, "Natural antioxidants for non-alcoholic fatty liver disease: molecular targets and clinical perspectives," *Liver International*, vol. 36, no. 1, pp. 5–20, 2016.

[18] F. Yu, T. Takahashi, J. Moriya et al., "Angiotensin-II receptor antagonist alleviates non-alcoholic fatty liver in KKAy obese mice with type 2 diabetes," *Journal of International Medical Research*, vol. 34, no. 3, pp. 297–302, 2016.

[19] I. Barchetta, F. Angelico, M. del Ben et al., "Effects of oral high-dose vitamin D supplementation on non-alcoholic fatty liver disease in patients with type 2 diabetes: a randomised, double-blind, placebo-controlled trial," *Journal of Hepatology*, vol. 64, no. 2, Supplement, p. S483, 2016.

[20] G.-L. Jin, Y. P. Su, M. Liu et al., "Medicinal plants of the genus *Gelsemium* (Gelsemiaceae, Gentianales)—a review of their phytochemistry, pharmacology, toxicology and traditional use," *Journal of Ethnopharmacology*, vol. 152, no. 1, pp. 33–52, 2014.

[21] X. Zhang, Y. Chen, B. Gao, D. Luo, Y. Wen, and X. Ma, "Apoptotic effect of koumine on human breast cancer cells and the mechanism involved," *Cell Biochemistry and Biophysics*, vol. 72, no. 2, pp. 411–416, 2015.

[22] J. Yang, H. D. Cai, Y. L. Zeng et al., "Effects of koumine on adjuvant- and collagen-induced arthritis in rats," *Journal of Natural Products*, vol. 79, no. 10, pp. 2635–2643, 2016.

[23] Y. Xu, H.-Q. Qiu, H. Liu et al., "Effects of koumine, an alkaloid of *Gelsemium elegans* Benth., on inflammatory and neuropathic pain models and possible mechanism with allopregnanolone," *Pharmacology Biochemistry and Behavior*, vol. 101, no. 3, pp. 504–514, 2012.

[24] G.-L. Jin, S.-D. He, S.-M. Lin et al., "Koumine attenuates neuroglia activation and inflammatory response to neuropathic pain," *Neural Plasticity*, vol. 2018, 13 pages, 2018.

[25] Y. Rotman and A. J. Sanyal, "Current and upcoming pharmacotherapy for non-alcoholic fatty liver disease," *Gut*, vol. 66, no. 1, pp. 180–190, 2016.

[26] D. E. Kleiner, E. M. Brunt, M. van Natta et al., "Design and validation of a histological scoring system for nonalcoholic fatty liver disease," *Hepatology*, vol. 41, no. 6, pp. 1313–1321, 2005.

[27] Z. Younossi and L. Henry, "Contribution of alcoholic and nonalcoholic fatty liver disease to the burden of liver-related morbidity and mortality," *Gastroenterology*, vol. 150, no. 8, pp. 1778–1785, 2016.

[28] K. Cusi, "Treatment of patients with type 2 diabetes and non-alcoholic fatty liver disease: current approaches and future directions," *Diabetologia*, vol. 59, no. 6, pp. 1112–1120, 2016.

[29] A. Ahmed, R. J. Wong, and S. A. Harrison, "Nonalcoholic fatty liver disease review: diagnosis, treatment, and outcomes," *Clinical Gastroenterology and Hepatology*, vol. 13, no. 12, pp. 2062–2070, 2015.

[30] J. K. C. Lau, X. Zhang, and J. Yu, "Animal models of non-alcoholic fatty liver disease: current perspectives and recent advances," *Journal of Pathology*, vol. 241, no. 1, pp. 36–44, 2017.

[31] H.-L. Zhang, X.-Y. Zheng, and J. Zhu, "Th1/Th2/Th17/Treg cytokines in Guillain–Barré syndrome and experimental autoimmune neuritis," *Cytokine & Growth Factor Reviews*, vol. 24, no. 5, pp. 443–453, 2013.

[32] E. M. Shevach, "Mechanisms of foxp3$^+$ T regulatory cell-mediated suppression," *Immunity*, vol. 30, no. 5, pp. 636–645, 2009.

[33] H. Lassmann, J. van Horssen, and D. Mahad, "Progressive multiple sclerosis: pathology and pathogenesis," *Nature Reviews Neurology*, vol. 8, no. 11, pp. 647–656, 2012.

[34] E. Bugianesi and M. Marietti, "Non-alcoholic fatty liver disease (NAFLD)," *Journal of Gastroenterology & Hepatology*, vol. 43, no. 10, pp. 360–368, 2016.

[35] D. Porras, E. Nistal, S. Martínez-Flórez et al., "Protective effect of quercetin on high-fat diet-induced non-alcoholic fatty liver disease in mice is mediated by modulating intestinal microbiota imbalance and related gut-liver axis activation," *Free Radical Biology and Medicine*, vol. 102, pp. 188–202, 2017.

[36] L. Probert, H.-P. Eugster, K. Akassoglou et al., "TNFR1 signalling is critical for the development of demyelination and the limitation of T-cell responses during immune-mediated CNS disease," *Brain*, vol. 123, no. 10, pp. 2005–2019, 2000.

[37] C. T. Weaver, R. D. Hatton, P. R. Mangan, and L. E. Harrington, "IL-17 family cytokines and the expanding diversity of effector T cell lineages," *Annual Review of Immunology*, vol. 25, no. 1, pp. 821–852, 2007.

Hindawi
Journal of Immunology Research
Volume 2019, Article ID 7657294, 15 pages
https://doi.org/10.1155/2019/7657294

Research Article

Overexpression of Tumor Necrosis Factor-Like Ligand 1 A in Myeloid Cells Aggravates Liver Fibrosis in Mice

Jinbo Guo,[1] Yuxin Luo,[1] Fengrong Yin,[1] Xiaoxia Huo,[1] Guochao Niu,[1] Mei Song,[1] Shuang Chen,[2] and Xiaolan Zhang[1]

[1]*Department of Gastroenterology, The Second Hospital of Hebei Medical University, Hebei Key Laboratory of Gastroenterology, Hebei Institute of Gastroenterology, Shijiazhuang, Hebei, China*
[2]*Department of Pediatric and Department of Biomedical Science, Cedars Sinai Medical Center, Los Angeles, USA*

Correspondence should be addressed to Xiaolan Zhang; xiaolanzh@126.com

Received 30 June 2018; Revised 26 October 2018; Accepted 15 November 2018; Published 14 February 2019

Guest Editor: Xiaoni Kong

Macrophages are the master regulator of the dynamic fibrogenesis–fibrosis resolution paradigm. TNF-like ligand 1 aberrance (TL1A) was found to be able to induce intestinal inflammation and fibrosis. Furthermore, significantly increased TL1A had been detected in liver tissues and mononuclear cells of patients with primary biliary cirrhosis (PBC). This study was to investigate the effect of myeloid cells with constitutive TL1A expression on liver fibrogenesis. We found that TL1A expressions in liver tissues and macrophages were significantly increased in mice with liver fibrosis induced by injection of carbon tetrachloride (CCl_4). TL1A overexpression in myeloid cells induced liver function injury, accelerated the necrosis and apoptosis of hepatocytes, recruited macrophages, and promoted activation of hepatic stellate cells (HSCs) and fibrosis. In vitro results of our study showed that TL1A overexpression in macrophages promoted secretion of platelet-derived growth factor-BB (PDGF-BB), tumor necrosis factor-α (TNF-α), and interleukin-1β (IL-1β). Culturing macrophages with TL1A overexpression could accelerate the activation and proliferation of primary HSCs. These results indicated that constitutive TL1A expression in myeloid cells exacerbated liver fibrosis, probably through macrophage recruitment and secretion of proinflammatory and profibrotic cytokines.

1. Introduction

Hepatic fibrosis is a common pathological consequence of chronic liver diseases, which is characterized by an extensive deposition of the extracellular matrix (ECM) mainly secreted by activated hepatic stellate cells (HSCs) [1]. HSC activation is the leading cause of liver fibrogenesis, and persistent chronic liver inflammation plays a vital role in HSC activation. It has been well known that macrophage plays an essential role during inflammatory, wound healing responses, as well as perpetuation of fibrosis [2]. In the stage of liver fibrogenesis, macrophages not only secrete proinflammatory and profibrotic cytokines which worsen hepatocellular damage and activate HSCs but also release chemokines such as C–C chemokine ligand 2 (CCL2) which recruit monocytes/macrophages in blood [3]. In recent years, the roles of macrophage in liver fibrosis have been emphasized. Chu et al. [4] found that C-C motif chemokine receptor 9-positive macrophages activated HSCs and promoted liver fibrosis, Lodder et al. [5] demonstrated that macrophage autophagy protected against liver fibrosis in mice, and He et al. [6] identified that myeloid-specific disruption of recombination signal-binding protein-Jkappa ameliorated hepatic fibrosis by attenuating inflammation.

Tumor necrosis factor-like ligand 1 A (TL1A), also known as vascular endothelial growth inhibitor (VEGI), is a recently recognized member of the TNF superfamily. TL1A is a transmembrane protein predominant in endothelial cells, playing a critical role in multiple chronic inflammatory processes [7]. It was illuminated that TL1A expressions were increased in serum, colonic tissues, and macrophages in mice with chronic colitis. Mice with constitutive TL1A expression

in myeloid cells (Kupffer cells and macrophages) exhibited enhanced intestinal and colonic inflammation and fibrosis compared to wild-type (WT) littermates [8, 9]. Furthermore, TL1A antibody could alleviate the inflammatory response and fibrosis of the colon [10]. Other than colonic disease, the roles of TL1A in organ fibrosis were also found in rheumatoid arthritis (RA), myocardial fibrosis, and idiopathic pulmonary fibrosis [11–13]. However, few studies focused on the roles of TL1A in liver fibrogenesis. Recently, it was reported that TL1A expression was markedly increased in the patients with primary biliary cirrhosis (PBC) [14]. It was mainly located in the Kupffer cells (KCs) and infiltrated macrophages in the liver, indicating that TL1A might play an important role in liver fibrosis. Pradere et al. [15] demonstrated that there was no contribution of dendritic cells to liver fibrosis development. Therefore, our research focused on the effect of TL1A overexpression in myeloid cells on liver fibrogenesis.

2. Materials and Methods

2.1. Mice and Experimental Models. The animal experiments were carried out in strict accordance with the recommendations in the Guide for the Care and Use of Laboratory Animals by the National Institutes of Health. The Chinese Academy of Sciences Animal Care and Use Committee gave approval for the animal experiments. Age-matched wild-type (WT) C57BL/6 mice and transgenic mice (Tg) with TL1A overexpression in myeloid cells (macrophages, dendritic cells), aged 6 to 8 weeks and weighted 18-21 g, were used in experiments, provided by the Experimental Animal Center of the Second Affiliated Hospital of Hebei Medical University (qualification certificate no. 911102) and by Cedars-Sinai Medical Center (America), respectively. Mice were genotyped by PCR with tail DNA as a template. Repeated administration of CCl_4 has become one of the most commonly used experimental models for inducing toxin-mediated liver fibrosis. CCl_4 is widely used as a solvent for dissolving nonpolar compounds, such as fats and oils. Olive oil was used to dissolve CCl_4 in our study. The WT mice and Tg mice were randomly divided into six groups (10 mice per group): Control/WT group, Oil/WT group, CCl_4/WT group, Control/Tg group, Oil/Tg group, and CCl_4/Tg group. The CCl_4/WT and CCl_4/Tg groups were injected intraperitoneally with 10% CCl_4 (5 μL/g, Sigma, St. Louis, MO) twice a week for 4 weeks to establish the hepatic fibrosis model. The Oil/WT and Oil/Tg groups were injected with olive oil, whereas the Control/WT group and Control/Tg group were injected with normal saline. All injections were given for 8 times. Mice were sacrificed at 48 h after the last injection. Blood was obtained from the retroorbital sinus of mice.

2.2. Detection of Liver Function. The levels of alanine aminotransferase (ALT), aspartate aminotransferase (AST), and total bilirubin (TBIL) in the serum were analyzed using an automatic biochemical analyzer (BECKMAN COULTER CX9, America).

2.3. Histological Analysis. Five μm-thick paraffin-embedded liver sections were stained with hematoxylin and eosin (H&E) and Sirius Red. The necrosis area and positive area were calculated by the software of Image-Pro Plus. For immunohistochemical analysis, liver specimens were fixed in 10% buffered formalin and incubated with α-smooth muscle actin antibody (α-SMA, Sigma) and Collagen1α1 antibody (Affinity, USA), followed by the appropriate secondary antibodies. For dual-color immunofluorescence, sections were incubated with F4/80 antibody (Abcam, USA), TL1A antibody (Affinity, USA), and fluorescent secondary antibodies. The positive areas showed the color of brown yellow. Immunohistochemical analysis was performed with the software of Image-Pro Plus for calculating integrate optical density (IOD). Apoptosis was assessed by the terminal deoxynucleotidyl transferase dUTP nick end labeling (TUNEL) assay (Promega, Madison, WI, USA, #G7132). The number of TUNEL-positive nuclei was determined in 10 randomly selected fields. To detect hydroxyproline, 100 mg of wet liver samples was subjected to acid hydrolysis according to the protocol in the Hydroxyproline Testing Kit (Nanjing Jiancheng Bioengineering Co. Ltd., China).

2.4. Cell Isolation and Culture. Bone marrow cells were obtained by flushing the femur and tibia. The culture medium contained 10% fetal bovine serum (FBS) and 10 ng/mL macrophage colony-stimulating factor (M-CSF). After culture for 10 d, 100 ng/mL lipopolysaccharide (LPS) and 25 ng/mL interferon-γ (IFN-γ) were added into the culture medium to activate and differentiate the bone marrow cells into bone marrow-derived macrophages (BMMs). The medium of BMMs would be collected 3 d after adding LPS and IFN-γ for cytokine detection or as conditioned medium (CM) for culture of HSCs. Peritoneal macrophages (PMs) were obtained by flushing the enterocoelia and cultured with culture medium (containing 10% of FBS) for 6 to 8 h. After PMs became adhesive, 100 ng/mL LPS and 25 ng/mL IFN-γ were added into the culture medium. The medium of PMs would be collected 3 d after adding LPS and IFN-γ for cytokine detection or as CM for culture of HSCs.

HSCs were isolated as previously described [16]. Briefly, the liver was digested by pronase and collagenase, followed by density gradient centrifugation. More than 95% of the purity of isolated HSCs was confirmed by immunostaining with anti-Desmin antibody. To detect the effect of macrophages on the activation and proliferation of HSCs, HSCs were cultured with CM from BMMs/PMs for 24 h. The groups would be deducted or added in some experiments according to the different aims. We divided the Control group (HSCs from C57BL/6 mice with DMEM), M-CSF + LPS + IFN-γ group (HSCs from C57BL/6 mice with DMEM containing M-CSF, LPS, and IFN-γ), CM/WT group (HSCs from C57BL/6 mice incubated in medium containing 40% CM from M-CSF + LPS + IFN-γ-stimulated BMMs from WT mice for 24 h), and CM/Tg group (HSCs from C57BL/6 mice incubated in medium containing 40% CM from M-CSF + LPS + IFN-γ-stimulated BMMs from Tg mice

Table 1: Oligonucleotide sequences used for Q-PCR analysis.

Transcript		Sequence (5′-3′ direction)	Product size
TL1A	F R	CGGGGAGACGACCAAACAAG AAGGAGAACGTGGCCCCAAGGTAG	160 bp
α-SMA	F R	TGCTGTCCCTCTATGCCTCT CGGCCAGCCAAGTCCAGACG	133 bp
Collagen1α1	F R	ACGGGAGGGCGAGTGCTGTG GGGGCCAGGCACGGAAACTC	277 bp
MMP-2	F R	TTTCCTGGGCAACAAGTATGAGAGC CTGGTCAGTGGCTTGGGGTATCCTC	618 bp
MMP-9	F R	CACCGCCAACTATGACCAGGAT GTTTAGAGCCACGACCATACAG	398 bp
F4/80	F R	CCTGCCACAACACTCTCGGAAGC TGGGCATGAGCAGCTGTAGGATC	191 bp
TNF-α	F R	CCGCGACGTGGAACTGGCAGAAG CCGATCACCCCGAAGTTCAGTAG	150 bp
Pro-IL-1β	F R	ACAGATGAAGTGCTCCTTCCA GTCGGAGATTCGTAGCTGGAT	73 bp
PDGF-BB	F R	GGGGCTTCCAGGAGTGATACCA GCCCGAGCAGGTCAGAACAAA	163 bp
TGF-β1	F R	CGCCAGTCCCCCAAGCCA CGCGGGTGACCTCTTTAGCATAG	155 bp
CCL2	F R	GCTGGAGAGCTACAAGAGGATCA TCTCTCTTGAGCTTGGTGACAAAA	78 bp
GAPDH	F R	TCGTCCCGTAGACAAAATGG TTGAGGTCAATGAAGGGGTC	132 bp

for 24 h). PM-based cells were divided into the Control group (HSCs from C57BL/6 mice with DMEM), LPS + IFN-γ group (HSCs from C57BL/6 mice with DMEM containing LPS and IFN-γ), CM/WT group (HSCs from C57BL/6 mice incubated in medium containing 40% CM from LPS + IFN-γ-stimulated PMs from WT mice for 24 h), and CM/Tg group (HSCs from C57BL/6 mice incubated in medium containing 40% CM from LPS + IFN-γ-stimulated PMs from Tg mice for 24 h).

2.5. Cell Immunofluorescence and ELISA Detection. The expressions of TL1A in macrophages were detected by immunofluorescence staining as previously described [5]. The immunofluorescence staining of F4/80 was used for macrophage identification. To detect the effect of high expression of TL1A cells on the activation of HSCs, HSCs were cultured with 40% conditioned medium (CM) from BMMs/PM. The expressions of α-SMA in HSCs were detected by immunofluorescence on the 2nd, 4th, and 6th day, respectively. TGF-β1, PDGF-BB, TNF-α, and IL-1β in serum and CM were detected under the recommended protocols. ELISA kits were purchased from Lianke Biotech Co. Ltd.

2.6. In Vitro Primary HSC Proliferation Assay. Cell proliferation was assessed by the Cell Counting Kit-8 (CCK-8) assay (Dojindo, Japan) according to the manufacturer's protocol. Briefly, cells were seeded in 96-well plates (2×10^3 cells/well) and incubated at 37°C with 5% CO_2 for 24 h. Then cells were incubated with 50% conditional medium from macrophages and cultured for an additional 24 h. For CCK-8 detection, 10 μL of CCK-8 solution was added into the wells and the cells were incubated at 37°C for 3 h. The absorbance (optical density (OD)) of cells was determined at 450 nm using a microplate reader.

2.7. Western Blot Analysis. Collagen 1α1, MMP-2, MMP-9, α-SMA, and CCL2 in liver tissues were detected. Preparation of protein extracts, electrophoresis, and subsequent blotting were performed as previously described [17]. The antibodies were all purchased from Sigma-Aldrich Co. LLC.

2.8. Real-Time Polymerase Chain Reaction (RT-PCR). RNA was extracted from liver tissue and cultured cells using the RNeasy and DNase Kits (QIAGEN, Valencia, CA, USA) and was reverse transcribed using the High-Capacity cDNA Reverse Transcription Kit (Applied Biosystems, Foster City, CA, USA). Quantitative RT-PCR was performed in duplicate with the QuantiTect SYBR Green PCR kit (QIAGEN, Mainz, Germany) using the LightCycler apparatus. QuantiTect primer assays (QIAGEN) were used to amplify the following mRNAs: TL1A, Collagen1α1, α-SMA, MMP-2, MMP-9, TGF-β1, PDGF-BB, TNF-α, pro-IL-1β, F4/80, and CCL2 in liver tissues and α-SMA in HSCs. Oligonucleotide sequences used for RT-PCR analysis could be found in Table 1.

2.9. Statistical Analysis. Statistical analyses were performed using SPSS for Windows version 22.0 (SPSS Inc., Chicago, Illinois) and were expressed as mean ± standard deviation of the mean (SEM). The one-way ANOVA, the Student-Newman-Keuls (SNK) test, the Nemenyi test, and the Kruskal-Wallis test were used to assess the differences between groups, as appropriate. The level of statistical significance was set at $p < 0.05$ for all the tests.

3. Results

3.1. TL1A Was Upregulated in Liver Tissues and Macrophages in Mice with Hepatic Fibrosis. The hepatic fibrosis model was established successfully verified by H&E and Sirius Red staining (Figure 1(a)). The RT-PCR was performed to analyze TL1A mRNA expression levels in liver tissues. There was no significant difference in terms of TL1A mRNA expression between the Control/WT group and Oil/WT group (1 ± 0.02 vs 1.29 ± 0.31, $p > 0.05$), and the expression of TL1A mRNA in the CCl_4/WT group was significantly higher than that in the Oil/WT group (3.57 ± 0.81 vs 11.5 ± 1.87, $p < 0.01$) (Figure 1(b)). As expected, TL1A expression in the CCl_4/Tg group was markedly increased, as compared with that in the Oil/Tg group (11.5 ± 1.87 vs 7.08 ± 1.15, $p < 0.01$). Furthermore, the expression of TL1A protein was also shown with significantly higher levels in the CCl_4/WT

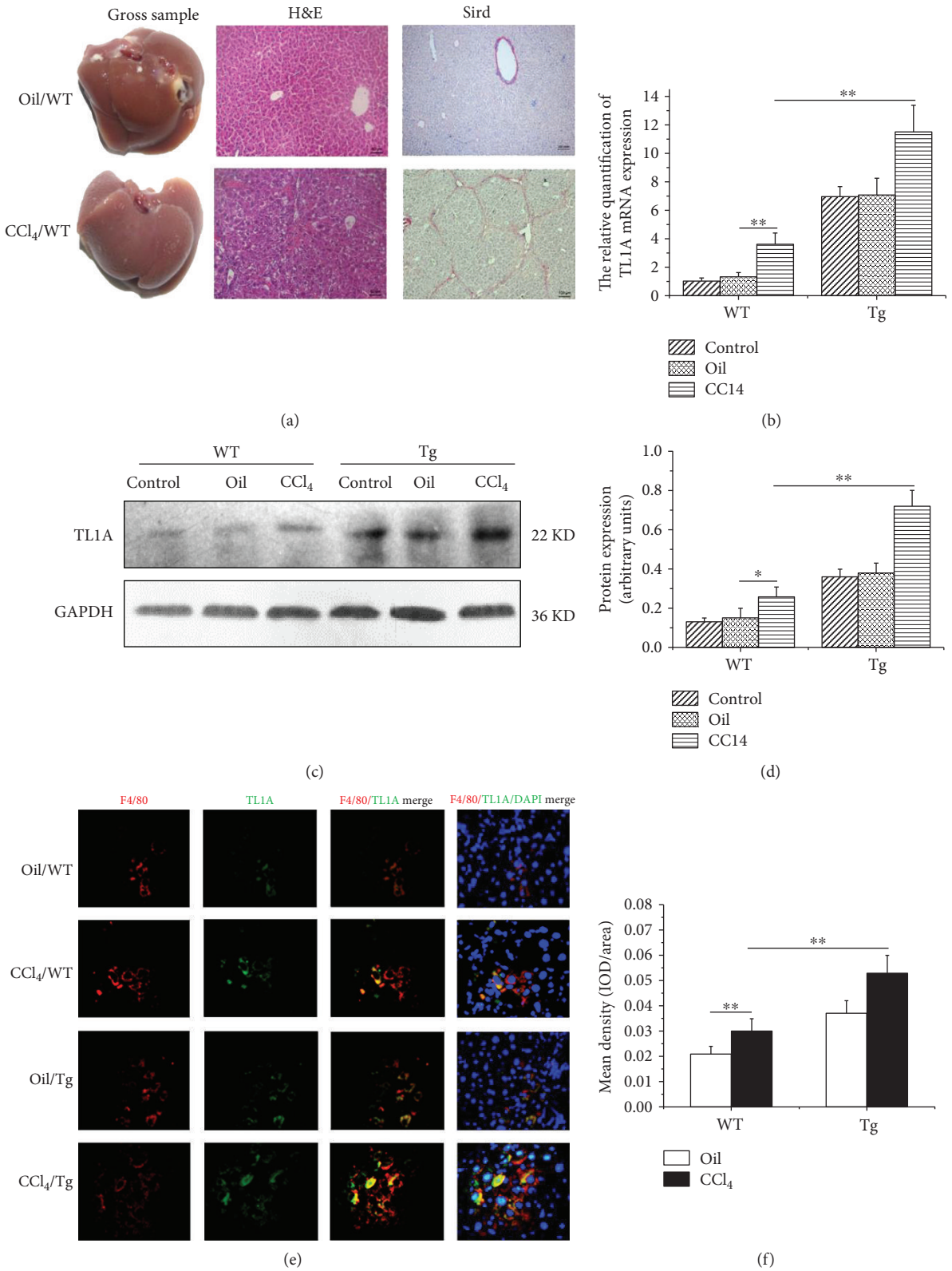

Figure 1: TL1A was upregulated in liver tissues and macrophages in mice with hepatic fibrosis. (a) The hepatic fibrosis model was established and verified by H&E and Sirius Red staining (200x). (b) The relative quantification of TL1A mRNA was measured by RT-PCR. (c, d) TL1A expression in the CCl_4/WT group was significantly higher than those in the Control/WT and Oil/WT group, which was markedly higher in the CCl_4/Tg group than that in the CCl_4/WT group detected by Western blot. (e, f) TL1A was discovered in macrophage through F4/80 and TL1A immunofluorescence double staining, which was markedly higher in the CCl_4/WT group than in the Oil/WT group and significantly higher in the CCl_4/Tg group than in the CCl_4/WT group. Data are expressed as mean ± SD, $^*p < 0.05$ and $^{**}p < 0.01$.

group (0.26 ± 0.05) and CCl_4/Tg group (0.72 ± 0.08) compared with the equivalent Oil/WT group (0.15 ± 0.05) and Oil/Tg group (0.38 ± 0.05) detected by Western blot (all $p < 0.01$) (Figures 1(c) and 1(d)). F4/80 is the surface marker of macrophages. TL1A expression in macrophages was detected by dual-color immunofluorescence. As shown in Figures 1(e) and 1(f), the red and green fluorescence areas represented the expressions of F4/80 and TL1A, respectively. The mean integral optical density (IOD) of coexpression areas was evaluated. The IOD of the CCl_4/WT group was obviously higher than that of the Oil/WT group (0.031 ± 0.005 vs 0.021 ± 0.003, $p < 0.01$). In addition, the IOD in the CCl_4/Tg group was significantly higher than that in the CCl_4/WT group (0.053 ± 0.007 vs 0.031 ± 0.005, $p < 0.01$). It was demonstrated that TL1A expression was increased in macrophages in liver tissue of mice with liver fibrosis.

3.2. High Expression of TL1A in Myeloid Cells Worsened Hepatic Inflammation. We next evaluated the consequences of overexpression of TL1A in myeloid cells on chronic liver injury in mice exposed to repeated injections of CCl_4 by studying the extent of hepatocyte necrosis and apoptosis. Analysis of liver histology in H&E staining showed that hepatocyte death was more pronounced in TL1A-Tg mice than in WT counterparts (Figures 2(a) and 2(b)). Moreover, the number of TUNEL-positive hepatocytes was significantly larger in CCl_4-exposed TL1A-Tg mice than in WT animals (46 ± 6 vs 28 ± 5, $p < 0.01$) (Figures 2(c) and 2(d)). The liver function test also showed that serum ALT, AST, and TBIL levels were markedly elevated in TL1A-Tg mice exposed to CCl_4 than in WT counterparts (ALT: 222.4 U/L ± 5.2 U/L vs 190.4 U/L ± 10.4 U/L, $p < 0.05$; AST: 70.8 U/L ± 19.7 U/L vs 220.5 U/L ± 19.3 U/L, $p < 0.05$; and TBIL: 9.09 μmol/L ± 0.9 μmol/L vs 6 μmol/L ± 1.07 μmol/L, $p < 0.05$) (Figure 2(e)).

3.3. Overexpression of TL1A in Myeloid Cells Aggravated Hepatic Fibrosis. We evaluated hepatic fibrosis by Sirius Red staining and hydroxyproline determination. The positive area of fibrous connective tissue showed obviously higher levels in TL1A-Tg mice compared with WT mice exposed to repeated injections of CCl_4 (1.85% ± 0.14% vs 1.43% ± 0.21%, $p < 0.05$) (Figure 3(a)). Hydroxyproline content was also markedly higher in TL1A-Tg mice than in WT counterparts following CCl_4 exposure (162 μg/g ± 14 μg/g vs 130 μg/g ± 10 μg/g, $p < 0.05$) (Figure 3(b)). Collagen1α1 is the major component of total collagen constituting the ECM, which is also used for measuring the degree of fibrosis. Collagen1α1 detected by RT-PCR, Western blotting, and immunohistochemical analysis showed similar tendencies with significantly higher levels in the CCl_4/Tg group compared with the CCl_4/WT group (Figures 3(c)–3(e)).

3.4. Overexpression of TL1A in Myeloid Cells Promoted the Activation of HSCs. The activation of HSCs is pivotal in hepatic fibrosis [1]. The α-SMA, as the marker of HSC activation, was detected. Immunostaining of liver sections showed that the levels of α-SMA increased remarkably in the livers of TL1A-Tg mice as compared with the Control after CCl_4 injection (Figure 4(a)), indicating that TL1A overexpression activated HSCs more extensively. The Western blotting and RT-PCR results of α-SMA also showed significantly higher levels in the CCl_4/Tg group compared with that in the CCl_4/WT group (Figures 4(b) and 4(c)). Gelatinases, including MMP-2 and MMP-9, were involved in the degradation of ECM components, which promoted the activation and proliferation of HSCs by degrading the basilar membrane. The expressions of MMP-2 and MMP-9 were detected by RT-PCR and Western blotting. The levels of MMP-2 protein and mRNA were significantly higher in the CCl_4/Tg group than in the CCl_4/WT group (Figures 4(d) and 4(e)). Similar tendency was observed in MMP-9 as in MMP-2 (Figures 4(f) and 4(g)).

3.5. Overexpression of TL1A in Myeloid Cells Enhanced Macrophage Recruitment. Several studies have emphasized the crucial role of infiltrating macrophages for the progression of liver inflammation and fibrosis in experimental mouse models [2, 4, 6]. Immunohistochemical staining and RT-PCR were used to detect F4/80 expression, which reflected macrophage infiltration. TL1A-Tg mice showed significantly increased liver macrophages after CCl_4-induced liver damage (Figures 5(a)–5(c)). Under conditions of liver damage, CCL2 promoted monocyte subset infiltration into the liver. We found markedly elevated CCL2 protein and mRNA in the CCl_4/Tg group compared with the CCl_4/WT group (Figures 5(d) and 5(e)).

3.6. Overexpression of TL1A in Myeloid Cells Increased the Expressions of PDGF-BB, TNF-α, and IL-1β in Serum, Liver Tissue, and Conditioned Medium for Macrophages. TGF-β1 is considered to accelerate liver fibrosis mainly secreted by activated HSCs, stimulating collagen gene transcription and inhibiting degradation of ECM [18]. As shown in Figure 6(a), TGF-β1 mRNA in liver tissue by RT-PCR was shown with a significantly higher level in the CCl_4/Tg group compared with the CCl_4/WT group (6.45 ± 1.35 vs 3.83 ± 1.23, $p < 0.05$) and the TGF-β1 level in serum by ELISA showed the similar tendency as well (253.6 pg/mL ± 11.4 pg/mL vs 184 pg/mL ± 17.3 pg/mL, $p < 0.05$). However, TGF-β1 concentration between CM for macrophages derived from TL1A-Tg mice and WT mice was not significantly different. PDGF-BB is essential for HSC proliferation which was secreted by macrophages, blood platelets, and activated HSCs. Remarkable elevations of PDGF-BB mRNA in liver tissue and PDGF-BB level in serum were observed in the CCl_4/Tg group compared with the CCl_4/WT group. Moreover, PDGF-BB concentration in CM for BMMs and PMs derived from TL1A-Tg mice was markedly higher than that from WT mice (Figure 6(b)). TNF-α and IL-1β are mostly produced by macrophages and infiltrated monocytes and involved in chronic hepatic inflammation and fibrosis. The results showed that TNF-α and IL-1β were remarkably higher in serum, liver tissue, and CM obtained from TL1A-Tg mice than WT mice (Figures 6(c) and 6(d)).

3.7. Overexpression of TL1A in Macrophages Promoted Activation and Proliferation of HSCs. We further evaluated

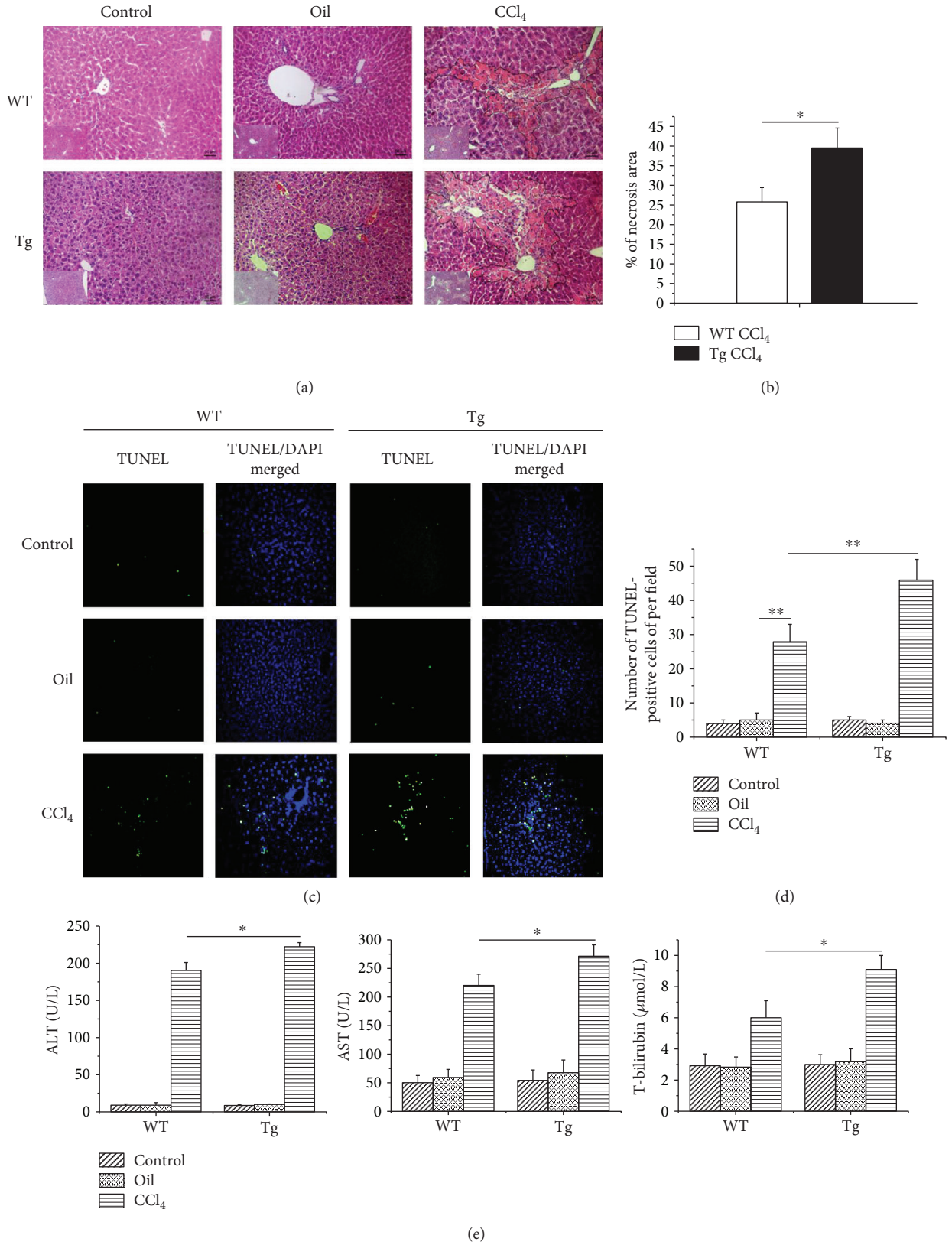

Figure 2: Constitutive TL1A expression on myeloid cells aggravated liver injury, hepatocyte necrosis, and apoptosis. (a, b) H&E staining showed that the hepatocyte necrosis area in the CCl_4/Tg group was significantly larger than that in the CCl_4/WT group (200x). (c, d) The apoptotic hepatocytes were significantly increased in the CCl_4/WT group than in the Control/WT group and Oil/WT group, and more apoptotic hepatocytes were found in the CCl_4/Tg group, compared with the CCl_4/WT group (200x). (e) Serum ALT, AST, and TBIL in the CCl_4/Tg group were significantly higher than those in the CCl_4/WT group. Data are expressed as mean ± SD, $^*p < 0.05$ and $^{**}p < 0.01$.

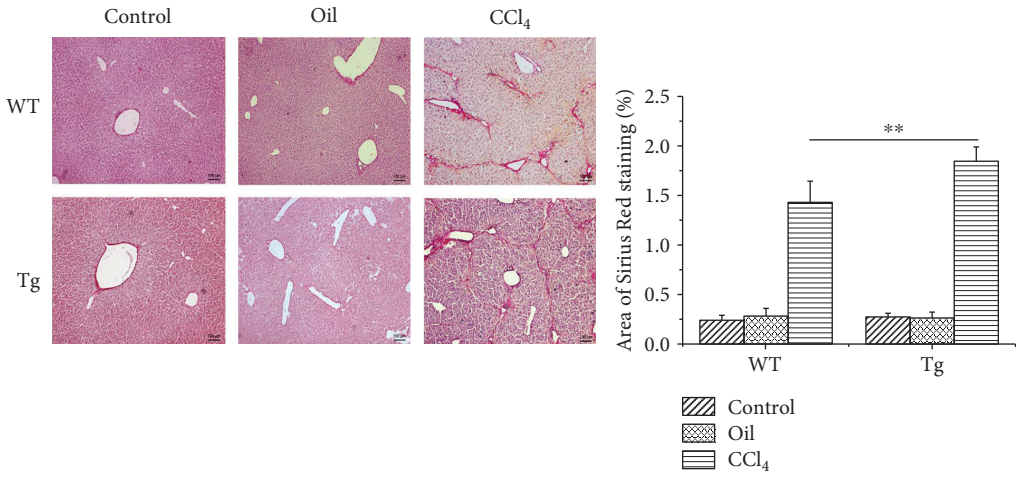

(a)

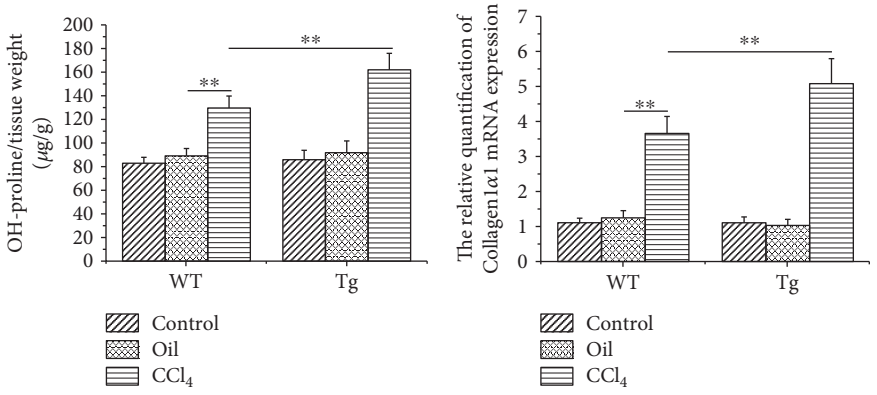

(b) (c)

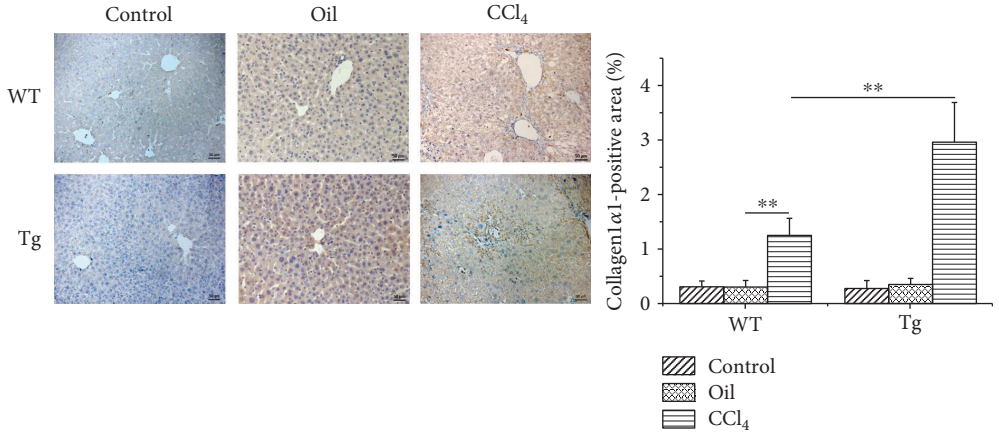

(d)

Figure 3: Continued.

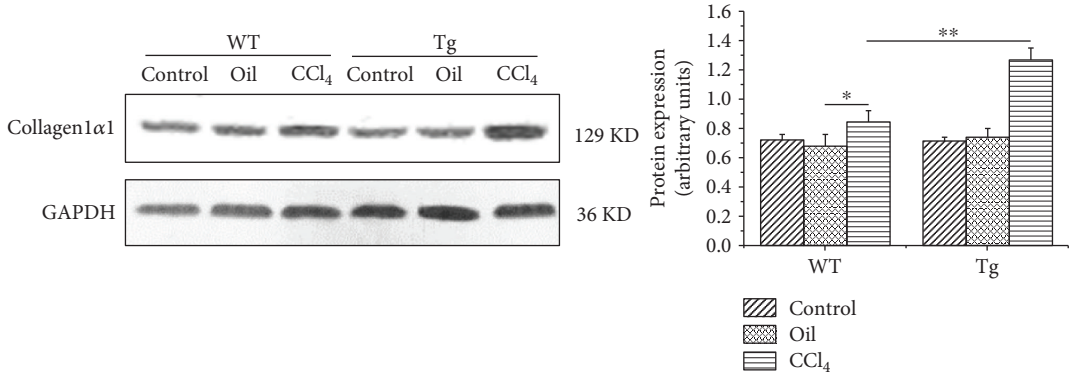

(e)

Figure 3: Constitutive TL1A expression on myeloid cells exacerbated liver fibrosis. (a) The Sirius Red-positive area in the CCl_4/Tg group was markedly larger than that in the CCl_4/WT group (200x). (b) The hydroxyproline content in the CCl_4/Tg group was higher than that in the CCl_4/WT group. (c–e) The Collagen1α1 expressions in the CCl_4/Tg group were remarkably higher than those in the CCl_4/WT group detected by RT-PCR, immunohistochemical staining (200x), and Western blot. Data are expressed as mean ± SD, $^*p < 0.05$ and $^{**}p < 0.01$.

the impact of TL1A overexpression of macrophage on the activation and proliferation of HSCs in conditioned medium experiments. The α-SMA as the marker of HSC activation was detected by immunofluorescence and RT-PCR. The protein expression of α-SMA in HSCs cultured with CM of BMMs isolated from TL1A-Tg mice showed no significant difference compared to that derived from WT mice on the 2nd and 6th day. However, the protein expression of α-SMA was significantly increased in HSCs cultured with CM of BMMs with TL1A overexpression on the 4th day (Figures 7(a) and 7(c)), which was consistent with the results of PMs (Figures 7(b) and 7(d)). The mRNA expression of α-SMA was significantly enhanced in HSCs exposed to CM collected from macrophages (BMMs and PMs, respectively) with TL1A overexpression on the 4th and 6th day (Figures 7(e) and 7(f)). The proliferation rate was detected by CCK-8 assay. As shown in Table 2, the proliferation rate of HSCs exposed to CM collected from macrophages (BMMs and PMs, respectively) with TL1A overexpression was significantly higher than that of HSCs exposed to CM collected from macrophages isolated from WT mice.

4. Discussion

The onset and progression of fibrosis is closely linked to chronic inflammatory reactions. Recruitment of immune cells such as macrophages and T-cells to the site of injury is an important event in the initiation of inflammation, as well as for wound healing and hepatic fibrosis [19]. TL1A is a tumor necrosis factor family member expressed by monocytes, macrophages, dendritic cells (DCs), and endothelial cells in response to stimulation by cytokines, immune complexes [20]. TL1A exerts pleiotropic effects on cell proliferation, activation, and differentiation of immune cells, which involves autoimmune diseases such as IBD, RA, and ankylosing spondylitis (AS). It has been proved that serum TL1A levels were significantly increased in patients with PBC, chronic hepatitis C, or autoimmune hepatitis. And its levels were significantly decreased in early-stage PBC patients after ursodeoxycholic acid (UDCA) treatment. TL1A was immunohistochemically located to biliary epithelial cells, Kupffer cells, blood vessels, and infiltrating mononuclear cells in the PBC liver [14]. However, the role of TL1A in liver fibrosis remains poorly understood.

To investigate the roles of TL1A in the process of hepatic fibrosis, the CCl_4-induced hepatic fibrosis model was established and a series of experiments at cellular, molecular, and protein levels were carried out in this study. Consistent with a previous clinical study that TL1A expression was found to be increased in serum and liver tissues in patients with PBC and advanced hepatitis cirrhosis [14], the present study showed that the expressions of TL1A protein and mRNA were significantly higher in mice with liver fibrosis than in the Control mice. In the clinical study on TL1A, mononuclear phagocytes are thought to be the main source of TL1A in patients with RA [21]. In the liver of PBC patients, TL1A expression is positive for infiltrating mononuclear cells as well. Therefore, we detected the TL1A expression in macrophages of liver tissues by dual-color immunofluorescence. As expected, TL1A was notably increased in macrophages after CCl_4-induced liver damage.

The key role of macrophages in promoting hepatic fibrogenesis has been demonstrated in a number of studies. In fibrotic mouse livers, the accumulation of macrophages greatly augments the local macrophage pool, perpetuates inflammation causing further hepatocyte injury, and activates fibrogenic HSCs [22, 23]. Furthermore, in CD11b-DTR mice, selective depletion of macrophages during ongoing injury led to a reduction of liver fibrosis [24]. Shih et al. [9] showed that an increased number of macrophages were found in transgenic mice with overexpression of TL1A in an intestinal fibrosis model. Similarly, we also found that the macrophages in hepatic tissues were significantly increased in TL1A-Tg mice than in WT mice, confirming that the high expression of TL1A in myeloid cells during hepatic fibrosis promoted the recruitment of macrophages to the liver. In the chronically inflamed liver, CCL2 is secreted mainly by injured hepatocytes, biliary epithelial

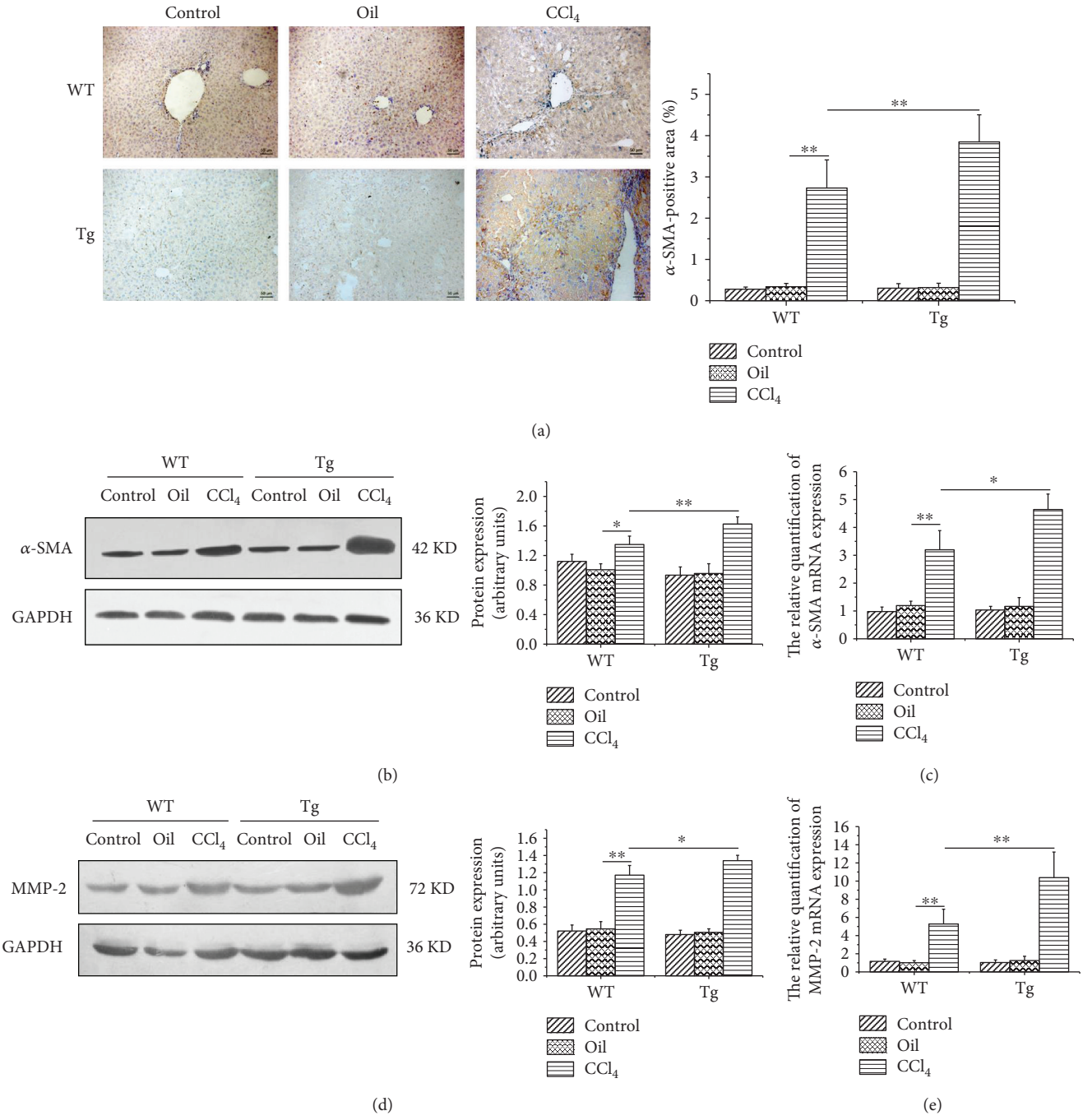

Figure 4: Continued.

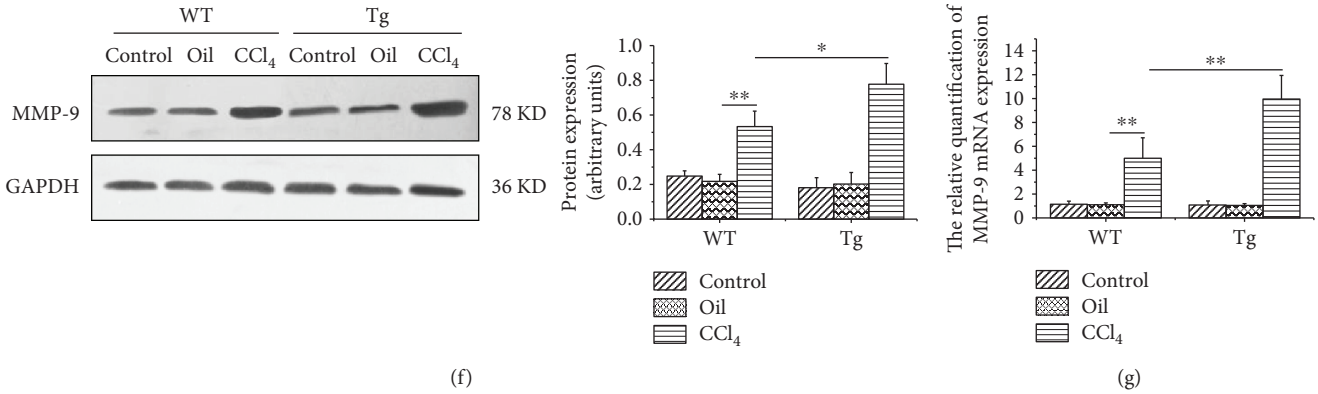

Figure 4: Constitutive TL1A expression on myeloid cells facilitated HSC activation and the expressions of MMP-2 and MMP-9. (a–c) The α-SMA expressions in the CCl_4/Tg group were markedly higher than that in the CCl_4/WT group detected by immunohistochemical staining (200x), Western blot, and RT-PCR. (d, e) The MMP-2 expressions in the CCl_4/Tg group were significantly increased than those in the CCl_4/WT group detected by Western blot and RT-PCR. (f, g) The MMP-9 expressions in the CCl_4/Tg group were notably increased than those in the CCl_4/WT group detected by Western blot and RT-PCR. Data are expressed as mean ± SD, $^{*}p < 0.05$ and $^{**}p < 0.01$.

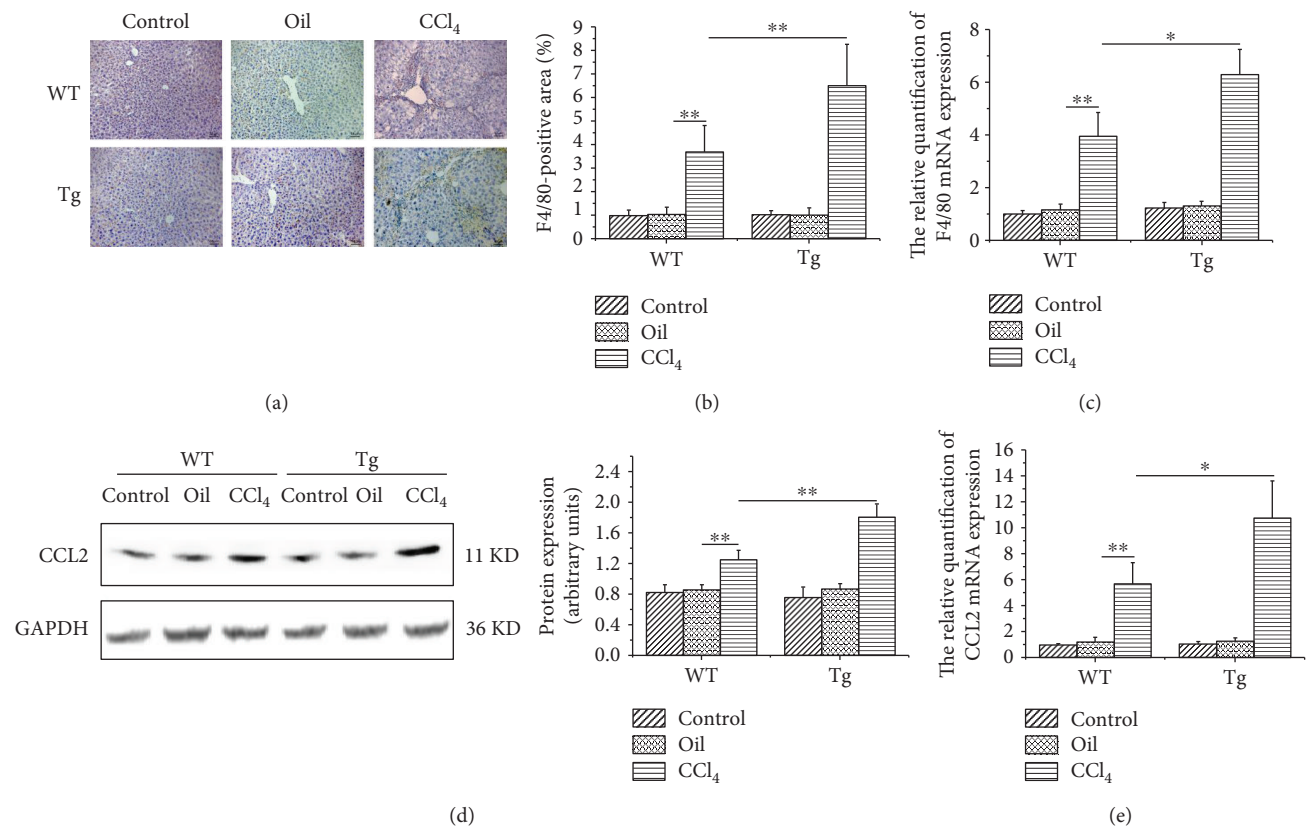

Figure 5: Constitutive TL1A expression on myeloid cells promoted macrophage recruitment to the liver. (a–c) The expression of F4/80 was significantly higher than that in the CCl_4/WT group detected by immunohistochemical staining (200x) and RT-PCR. (d, e) CCL2 in the CCl_4/Tg group was significantly higher than that in the CCl_4/WT group detected by Western blot and RT-PCR. Data are expressed as mean ± SD, $^{*}p < 0.05$ and $^{**}p < 0.01$.

cells, and HSCs [25], which is associated with the infiltration of macrophages [26]. In our study, CCL2 expression was significantly higher in TL1A-Tg mice than in the WT mice, indicating that the promotion of TL1A in the recruitment of macrophages might be related to the upregulation of CCL2 expression in liver tissues.

Chronic persistent inflammation is a main cause of liver fibrosis. Liver inflammation induces necrosis and apoptosis in liver cells and releases enzymes in liver cells. In this study, the levels of ALT, AST, and TBIL in serum were significantly higher in TL1A-Tg mice than in the WT mice with liver fibrosis, indicating that overexpression of TL1A in myeloid

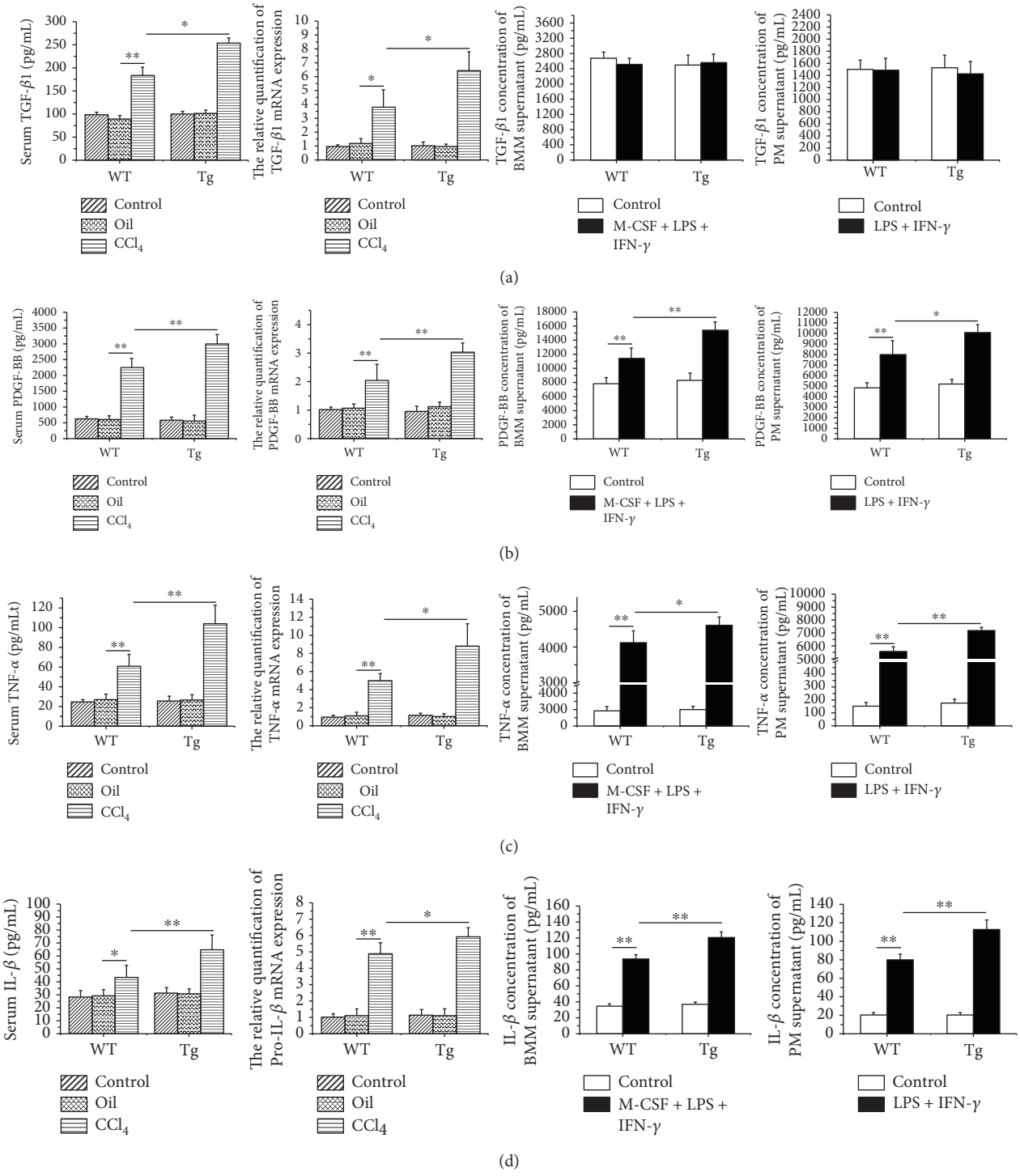

Figure 6: Constitutive TL1A expression on macrophages upregulated the PDGF-BB, TNF-α, and IL-1β in the serum, liver tissues, and macrophages. (a) The expression of TGF-β1 in serum, liver tissue, and the medium of BMMs and PMs was detected by ELISA and RT-PCR. Serum TGF-β1 in the CCl_4/Tg group were significantly higher than those in the CCl_4/WT group, and TGF-β1 mRNA in the CCl_4/Tg group were also higher than those in the CCl_4/WT group. But there was no statistical significance between the Tg group and WT group of CM derived from BMMs and PMs. (b, c, d) The expressions of PDGF-BB, TNF-α, and IL-1β in serum, liver tissue, and the medium of BMMs and PMs were detected by ELISA and RT-PCR, respectively. The cytokines in serum and mRNA in liver tissue in the CCl_4/Tg group were significantly higher than those in the CCl_4/WT group. And those derived from BMM and PM supernatant in the LPS + IFN-γ + M-CSF/Tg group were significantly higher than those in the LPS + IFN-γ + M-CSF/WT group. Data are expressed as mean $\pm$ SD, $^{*}p < 0.05$ and $^{**}p < 0.01$.

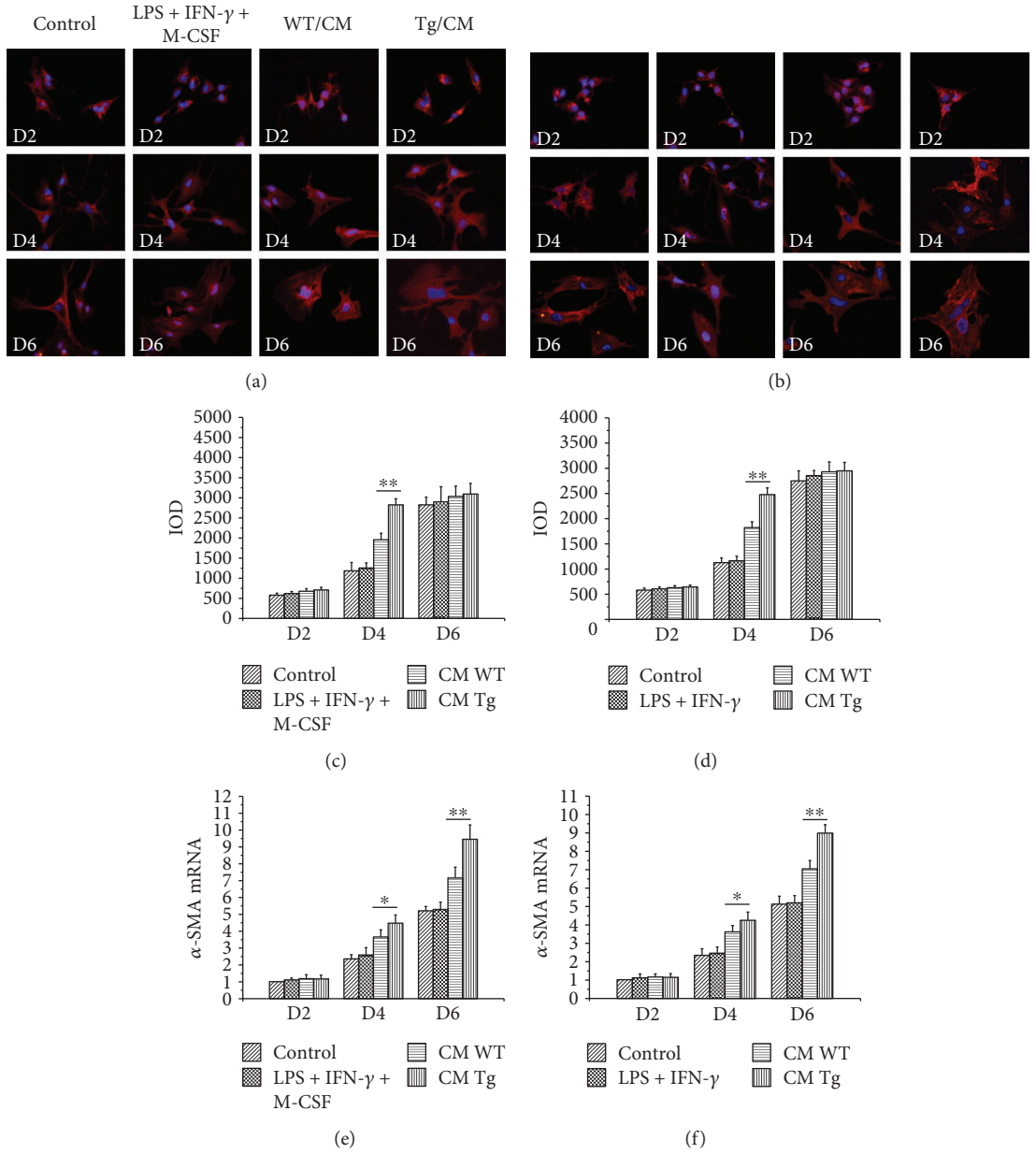

Figure 7: Constitutive TL1A expression on macrophages promoted the activation of HSCs. (a, c, e) The α-SMA expressions of HSCs cultured with BMM-derived CM in the CM/Tg group were markedly higher than those in the CM/WT group detected by immunofluorescence staining (400x) and RT-PCR. (b, d, f) The α-SMA expressions of HSCs cultured with PM-derived CM in the CM/Tg group were significantly higher than those in the CM/WT group detected by immunofluorescence staining (400x) and RT-PCR. Data are expressed as mean ± SD, $^{*}p < 0.05$ and $^{**}p < 0.01$.

Table 2: Effect of macrophages with high expression of TL1A on the proliferation of HSCs.

Cells	Groups			
	Control	LPS + IFN-γ + M-CSF	CM/WT	CM/Tg
BMMs	100.82 ± 8.48	100.54 ± 8.11	203.24 ± 10.50	246.21±8.34**
PMs	100.00 ± 8.13	101.63 ± 7.97	162.23 ± 9.40	194.29±6.82**

$^{**}p < 0.01$ vs the CM/WT group.

cells aggravated hepatocyte injury. Moreover, the H&E staining and TUNEL assay revealed that the necrotic area of hepatocyte was significantly wider and the apoptosis number of hepatocytes was significantly larger in TL1A-Tg mice than in WT counterparts. The above results confirmed that overexpression of TL1A in myeloid cells caused more necrosis

and apoptosis of liver cells, as well as more severe liver injury and inflammation.

HSCs are typically found in the space of Disse in a quiescent state, which are activated to myofibroblasts expressing α-SMA by several stimuli such as cytokines and inflammatory mediators. Collagen1α1, a major component of total collagen constituting the ECM, are mainly released by activated HSCs. The results revealed that α-SMA and Collagen1α1 expressions were markedly higher in TL1A-Tg mice than in WT mice detected by immunohistochemical staining, RT-PCR, and Western blot assay. Hydroxyproline is a special amino acid of collagen, and its content can reflect the total collagen condition and assess the degree of fibrosis. In this study, we found that the content of hydroxyproline in TL1A-Tg mice treated with CCl4 was significantly higher than that in WT mice. It was also confirmed that the TL1A-Tg mice were combined with more severe liver fibrosis by Sirius Red staining. In the early stage of hepatic fibrogenesis, gelatinases, including MMP-2 and MMP-9, are involved in the degradation of ECM components around HSCs. Previous studies have demonstrated that MMP-2 and MMP-9 promote the activation and proliferation of HSCs by degrading the basilar membrane and increase the biological activity of IL-1β and TGF-β [27, 28]. Infiltrated macrophages are the important source of MMP-2 and MMP-9 [29]. Our study confirmed significantly higher levels of MMP-2 and MMP-9 in TL1A-Tg mice than in WT counterparts. The above results demonstrated that overexpression of TL1A in myeloid cells accelerated HSC activation, which might be related to macrophage recruitment, thereby releasing more MMP-2 and MMP-9.

The important mechanism for macrophages to participate in liver fibrosis is to secrete a series of proinflammatory and profibrotic factors, which can act on the HSCs to induce a profibrotic phenotype. Specifically, macrophages can produce and activate the archetypal profibrotic cytokine TGF-β1, which acts to increase myofibroblast ECM and TIMP-1 production [30]. Additionally, hepatic macrophages can produce PDGF-BB (a potent stimulator of myofibroblast proliferation), IL-1β, and TNF-α (proinflammatory cytokines) to perpetuate the proinflammatory pro-fibrotic stimulus [31]. Our study showed that overexpression of TL1A in myeloid cells promoted the expression of TGF-β1 in liver tissues and serum, whereas TL1A had no effect on the secretion of TGF-β1 by macrophages themselves. We speculated that the TGF-β1 was secreted primarily by M2 macrophages, which in our study involved M1 macrophages. The others including PDGF-BB, TNF-α, and IL-1β were obviously increased in serum and liver tissues in TL1A-Tg mice compared to WT mice. Consistent with in vivo experiment, the concentration of PDGF-BB, TNF-α, and IL-1β in CM of macrophages derived from TL1A-Tg mice was markedly higher than that from equivalent WT mice. The results in this study confirmed that TL1A was able to enhance the proinflammatory factor (PDGF-BB, TNF-α, and IL-1β) secretion of macrophages directly. We cultured primary HSCs with CM of macrophages with or without TL1A overexpression, respectively, to further investigate the activation and proliferation of HSCs. Previous studies had confirmed cultured HSCs with macrophage medium promoting the activation and proliferation of HSCs [5, 15, 32], which accorded with the present results. Additionally, macrophages with overexpression of TL1A accelerated the activation and proliferation more obviously.

In conclusion, overexpression of TL1A in myeloid cells could accelerate the process of hepatic fibrosis, worsen the liver function, promote macrophages recruitment, upregulate the levels of PDGF-BB, TNF-α, and IL-1β in liver tissues and macrophages, and further stimulate the activation and proliferation of HSCs.

Data Availability

The data used to support the findings of this study are available from the corresponding author upon request.

Disclosure

In addition, an earlier version of this paper has been presented as conference abstract in Abstracts of the 26th Annual Conference of APASL, February 15-19, 2017, Shanghai, China.

Conflicts of Interest

The authors declare that there is no conflict of interest regarding the publication of this paper.

Authors' Contributions

Jinbo Guo was involved in the study's conception, design, data acquisition, analysis, and interpretation and drafted the manuscript. Yuxin Luo contributed to data acquisition and the laboratory work. Fengrong Yin and Xiaoxia Huo contributed to conception, design, and revision of the manuscript. Guochao Niu contributed to data acquisition and data analysis. Mei Song contributed to culture cells. Shuang Chen contributed to the revision of the manuscript. Xiaolan Zhang contributed to the design and interpretation, drafted, and critically revised the manuscript. All authors gave final approval and agreed to be accountable for all aspects of the work.

Acknowledgments

This study was supported by grants from the Natural Science Foundation of Hebei Province (Grant no. H2018206363) and the Foundation of the Second Hospital of Hebei Medical University (Grant no. 2h2017052). And the authors are grateful for the donation of transgenic mice by David Q. Shih and Stephan R. Targan from the Cedars-Sinai Medical Center, USA. The authors wish to thank Libo Zheng for important suggestions about the experiment.

References

[1] M. M. Ni, Y. R. Wang, W. W. Wu et al., "Novel insights on Notch signaling pathways in liver fibrosis," *European Journal of Pharmacology*, vol. 826, pp. 66–74, 2018.

[2] O. Krenkel, T. Puengel, O. Govaere et al., "Therapeutic inhibition of inflammatory monocyte recruitment reduces steatohepatitis and liver fibrosis," *Hepatology*, vol. 67, no. 4, pp. 1270–1283, 2018.

[3] P. Ramachandran and J. P. Iredale, "Macrophages: central regulators of hepatic fibrogenesis and fibrosis resolution," *Journal of Hepatology*, vol. 56, no. 6, pp. 1417–1419, 2012.

[4] P. S. Chu, N. Nakamoto, H. Ebinuma et al., "C-C motif chemokine receptor 9 positive macrophages activate hepatic stellate cells and promote liver fibrosis in mice," *Hepatology*, vol. 58, no. 1, pp. 337–350, 2013.

[5] J. Lodder, T. Denaës, M. N. Chobert et al., "Macrophage autophagy protects against liver fibrosis in mice," *Autophagy*, vol. 11, no. 8, pp. 1280–1292, 2015.

[6] F. He, F. C. Guo, Z. Li et al., "Myeloid-specific disruption of recombination signal binding protein Jκ ameliorates hepatic fibrosis by attenuating inflammation through cylindromatosis in mice," *Hepatology*, vol. 61, no. 1, pp. 303–314, 2015.

[7] Y. Aiba and M. Nakamura, "The role of TL1A and DR3 in autoimmune and inflammatory diseases," *Mediators of Inflammation*, vol. 2013, Article ID 258164, 9 pages, 2013.

[8] R. Barrett, X. Zhang, H. W. Koon et al., "Constitutive TL1A expression under colitogenic conditions modulates the severity and location of gut mucosal inflammation and induces fibrostenosis," *The American Journal of Pathology*, vol. 180, no. 2, pp. 636–649, 2012.

[9] D. Q. Shih, R. Barrett, X. Zhang et al., "Constitutive TL1A (TNFSF15) expression on lymphoid or myeloid cells leads to mild intestinal inflammation and fibrosis," *PLoS One*, vol. 6, no. 1, article e16090, 2011.

[10] D. Q. Shih, L. Zheng, X. Zhang et al., "Inhibition of a novel fibrogenic factor Tl1a reverses established colonic fibrosis," *Mucosal Immunology*, vol. 7, no. 6, pp. 1492–1503, 2014.

[11] M. Al-Azab, J. Wei, X. Ouyang et al., "TL1A mediates fibroblast-like synoviocytes migration and Indian Hedgehog signaling pathway via TNFR2 in patients with rheumatoid arthritis," *European Cytokine Network*, vol. 29, no. 1, pp. 27–35, 2018.

[12] J. E. McLaren, C. J. Calder, B. P. McSharry et al., "The TNF-like protein 1A–death receptor 3 pathway promotes macrophage foam cell formation in vitro," *The Journal of Immunology*, vol. 184, no. 10, pp. 5827–5834, 2010.

[13] E. Bouros, E. Filidou, K. Arvanitidis et al., "Lung fibrosis-associated soluble mediators and bronchoalveolar lavage from idiopathic pulmonary fibrosis patients promote the expression of fibrogenic factors in subepithelial lung myofibroblasts," *Pulmonary Pharmacology & Therapeutics*, vol. 46, pp. 78–87, 2017.

[14] Y. Aiba, K. Harada, A. Komori et al., "Systemic and local expression levels of TNF-like ligand 1A and its decoy receptor 3 are increased in primary biliary cirrhosis," *Liver International*, vol. 34, no. 5, pp. 679–688, 2014.

[15] J.-P. Pradere, J. Kluwe, S. de Minicis et al., "Hepatic macrophages but not dendritic cells contribute to liver fibrosis by promoting the survival of activated hepatic stellate cells in mice," *Hepatology*, vol. 58, no. 4, pp. 1461–1473, 2013.

[16] I. Mederacke, D. H. Dapito, S. Affò, H. Uchinami, and R. F. Schwabe, "High-yield and high-purity isolation of hepatic stellate cells from normal and fibrotic mouse livers," *Nature Protocols*, vol. 10, no. 2, pp. 305–315, 2015.

[17] T. Aoyama, K. Ikejima, K. Kon, K. Okumura, K. Arai, and S. Watanabe, "Pioglitazone promotes survival and prevents hepatic regeneration failure after partial hepatectomy in obese and diabetic KK-A^y mice," *Hepatology*, vol. 49, no. 5, pp. 1636–1644, 2009.

[18] X. Cai, Z. Li, Q. Zhang et al., "CXCL6-EGFR-induced Kupffer cells secrete TGF-β1 promoting hepatic stellate cell activation via the SMAD2/BRD4/C-MYC/EZH2 pathway in liver fibrosis," *Journal of Cellular and Molecular Medicine*, vol. 22, no. 10, pp. 5050–5061, 2018.

[19] K. R. Karlmark, H. E. Wasmuth, C. Trautwein, and F. Tacke, "Chemokine-directed immune cell infiltration in acute and chronic liver disease," *Expert Review of Gastroenterology & Hepatology*, vol. 2, no. 2, pp. 233–242, 2008.

[20] D. Q. Shih, L. Y. Kwan, V. Chavez et al., "Microbial induction of inflammatory bowel disease associated gene TL1A (TNFSF15) in antigen presenting cells," *European Journal of Immunology*, vol. 39, no. 11, pp. 3239–3250, 2009.

[21] M. A. Cassatella, G. P. da Silva, I. Tinazzi et al., "Soluble TNF-like cytokine (TL1A) production by immune complexes stimulated monocytes in rheumatoid arthritis," *The Journal of Immunology*, vol. 178, no. 11, pp. 7325–7333, 2007.

[22] C. Baeck, A. Wehr, K. R. Karlmark et al., "Pharmacological inhibition of the chemokine CCL2 (MCP-1) diminishes liver macrophage infiltration and steatohepatitis in chronic hepatic injury," *Gut*, vol. 61, no. 3, pp. 416–426, 2012.

[23] J. Ehling, M. Bartneck, X. Wei et al., "CCL2-dependent infiltrating macrophages promote angiogenesis in progressive liver fibrosis," *Gut*, vol. 63, no. 12, pp. 1960–1971, 2014.

[24] J. S. Duffield, S. J. Forbes, C. M. Constandinou et al., "Selective depletion of macrophages reveals distinct, opposing roles during liver injury and repair," *The Journal of Clinical Investigation*, vol. 115, no. 1, pp. 56–65, 2005.

[25] G. A. Ramm, "Chemokine (C-C motif) receptors in fibrogenesis and hepatic regeneration following acute and chronic liver disease," *Hepatology*, vol. 50, no. 5, pp. 1664–1668, 2009.

[26] F. Marra, R. DeFranco, C. Grappone et al., "Increased expression of monocyte chemotactic protein-1 during active hepatic fibrogenesis: correlation with monocyte infiltration," *The American Journal of Pathology*, vol. 152, no. 2, pp. 423–430, 1998.

[27] E. Olaso, K. Ikeda, F. J. Eng et al., "DDR2 receptor promotes MMP-2–mediated proliferation and invasion by hepatic stellate cells," *The Journal of Clinical Investigation*, vol. 108, no. 9, pp. 1369–1378, 2001.

[28] T. H. Vu and Z. Werb, "Matrix metalloproteinases: effectors of development and normal physiology," *Genes & Development*, vol. 14, no. 17, pp. 2123–2133, 2000.

[29] M. J. P. Arthur, A. Stanley, J. P. Iredale, J. A. Rafferty, R. M. Hembry, and S. L. Friedman, "Secretion of 72 kDa type IV collagenase/gelatinase by cultured human lipocytes. Analysis of gene expression, protein synthesis and proteinase activity," *Biochemical Journal*, vol. 287, no. 3, pp. 701–707, 1992.

[30] K. R. Karlmark, R. Weiskirchen, H. W. Zimmermann et al., "Hepatic recruitment of the inflammatory $Gr1^+$ monocyte subset upon liver injury promotes hepatic fibrosis," *Hepatology*, vol. 50, no. 1, pp. 261–274, 2009.

[31] T. A. Wynn and L. Barron, "Macrophages: master regulators of inflammation and fibrosis," *Seminars in Liver Disease*, vol. 30, no. 3, pp. 245–257, 2010.

[32] N. Nieto, "Oxidative-stress and IL-6 mediate the fibrogenic effects of rodent Kupffer cells on stellate cells," *Hepatology*, vol. 44, no. 6, pp. 1487–1501, 2006.

Hindawi
Journal of Immunology Research
Volume 2019, Article ID 8983903, 10 pages
https://doi.org/10.1155/2019/8983903

Research Article

Immunomodulatory Effects of Combination Therapy with Bushen Formula plus Entecavir for Chronic Hepatitis B Patients

Long-Shan Ji,[1] Qiu-Tian Gao,[2] Ruo-Wen Guo,[1] Xin Zhang,[1] Zhen-Hua Zhou,[3] Zhuo Yu,[3] Xiao-Jun Zhu,[3] Ya-Ting Gao,[1] Xue-Hua Sun,[3] Yue-Qiu Gao,[1] and Man Li[1]

[1]*Laboratory of Cellular Immunity, Institute of Clinical Immunology, Shanghai Key Laboratory of Traditional Chinese Clinical Medicine, Shuguang Hospital, Affiliated to Shanghai University of Traditional Chinese Medicine, China*
[2]*The Pennington School, 112 W Delaware Ave, Pennington, NJ 08534, USA*
[3]*Department of Hepatopathy, Shuguang Hospital, Affiliated to Shanghai University of Traditional Chinese Medicine, Shanghai 201203, China*

Correspondence should be addressed to Man Li; liman121000@126.com

Received 29 June 2018; Accepted 3 October 2018; Published 13 January 2019

Guest Editor: YinYing Lu

Aim. To compare the clinical efficacy of the combination therapy with Bushen formula (BSF) plus entecavir (ETV) in naïve chronic hepatitis B (CHB) patients and that in CHB patients with partial virological response to ETV and explore the relevant immunoregulatory mechanism. *Materials and Methods*. Two hundred and twenty CHB patients were enrolled in the historical prospective cohort study. Patients were categorized into a treatment group (T-Group: combination therapy with BSF plus ETV) and a control group (C-Group: ETV). Patients in T-Group and C-Group were grouped into T1/C1 (treatment-naïve patients) and T2/C2 (patients with partial virological response to ETV). Biochemical assessment, viral load quantitation, and HBV markers were tested. Chinese medicine symptom complex score was evaluated and recorded as well. In addition, peripheral blood mononuclear cells were separated from blood samples in 56 patients and 11 healthy donors. The frequencies of Th1, Treg, and dendritic cells (DCs) and expression levels of PD-1/PD-L1 were examined by flow cytometry. *Results*. In treatment-naïve CHB patients, complete viral suppression rates in HBeAg(−) patients were higher than those in HBeAg(+) patients in both T and C groups. In patients with partial virological response to ETV, the rate of HBsAg decline $\geq 20\%$ in HBeAg(+) patients of T2-Group was higher than that in HBeAg(+) patients of C2-Group. A significant reduction of Chinese medicine symptom complex score was only observed in T-Group. The study of mechanism showed that, compared with healthy controls, Th1 and DC frequencies were decreased in all CHB patients, while Treg frequency was increased only in treatment-naïve patients. In addition, compared with healthy controls, PD-1 expression levels on Th1 and Treg were increased in all patients and PD-L1 expression levels on DCs were increased only in treatment-naïve patients. In treatment-naïve patients, the combination therapy with BSF plus ETV increased Th1 and DC frequencies and decreased Treg frequency, which was correlated with HBsAg decline. In addition, in patients with partial virological response to ETV, the combination therapy downregulated PD-L1 levels on DCs and the frequency of Treg, which was related with HBsAg decline. *Conclusions*. In patients with partial virological response to ETV, HBeAg(+) patients tend to achieve ideal effects after the combination therapy with BSF plus ETV, which may correlate with the decrease of Treg frequency and the downregulation of PD-L1 levels on DCs.

1. Introduction

Hepatitis B is a potentially serious liver disease caused by hepatitis B virus (HBV), which is a general worldwide health problem. According to the reports from WTO, an estimate of 240 million people are persistently infected with HBV and more than 686,000 people die each year due to severe complications caused by hepatitis B, including cirrhosis and liver cancer [1]. The prevalence of hepatitis B is the utmost in sub-Saharan Africa and East Asia. In China, hepatitis B is one of the top 3 infectious diseases reported by the Ministry of Health [2] and 300,000 people die from HBV-related liver

Table 1: Baseline characteristics of 220 CHB patients [$M(Q1 - Q3)$].

Group (n)	Sex (M/F)	Age (years)	ALT (U/l)	AST (U/l)	HBV DNA (lgIU/ml)	HBsAg (lgIU/ml)	HBeAg(+) (n)
T1 (59)	38/21	37.0 (32.0–42.0)	40.0 (26.0–73.0)	33.0 (26.0–60.0)	5.48 (4.31–7.05)	3.64 (3.22–4.12)	38
T2 (42)	26/16	41.5[a] (37.3–46.8)	22.0[b] (14.5–28.2)	24.0[e] (19.0–30.5)	N.A.	3.37 (2.92–4.00)	18
C1 (78)	59/19	34.0 (29.0–41.0)	53.0[c] (34.0.0–93.0)	42.0[f] (29.0–65.0)	7.11 (5.17–7.95)	3.99 (3.34–4.16)	54
C2 (41)	36/5	39.0 (33.0–52.5)	25.0[d] (22.0–28.8)	25.0[g] (22.0–28.8)	N.A.	3.56 (3.10–3.80)	19

Notes: M: male; F: female; ALT: alanine aminotransferase; AST: aspartate transaminase; HBV: hepatitis B virus; HBsAg: hepatitis B surface antigen; HBeAg: hepatitis B e antigen. [a]$P < 0.05$, compared with C1; [b]$P < 0.05$, compared with T1; [c]$P < 0.05$, compared with T1; [d]$P < 0.05$, compared with C1; [e]$P < 0.05$, compared with T1; [f]$P < 0.05$, compared with T1; [g]$P < 0.05$, compared with C1.

diseases each year [3], which holds 40%–50% of the total HBV-related deaths worldwide [4].

Peginterferon and nucleoside/nucleotide analogues are currently approved first-line treatments of chronic HBV infection and have been applied for many years [5, 6]. However, these therapies can hardly cure most chronic hepatitis B (CHB) patients and merely suppress HBV replication. Therefore, most CHB patients have to be treated for a long period of life. The outcome of HBV infection depends on the multifaceted interactions between HBV and the host immune system. Innate and adaptive immunities play a pivotal role in HBV clearance [7, 8]. The efficient suppression of HBV replication depends on a combination of innate immunity, adaptive cellular, and humoral immunities [9]. It has been shown that the cellular immune responses, including CTL, Th1, Treg, and DC, are crucial for governing HBV replication [10]. It was also shown that Th1/Th2 imbalance [11], as well as the increased expression of Treg and Th17 cells, acts as an independent risk factor in CHB patients [12].

There has been an obvious growth in the practice of ?complementary and alternative medicine in recent years worldwide. As an important complementary and alternative medicine, traditional Chinese medicine (TCM) based on syndrome differentiation has been used widely to treat CHB patients in Asian countries [13, 14]. The theory and practice of immunology and infectious diseases were actually applied in TCM from earlier dynasties. Beginning around 1950, scientific evaluation of herb materials used for treatment of viral hepatitis was accepted in China and Japan. Current studies from Gao et al. showed that the combination therapy with peginterferon plus Chinese herbs exerted combinatorial effects in HBeAg(+) CHB patients [15]. Our previous studies showed that BSF had beneficial effects on CHB patients with mildly elevated ALT (1–2 times ULN) by reducing serum ALT and HBV DNA levels, which was relevant with the decrease of $CD4^+CD25^+$ T cell frequency and the increase of the IFN-γ level in $CD4^+$ T cells [16]. Entecavir (ETV) is one of first-line antiviral agents for treating CHB patients. However, some patients are likely to exhibit a suboptimal response to ETV. Currently, there are limited data on how to approach these patients. In this study, the anti-HBV efficacies of the combination therapy with BSF plus ETV in naive CHB patients and that in CHB patients with partial virological response to ETV were compared and then the underlying immunoregulatory mechanisms were explored, which will be helpful for clinicians to make effective treatment project for CHB patients.

2. Materials and Methods

2.1. Subjects. This is a historical prospective cohort study. Two hundred and twenty CHB patients with liver and kidney Yin deficiency and damp-heat syndrome were enrolled in this study. The inclusion criteria were patients enrolled for antiviral therapy [17], ETV monotherapy, or combination therapy with BSF plus ETV applied. The normal control group comprised 11 healthy donors who had no evidence of exposure to HBV (HBV surface antigen- (HBsAg-) negative, anti-HBc-negative). All subjects were given written informed consent before the blood samples were collected. This study was conducted in accordance with the ethics principles of the Declaration of Helsinki and regulation of clinical trial. This study was approved by the IRB of Shuguang Hospital affiliated to Shanghai University of TCM.

2.2. Drugs and Grouping. According to the treatment project, 220 patients were categorized into treatment-naïve patients and patients with partial virological response to ETV. Then, treatment-naïve patients were categorized into T1-Group and C1-Group, and patients with partial response to ETV were categorized into T2-Group and C2-Group. Patients in T1-Group and T2-Group were administrated with BSF combined with ETV, and patients in C1-Group and C2-Group were administrated with ETV. The above patients were followed up for 6 months. Eleven healthy controls were enrolled as a healthy control group. Peripheral blood mononuclear cells (PBMCs) were separated from blood of 56 patients and 11 healthy controls. The baseline characteristics of 220 CHB patients are shown in Table 1. There were significant differences among four groups in basic levels including ALT, AST, HBV DNA, HBsAg, and HBeAg.

2.3. Drugs. The BSF granule (oral agents, one dose) [16] was prepared and provided by Jiangyin River Pharmaceutical Company Limited and included Astragalus mongholicus, Fructus Ligustri Lucidi, Longspur epimedium, ClawVine, Rhizoma Picrorhizae, and Pericarpium citri reticulatae viride, and the manufacturing procedure involved boiling, filtering, plastering, and drying. Patients were given 0.5 mg/day ETV and 4.5 g/day BSF granule, oral administration.

2.4. Serum Viral Load HBV Serum Markers and ALT/AST Determination. Serum HBV DNA levels in CHB patients were tested with real-time PCR using a LightCycler PCR system (FQD-33A) with a lower limit of approximately 1000 viral genome copies/ml. The results were considered

abnormal when HBV DNA was >1000 copies/ml. Serum HBsAg and HBeAg levels were detected by ELISA with commercially available kits (Sino-American Biotechnology Company).

The serum ALT/AST levels were assayed by DXC 800 Fully Auto Biochemistry Analyzer, at the Department of Clinical Laboratory, Shuguang Hospital affiliated to Shanghai University of TCM, China. The results were considered abnormal when ALT was >40 U/l.

2.5. Isolation of PBMCs. PBMCs were isolated from heparinized blood by standard density gradient centrifugation with Lympholyte-H (Cedarlane) according to manufacturer's protocol. The cell viability was over 90%, as assessed by the trypan blue exclusion test.

2.6. Flow Cytometry (FCM). The CD8-FITC, IFN-γ-APC-Cy7, CD4-FITC, CD25-APC, FoxP3-PE, lin1-FITC, CD11c-APC, HLA-DR-PE, PD-1-PE-cy7, and PD-L1-PE-cy7 mAbs were obtained from BioLegend (BioLegend, CA). Fix and Perm kit was obtained from BioLegend (BioLegend, CA). Intracellular cytokine production was detected by four-color flow cytometry [16, 18], as described in previous papers. What need to be illustrated is that PMA-ionomycin stimulation causes the prominent alternation of cell membrane expression of CD4, so $CD3^+CD8^-$ cells are identified as $CD4^+$ T cells [19]. After washing with PBS, the stained cells were analyzed by flow cytometry.

2.7. Symptom Scores. According to our previous paper [20], symptoms in CHB patients were recorded before and after treatment including hypodynamia, shortness of breath, sweating, palpitations, poor appetite, insomnia, characteristics of urine and stools, appearance of tongue, and characteristics of pulse. Then, Chinese medicine symptom complex score was calculated by recording the severity of the symptoms: none, light, moderate, and severe were scored as 0, 1, 2, and 3, respectively.

2.8. Statistical Analysis. Statistical analyses were performed using SPSS statistics software (version 21.0, IBM Inc., NY, USA). Nonparametric test of rank transformation was used to compare the differences of intergroups and intragroups. The measurement data and numeration data were statistically analyzed with the t-test and Fisher exact tests χ^2, respectively. All statistical tests were a two-sided test; $P < 0.05$, and the difference was statistically significant.

3. Results

3.1. The Clinical Effects of the Combination Therapy with BSF plus ETV in CHB Patients. In treatment-naïve patients, the HBV DNA-negative rates in HBeAg(−) patients were markedly higher than those in HBeAg(+) patients in both T and C groups (Figure 1(a)). In patients with partial virological response to ETV, HBeAg-negative rate in T2-Group was higher than that in C2-Group, although there was no significant difference (Figure 1(b)), and the rate of HBsAg decline ≥ 20% in HBeAg(+) patients of T2-Group was higher than that in HBeAg(+) patients of C2-Group (Figure 1(c)). The above results reminded us that the combination therapy with BSF plus ETV may be a potential effective therapy for patients with partial response to ETV.

3.2. The Combination Therapy with BSF plus ETV Improved Chinese Medicine Symptoms in CHB Patients. Chinese medicine symptom complex score is the conventional method for assessing the adjustment of Chinese medicine symptoms. Damp-heat stasis syndrome and liver and kidney Yin deficiency syndrome, classified as excess syndrome and deficiency syndrome, respectively, are the common syndromes in CHB patients [21]. The standard for Chinese medicine symptom complex score is based on guiding principles for clinical research on new drugs of TCM. In this study, our results showed that Chinese medicine symptom complex score in CHB patients was decreased from 14.57 ± 4.83 to 8.45 ± 1.09 after treatment in T-Group and there was no significant difference after treatment in C-group, as shown in Table 2, which suggested that BSF substantially improved Chinese medicine symptoms in CHB patients.

3.3. Characteristics of Peripheral Th1, Treg, and DCs in CHB Patients. PBMCs from 11 healthy controls, 32 treatment-naïve patients, and 24 patients with partial virological response to ETV were separated, and the frequencies of Th1, Treg, and DCs were analyzed by flow cytometry. Baseline characteristics of the above subjects are shown in Tables 3 and 4. Phenotypic characterization of circulating Th1, Treg, and DCs and expression levels of PD-1 and PD-L1 on immune cells in CHB patients are shown in Figure 2.

Results showed that the frequencies of $CD4^+$ T cells, Th1, and DCs in all patients were markedly lower than those in healthy controls ($P < 0.01$) and the frequencies of $CD4^+$ T cells and DCs in patients with partial virological response to ETV were obviously higher than those in treatment-naïve patients ($P < 0.05$ or $P < 0.01$). In addition, the Treg frequency in treatment-naïve patients was higher than that in the normal group ($P < 0.05$) and the Treg frequency in patients with partial virological response to ETV was significantly lower than that in treatment-naïve patients ($P < 0.01$), as shown in Table 5.

PD-1 expression levels on Th1 and Treg in all patients were notably higher than those in normal controls ($P < 0.05$ or $P < 0.01$), and PD-1 levels on Th1 in patients with partial virological response to ETV were higher than those in treatment-naïve patients ($P < 0.05$). PD-L1 levels on DCs in treatment-naïve patients were markedly higher than those in normal controls ($P < 0.01$) as shown in Table 5.

3.4. Correlation between the Changes of Immune Cell Subsets and HBsAg Decline after the Combination Therapy with BSF plus ETV. The clinical effects of the combination therapy on CHB patients were analyzed, and the results showed that there was no difference in the viral response rate between T1-Group and C1-Group. However, the rate of HBsAg decline ≥ 10% in T1-Group was higher than that in C1-Group, although the difference was not statistically significant ($P > 0.05$), as shown in Table 5.

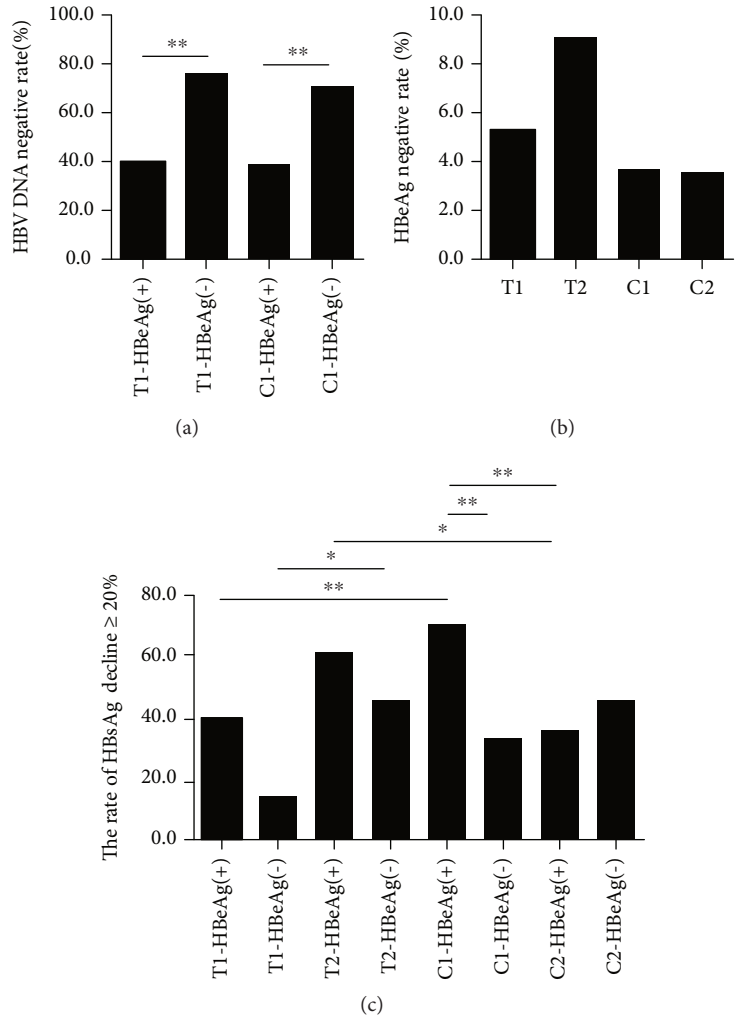

Figure 1: The clinical effects of the combination therapy with BSF plus ETV in CHB patients. Serum HBV DNA, HBsAg, and HBeAg levels were evaluated before and after treatment. (a) HBV DNA-negative rates in HBeAg(−) patients were higher than those in HBeAg(+) patients in both T1-Group and C1-Group. (b) HBeAg-negative rate in T2-Group was higher than that in C2-Group, although there was no significant difference. (c) The rate of HBsAg decline ≥ 20% in HBeAg(+) patients in T2-Group was higher than that in HBeAg(+) patients in C2-Group.

Table 2: Changes of Chinese medicine symptom complex score in CHB patients ($x \pm s$).

Group	Case	Before treatment	After treatment
T-Group	101	14.57 ± 4.83	$8.45 \pm 1.09^*$
C-Group	119	14.90 ± 4.25	12.38 ± 2.50

Note: $^*P < 0.05$, compared with that before treatment

To explore the immunological mechanism of the combination therapy for treating CHB, the relationships between the changes of frequencies of Th1, Treg, and DCs and HBsAg decline were analyzed. In treatment-naive patients with HBsAg decline ≥ 10%, Th1 and DC frequencies were increased and Treg frequency was decreased in T1-Group, but Th1 and DC frequencies were decreased in C1-Group (Figures 3(a) and 3(b)). In patients with partial virological response to ETV with HBsAg decline ≥ 10%, Treg frequency was decreased in T2-Group, but Treg frequency was not changed and Th1 frequency was decreased in C2-Group (Figures 3(c) and 3(d)). The above results showed that the combination therapy with BSF plus ETV contributed to the increase of Th1 and DC frequencies and the decrease of Treg frequency in treatment-naïve patients and the therapy contributed to the decrease of Treg in patients with partial virological response to ETV. Therefore, the mechanism of the combination therapy with BSF plus ETV downregulating HBsAg levels may lie in regulating frequencies of immune cell subsets.

In addition, the correlations between PD-1 and PD-L1 expression levels on immune cell subsets and HBsAg decline were analyzed. In treatment-naive patients with HBsAg decline ≥ 10%, the PD-1 level on Treg and the PD-L1 level on DCs were decreased both in C1-Group and T1-Group (Figures 4(a) and 4(b)). In patients with partial virological response to ETV with HBsAg ≥ 10%, PD-1 levels on Th1

Table 3: Baseline characteristics of CHB patients and normal controls [$M(Q1 - Q3)$].

Group	Sex M	Sex F	Age (years)	ALT (U/l)	HBV DNA (log10IU/ml)	HBeAg (log10COI)	HBsAg (log10IU/ml)
Normal controls	6	5	25.0 (25.0–26.0)	17.5 (10.6–35.8)	N.A.	N.A.	N.A.
Treatment-naïve patients	26	6	41.0 (35.3–48.5)	57.5 (41.5–96.0)	6.63 (5.13–7.48)	2.28 (0.00–2.88)	3.85 (3.31–4.01)
Patients with partial virological response to ETV	21	3	32.0 (28.3–37.5)	34.0 (23.3–47.0)	N.A.	1.98 (0.23–3.09)	3.85 (3.41–4.14)

Table 4: Comparative analysis of peripheral Th1, Treg, and DCs between healthy controls and CHB patients [$M(Q1 - Q3)$].

	Healthy controls	Treatment-naïve patients	Patients with partial response to ETV
$CD4^+$ T cell of PBMCs (%)	60.30 (56.50–64.60)	16.20^{**} (7.30–56.40)	$49.30^{**,\triangle}$ (46.00–63.30)
Th1 of $CD4^+$ T cells (%)	60.40 (58.80–62.2)	10.50^{**} (8.70–14.1)	10.00^{**} (3.10–14.20)
Treg of $CD4^+$ T cells (%)	4.00 (3.09–5.18)	12.68^{*} (4.98–41.48)	$2.88^{\triangle\triangle}$ (0.50–8.32)
DCs of PBMCs (%)	0.29 (0.27–0.40)	0.07^{**} (0.01–0.13)	$0.15^{**,\triangle\triangle}$ (0.10–0.22)
PD-1 on Th1 (MFI)	437.5 (412.8–452.8)	523.1^{*} (423.2–639.4)	$594.5^{**,\triangle\triangle}$ (553.0–696.4)
PD-1 on Treg (MFI)	1118.2 (856.8–2628.9)	7164.1^{**} (3022.4–25690.6)	5677.8^{*} (1372.3–11151.0)
PD-L1 on DCs (MFI)	2010.30 (1683.5–2852.5)	3432.1^{**} (2080.6–6800.3)	2530.3 (1764.3–4098.9)

Notes: $^{*}P < 0.05$, compared with healthy controls; $^{**}P < 0.01$, compared with healthy controls; $^{\triangle}P < 0.05$, compared with treatment-naïve patients; $^{\triangle\triangle}P < 0.01$, compared with treatment-naïve patients.

and Treg were decreased in C2-Group and the PD-L1 level on DCs was decreased in T2-Group (Figures 4(c) and 4(d)). The above results showed that the decrease of PD-L1 on DCs may be correlated with HBsAg decline in patients with partial virological response to ETV after the combination therapy.

4. Discussion

According to current guidelines, the goal of therapy for CHB is to improve quality of life and survival by preventing the progression of the disease to cirrhosis, decompensated cirrhosis, end-stage liver disease, HCC, and death and ETV and tenofovir can be confidently used as first-line monotherapies [6, 17]. However, there are more and more patients who experienced treatment failure to different nucleotide analogue treatment regimens. So what should they do? This is a growing problem in daily clinical practice. One meta-analysis showed that Kushenin combined with nucleotide analogues increased the frequency of loss of serum HBeAg, HBeAg seroconversion, undetectable HBV-DNA levels, and ALT normalization compared with nucleotide analogues [22]. One recent study showed that the liver histological response rate in the combination treatment group with Diwu Yanggan capsule plus ETV was significantly higher than that in the group with ETV (71.43% versus 22.22%; $P = 0.036$) after 48 weeks of treatment [23]. In our study, the clinical effects of combination therapy with BSF plus ETV on CHB patients were observed. The results showed that the combination therapy contributed to the decrease of HBsAg in patients with partial response to ETV, which gave us a hint that the patients who experienced treatment failure to different nucleotide analogue treatment regimens may be administrated with the combination therapy.

According to the TCM symptoms of CHB patients, liver-gallbladder damp-heat and liver stagnation-spleen deficiency are the most abundant syndromes [21]. BSF was composed of Astragalus mongholicus, Fructus Ligustri Lucidi, Longspur epimedium, ClawVine, Rhizoma Picrorhizae, and Pericarpium citri reticulatae viride, which was used to tonify kidney, invigorate spleen, and remove dampness. Our results showed that Chinese medicine symptom complex score in CHB patients was significantly decreased after the combination therapy. In addition, the rate of HBsAg decline $\geq 20\%$ in HBeAg(+) patients of T2-Group was higher than that in HBeAg(+) patients of C2-Group, which suggested that the combination therapy with BSF plus ETV contributed to the decrease of HBsAg, especially in patients with partial response to ETV. So, the combination therapy with BSF plus ETV will provide a potential treatment method for patients with partial response to ETV.

It has been shown that the components of BSF have a broad-spectrum immunoregulatory effects. Astragalus polysaccharides might suppress Treg activity by binding TLR4 on Treg and trigger a shift of Th2 to Th1 with the activation of $CD4^+$ T cells in burned mice with P. aeruginosa infection [24]. The supercritical fluid extract of Fructus Ligustri Lucidi regulated the expression of Th1- and Th2-related cytokines, elevated the levels of IL-2, IFN-γ, and TNF-α produced by Th1 lymphocytes, and decreased the levels of IL-4 and IL-10 produced by Th2 lymphocytes [25]. Our results showed that the combination therapy with BSF plus ETV

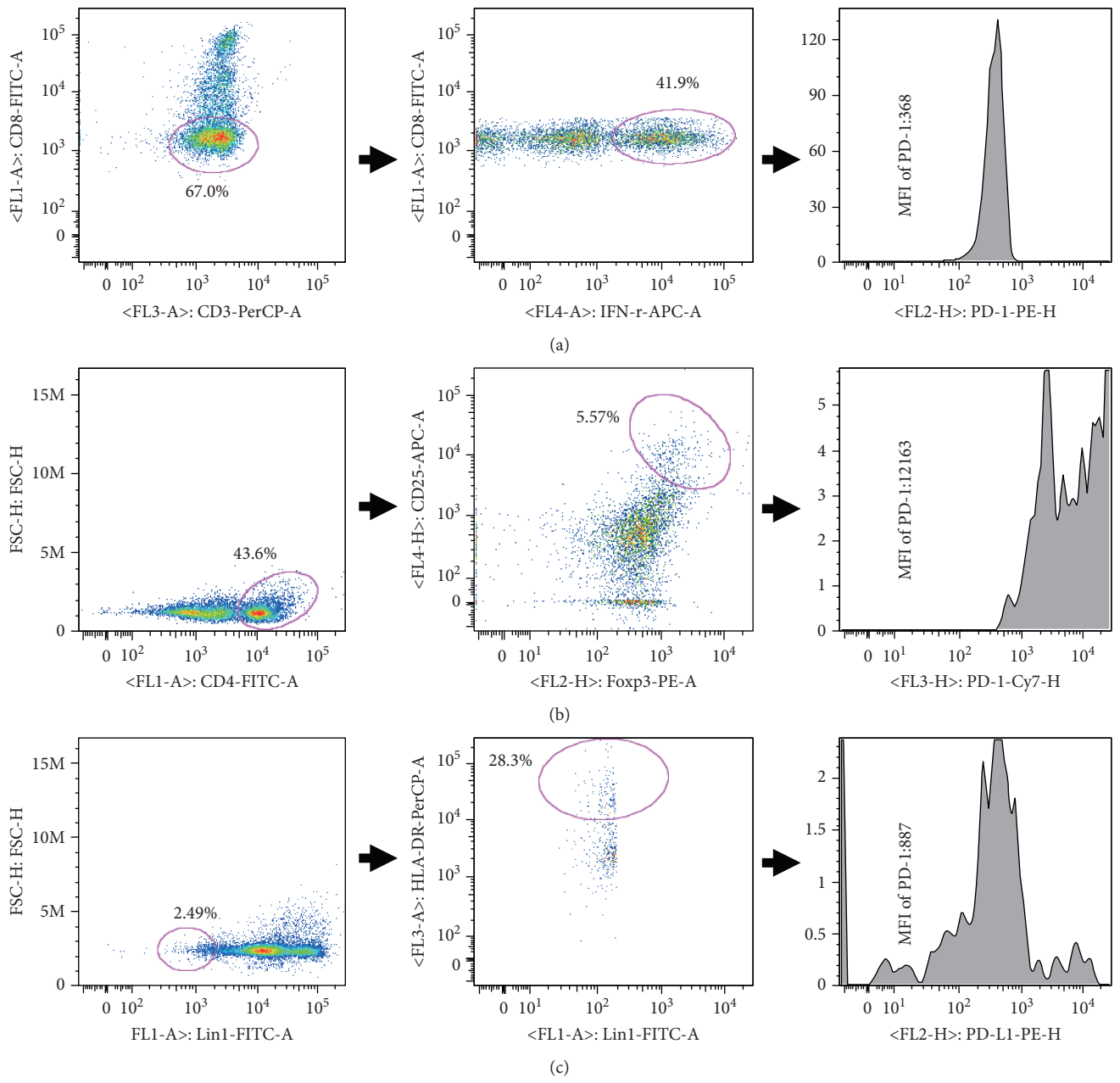

Figure 2: Phenotypic characterization of circulating Th1, Treg, and DCs and expression levels of PD-1 and PD-L1 on immune cells in CHB patients. This panel is based on surface markers CD3, CD8, IFN-γ, CD4, CD25, Foxp3, LIN1, HLA-DR, PD-1, and PD-L1. All cells were gated using a FSC-H/SSC-A dot plot. (a) Among PBMCs, $CD3^+CD8^-$ cells were defined as $CD4^+$ T cells. Among $CD4^+$ T cells, $CD4^+IFN\text{-}\gamma^+$ cells were Th1 and then MFI of PD-1 expression on Th1 was analyzed. (b) Among PBMCs, $CD4^+$ cells were gated and then $CD4^+CD25^+FoxP3^+$ cells were defined as Treg. MFI of PD-1 expression on Treg was analyzed. (c) Among PBMCs, $LIN1^-$ cells were gated and then $LIN1^-HLA\text{-}DR^+$ cells were defined as DCs. MFI of PD-L1 expression on DCs was analyzed.

Table 5: Clinical effects of the combination therapy with ETV plus BSF.

Group	Case	Sex (F/M)	Age (years) [$M(Q1 - Q3)$]	Rates of virological response (%)	Rates of HBsAg decline ≥ 10% (%)
T1-Group	18	14/4	46.0 (36.5–49.5)	94.4	66.7
T2-Group	7	5/2	32.0 (29.0–36.0)	/	57.1
C1-Group	14	12/2	43.0 (37.5–49.5)	85.7	50.0
C2-Group	17	16/1	32.0 (27.0–42.0)	/	52.9

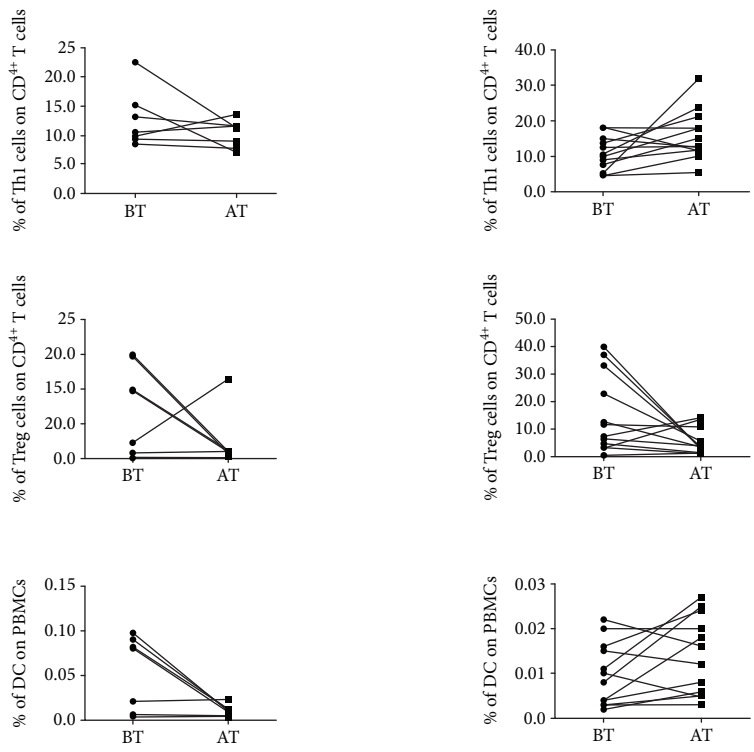

(a) Patients with HBsAg decline ≥ 10% in C1-Group (b) Patients with HBsAg decline ≥ 10% in T1-Group

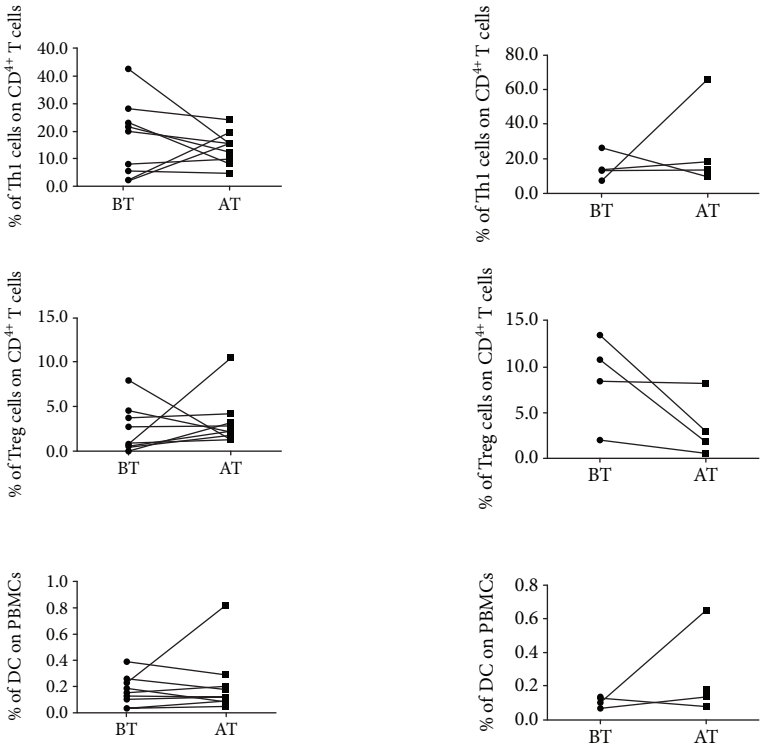

(c) Patients with HBsAg decline ≥ 10% in C2-Group (d) Patients with HBsAg decline ≥ 10% in T2-Group

Figure 3: Relationship between the changes of frequencies of Th1, Treg, and DCs and HBsAg decline. (a) Changes of frequencies of Th1, Treg, and DCs were analyzed before and after treatment in patients with HBsAg decline ≥ 10% of C1-Group. BT: before treatment; AT: after treatment. (b) Changes of frequencies of Th1, Treg, and DCs were analyzed before and after treatment in patients with HBsAg decline ≥ 10% of T1-Group. (c) Changes of frequencies of Th1, Treg, and DCs were analyzed before and after treatment in patients with HBsAg decline ≥ 10% of C2-Group. (d) Changes of frequencies of Th1, Treg, and DCs were analyzed before and after treatment in patients with HBsAg decline ≥ 10% of T2-Group.

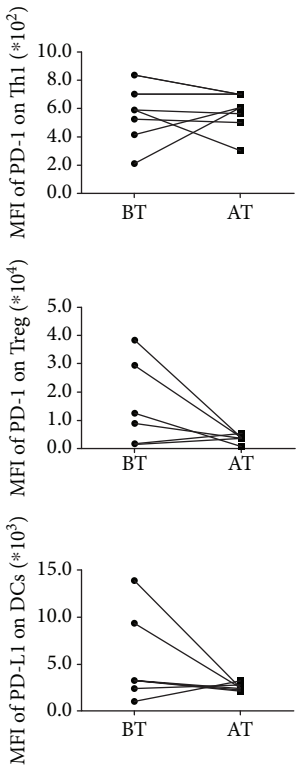

(a) Patients with HBsAg decline ≥ 10% in C1-Group

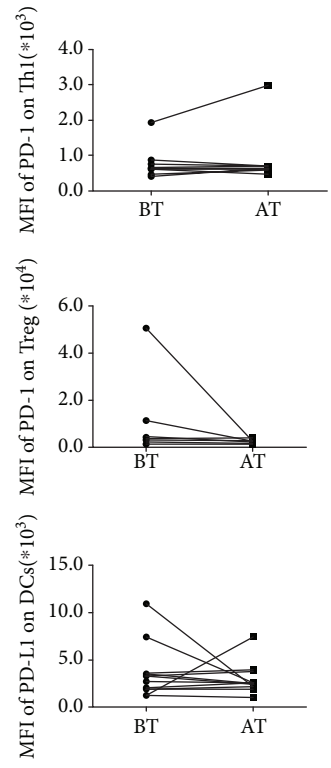

(b) Patients with HBsAg decline ≥ 10% in T1-Group

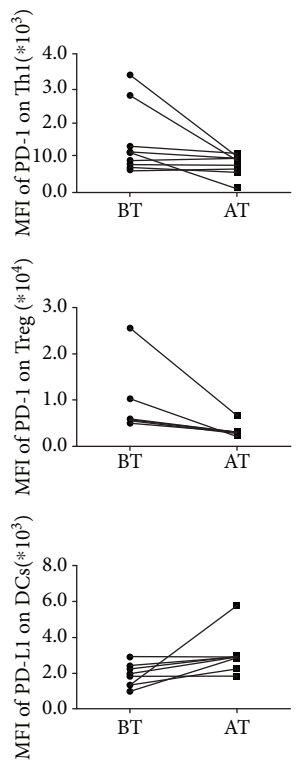

(c) Patients with HBsAg decline ≥ 10% in C2-Group

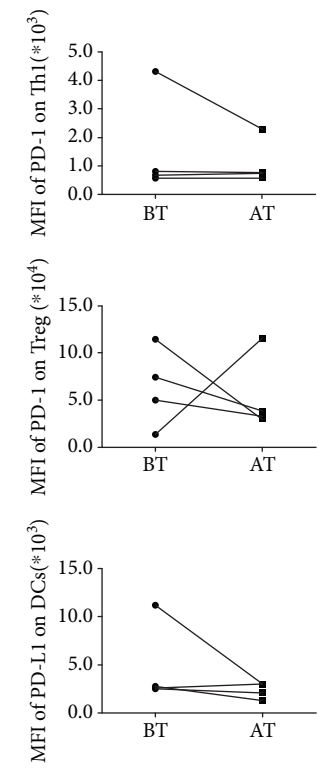

(d) Patients with HBsAg decline ≥ 10% in T2-Group

Figure 4: Relationship between PD-1 and PD-L1 levels on immune cell subsets and HBsAg decline. (a) Changes of PD-1 levels on Th1 and Treg and the PD-L1 level on DCs were analyzed before and after treatment in patients with HBsAg decline ≥ 10% of C1-Group. BT: before treatment; AT: after treatment. (b) Changes of PD-1 levels on Th1 and Treg and the PD-L1 level on DCs were analyzed before and after treatment in patients with HBsAg decline ≥ 10% of T1-Group. (c) Changes of PD-1 levels on Th1 and Treg and the PD-L1 level on DCs were analyzed before and after treatment in patients with HBsAg decline ≥ 10% of C2-Group. (d) Changes of PD-1 levels on Th1 and Treg and the PD-L1 level on DCs were analyzed before and after treatment in patients with HBsAg decline ≥ 10% of T2-Group.

increased Th1 and DC frequencies in treatment-naïve patients, which was correlated with the decrease of HBsAg levels. Therefore, Astragalus polysaccharides and Fructus Ligustri Lucidi may play a key role in contributing to the increase of Th1 frequencies. In future studies, we will explore in depth the immunoregulatory mechanism of BSF in treating CHB patients by collecting more samples from patients.

Data Availability

Data are made available to all interested researchers upon request.

Conflicts of Interest

The authors declare that they have no conflicts of interest.

Acknowledgments

This work was supported by the National Natural Science Foundation of China (81473477, 81473629, 81503545, 81673767, 81673938, 81673935, and 81774256), Training Plan for Excellent Academic Leaders of Shanghai Health System (2017BR007), Municipal Hospital Emerging Cutting Edge Technology Joint Research Project (SHDC12016121), and Science Research Project of Thirteen Five-year Plan (2018ZX10725504).

References

[1] GBD 2013 Mortality and Causes of Death Collaborators, "Global, regional, and national age-sex specific all-cause and cause-specific mortality for 240 causes of death, 1990–2013: a systematic analysis for the global burden of disease Study 2013," *The Lancet*, vol. 385, no. 9963, pp. 117–171, 2015.

[2] L. Zou, W. Zhang, and S. Ruan, "Modeling the transmission dynamics and control of hepatitis B virus in China," *Journal of Theoretical Biology*, vol. 262, no. 2, pp. 330–338, 2010.

[3] J. D. Jia and H. Zhuang, "The overview of the seminar on chronic hepatitis B," *Zhonghua gan zang bing za zhi= Zhonghua ganzangbing zazhi= Chinese journal of hepatology*, vol. 12, no. 11, pp. 698-699, 2004.

[4] S. T. Goldstein, F. Zhou, S. C. Hadler, B. P. Bell, E. E. Mast, and H. S. Margolis, "A mathematical model to estimate global hepatitis B disease burden and vaccination impact," *International Journal of Epidemiology*, vol. 34, no. 6, pp. 1329–1339, 2005.

[5] A. S. F. Lok and B. J. McMahon, "Chronic hepatitis B: update 2009," *Hepatology*, vol. 50, no. 3, pp. 661-662, 2009.

[6] European Association for the Study of the Liver, "EASL clinical practice guidelines: management of chronic hepatitis B virus infection," *Journal of Hepatology*, vol. 57, no. 1, pp. 167–185, 2012.

[7] M. K. Maini and A. J. Gehring, "The role of innate immunity in the immunopathology and treatment of HBV infection," *Journal of Hepatology*, vol. 64, no. 1, pp. S60–S70, 2016.

[8] A. Bertoletti and C. Ferrari, "Adaptive immunity in HBV infection," *Journal of Hepatology*, vol. 64, no. 1, pp. S71–S83, 2016.

[9] S. Ducheix, A. Montagner, A. Polizzi et al., "Essential fatty acids deficiency promotes lipogenic gene expression and hepatic steatosis through the liver X receptor," *Journal of Hepatology*, vol. 58, no. 5, pp. 984–992, 2013.

[10] M. Yamamoto, T. Tatsumi, T. Miyagi et al., "α-Fetoprotein impairs activation of natural killer cells by inhibiting the function of dendritic cells," *Clinical and Experimental Immunology*, vol. 165, no. 2, pp. 211–219, 2011.

[11] S. H. Aalaei-Andabili and S. M. Alavian, "Regulatory T cells are the most important determinant factor of hepatitis B infection prognosis: a systematic review and meta-analysis," *Vaccine*, vol. 30, no. 38, pp. 5595–5602, 2012.

[12] H. Feng, J. Yin, Y. P. Han et al., "Regulatory T cells and IL-17(+) T helper cells enhanced in patients with chronic hepatitis B virus infection," *International Journal of Clinical and Experimental Medicine*, vol. 8, no. 6, pp. 8674–8685, 2015.

[13] E. Chan, M. Tan, J. Xin, S. Sudarsanam, and D. E. Johnson, "Interactions between traditional Chinese medicines and Western therapeutics," *Current Opinion in Drug Discovery & Development*, vol. 13, no. 1, pp. 50–65, 2010.

[14] W. Dai, C. Wei, H. Kong et al., "Effect of the traditional Chinese medicine tongxinluo on endothelial dysfunction rats studied by using urinary metabonomics based on liquid chromatography-mass spectrometry," *Journal of Pharmaceutical and Biomedical Analysis*, vol. 56, no. 1, pp. 86–92, 2011.

[15] Y. An, S. Gao, D. Cheng et al., "Peginterferon and Chinese herbs exert a combinatorial effect in HBeAg-positive chronic hepatitis B," *Journal of Infection in Developing Countries*, vol. 10, no. 04, pp. 369–376, 2016.

[16] M. Li, X. H. Sun, Z. H. Zhou et al., "Beneficial therapeutic effect of Chinese herbal Bushen formula on CHB patients with mildly elevated alanine aminotransferase by down-regulating $CD4^+CD25^+$ T cells," *Journal of Ethnopharmacology*, vol. 146, no. 2, pp. 614–622, 2013.

[17] Chinese Society of Hepatology, Chinese Medical Association, Chinese Society of Infectious Diseases, Chinese Medical Association, J. L. Hou, and W. Lai, "The guideline of prevention and treatment for chronic hepatitis B: a 2015 update," *Zhonghua gan zang bing za zhi= Zhonghua ganzangbing zazhi= Chinese journal of hepatology*, vol. 23, no. 12, pp. 888–905, 2015.

[18] M. Li, Z. H. Zhou, X. H. Sun et al., "The dynamic changes of circulating invariant natural killer T cells during chronic hepatitis B virus infection," *Hepatology International*, vol. 10, no. 4, pp. 594–601, 2016.

[19] J. Baran, D. Kowalczyk, M. Ozog, and M. Zembala, "Three-color flow cytometry detection of intracellular cytokines in peripheral blood mononuclear cells: comparative analysis of phorbol myristate acetate-ionomycin and phytohemagglutinin stimulation," *Clinical and Diagnostic Laboratory Immunology*, vol. 8, no. 2, pp. 303–313, 2001.

[20] X. J. Zhu, X. H. Sun, Z. H. Zhou et al., "Lingmao formula combined with entecavir for HBeAg-positive chronic hepatitis B patients with mildly elevated alanine aminotransferase: a multicenter, randomized, double-blind, placebo-controlled trial," *Evidence-based Complementary and Alternative Medicine*, vol. 2013, Article ID 620230, 7 pages, 2013.

[21] Y. Liu, P. Liu, R. Dai et al., "Analysis of plasma proteome from cases of the different traditional Chinese medicine syndromes in patients with chronic hepatitis B," *Journal of Pharmaceutical and Biomedical Analysis*, vol. 59, pp. 173–178, 2012.

[22] Z. Chen, X. Ma, Y. Zhao et al., "Kushenin combined with nucleos(t)ide analogues for chronic hepatitis B: a systematic review and meta-analysis," *Evidence-based Complementary and Alternative Medicine*, vol. 2015, Article ID 529636, 12 pages, 2015.

[23] H. Li, Z. Ye, X. Gao et al., "Diwu Yanggan capsule improving liver histological response for patients with HBeAg-negative chronic hepatitis B: a randomized controlled clinical trial," *American Journal of Translational Research*, vol. 10, no. 5, pp. 1511–1521, 2018.

[24] Q. Y. Liu, Y. M. Yao, Y. Yu, N. Dong, and Z. Y. Sheng, "Astragalus polysaccharides attenuate postburn sepsis via inhibiting negative immunoregulation of $CD4^+$ CD25 (high) T cells," *PLoS One*, vol. 6, no. 6, article e19811, 2011.

[25] Y. H. Chen, X. F. Wu, J. Hao, M. L. Chen, and G. Y. Zhu, "Selection and purification potential evaluation of woody plant in vertical flow constructed wetlands in the subtropical area," *Huan Jing Ke Xue*, vol. 35, no. 2, pp. 585–591, 2014.

Hindawi
Journal of Immunology Research
Volume 2019, Article ID 3954890, 10 pages
https://doi.org/10.1155/2019/3954890

Review Article

The Crosstalk between Fat Homeostasis and Liver Regional Immunity in NAFLD

Minjuan Ma,[1] Rui Duan,[1] Hong Zhong,[1] Tingming Liang,[1] and Li Guo[2]

[1]*Jiangsu Key Laboratory for Molecular and Medical Biotechnology and College of Life Sciences, Nanjing Normal University, Nanjing, Jiangsu 210023, China*
[2]*Department of Bioinformatics, School of Geographic and Biologic Information, Nanjing University of Posts and Telecommunications, Nanjing, Jiangsu 210023, China*

Correspondence should be addressed to Tingming Liang; tmliang@njnu.edu.cn and Li Guo; lguo@njupt.edu.cn

Received 24 June 2018; Revised 11 November 2018; Accepted 9 December 2018; Published 3 January 2019

Guest Editor: Xiaoni Kong

The liver is well known as the center of glucose and lipid metabolism in the human body. It also functions as an immune organ. Previous studies have suggested that liver nonparenchymal cells are crucial in the progression of NAFLD. In recent years, NAFLD's threat to human health has been becoming a global issue. And by far, there is no effective treatment for NAFLD. Liver nonparenchymal cells are stimulated by lipid antigens, adipokines, or other factors, and secreted immune factors can alter the expression of key proteins such as SREBP-1c, ChREBP, and PPARγ to regulate lipid metabolism, thus affecting the pathological process of NAFLD. Interestingly, some ncRNAs (including miRNAs and lncRNAs) participate in the pathological process of NAFLD by changing body fat homeostasis. And even some ncRNAs could regulate the activity of HSCs, thereby affecting the progression of inflammation and fibrosis in the course of NAFLD. In conclusion, immunotherapy could be an effective way to treat NAFLD.

1. Introduction

The liver, consisting of 80% hepatic parenchymal cells and 20% hepatic nonparenchymal cells, is the largest metabolism organ in the human body. It not only maintains the homeostasis of sugars and fats but also participates in immune regulation (innate immunity, adaptive immunity, and immune tolerance) [1–3] Hepatocytes are hepatic parenchymal cells, while the other 20% of nonparenchymal cells in the liver include liver sinusoidal endothelial cells (LSECs), natural killer (NK) cells, natural killer T (NKT) cells, Kupffer cells (KCs), hepatic stellate cells (HSCs), and dendritic cells (DCs). Hepatocytes, the parenchymal cells of the liver, are stimulated by a number of inflammatory factors, such as interleukin 6 (IL-6) and interleukin 1 beta (IL-1β), producing a large number of acute-phase proteins (APPs) that can kill foreign antigens and regulate immune responses [4]. KCs play an important role in the initial response to injury. When liver damage occurs, it can rapidly produce cytokines and chemokines, such as IL-1β and tumor necrosis factor α (TNF-α), resulting in the recruitment of other immune cells, such as monocytes. After entering the liver, the phenotype of monocytes changes, showing proinflammatory and profibrotic functions [5]. NK cells play an important role in liver host defense and immune balance by secreting cytokines, such as interferon gamma (IFN-γ) [6]. NKT cells serve as a bridge connecting innate immunity and adaptive immunity in the liver. They are activated by stimulation with lipid antigens, rapidly secrete anti-inflammatory or proinflammatory cytokines and chemokines, and participate in liver diseases [7]. A recent study shows that LSECs are serving as sentinel cells to detect microbial infection through pattern recognition receptor activation and as antigen (cross)--presenting cells [8]. Under normal physiological conditions, HSCs store liver lipids and 70% of the body's vitamin A. Conversely, after being stimulated by insulin, they can secrete type I collagen (Col-1) and connective tissue growth factor, causing inflammation and liver fibrosis [9]. Liver DCs internalize antigens and present them to surrounding lymphocytes as APCs and regulate T cells via the interleukin 10

Table 1: ncRNAs link the fat homeostasis and immunity in the pathological process of NAFLD.

Noncoding RNAs	Target genes	Signaling pathways	References
MiR-373	*AKT1*	AKT–mTOR-S6K	[91]
MiR-7a	*YY1*	YY1-CHOP-10-C/EBP-α/PPARγ	[92]
MiR-130a-3p	*TGFBR1*/*TGFBR2*	GF-β/SMAD	[93]
MiR-26a	*IL-6* mRNA	miR-26a-IL-6-IL-17 axis	[94]
MiR-146a-5p	*Wnt1* and *Wnt5a*	Wnt	[95]
LncRNA MRAK052686	*Nrf2* and *Eif2ak2*	PERK	[99]
LncRNA SRA	*FoxO1*	FFA β-oxidation	[100]
LncRNA MALAT1	*CXCL5*	Extracellular space	[101]
LncRNA NONRATT013819.2	*Lox*	ECM-related pathways	[102]

(IL-10) mechanism [10, 11]. The hepatic metabolic homeostasis is maintained by the precise mechanism that each liver cell performs its own duties while maintaining crosstalk. Disorders of this mechanism can cause liver metabolic disorders and liver disease.

Liver disease (viral hepatitis, liver fibrosis, fatty liver, alcoholic liver, drug-induced liver damage and cirrhosis, and liver cancer), relating to liver immune cell disorders, is one of the reasons for high mortality in some countries and regions of the world [12–14]. Nonalcoholic fatty liver disease (NAFLD) is the most common cause of liver disease, the primary feature of which is simple steatosis caused by accumulation of liver triglycerides (TG), followed by nonalcoholic steatohepatitis (NASH) with inflammation, fibrosis, and liver damage, eventually developing into cirrhosis and hepatocellular carcinoma (HCC). Importantly, it is also closely related to obesity and type 2 diabetes, insulin resistance (IR), and other metabolic abnormalities [15, 16]. It has been reported that the prevalence of NAFLD is about 27%-34% in America [17], 25% in Europe [18], and 15-20% in Asia [19]. With economic development and changes in lifestyle, the upward trend of people's weights, especially in some high-income countries and regions, is causing global obesity and type 2 diabetes [20, 21]. Population-based studies showed that 2.6–9.6% of children have NAFLD, increasing up to 38–53% among obese children [22, 23]. Therefore, prevention and treatment of NAFLD is an imminent global issue.

NAFLD begins with excessive accumulation of TG in the liver. Studies have shown that approximately 60% of TG comes from adipose tissue free fatty acid pools, 26% from lipid de novo synthesis, and 15% from unhealthy diets [24]. Obesity and type 2 diabetes promote liver overload of glucose and insulin, which can activate carbohydrate response element binding protein (ChREBP) and sterol regulatory element binding protein-1c (SREBP-1c), respectively, thereby upregulating glycolytic enzymes and fatty acid synthase to promote hepatic lipogenesis [25]. Interestingly, IL-1β signaling mediates hepatocyte TG accumulation by driving the de novo lipogenic signaling pathway in obese mouse livers [26]. The main reason for the development of NASA from simple steatosis is abnormal release of adipokines and excessive accumulation of liver TG to activate hepatic nonparenchymal cells such as KCs, DCs, NK, and NKT. These cells can release proinflammatory factors including TNF-α, IL-6, and TGF-β, thereby leading to hepatitis, liver fibrosis, and liver damage [27].

Complex crosstalk between hepatocytes and other hepatocytes plays a decisive role in the pathogenesis of NAFLD. Surprisingly, some noncoding RNAs (ncRNAs) are involved in the pathological process of NAFLD and can even directly regulate certain pathways in liver nonparenchymal cells to influence the progression of NAFLD (Table 1). Therefore, this paper mainly clarifies the interaction between immune factors and ncRNA and protein in each stage of NAFLD, in order to provide potential targets for the treatment and prognosis of NAFLD.

2. Crosstalk between Hepatocytes, Hepatic Nonparenchymal Cells, and Adipocytes in the Pathological Process of NAFLD

2.1. Main Signal Pathways in Simple Hepatic Steatosis. Liver fat is mainly derived from dietary fatty acids, de novo lipogenesis, and adipose tissue. Hepatic steatosis occurs when fatty acid uptake, de novo lipogenesis, lipid secretion, or disposal via free fatty acid (FFA) oxidation are unbalanced [28].

Dietary fat is stored in fat tissue in the form of FFA to form an FFA pool. Obesity causes dysfunction of adipocytes and releases a large number of proinflammatory factors such as TNF-α [29], IL-6 [30], and leptin. This causes FFAs in the FFA pool to translocate to nonadipose tissues such as the liver and skeletal muscle [31]. At the same time, TNF-α inhibits the release of adiponectin by adipocytes, thereby increasing the uptake of hepatic FFAs and reducing hepatic fatty acid oxidation and TG output [32]. Excessive accumulation of FFAs causes IR [33], which can mobilize peripheral fat to form new FFAs. FFAs translocate to the liver, exacerbate liver TG accumulation, and ultimately cause hepatic steatosis [34].

De novo fatty acid synthesis is a complex reaction, and it is regulated by multiple factors [35]. This paper mainly describes the FFAs from de novo fatty acid synthesis through the pathways involved in the three proteins SREBP-1c, ChREBP, and PPARγ. SREBP-1c, is an isoform of SREBPs (a family of TFs anchored in the ER membrane). It mainly regulates the synthesis of fatty acids [36]. ChREBP is a

transcription factor that recognizes the carbohydrate response element (ChRE) in glycolysis and lipid synthesis gene promoter [37, 38]. The peroxisome proliferator-activated receptors (PPARs), transcription factors that regulate lipid metabolism and insulin sensitivity [39], consist of three isoforms: PPARγ, PPARα, and PPARδ [40]. PPARγ is highly expressed in adipocytes while it is also present in other hepatocytes, especially in resting HSCs [41].

IR can upregulate SREBP-1c, ChREBP, and PPARγ to promote hepatic steatosis, which in turn can promote IR by SREBP-1c, ChREBP, and PPARγ. (1) The proinflammatory factors TNF-α and IL-6 released by M1-type KCs (regulated by lipopolysaccharide and other factors) reach the hepatic portal vein with blood flow and form a functional complex with hepatocyte membrane receptors TNFR1 and IL-6R [42–44]. The complex formed by TNF-α and TNFR1 recruits upstream kinases such as nuclear factor-κB- (NF-κB-) inducible kinase (NIK) and transforming growth factor--β-activated kinase to activate NF-κB, which upregulates IL-6 expression and cytokine signaling inhibitor-3 (SOCS-3) by binding to DNA [45]. IL-6 activates the Janus-activated kinase (JAK), which in turn is activated by phosphorylation of signal transduction and activator of transcription 3 (STAT3), which upregulates SOCS-3 [46]. SOCS-3 promotes IR by inducing the expression of SREBP-1c, which suppresses insulin receptor-mediated IRS1/2 synthesis [47]. (2) When IR causes severe extrahepatic injury, the liver tissue receives overloaded glucose and insulin. Insulin activates SREBP-1c [48]. SREBP-1c activates transcription of transcription factors involved in FFA metabolism, including the cluster of differentiation 36 (CD36) required for FFA uptake [49], FFA synthesis of required fatty acid synthase (FASN) and acetyl-CoA carboxylase (ACC), and TG synthesis-required glycerol-3-phosphate acyltransferase [50, 51]. High concentration of glucose induces the transfer of ChREBP from the cytoplasm to the nucleus; ChREBP in the nucleus upregulates FASN and ACC [52] and also induces glucose-6 phosphatase (G6P) and liver pyruvate kinase (LPK) expression to accelerate glycolysis and gluconeogenesis [53]. Interestingly, a recent study [54] found that activated ChREBP can directly target SREBP-1c and promote the accumulation of FFAs. (3) The large amount of FFAs released by adipose tissue activates liver PPARγ, which upregulates fatty acid transporters (such as CD36), resulting in a significant increase in fatty acid uptake in hepatocytes. The fatty acid is then converted to fatty acyl CoA, which is ultimately esterified to TG. In addition, hepatic PPARγ upregulates monoacylglycerol O-acyltransferase 1 (MGAT1) expression to promote TG accumulation [55]. PPARγ also upregulates SREBP-1c expression to promote de novo synthesis of lipids [56].

2.2. Main Signal Pathways in NASH. The main pathological features of NASH are (1) oxidative stress (OS) [57], (2) systemic and hepatic inflammation [58], (3) fibrosis [59], and (4) hepatocyte apoptosis [60]. The appearance of these pathological features is mainly trigged by the accumulation of excessive FFAs in the liver to activate the signaling pathways that promote prooxidation, proinflammation, profibrosis, and proapoptosis [61].

FFAs are stored in lipid droplets in the form of TG, exported as very low-density lipoprotein (VLDL), and oxidized by mitochondrial β-oxidation. Excessive activation of mitochondrial β-oxidation and cytochrome P450 family 2 subfamily E member 1 (CYP2E1), a cytochrome that performs futile cycles with release of electrons into the cytosol, which destroy the electron transport chain, produces a large amount of reactive oxygen species (ROS), which ultimately leads to OS [62, 63]. TNF-α can effectively stimulate the production of mitochondrial ROS [64]. In order to reduce ROS, a large amount of mitochondrial uncoupling protein is produced to reduce superoxide anions, which unfortunately leads to a decrease in membrane potential, thereby limiting ATP production. When the ATP supply is insufficient, dying KCs release the proinflammatory factor interleukin 8 (IL-8). This recruits inflammatory cells into the liver [65].

FFAs activate proinflammatory signals through TLR4 and in a synergistic manner with LPS [66, 67]. Proinflammatory cells (including hepatocytes, KCs, and adipocytes) produce proinflammatory factors through NF-κB activation [68]. LPS targets and activates TLR4 in hepatocytes and KCs, which upregulates NF-κB transcription to produce a large number of proinflammatory factors including IL-β, TNF-α, IL-6, IL-8, and TGF-β [69]. KCs can also be activated by OS to promote the release of proinflammatory factors (IL-β, TNF-α, IL-6, IL-8, and TGF-β) [70]. The dysfunctional adipocytes release a large amount of the proinflammatory factors TNF-α and IL-6 [30]. The massive release of proinflammatory factors promotes the conversion of simple hepatic steatosis to NASH. At the same time, proinflammatory factors in turn promote IR, thus aggravating NAFLD. Adipocytes can release two adipokines, leptin and adiponectin, which are involved in inflammation and fibrosis to affect the pathological process of NASH [71]. Adiponectin reduces inflammation by stimulating KCs to secrete anti-inflammatory cytokines (such as IL-10), blocking the activation of NF-κB [72], and inhibiting the release of TNF-α, IL-6, and chemokines, and antifibrosis by activating AMP-activated protein kinase (AMPK) in HSCs [73, 74]. Leptin accelerates the development of NASH by upregulating the expression of CD14 in KCs (enhancing the response of hepatocytes to low-dose LPS) [75]. It can also promote fibrosis by targeting KCs and sinusoidal endothelial cells, releasing a large amount of TGF-β, which promotes HSC production of collagen [76–79]. Unfortunately, low expression of adiponectin and high expression of leptin promote the development of inflammation and fibrosis in the NAFLD.

NF-κB upregulates the expression of TNF-α, Fas ligand (FasL), and TGF-β, which are considered to be major factors in the response to apoptosis and fibrosis that drive NASH progression [80]. After TNF-α and FasL recognize and bind to receptor TNFR and Fas on hepatocytes, respectively, TNFR and Fas are activated, which triggers a series of apoptotic events. Homologous dimerization of activated TNFR and Fas induces the formation of the death-inducing signaling complex (DISC), which induces activation of caspases 8 and 10, and induction of caspase 3, 6, and 7, eventually

leading to hepatocyte apoptosis [81, 82]. Upon activation of NKT cells by lipid antigens, CD40L expression is upregulated on the surface of NKT cells, which interacts with CD40 expressed on DCs, resulting in the production of IL-12 by DCs [83]. Increased liver IL-12 levels further stimulate liver NKT cells to enhance cytotoxicity by releasing perforin and granzymes and increasing the expression of FasL on the surface, which expresses binding to Fas receptors expressed on hepatocytes, leading to apoptosis [84]. Activation of NKT cells can also indirectly induce hepatocyte apoptosis by the release of cytokines, including IFN-γ and TNF-α. NKT-derived IFN-γ activates and recruits NK cells and DCs. Specifically, NK cell-induced transactivation of NK cells enhances cytolysis and production of NK cell IFN-γ, thereby further promoting hepatocyte apoptosis [85, 86].

The phosphorylation of SMAD2/3 is triggered by the interaction of TGF-β produced by KCs with specific receptors on the membrane of HSCs. Phosphorylated SMAD2/3 forms a complex with SMAD4 and is transferred to the nucleus to upregulate Col-1 in combination with target genes, thereby promoting fibrosis [87, 88].

3. ncRNAs Link the Fat Homeostasis and Immunity in the Progression of NAFLD

Noncoding RNA (ncRNA) refers to an RNA that does not encode any protein. ncRNA includes RNAs of known functions such as rRNA, tRNA, snRNA, snoRNA, and microRNA, as well as RNAs of unknown function. ncRNA plays an important role in the process of life. For example, ncRNAs can regulate mRNA stability and translation and ncRNAs affect protein stability and transport [89]. In the chapter, we will focus on the role of microRNA and lncRNA in the progression of NAFLD.

microRNAs (miRNAs) are endogenous, noncoding RNAs of about 20-24 nucleotides in length that can interact with messenger RNA and participate in posttranscriptional regulation of gene expression [90]. Studies have showed that the upregulation of microRNA-373 (miR-373) lowers its target gene AKT serine/threonine kinase 1 (AKT1) mRNA levels, resulting in suppression of the AKT-mTOR-S6K signaling pathway in hepatocytes and eventually weakening hepatic lipid abnormal deposition [91]. In zebrafish, the depletion of miR-7a increases the expression of Yin Yang 1 (YY1). YY1 induces the expression of C/EBP-α and PPARγ by inhibiting the expression of CHOP-10, leading to the accumulation of FFAs and triglyceride, and finally causing NASH [92]. MiR-130a-3p promotes the apoptosis of HSCs and inhibits the production of collagen by inhibiting the TGF-β/SMAD signaling pathway, thereby improving the pathological process of the liver [93]. Overexpression of miR-26a improves NAFLD and reduces IL-17 expression by partially reducing IL-6 expression, indicating the immunomodulatory effects of the miR-26a-IL-6-IL-17 axis in the pathological process of NAFLD. However, the specific mechanism of immune regulation has not been elucidated [94]. MiR-146a-5p inhibits the activity and proliferation of HSCs by downregulating Wnt1 and Wnt5a; the amount of Col-1 is decreased, thereby inhibiting the occurrence of fibrosis in the progression of NAFLD [95]. Several of the above studies indicate that miRNAs affect a particular signaling pathway by targeting their specific target genes, thereby regulating lipid-metabolizing proteins, as well as hepatic nonparenchymal cells involved in NAFLD progression. So, miRNAs may serve as new targets for NAFLD.

Long-chain noncoding RNAs are noncoding RNAs with a length of more than 200 nt, which have important functions in transcriptional silencing, transcriptional activation, chromosome modification, and nuclear transport [96, 97]. As transcription factors, lncRNAs play an important role in normal physiological and pathological processes [98]. In 2015, a study reported that Berberine (BBR) can upregulate the expression of lncRNA MRAK052686 and its target genes *Nrf2* and *Eif2ak2* in a high-fat diet- (HFD-) induced steatotic animal model, thereby inhibiting the PERK (PKR-like ER-kinase) pathway in ER stress, indicating that lncRNA MRAK052686 plays a role in NAFLD by affecting ER stress. This study opened the prelude to the study of the role of lncRNAs in NAFLD [99]. lncRNA SRA inhibits the transcription of forkhead box protein O1 (FoxO1) through an insulin-independent pathway in hepatocytes, thereby reducing the expression of the downstream gene adipose triglyceride lipase (ATGL) and subsequently lowering the FFA β-oxidation of hepatocytes, resulting in hepatic steatosis [100]. Some lncRNAs are involved in immune regulation by regulating nonparenchymal liver cells. Studies have found that in activated HSCs, lncRNA MALAT1 expression is upregulated and upregulates its target C-X-C motif chemokine ligand 5 (CXCL5), thereby promoting the development of inflammation and fibrosis in NASH [101]. Correspondingly, the study found that lncRNA NONRATT013819.2 was involved in ECM-related pathways to mediate activation of HSCs by upregulating the expression of lysyl oxidase (Lox) [102]. LncRNAs are not only involved in the development of NAFLD, but also related to the occurrence of HCC [103]. Most importantly, lncRNAs are involved in immune regulation [104], indicating that lncRNAs can be used as a novel target for liver immunotherapy.

4. Conclusions and Immune Treatment Strategies in NAFLD

Nowadays, the number of people suffering from NAFLD is increasing rapidly [105]. However, because of the complicated pathogenic mechanism behind NAFLD, there is currently no effective treatment for NAFLD. During the NAFLD process, hepatocytes, hepatic nonparenchymal cells, and adipocytes crosstalk, releasing factors involved in hepatic steatosis, nonalcoholic steatohepatitis, fibrosis, and even HCC [106]. Accumulation of fatty acids causes liver steatosis [107], endoplasmic reticulum resistance, and reactive oxygen species to promote steatosis and development into NASH [108]. By far, the existing methods for treating NAFLD include improving diet, strengthening exercise, changing lifestyles, and performing weight loss surgery, all with the purpose of reducing the accumulation of liver fat in patients [109–114]. Studies on NAFLD have reported that there is a

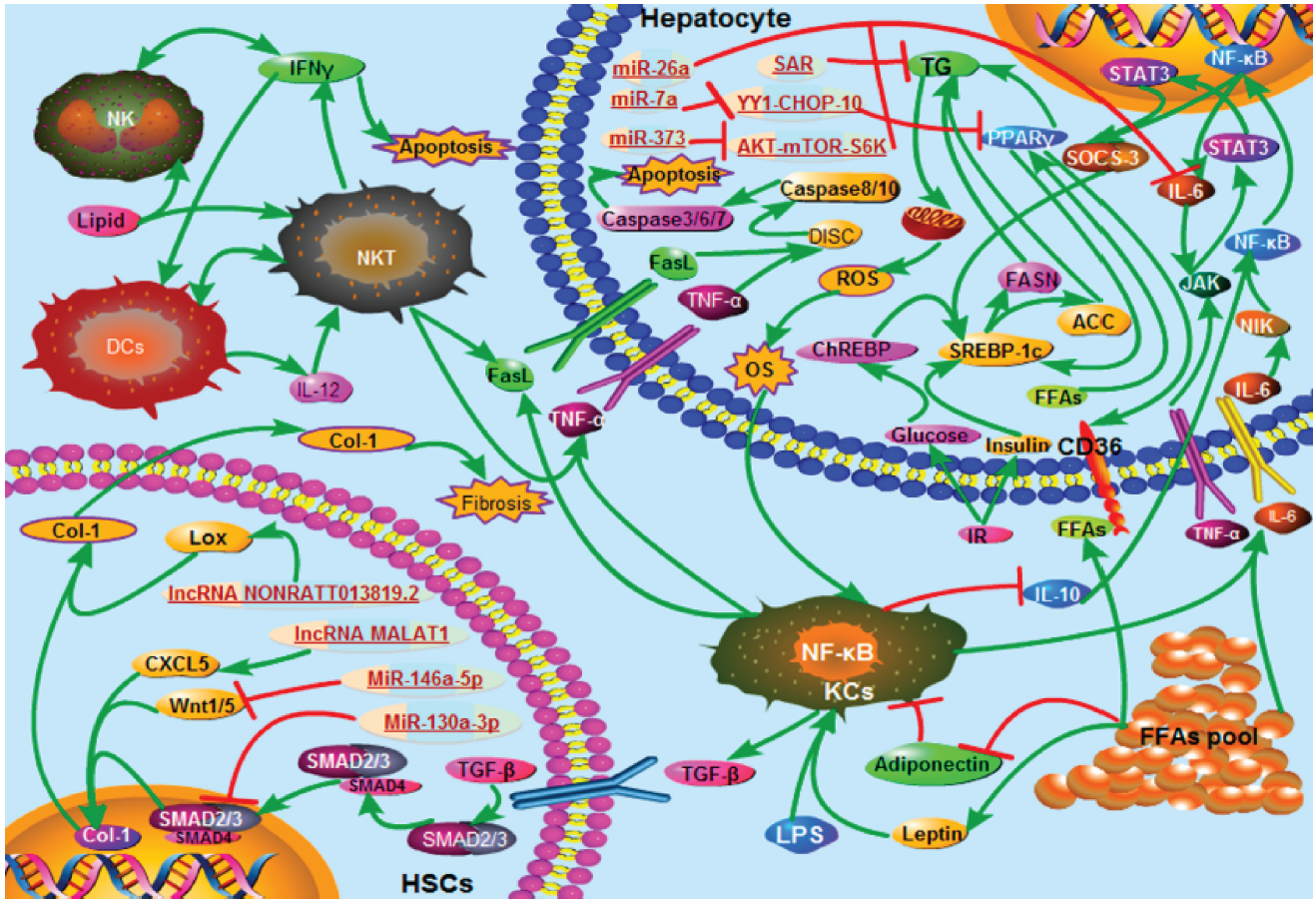

Figure 1: Crosstalk between hepatocytes, hepatic nonparenchymal cells, and ncRNA during the pathology of NAFLD. (1) Hepatic steatosis. Obesity and LPS from the intestine promote the release of proinflammatory cytokines TNF-α and IL-6 from KCs and adipocytes, which interact with ligands on the hepatocyte membrane. TNF-α activates SREBP-1c via the JAK/STAT3/SOCS-3 pathway, which activates FASN and ACC to promote hepatic TG accumulation. IL-6 upregulates IL-6 and SOCS-3 by NIK/NF-κB. The FFAs released from the FFA pool in the adipocytes directly activate PPARγ, which upregulates SREBP-1c to promote TG accumulation through other pathways. IR causes liver overload of glucose and insulin, and glucose activates ChREBP, which not only activates FASN and ACC but also activates SREBP-1c. Eventually, TG overload in hepatocytes causes hepatic steatosis. (2) NASH. Deregulation of adipocytes causes an increase in leptin levels, but adiponectin levels decrease. Decreased adiponectin causes a decrease in the release of the anti-inflammatory factor IL-10 from KCs, thereby promoting inflammation. TG overload causes excessive mitochondrial β-oxidation, which produces large amounts of ROS, which causes OS, causing KCs to release large amounts of proinflammatory factors (TNF-α, IL-6, and TGF-β) and FasL. Upon recognition of TNF-α and FasL with ligands on the hepatocyte membrane, they induce the formation of a death-inducing signaling complex (DISC), which induces hepatocyte apoptosis via the caspase pathway. Leptin can promote the release of TGF-β by KCs. After binding of TGF-β to ligand recognition on HSCs, liver fibrosis is promoted through the SMAD/Col-1 pathway. Lipids can induce NK and NKT release of apoptotic factors IFN-γ, FasL, and TNF-α. Activated NKT activates DCs, which produce IL-12 that stimulates NKT and ultimately aggravates inflammation and apoptosis. microRNA-373 (miR-373) reduces inflammation by inhibiting the AKT-mTOR-S6K signaling pathway, which inhibits IL-6 production; miR-7a upregulates YY1, which induces the expression of PPARγ by inhibiting the expression of CHOP-10, leading to the accumulation of FFAs and triglyceride, and finally causing NASH; MiR-130a-3p promotes the apoptosis of HSCs and inhibits the production of collagen by inhibiting the TGF-β/SMAD signaling pathway, thereby improving the pathological process of the liver; miR-26a improves NAFLD by partially reducing IL-6 expression; MiR-146a-5p inhibits the activity and proliferation of HSCs by downregulating Wnt1 and Wnt5a, and the amount of Col-1 is decreased, thereby inhibiting the occurrence of fibrosis in the progression of NAFLD; lncRNA SRA aggravates hepatic steatosis by reducing mitochondrial β-oxidation. lncRNA MALAT1 upregulates its target C-X-C motif chemokine ligand 5 (CXCL5), promoting the development of inflammation and fibrosis in NASH; and lncRNA NONRATT013819.2 promotes fibrosis by upregulating the expression of lysyl oxidase (Lox).

complicated relationship between liver immunity and fat homeostasis [115–117], while there is evidence that ncRNAs can interact with nonparenchymal liver cells and affect NAFLD [118]. Many functions of ncRNAs are not to be noted. Liver nonparenchymal cells play a crucial role in the maintenance of liver morphological structure and function (Figure 1). Although there are no reports of immunotherapy of NAFLD associated with fatty acid metabolism, future researches on the relationship between ncRNAs and NAFLD, between liver nonparenchymal cells and NAFLD, or the effect of interaction between ncRNAs and liver nonparenchymal cells on NAFLD, and liver immunotherapy for NAFLD

could be a breakthrough point in addressing current treatment deficiencies. Therefore, searching the target of NAFLD immunotherapy could be a new direction in the research for the treatment of NAFLD.

Abbreviations

NK: Natural killer cells
NKT: Natural killer T cells
LSECs: Liver sinusoidal endothelial cells
IL-6: Interleukin 6
IL-1β: Interleukin 1 beta
APPs: Acute-phase proteins
KCs: Kupffer cells
TNF-α: Tumor necrosis factor α
IFN-γ: Interferon gamma
HSCs: Hepatic stellate cells
NAFLD: Nonalcoholic fatty liver disease
Col-1: Type I collagen
NASH: Nonalcoholic steatohepatitis
IR: Insulin resistance
SphK1: Sphingosine kinase 1
FFAs: Free fatty acids
SREBP-1c: Sterol regulatory element binding protein-1c
ChREBP: Carbohydrate response element binding protein
PPARγ: Peroxisome proliferator-activated receptor-γ
SOCS-3: Cytokine signaling-3
G6p: Glucose-6-phosphatase
LPK: L-type pyruvate kinase
OS: Oxidative stress
VLDL: Low-density lipoprotein
CYP2E1: Cytochrome P450 family 2 subfamily E member 1
FasL: Fas ligand
DISC: Death-inducing signaling complex
FASN: Fatty acid synthase
ACC: Acetyl-CoA carboxylase
IL-10: Interleukin 10
HCC: Hepatocellular carcinoma
ROS: Reactive oxygen species production
JNK: c-Jun N-terminal kinase
MGAT1: Monoacylglycerol O-acyltransferase 1
LPS: Lipopolysaccharide
AMPK: AMP-activated protein kinase
ncRNA: Noncoding RNA
AKT1: AKT serine/threonine kinase 1
YY1: Yin Yang 1.

Conflicts of Interest

The authors declare no conflict of interest.

Acknowledgments

This work was supported by the National Natural Science Foundation of China (Nos. 31401009 and 61771251), the Key Project of Social Development in Jiangsu Province (No BE2016773), the Natural Science Foundation of Jiangsu (No. BK20171443), the Priority Academic Program Development of Jiangsu Higher Education Institutions (PAPD), and the Qing-lan Project of Nanjing Normal University sponsored by NUPTSF (No. NY215068), and sponsored by NUPTSF (Nos. NY215068 and NY217100).

References

[1] B. Gao, "Basic liver immunology," *Cellular & Molecular Immunology*, vol. 13, no. 3, pp. 265-266, 2016.

[2] Z. Kmiec, "Cooperation of liver cells in health and disease," *Advances in Anatomy, Embryology, and Cell Biology*, vol. 161, article 11729749, pp. 1–151, 2001.

[3] M. W. Robinson, C. Harmon, and C. O'Farrelly, "Liver immunology and its role in inflammation and homeostasis," *Cellular & Molecular Immunology*, vol. 13, no. 3, pp. 267–276, 2016.

[4] Z. Zhou, M. J. Xu, and B. Gao, "Hepatocytes: a key cell type for innate immunity," *Cellular & Molecular Immunology*, vol. 13, no. 3, pp. 301–315, 2016.

[5] C. Ju and F. Tacke, "Hepatic macrophages in homeostasis and liver diseases: from pathogenesis to novel therapeutic strategies," *Cellular & Molecular Immunology*, vol. 13, no. 3, pp. 316–327, 2016.

[6] H. Peng, E. Wisse, and Z. Tian, "Liver natural killer cells: subsets and roles in liver immunity," *Cellular & Molecular Immunology*, vol. 13, no. 3, pp. 328–336, 2016.

[7] K. Bandyopadhyay, I. Marrero, and V. Kumar, "NKT cell subsets as key participants in liver physiology and pathology," *Cellular & Molecular Immunology*, vol. 13, no. 3, pp. 337–346, 2016.

[8] P. A. Knolle and D. Wohlleber, "Immunological functions of liver sinusoidal endothelial cells," *Cellular & Molecular Immunology*, vol. 13, no. 3, pp. 347–353, 2016.

[9] S. Sanz, J. B. Pucilowska, S. Liu et al., "Expression of insulin-like growth factor I by activated hepatic stellate cells reduces fibrogenesis and enhances regeneration after liver injury," *Gut*, vol. 54, no. 1, pp. 134–141, 2005.

[10] Z. M. Bamboat, J. A. Stableford, G. Plitas et al., "Human liver dendritic cells promote T cell hyporesponsiveness," *Journal of Immunology*, vol. 182, no. 4, pp. 1901–1911, 2009.

[11] K. Palucka and J. Banchereau, "Cancer immunotherapy via dendritic cells," *Nature Reviews Cancer*, vol. 12, no. 4, pp. 265–277, 2012.

[12] J. Herkel, "Regulatory T cells in hepatic immune tolerance and autoimmune liver diseases," *Digestive Diseases*, vol. 33, no. 2, pp. 70–74, 2015.

[13] Z. Li, M. J. Soloski, and A. M. Diehl, "Dietary factors alter hepatic innate immune system in mice with nonalcoholic fatty liver disease," *Hepatology*, vol. 42, no. 4, pp. 880–885, 2005.

[14] W. R. Kim, Brown RS Jr, N. A. Terrault, and H. el-Serag, "Burden of liver disease in the United States: summary of a workshop," *Hepatology*, vol. 36, no. 1, pp. 227–242, 2002.

[15] B. A. Neuschwander-Tetri, "Non-alcoholic fatty liver disease," *BMC Medicine*, vol. 15, p. 45, 2017.

[16] J. T. Haas, S. Francque, and B. Staels, "Pathophysiology and mechanisms of nonalcoholic fatty liver disease," *Annual Review of Physiology*, vol. 78, no. 1, pp. 181–205, 2016.

[17] M. Lazo, R. Hernaez, M. S. Eberhardt et al., "Prevalence of nonalcoholic fatty liver disease in the United States: the third National Health and Nutrition Examination Survey, 1988–

1994," *American Journal of Epidemiology*, vol. 178, no. 1, pp. 38–45, 2013.

[18] M. Blachier, H. Leleu, M. Peck-Radosavljevic, D. C. Valla, and F. Roudot-Thoraval, "The burden of liver disease in Europe: a review of available epidemiological data," *Journal of Hepatology*, vol. 58, no. 3, pp. 593–608, 2013.

[19] G. C. Farrell, V. W. S. Wong, and S. Chitturi, "NAFLD in Asia–as common and important as in the West," *Nature Reviews Gastroenterology & Hepatology*, vol. 10, no. 5, pp. 307–318, 2013.

[20] S. Vandevijvere, C. C. Chow, K. D. Hall, E. Umali, and B. A. Swinburn, "Increased food energy supply as a major driver of the obesity epidemic: a global analysis," *Bulletin of the World Health Organization*, vol. 93, no. 7, pp. 446–456, 2015.

[21] T. Bhurosy and R. Jeewon, "Overweight and obesity epidemic in developing countries: a problem with diet, physical activity, or socioeconomic status?," *The Scientific World Journal*, vol. 2014, Article ID 964236, 7 pages, 2014.

[22] N. N. Than and P. N. Newsome, "A concise review of non-alcoholic fatty liver disease," *Atherosclerosis*, vol. 239, no. 1, pp. 192–202, 2015.

[23] Y. Falck-Ytter, Z. M. Younossi, G. Marchesini, and A. J. McCullough, "Clinical features and natural history of nonalcoholic steatosis syndromes," *Seminars in Liver Disease*, vol. 21, no. 1, pp. 017–026, 2001.

[24] K. L. Donnelly, C. I. Smith, S. J. Schwarzenberg, J. Jessurun, M. D. Boldt, and E. J. Parks, "Sources of fatty acids stored in liver and secreted via lipoproteins in patients with nonalcoholic fatty liver disease," *Journal of Clinical Investigation*, vol. 115, no. 5, pp. 1343–1351, 2005.

[25] R. Dentin, J. Girard, and C. Postic, "Carbohydrate responsive element binding protein (ChREBP) and sterol regulatory element binding protein-1c (SREBP-1c): two key regulators of glucose metabolism and lipid synthesis in liver," *Biochimie*, vol. 87, no. 1, pp. 81–86, 2005.

[26] K. A. Negrin, R. J. Roth Flach, M. T. DiStefano et al., "IL-1 signaling in obesity-induced hepatic lipogenesis and steatosis," *PLoS One*, vol. 9, no. 9, article e107265, 2014.

[27] I. C. Bocsan, M. V. Milaciu, R. M. Pop et al., "Cytokines Genotype-Phenotype Correlation in Nonalcoholic Steatohepatitis," *Oxidative Medicine and Cellular Longevity*, vol. 2017, Article ID 4297206, 7 pages, 2017.

[28] J. M. Lou-Bonafonte, C. Arnal, and J. Osada, "New genes involved in hepatic steatosis," *Current Opinion in Lipidology*, vol. 22, no. 3, pp. 159–164, 2011.

[29] I. Nieto-Vazquez, S. Fernandez-Veledo, D. K. Kramer, R. Vila-Bedmar, L. Garcia-Guerra, and M. Lorenzo, "Insulin resistance associated to obesity: the link TNF-alpha," *Archives of Physiology and Biochemistry*, vol. 114, no. 3, pp. 183–194, 2008.

[30] T. Wang and C. He, "Pro-inflammatory cytokines: the link between obesity and osteoarthritis," *Cytokine & Growth Factor Reviews*, vol. 44, pp. 38–50, 2018.

[31] F. Bessone, M. V. Razori, and M. G. Roma, "Molecular pathways of nonalcoholic fatty liver disease development and progression," in *Cellular and Molecular Life Sciences*, pp. 1–30, Springer, 2018.

[32] H. Y. Zhang, Z. X. du, and X. Meng, "Resveratrol prevents TNFα-induced suppression of adiponectin expression via PPARγ activation in 3T3-L1 adipocytes," *Clinical and Experimental Medicine*, vol. 13, no. 3, pp. 193–199, 2013.

[33] B. Sears and M. Perry, "The role of fatty acids in insulin resistance," *Lipids in Health and Disease*, vol. 14, p. 121, 2015.

[34] S. H. Koo, "Nonalcoholic fatty liver disease: molecular mechanisms for the hepatic steatosis," *Clinical and Molecular Hepatology*, vol. 19, no. 3, pp. 210–215, 2013.

[35] Y. Kawano and D. E. Cohen, "Mechanisms of hepatic triglyceride accumulation in non-alcoholic fatty liver disease," *Journal of Gastroenterology*, vol. 48, no. 4, pp. 434–441, 2013.

[36] J. Ou, H. Tu, B. Shan et al., "Unsaturated fatty acids inhibit transcription of the sterol regulatory element-binding protein-1c (SREBP-1c) gene by antagonizing ligand-dependent activation of the LXR," *Proceedings of the National Academy of Sciences of the United States of America*, vol. 98, no. 11, pp. 6027–6032, 2001.

[37] H. Yamashita, M. Takenoshita, M. Sakurai et al., "A glucose-responsive transcription factor that regulates carbohydrate metabolism in the liver," *Proceedings of the National Academy of Sciences of the United States of America*, vol. 98, no. 16, pp. 9116–9121, 2001.

[38] C. Rufo, M. Teran-Garcia, M. T. Nakamura, S. H. Koo, H. C. Towle, and S. D. Clarke, "Involvement of a unique carbohydrate-responsive factor in the glucose regulation of rat liver fatty-acid synthase gene transcription," *The Journal of Biological Chemistry*, vol. 276, no. 24, pp. 21969–21975, 2001.

[39] C. Janani and B. D. Ranjitha Kumari, "PPAR gamma gene–a review," *Diabetes & Metabolic Syndrome*, vol. 9, no. 1, pp. 46–50, 2015.

[40] E. Esposito, S. Cuzzocrea, and R. Meli, "Peroxisome proliferator-activated receptors and shock state," *The Scientific World Journal*, vol. 6, 1782 pages, 2006.

[41] Q. Zhou, W. Guan, H. Qiao et al., "GATA binding protein 2 mediates leptin inhibition of PPARγ1 expression in hepatic stellate cells and contributes to hepatic stellate cell activation," *Biochimica et Biophysica Acta (BBA) - Molecular Basis of Disease*, vol. 1842, no. 12, pp. 2367–2377, 2014.

[42] O. H. Al-Jiffri and F. M. Alsharif, "Adipokines profile and glucose control of Saudi patients with nonalcoholic fatty liver disease," *Advanced Research in Gastroenterology & Hepatology*, vol. 5, no. 2, article 555660, 2017.

[43] C. N. Lumeng, J. L. Bodzin, and A. R. Saltiel, "Obesity induces a phenotypic switch in adipose tissue macrophage polarization," *The Journal of Clinical Investigation*, vol. 117, no. 1, pp. 175–184, 2007.

[44] Y. S. Park, M. J. Uddin, L. Piao, I. Hwang, J. H. Lee, and H. Ha, "Novel role of endogenous catalase in macrophage polarization in adipose tissue," *Mediators of Inflammation*, vol. 2016, Article ID 8675905, 14 pages, 2016.

[45] M. S. Hayden and S. Ghosh, "Regulation of NF-κB by TNF family cytokines," *Seminars in Immunology*, vol. 26, no. 3, pp. 253–266, 2014.

[46] G. Huang, M. Yuan, J. Zhang et al., "IL-6 mediates differentiation disorder during spermatogenesis in obesity-associated inflammation by affecting the expression of Zfp637 through the SOCS3/STAT3 pathway," *Scientific Reports*, vol. 6, no. 1, p. 28012, 2016.

[47] K. Ueki, T. Kadowaki, and C. Kahn, "Role of suppressors of cytokine signaling SOCS-1 and SOCS-3 in hepatic steatosis and the metabolic syndrome," *Hepatology Research*, vol. 33, no. 2, pp. 185–192, 2005.

[48] Z. G. Hua, L. J. Xiong, C. Yan et al., "Glucose and insulin stimulate lipogenesis in porcine adipocytes: dissimilar and identical regulation pathway for key transcription factors," *Molecules and Cells*, vol. 39, no. 11, pp. 797–806, 2016.

[49] J. F. C. Glatz and J. J. F. P. Luiken, "From fat to FAT (CD36/SR-B2): understanding the regulation of cellular fatty acid uptake," *Biochimie*, vol. 136, pp. 21–26, 2017.

[50] X. Xu, J. S. So, J. G. Park, and A. H. Lee, "Transcriptional control of hepatic lipid metabolism by SREBP and ChREBP," *Seminars in Liver Disease*, vol. 33, no. 4, pp. 301–311, 2013.

[51] N. Harada, E. Fujimoto, M. Okuyama, H. Sakaue, and Y. Nakaya, "Identification and functional characterization of human glycerol-3-phosphate acyltransferase 1 gene promoters," *Biochemical and Biophysical Research Communications*, vol. 423, no. 1, pp. 128–133, 2012.

[52] S. Ishii, K. Iizuka, B. C. Miller, and K. Uyeda, "Carbohydrate response element binding protein directly promotes lipogenic enzyme gene transcription," *Proceedings of the National Academy of Sciences of the United States of America*, vol. 101, no. 44, pp. 15597–15602, 2004.

[53] R. Dentin, L. Tomas-Cobos, F. Foufelle et al., "Glucose 6-phosphate, rather than xylulose 5-phosphate, is required for the activation of ChREBP in response to glucose in the liver," *Journal of Hepatology*, vol. 56, no. 1, pp. 199–209, 2012.

[54] A. G. Linden, S. Li, H. Y. Choi et al., "Interplay between ChREBP and SREBP-1c coordinates postprandial glycolysis and lipogenesis in livers of mice," *Journal of Lipid Research*, vol. 59, no. 3, pp. 475–487, 2018.

[55] J. H. Yu, Y. J. Lee, H. J. Kim et al., "Monoacylglycerol O-acyltransferase 1 is regulated by peroxisome proliferator-activated receptor γ in human hepatocytes and increases lipid accumulation," *Biochemical and Biophysical Research Communications*, vol. 460, no. 3, pp. 715–720, 2015.

[56] V. Souza-Mello, "Peroxisome proliferator-activated receptors as targets to treat non-alcoholic fatty liver disease," *World Journal of Hepatology*, vol. 7, no. 8, pp. 1012–1019, 2015.

[57] S. Spahis, E. Delvin, J.-M. Borys, and E. Levy, "Oxidative stress as a critical factor in nonalcoholic fatty liver disease pathogenesis," *Antioxidants & Redox Signaling*, vol. 26, no. 10, pp. 519–541, 2017.

[58] W. Liu, R. D. Baker, T. Bhatia, L. Zhu, and S. S. Baker, "Pathogenesis of nonalcoholic steatohepatitis," *Cellular and Molecular Life Sciences*, vol. 73, no. 10, pp. 1969–1987, 2016.

[59] P. S. Dulai, S. Singh, J. Patel et al., "Increased risk of mortality by fibrosis stage in nonalcoholic fatty liver disease: systematic review and meta-analysis," *Hepatology*, vol. 65, no. 5, pp. 1557–1565, 2017.

[60] T. Kanda, S. Matsuoka, M. Yamazaki et al., "Apoptosis and non-alcoholic fatty liver diseases," *World Journal of Gastroenterology*, vol. 24, no. 25, pp. 2661–2672, 2018.

[61] E. Buzzetti, M. Pinzani, and E. A. Tsochatzis, "The multiple-hit pathogenesis of non-alcoholic fatty liver disease (NAFLD)," *Metabolism - Clinical and Experimental*, vol. 65, no. 8, pp. 1038–1048, 2016.

[62] A. P. Rolo, J. S. Teodoro, and C. M. Palmeira, "Role of oxidative stress in the pathogenesis of nonalcoholic steatohepatitis," *Free Radical Biology and Medicine*, vol. 52, no. 1, pp. 59–69, 2012.

[63] M. A. Abdelmegeed, A. Banerjee, S. H. Yoo, S. Jang, F. J. Gonzalez, and B. J. Song, "Critical role of cytochrome P450 2E1 (CYP2E1) in the development of high fat-induced non-alcoholic steatohepatitis," *Journal of Hepatology*, vol. 57, no. 4, pp. 860–866, 2012.

[64] R. A. Muluye, Y. Bian, L. Wang et al., "Placenta peptide can protect mitochondrial dysfunction through inhibiting ROS and TNF-α generation, by maintaining mitochondrial dynamic network and by increasing IL-6 level during chronic fatigue," *Frontiers in Pharmacology*, vol. 7, p. 328, 2016.

[65] A. M. Diehl, "Tumor necrosis factor and its potential role in insulin resistance and nonalcoholic fatty liver disease," *Clinics in Liver Disease*, vol. 8, no. 3, pp. 619–638, 2004.

[66] J. M. Lowe, D. Menendez, P. R. Bushel et al., "p53 and NF-κB coregulate proinflammatory gene responses in human macrophages," *Cancer Research*, vol. 74, no. 8, pp. 2182–2192, 2014.

[67] H. Shi, M. V. Kokoeva, K. Inouye, I. Tzameli, H. Yin, and J. S. Flier, "TLR4 links innate immunity and fatty acid-induced insulin resistance," *The Journal of Clinical Investigation*, vol. 116, no. 11, pp. 3015–3025, 2006.

[68] J. D. Schilling, H. M. Machkovech, L. He et al., "Palmitate and lipopolysaccharide trigger synergistic ceramide production in primary macrophages," *The Journal of Biological Chemistry*, vol. 288, no. 5, pp. 2923–2932, 2013.

[69] X. Liu, J. Li, X. Peng et al., "Geraniin inhibits LPS-induced THP-1 macrophages switching to M1 phenotype via SOCS1/NF-κB pathway," *Inflammation*, vol. 39, no. 4, pp. 1421–1433, 2016.

[70] G. H. Koek, P. R. Liedorp, and A. Bast, "The role of oxidative stress in non-alcoholic steatohepatitis," *Clinica Chimica Acta*, vol. 412, no. 15-16, pp. 1297–1305, 2011.

[71] S. I. Fujii and K. Shimizu, "Exploiting antitumor immunotherapeutic novel strategies by deciphering the cross talk between invariant NKT cells and dendritic cells," *Frontiers in Immunology*, vol. 8, p. 886, 2017.

[72] H. Tilg and A. R. Moschen, "Adipocytokines: mediators linking adipose tissue, inflammation and immunity," *Nature Reviews Immunology*, vol. 6, no. 10, pp. 772–783, 2006.

[73] A. Caligiuri, C. Bertolani, C. T. Guerra et al., "Adenosine monophosphate-activated protein kinase modulates the activated phenotype of hepatic stellate cells," *Hepatology*, vol. 47, no. 2, pp. 668–676, 2008.

[74] M. Adachi and D. A. Brenner, "High molecular weight adiponectin inhibits proliferation of hepatic stellate cells via activation of adenosine monophosphate-activated protein kinase," *Hepatology*, vol. 47, no. 2, pp. 677–685, 2008.

[75] K. Imajo, K. Fujita, M. Yoneda et al., "Hyperresponsivity to low-dose endotoxin during progression to nonalcoholic steatohepatitis is regulated by leptin-mediated signaling," *Cell Metabolism*, vol. 16, no. 1, pp. 44–54, 2012.

[76] C. Bertolani and F. Marra, "Role of adipocytokines in hepatic fibrosis," *Current Pharmaceutical Design*, vol. 16, no. 17, pp. 1929–1940, 2010.

[77] S. S. Choi, W. K. Syn, G. F. Karaca et al., "Leptin promotes the myofibroblastic phenotype in hepatic stellate cells by activating the hedgehog pathway," *The Journal of Biological Chemistry*, vol. 285, no. 47, pp. 36551–36560, 2010.

[78] S. Aleffi, I. Petrai, C. Bertolani et al., "Upregulation of proinflammatory and proangiogenic cytokines by leptin in human hepatic stellate cells," *Hepatology*, vol. 42, no. 6, pp. 1339–1348, 2005.

[79] J. Wang, I. Leclercq, J. M. Brymora et al., "Kupffer cells mediate leptin-induced liver fibrosis," *Gastroenterology*, vol. 137, no. 2, pp. 713–723.e1, 2009.

[80] J. M. Hui, A. Hodge, G. C. Farrell, J. G. Kench, A. Kriketos, and J. George, "Beyond insulin resistance in NASH: TNF-α or adiponectin?," *Hepatology*, vol. 40, no. 1, pp. 46–54, 2004.

[81] H. Tian, S. T. Yao, N. N. Yang et al., "D4F alleviates macrophage-derived foam cell apoptosis by inhibiting the NF-κB-dependent Fas/FasL pathway," *Scientific Reports*, vol. 7, article 7333, 2017.

[82] J. Huang, S. Yu, C. Ji, and J. Li, "Structural basis of cell apoptosis and necrosis in TNFR signaling," *Apoptosis*, vol. 20, no. 2, pp. 210–215, 2015.

[83] L. Cong, K. Chen, J. Li et al., "Regulation of adiponectin and leptin secretion and expression by insulin through a PI3K-PDE3B dependent mechanism in rat primary adipocytes," *The Biochemical Journal*, vol. 403, no. 3, pp. 519–525, 2007.

[84] M. C. Leite-de-Moraes, A. Herbelin, C. Gouarin, Y. Koezuka, E. Schneider, and M. Dy, "Fas/Fas ligand interactions promote activation-induced cell death of NK T lymphocytes," *The Journal of Immunology*, vol. 165, no. 8, pp. 4367–4371, 2000.

[85] W.-K. Syn, Y. Htun Oo, T. A. Pereira et al., "Accumulation of natural killer T cells in progressive nonalcoholic fatty liver disease," *Hepatology*, vol. 51, no. 6, pp. 1998–2007, 2010.

[86] T. Santodomingo-Garzon and M. G. Swain, "Role of NKT cells in autoimmune liver disease," *Autoimmunity Reviews*, vol. 10, no. 12, pp. 793–800, 2011.

[87] F. Xu, C. Liu, D. Zhou, and L. Zhang, "TGF-β/SMAD pathway and its regulation in hepatic fibrosis," *The Journal of Histochemistry and Cytochemistry*, vol. 64, no. 3, pp. 157–167, 2016.

[88] A. Biernacka, M. Dobaczewski, and N. G. Frangogiannis, "TGF-β signaling in fibrosis," *Growth Factors*, vol. 29, no. 5, pp. 196–202, 2011.

[89] G. Storz, "An expanding universe of noncoding RNAs," *Science*, vol. 296, no. 5571, pp. 1260–1263, 2002.

[90] S. Qin, P. Jin, X. Zhou, L. Chen, and F. Ma, "The role of transposable elements in the origin and evolution of microRNAs in human," *PLoS One*, vol. 10, no. 6, article e0131365, 2015.

[91] C. H. Li, S. C. Tang, C. H. Wong, Y. Wang, J. D. Jiang, and Y. Chen, "Berberine induces miR-373 expression in hepatocytes to inactivate hepatic steatosis associated AKT-S6 kinase pathway," *European Journal of Pharmacology*, vol. 825, pp. 107–118, 2018.

[92] C. Y. Lai, C. Y. Lin, C. C. Hsu, K. Y. Yeh, and G. M. Her, "Liver-directed microRNA-7a depletion induces nonalcoholic fatty liver disease by stabilizing YY1-mediated lipogenic pathways in zebrafish," *Biochimica et Biophysica Acta (BBA) – Molecular and Cell Biology of Lipids*, vol. 1863, no. 8, pp. 844–856, 2018.

[93] Y. Wang, J. du, X. Niu et al., "MiR-130a-3p attenuates activation and induces apoptosis of hepatic stellate cells in nonalcoholic fibrosing steatohepatitis by directly targeting TGFBR1 and TGFBR2," *Cell Death & Disease*, vol. 8, article e2792, 2017.

[94] Q. He, F. Li, J. Li et al., "MicroRNA-26a-interleukin (IL)-6-IL-17 axis regulates the development of non-alcoholic fatty liver disease in a murine model," *Clinical and Experimental Immunology*, vol. 187, no. 1, pp. 174–184, 2017.

[95] J. Du, X. Niu, Y. Wang et al., "MiR-146a-5p suppresses activation and proliferation of hepatic stellate cells in nonalcoholic fibrosing steatohepatitis through directly targeting Wnt1 and Wnt5a," *Scientific Reports*, vol. 5, no. 1, p. 16163, 2015.

[96] C. P. Ponting, P. L. Oliver, and W. Reik, "Evolution and functions of long noncoding RNAs," *Cell*, vol. 136, no. 4, pp. 629–641, 2009.

[97] P. Johnsson, L. Lipovich, D. Grander, and K. V. Morris, "Evolutionary conservation of long non-coding RNAs; sequence, structure, function," *Biochimica et Biophysica Acta (BBA) – General Subjects*, vol. 1840, no. 3, pp. 1063–1071, 2014.

[98] K. C. Wang and H. Y. Chang, "Molecular mechanisms of long noncoding RNAs," *Molecular Cell*, vol. 43, no. 6, pp. 904–914, 2011.

[99] X. Yuan, J. Wang, X. Tang, Y. Li, P. Xia, and X. Gao, "Berberine ameliorates nonalcoholic fatty liver disease by a global modulation of hepatic mRNA and lncRNA expression profiles," *Journal of Translational Medicine*, vol. 13, no. 1, p. 24, 2015.

[100] G. Chen, D. Yu, X. Nian et al., "LncRNA SRA promotes hepatic steatosis through repressing the expression of adipose triglyceride lipase (ATGL)," *Scientific Reports*, vol. 6, article 35531, 2016.

[101] F. Leti, C. Legendre, C. D. Still et al., "Altered expression of MALAT1 lncRNA in nonalcoholic steatohepatitis fibrosis regulates CXCL5 in hepatic stellate cells," *Translational Research*, vol. 190, pp. 25–39.e21, 2017.

[102] C.-J. Guo, X. Xiao, L. Sheng et al., "RNA sequencing and bioinformatics analysis implicate the regulatory role of a long noncoding RNA-mRNA network in hepatic stellate cell activation," *Cellular Physiology and Biochemistry*, vol. 42, no. 5, pp. 2030–2042, 2017.

[103] X. Yang, X. Xie, Y. F. Xiao et al., "The emergence of long non-coding RNAs in the tumorigenesis of hepatocellular carcinoma," *Cancer Letters*, vol. 360, no. 2, pp. 119–124, 2015.

[104] S. Carpenter, "Long noncoding RNA: novel links between gene expression and innate immunity," *Virus Research*, vol. 212, pp. 137–145, 2016.

[105] B. J. Perumpail, M. A. Khan, E. R. Yoo, G. Cholankeril, D. Kim, and A. Ahmed, "Clinical epidemiology and disease burden of nonalcoholic fatty liver disease," *World Journal of Gastroenterology*, vol. 23, no. 47, pp. 8263–8276, 2017.

[106] J. K. J. Gaidos, B. E. Hillner, and A. J. Sanyal, "A decision analysis study of the value of a liver biopsy in nonalcoholic steatohepatitis," *Liver International*, vol. 28, no. 5, pp. 650–658, 2008.

[107] A. Lonardo and P. Loria, "Apolipoprotein synthesis in nonalcoholic steatohepatitis," *Hepatology*, vol. 36, no. 2, pp. 514-515, 2002.

[108] K. Cusi, "Role of insulin resistance and lipotoxicity in non-alcoholic steatohepatitis," *Clinics in Liver Disease*, vol. 13, no. 4, pp. 545–563, 2009.

[109] F. S. Wang, J. G. Fan, Z. Zhang, B. Gao, and H. Y. Wang, "The global burden of liver disease: the major impact of China," *Hepatology*, vol. 60, no. 6, pp. 2099–2108, 2014.

[110] A. Chaney, "Treating the patient with nonalcoholic fatty liver disease," *The Nurse Practitioner*, vol. 40, no. 11, pp. 36–42, 2015.

[111] N. Chalasani, Z. Younossi, J. E. Lavine et al., "The diagnosis and management of non-alcoholic fatty liver disease: practice guideline by the American Association for the Study of Liver Diseases, American College of Gastroenterology, and the American Gastroenterological Association," *Hepatology*, vol. 55, no. 6, pp. 2005–2023, 2012.

[112] J. Weiss, M. Rau, and A. Geier, "Non-alcoholic fatty liver disease: epidemiology, clinical course, investigation, and treatment," *Deutsches Ärzteblatt International*, vol. 111, no. 26, pp. 447–452, 2014.

[113] R. R. Mummadi, K. S. Kasturi, S. Chennareddygari, and G. K. Sood, "Effect of bariatric surgery on nonalcoholic fatty liver disease: systematic review and meta-analysis," *Clinical Gastroenterology and Hepatology*, vol. 6, no. 12, pp. 1396–1402, 2008.

[114] J. Dyson and C. Day, "Treatment of non-alcoholic fatty liver disease," *Digestive Diseases*, vol. 32, no. 5, pp. 597–604, 2014.

[115] A. Federico, "Fat: a matter of disturbance for the immune system," *World Journal of Gastroenterology*, vol. 16, no. 38, p. 4762, 2010.

[116] S. Shono, Y. Habu, M. Nakashima et al., "The immunologic outcome of enhanced function of mouse liver lymphocytes and Kupffer cells by high-fat and high-cholesterol diet," *Shock*, vol. 36, no. 5, pp. 484–493, 2011.

[117] T. Geng, A. Sutter, M. D. Harland et al., "SphK1 mediates hepatic inflammation in a mouse model of NASH induced by high saturated fat feeding and initiates proinflammatory signaling in hepatocytes," *Journal of Lipid Research*, vol. 56, no. 12, pp. 2359–2371, 2015.

[118] Y. Chen, H. Huang, C. Xu, C. Yu, and Y. Li, "Long non-coding RNA profiling in a non-alcoholic fatty liver disease rodent model: new insight into pathogenesis," *International Journal of Molecular Sciences*, vol. 18, no. 1, 2017.

Hindawi
Journal of Immunology Research
Volume 2018, Article ID 9807139, 14 pages
https://doi.org/10.1155/2018/9807139

Research Article

Alda-1 Ameliorates Liver Ischemia-Reperfusion Injury by Activating Aldehyde Dehydrogenase 2 and Enhancing Autophagy in Mice

Meng Li,[1] Min Xu,[1] Jichang Li,[1] Lili Chen,[1] Dongwei Xu,[1] Ying Tong,[1] Jianjun Zhang,[1] Hailong Wu,[2] Xiaoni Kong,[1] and Qiang Xia[1]

[1]*Department of Liver Surgery, Renji Hospital, School of Medicine, Shanghai Jiao Tong University, Shanghai, China*
[2]*Shanghai Key Laboratory for Molecular Imaging, Collaborative Research Center, Shanghai University of Medicine & Health Science, Shanghai, China*

Correspondence should be addressed to Hailong Wu; wuhailong2@hotmail.com.cn, Xiaoni Kong; xiaoni-kong@126.com, and Qiang Xia; xiaqiang@shsmu.edu.cn

Received 26 March 2018; Revised 14 July 2018; Accepted 7 August 2018; Published 24 December 2018

Academic Editor: Peirong Jiao

Aldehyde dehydrogenase 2 (ALDH2) is a key enzyme for metabolism of reactive aldehydes, but its role during liver ischemia-reperfusion injury (IRI) remains unclear. In the present study, we investigated the effects of the ALDH2 activator, Alda-1, in liver IRI and elucidated the underlying mechanisms. Mice were pretreated with Alda-1 and subjected to a 90 min hepatic 70% ischemia model, and liver tissues or serum samples were collected at indicated time points after reperfusion. We demonstrated that Alda-1 pretreatment had a hepatoprotective role in liver IRI as evidenced by decreased liver necrotic areas, serum ALT/AST levels, and liver inflammatory responses. Mechanistically, Alda-1 treatment enhanced ALDH2 activity and subsequently reduced the accumulation of reactive aldehydes and toxic protein adducts, which result in decreased hepatocyte apoptosis and mitochondrial dysfunction. We further demonstrated that Alda-1 treatment could activate AMPK and autophagy and that AMPK activation was required for Alda-1-mediated autophagy enhancement. These findings collectively indicate that Alda-1-mediated ALDH2 activation could be a promising strategy to improve liver IRI by clearance of reactive aldehydes and enhancement of autophagy.

1. Introduction

Liver ischemia-reperfusion injury (IRI) is an ineluctable pathological process during a series of clinical procedures, such as liver transplantation, liver resection, and hemorrhagic shock [1]. Although liver IRI accounts for up to 10% of early graft failure and leads to a higher prevalence of acute or chronic rejection after liver transplantation, no effective pharmacological interventions have been developed to protect the liver from IRI so far [2]. Hepatocyte death and the subsequent inflammatory response are two key features of liver IRI, which form a vicious pathogenesis circle to drive the progression of liver IRI [3]. Therefore, strategies to effectively ameliorate hepatocyte death and interrupt the following inflammatory cascade reactions are urgently needed to improve liver IRI.

Autophagy is widely recognized as a critical protective cellular pathway in response to multiple intra- or extracellular stresses [4]. It has been reported that autophagy is deeply involved in various liver diseases including metabolic diseases, infectious diseases, and cancer [5]. However, the defined function of autophagy in the pathogenesis of IRI remains controversial [6]. We and other groups have demonstrated that the activation of autophagy plays a protective role in liver IRI [7–9].

Oxidative stress is one of the detrimental factors in the pathogenesis of liver IRI and accounts for the major reason of hepatocyte death [10, 11]. As such, excessive ROS could cause the accumulation of reactive aldehydes, including 4-hydroxy-2-nonenal (4HNE) and malondialdehyde (MDA), by lipid peroxidation [12], which can directly attack cellular proteins to form toxic protein to further

aggravate liver IRI [13]. Mitochondrial aldehyde dehydrogenase 2 (ALDH2) is a key enzyme responsible for detoxification of those reactive aldehydes to carboxylic acids [14]. Previous studies have indicated that ALDH2 activity is significantly decreased parallel with the remarkable accumulation of reactive aldehydes during liver IRI [15], suggesting that ALDH2 activation may play a protective role in liver IRI through cleaning up toxic aldehydes. Alda-1, a well-characterized ALDH2 activator, serves to activate or restore ALDH2 catalytic activity by modifying the kinetic properties of ALDH2 and increasing the substrate-enzyme interaction [16–18]. Previous studies have demonstrated that Alda-1 treatment significantly improves IRI in various types of organs including the heart, brain, lung, kidney, and intestine [16, 19–22]. However, whether Alda-1 plays a protective role in liver IRI remains unknown.

Here, we adopted an in vivo mouse liver IRI model together with an *in vitro* primary hepatocyte hypoxia/reoxygenation (H/R) injury model to investigate whether Alda-1 plays a protective role in liver IRI by activating ALDH2-mediated cleanup of reactive aldehydes. We found that Alda-1-induced pharmacological activation of ALDH2 increased the clearance of reactive aldehydes, enhanced hepatic autophagy, and ameliorated liver IRI. Thus, we claim that Alda-1 treatment may have clinical implications to protect against liver IRI.

2. Materials and Methods

2.1. Animal. 8–10-week-old male C57BL/6 wild-type (WT) mice (23-27 g body weight (BW)) were purchased from Shanghai SLAC Co. Ltd (Shanghai, China) and housed in an environment with controlled light (12 h light-dark cycle), temperature, and humidity, with free access to water and food. Animal protocols were approved by the Institutional Animal Care and Use Committee of Renji Hospital, School of Medicine, Shanghai Jiao Tong University.

2.2. Mouse Warm Liver IRI Model. An established and stable mouse model of warm liver IRI was used as we previously described [7]. Briefly, under sodium pentobarbital (40 mg/kg, i.p.) anesthesia, a midline laparotomy was performed. An atraumatic clip was placed across the portal triad, above the right lateral lobe. After 90 min of ischemia, the clamp was removed for reperfusion, animals were sacrificed after reperfusion at indicated time points, and liver tissues or serum samples were immediately collected for further analysis. Sham-operated mice underwent the same surgical procedure, but without vascular occlusion. Anesthetized mice were maintained at 37°C by means of a warming pad and heat lamp during the anesthesia process. Alda-1 (20 mg/kg BW, MCE, Monmouth Junction, NJ, USA) dissolved in solution (5% DMSO + 45% PEG400 + water) was administered intraperitoneally 2 h prior to the operation of liver ischemia, while 3-methyladenine (3MA, 30 mg/kg BW, MCE) dissolved in PBS or compound C (CC, 5 mg/kg BW, MCE) dissolved in PBS was administered intraperitoneally 1 h before the operation of liver ischemia; an equal volume of solution was administered in the same manner as the vehicle control. To distinguish the order in which the vehicle controls are administered, the vehicle controls of Alda-1 will be described as DMSO controls and the others as vehicle controls in this article.

2.3. Serum Sample Assays. The levels of ALT/AST in serum were measured by a standard clinical automatic analyzer (Dimension Xpand; Siemens Dade Behring, Munich, Germany). Serum TNF-α and IL-6 levels were measured using commercially available enzyme-linked immunosorbent assay (ELISA) kits (NeoBioscience Technology, Shenzhen, China) according to the manufacturer's protocols.

2.4. Liver Histopathology, Immunohistochemical, and TUNEL Staining. Standard procedures of liver histopathology, immunohistochemical, and TUNEL staining were used as we previously described [7]. Briefly, liver tissues were fixed in 4% paraformaldehyde, embedded in paraffin, and were cut into 5 μm thick sections. For histopathological analysis, the sections were stained with hematoxylin and eosin (H&E), Suzuki's criteria were used to evaluate the severity of liver IRI [23], and cytoplasmic vacuolization, sinusoidal congestion, and parenchymal cell necrosis were graded from 0 to 4. For immunohistochemical staining, after deparaffinization and rehydration of the sections which were then processed for an antigen-unmasking procedure and after overnight incubation with the primary antibodies against 4HNE (rabbit polyclonal, 1 : 300, Abcam), MPO (rabbit polyclonal, 1 : 300, Abcam), cleaved caspase-3 (rabbit polyclonal, 1 : 200, Cell Signaling Technology), and F4/80 (rat monoclonal, 1 : 250, AbD Serotec) at 4°C, the sections were incubated with HRP-conjugated secondary antibodies, and immunoreactive cells were visualized using DAB. For TUNEL staining, cell death in liver paraffin sections was detected by the TUNEL method (Roche Diagnostics, Indianapolis, USA) according to the manufacturer's instructions. For each stained section, at least three images from random fields were taken, and at least three mice per group were subjected to each experiment. Image-Pro Plus software (version 6.0) was used for image analysis of the sections.

2.5. Isolation, Culture, and Treatment of Hepatocytes. Primary hepatocytes were isolated as we previously described [24]. For hypoxia/reoxygenation assays, hepatocytes were cultured at 37°C in a modular incubator chamber (BioSpherix, Lacona, NY, USA) gassed with a 5% CO_2 and 95% N_2 gas mixture for 4 h followed by 2 h reoxygenation under normoxic conditions (air/5% CO_2). Alda-1 (20 μM), 3MA (5 mM), or CC (5 μM) was added to the medium for 1 hour before hypoxia. Cell viability was assessed using the CCK8 Cell Viability Assay Kit (Dojindo, Japan), and cytotoxicity was determined by lactate dehydrogenase (LDH) release (Beyotime, Shanghai, China) according to the manufacturer's instructions. All experiments were performed at least 3 times to confirm the results. Mitochondrial transmembrane potential in hepatocytes was assessed by the $\Delta\Psi m$ assay kit with JC-1 (Beyotime) according to the manufacturer's instructions. Mitochondrial generation of superoxide

was stained with MitoSOX Red (Invitrogen, Waltham, MA, USA).

2.6. ALDH2 Activity and MDA Content. ALDH2 activities in liver tissues were measured using an ALDH2 activity assay kit (GMS50131; GENMED, Pfizer, USA), according to the manufacturer's instruction. Briefly, the activities were measured with a spectrophotometer by monitoring the production of NADPH (340 nm). ALDH2 activity was expressed as nmol of NADH/min per mg protein (one unit). Malondialdehyde (MDA) contents were measured by commercially available kits (Nanjing Jiancheng Bioengineering Institute, Nanjing, China) according to the manufacturer's instructions.

2.7. Quantitative RT-PCR and Western Blot Analyses. Liver tissues and PMH were processed using RT-PCR and Western blot analysis as we previously described [24]. The relative expression levels of mRNA and protein for a target gene were normalized to relative changes with β-actin. The primers used for RT-PCR analysis are as follows:

(i) MCP1: F GGGCCTGCTGTTCACAGTT

(ii) MCP1: R CCAGCCTACTCATTGGGAT

(iii) IL-6: F TAGTCCTTCCTACCCCAATTTCC

(iv) IL-6: R TTGGTCCTTAGCCACTCCTTC

(v) TNF-α: F CCCTCACACTCAGATCATCTTCT

(vi) TNF-α: R GCTACGACGTGGGCTACAG

(vii) IL-1β: F TGGACCTTCCAGGATGAGGACA

(viii) IL-1β: R GTTCATCTCGGAGCCTGTAGTG

(ix) β-Actin: F TGACAGGATGCAGAAGGAGA

(x) β-Actin: R ACCGATCCACACAGAGTACT

The primary antibodies against P62 (rabbit monoclonal, 1 : 1000, Cell Signaling Technology), cleaved caspase-3 (rabbit polyclonal, 1 : 1000, Cell Signaling Technology), Bax (rabbit polyclonal, 1 : 1000, Cell Signaling Technology), Bcl2 (rabbit monoclonal, 1 : 1000, Cell Signaling Technology), 4HNE (rabbit polyclonal, 1 : 1000, Abcam), ALDH2 (rabbit polyclonal, 1 : 3000, Proteintech), LC3B (rabbit polyclonal, 1 : 1000, Proteintech), and β-actin (1 : 20000, Sigma-Aldrich) were used.

2.8. Ultrastructure Observation of Liver Tissues by a Transmission Electron Microscope. The liver tissues were dissected, and small pieces were fixed in 2.5% glutaraldehyde. Ultrathin sections were cut and contrasted with uranyl acetate buffer by lead citrate and then observed with a Hitachi HT-7700 transmission electron microscope.

2.9. Statistical Analysis. All values were expressed as mean ± SEM. The unpaired Student t-test or one-way ANOVA test was used to compare two groups or more than two groups, respectively. For nonparametric tests, the Mann-Whitney test or Kruskal-Wallis test was used. A P value less than 0.05 was used to indicate a statistically significant difference in all statistical comparisons, and data were analyzed using GraphPad Prism7 (GraphPad Software Inc., San Diego, CA, USA).

3. Results

3.1. Alda-1 Pretreatment Protects Liver from IRI. To investigate whether Alda-1 has the protective effects on liver IRI, we first determined the proper dosage and time window for Alda-1 treatment in mice by measuring ALT/AST levels and found that Alda-1 treatment at 20 mg/kg and 2 h prior to liver ischemia achieved a better protection outcome (Supplementary Figures 1A and 1B). Compared to DMSO controls, mice pretreated with Alda-1 showed markedly decreased necrotic areas and Suzuki's scores at 6 h and 12 h after reperfusion (Figures 1(a) and 1(b)). Consistent with these histological alterations, Alda-1-pretreated mice also exhibited lower serum ALT/AST levels (Figure 1(c)). To detect the function of Alda-1 on primary hepatocytes, we adopted the hypoxia/reoxygenation (H/R) model to treat primary hepatocytes *in vitro*. Compared to DMSO controls, the primary hepatocyte treated with Alda-1 showed fewer morphology abnormalities, higher cell viability, and lower cytotoxicity (Figures 1(d)–1(f)). Collectively, these findings demonstrated that Alda-1 had a protective role in liver IRI.

3.2. Alda-1 Protects Hepatocytes from IR-Induced Apoptosis. Apoptosis is a crucial mechanism to induce hepatocyte death in the process of liver IRI [25]. We then examined hepatic apoptosis by measuring levels of TUNEL, cleaved caspase-3, Bax, and Bcl2. Compared to DMSO controls, mice pretreated with Alda-1 showed significantly reduced hepatic apoptosis levels as evidenced by decreased TUNEL, cleaved caspase-3, and Bax signals and increased Bcl2 levels (Figures 2(a)–2(e)). In addition, Alda-1 treatment caused an increase in Bcl2 and a decrease in Bax levels in primary hepatocytes subjected to H/R challenge *in vitro* (Figure 2(f)). These findings demonstrated that Alda-1 could reduce hepatic apoptosis during liver IRI.

3.3. Alda-1 Ameliorates Inflammatory Responses in Liver IRI. During liver IRI, hepatocyte death-induced inflammatory responses can further exacerbate the severity of liver IRI [26]. We then sought to assess whether Alda-1 also affects inflammatory responses after liver IRI. As shown in Figures 3(a)–3(d), the hepatic infiltration of neutrophil (MPO) and macrophage (F4/80) was significantly decreased in Alda-1-pretreated mice compared to DMSO controls. In addition, both serum and hepatic levels of proinflammatory cytokines and chemokines such as MCP-1, IL-1β, TNF-α, and IL-6 were lower in Alda-1-pretreated mice than in control mice (Figures 3(e) and 3(f)). Collectively, these findings manifested that Alda-1 decreased inflammatory responses in liver IRI.

3.4. Alda-1 Administration Reduces Mitochondrial Dysfunction and ROS Production after H/R Challenge In Vitro. At the cellular level, mitochondrial dysfunction and excessive ROS production are two initial detrimental events

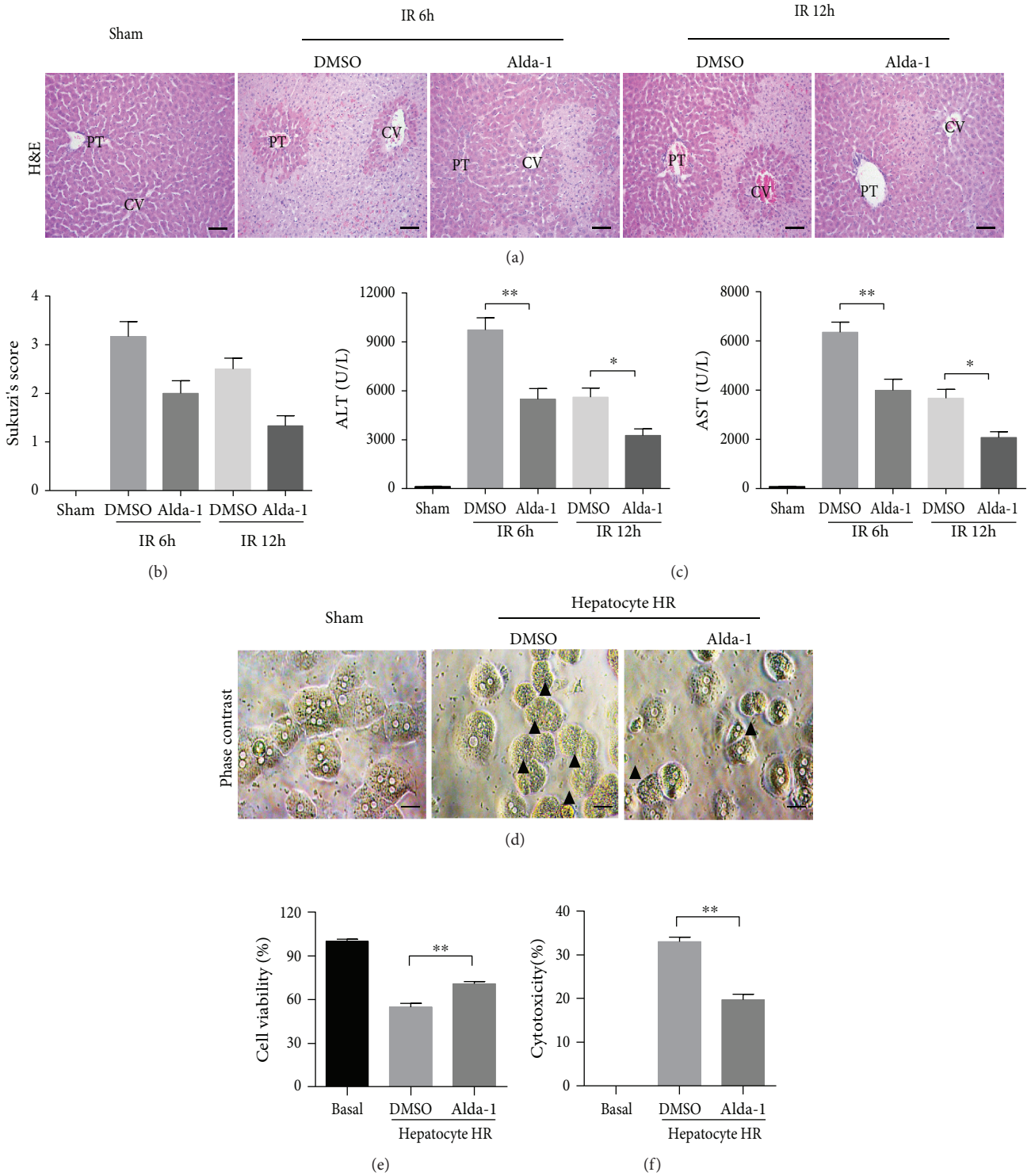

Figure 1: Alda-1 pretreatment protects liver from IRI. (a) Representative H&E-stained images at 6 and 12 hours after reperfusion or sham operation. PT: portal triads; CV: central veins. Scale bars: 50 μm. (b) Suzuki's scores of liver sections in (a). (c) Serum ALT/AST at 6 and 12 hours after liver IRI or sham operation ($n = 5$–6 per group). (d) Visible light microphotographs were taken in primary hepatocytes after HR challenge with or without Alda-1 pretreatment. Black arrows denote damaged hepatocytes. Scale bars: 25 μm. (e, f) Cell viability and cytotoxicity of primary hepatocytes after HR challenge with or without Alda-1 pretreatment were measured. Three to five independent experiments were performed. All data are shown as mean ± SEM. $^{**}P < 0.01$, $^{*}P < 0.05$.

to drive hepatocyte death and inflammatory responses during liver IRI [10]. To investigate whether Alda-1-mediated hepatoprotection during IRI is due to improved mitochondrial dysfunction and ROS production, we measured the mitochondrial membrane potential and ROS levels in primary hepatocytes during H/R treatment *in vitro*. Compared

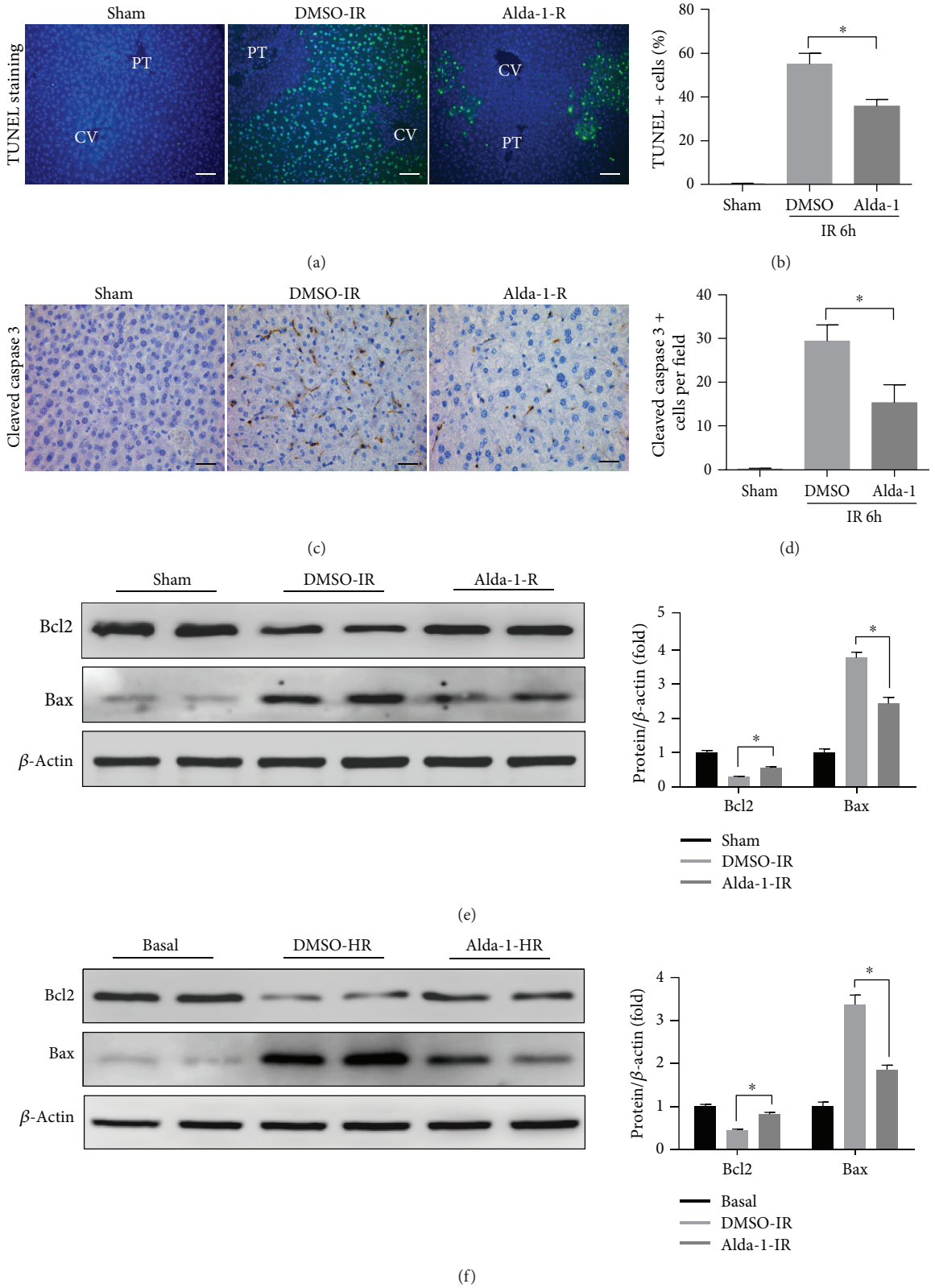

FIGURE 2: Alda-1 pretreatment alleviates apoptosis in liver IRI both in vivo and in vitro. (a, b) Representative sections of TUNEL staining and the numbers of TUNEL-positive cells in liver sections at 6 h after reperfusion or sham operation. Scale bars: 50 μm. (c, d) Representative sections of cleaved caspase-3 staining and the number of cleaved caspase-3-positive cells at 6 h after reperfusion or sham operation. Scale bars: 25 μm. (e) Western blot analysis of Bcl2 and Bax expression in liver tissues at 6 hours after reperfusion or sham operation (β-actin is used as a loading control). (f) Western blot analysis of Bcl2 and Bax expression in primary hepatocytes after HR challenge (β-actin is used as a loading control). All data are shown as mean ± SEM ($n = 4$–6). $^*P < 0.05$.

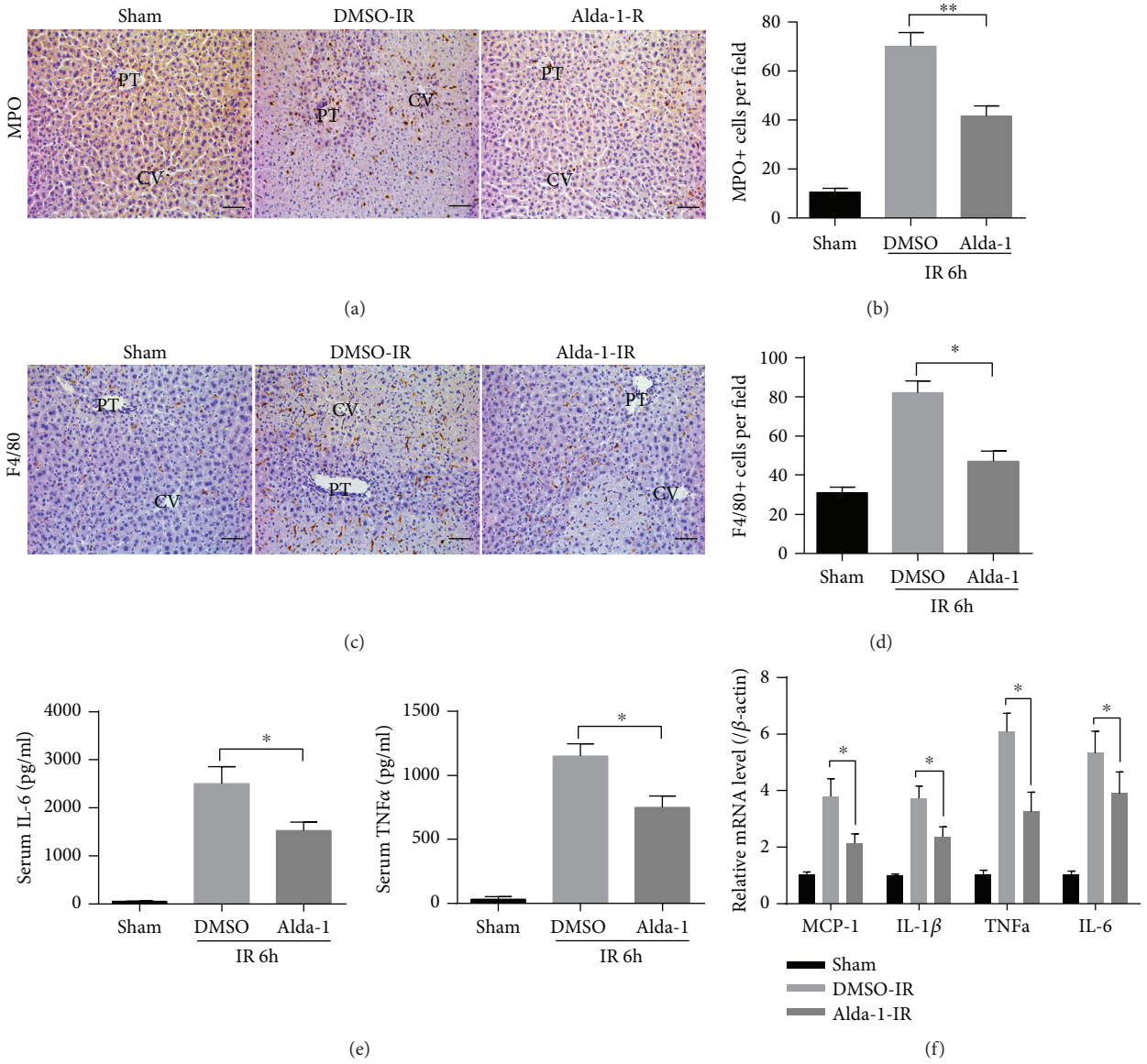

FIGURE 3: Alda-1 pretreatment restrains inflammatory responses in livers during IR injury. (a, b) Representative sections of MPO staining and the numbers of MPO-positive cells in liver sections at 6 h after reperfusion or sham operation. PT: portal triads; CV: central veins. Scale bars: 50 μm. (c, d) Representative sections of F4/80 staining and the numbers of F4/80-positive cells in liver sections at 6 h after reperfusion or sham operation. PT: portal triads; CV: central veins. Scale bars: 50 μm. (e) Serum IL-6 and TNF-α levels at 6 h after reperfusion or sham operation were measured by ELISA. (f) The mRNA levels of cytokines and chemokines at 6 h after reperfusion or sham operation were determined by quantitative RT-PCR. All data are shown as mean ± SEM ($n = 4$–6). $^{**}P < 0.01$, $^{*}P < 0.05$.

with the DMSO controls, Alda-1 significantly prevented the decrease in mitochondrial membrane potential (using JC-1 fluorescent dye) and the increase in ROS production (using mitoSOX Red dye) during H/R challenge (Figures 4(a)–4(d)). Thus, we concluded that Alda-1 pretreatment could protect against mitochondrial dysfunction and inhibit oxidative stress during liver IRI.

3.5. Alda-1 Pretreatment Enhances ALDH2 Activity and Decreases Toxic Aldehydes during Liver IRI. As Alda-1 is an ALDH2 activator, we then examined whether Alda-1 treatment activates ALDH2. During liver IRI, although ALDH2 activity was significantly decreased at 6 h and 12 h after reperfusion, Alda-1 pretreatment markedly increased hepatic ALDH2 activity (Figure 5(a)). Interestingly, such ALDH2 activity changes have nothing to do with ALDH2 expression because Western blot assays showed that there were no ALDH2 protein level changes in either sham mice, vehicle controls, or Alda-1 pretreated mice (Supplementary Figures 2A and 2B). As ALDH2 is a key enzyme responsible for the removal of reactive aldehydes, we then investigated whether Alda-1 pretreatment could reduce the accumulation of reactive aldehydes during liver IRI. Both Western blot and IHC assays showed that compared to the vehicle control, Alda-1 pretreatment significantly reduced the levels of 4HNE adducts at 6 h or 12 h after liver reperfusion (Figures 5(b)–

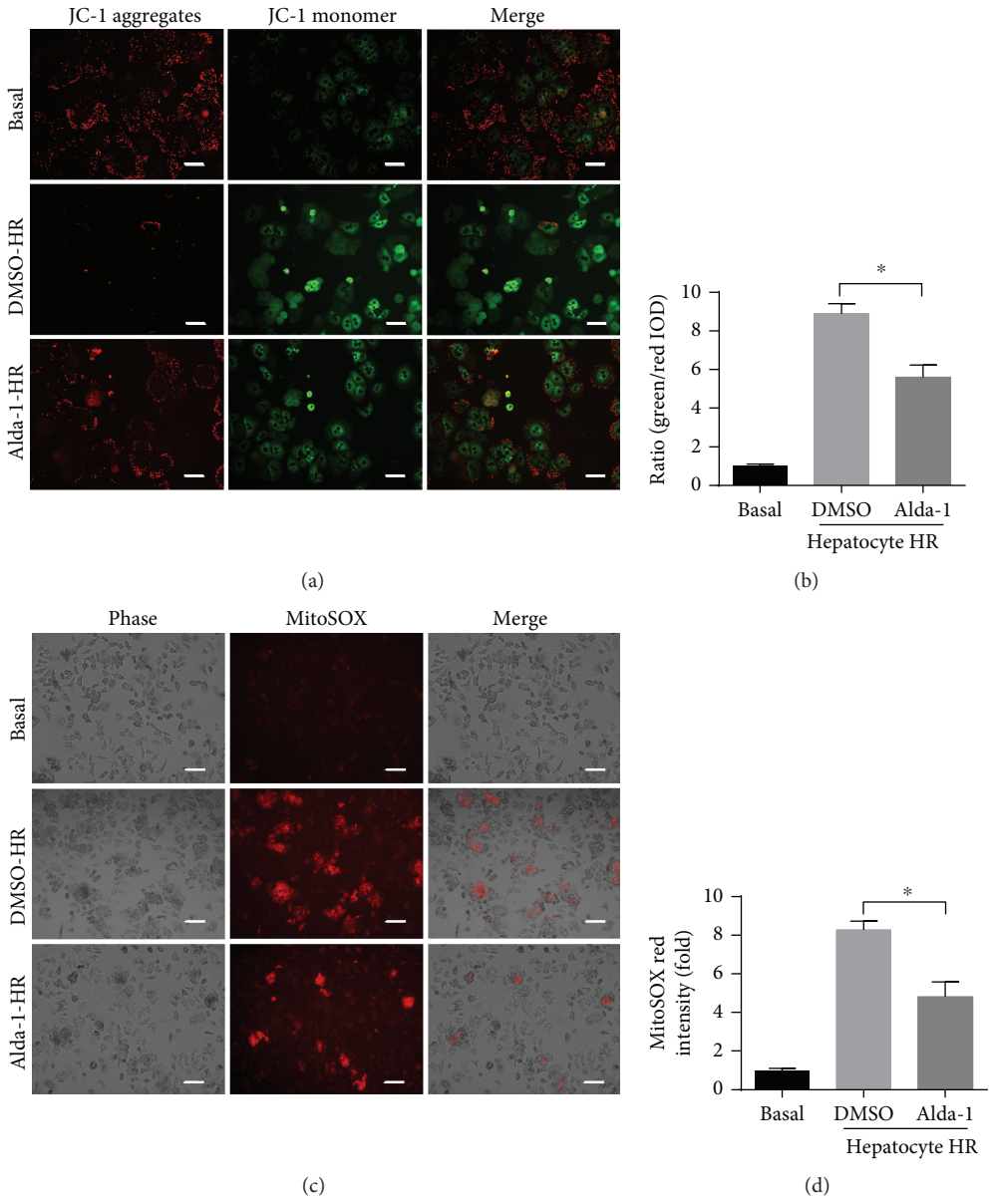

Figure 4: Alda-1 pretreatment alleviates mitochondrial injury and ROS production after HR challenge in vitro. (a, b) Representative pictures of mitochondrial membrane potential of primary hepatocytes after HR challenge with or without Alda-1 pretreatment. The ratio of green to red fluorescence intensity was determined. Scale bars: 25 μm. (c, d) Representative pictures of mitochondrial ROS accumulation of primary hepatocytes after HR injury. The mitochondrial ROS was expressed by the relative red area of the total picture. Scale bars: 50 μm. Data are shown as mean ± SEM ($n = 4$–6). $^*P < 0.05$.

5(d)). In addition, Alda-1 pretreatment also prevented the accumulation of MDA, another type of reactive aldehyde, at 6 h and 12 h after reperfusion (Figure 5(e)). Therefore, these results demonstrated that Alda-1 pretreatment could increase ALDH2 activity and in turn scavenge reactive aldehydes.

3.6. Alda-1-Mediated Hepatoprotection during Liver IRI Is Dependent on Enhanced Autophagy. Previous studies have demonstrated that ALDH2 activation is sufficient to induce autophagy in different physiological and pathological conditions [27, 28]. Consistent with those findings, compared to DMSO controls, Alda-1 treatment significantly enhanced liver autophagy as indicated by increased LC3BII and decreased P62 levels (Figure 6(a) and Supplementary Figure 3A). Correspondingly, the number of autophagosomes in the liver of Alda-1-pretreated mice was considerably increased (Figures 6(b) and 6(c)). To test whether Alda-1-mediated hepatoprotection was dependent on the enhanced autophagy, we investigated the effect of Alda-1 by blocking autophagy with 3-methyladenine (3MA, an autophagy inhibitor). H&E staining and Suzuki's scores showed that the necrotic areas in the liver of Alda-1-pretreated mice were significantly decreased compared to those of the DMSO controls, whereas inhibition of autophagy reversed the protective effect of Alda-1 (Figures 6(d) and 6(e)). In line with the histological data, 3MA-mediated autophagy

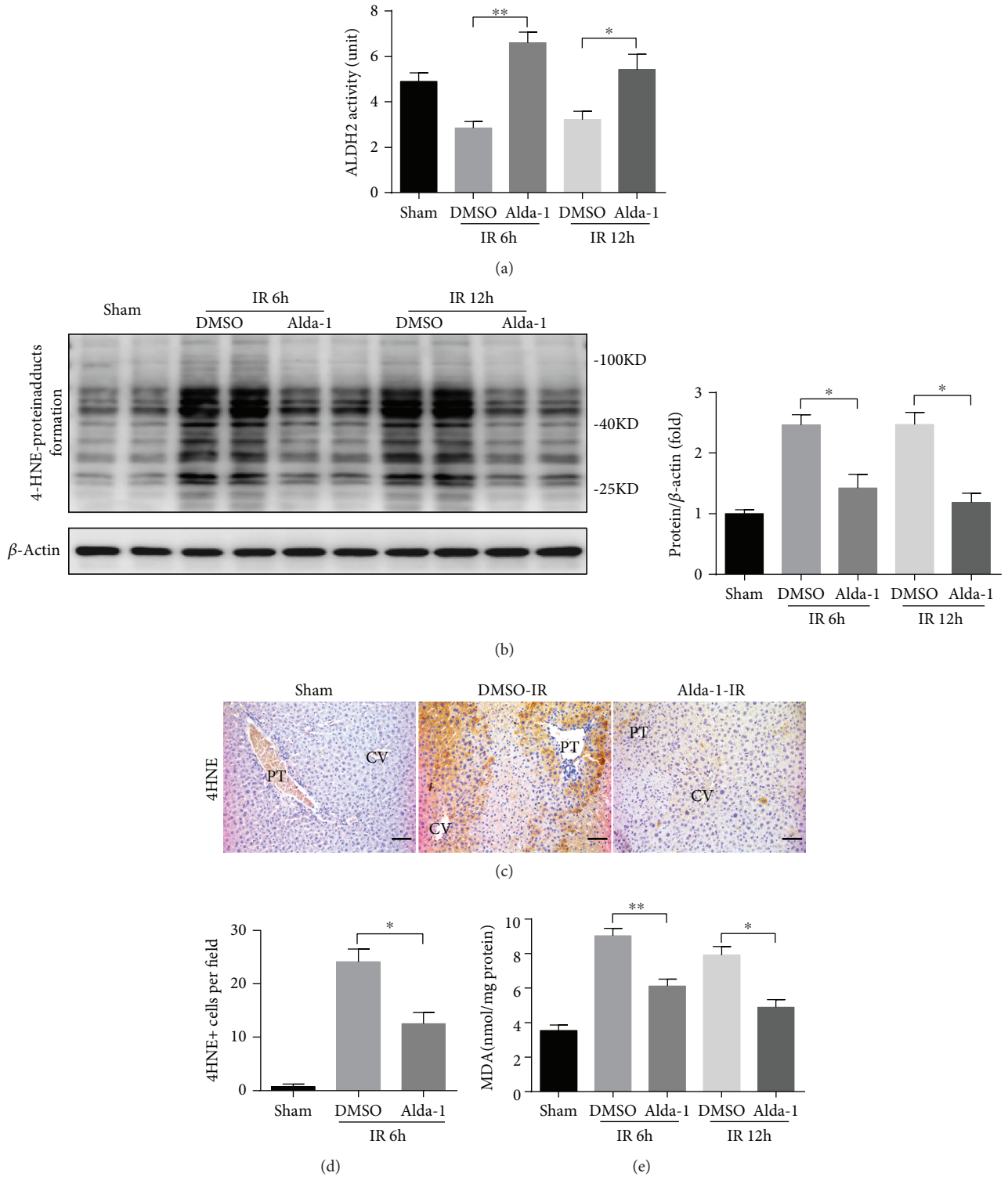

Figure 5: Alda-1 has the efficacy of ALDH2 activity activation and toxic aldehyde clearance during liver IR. (a) ALDH2 activity was observed in liver tissues at 6 and 12 hours after reperfusion or sham operation ($n = 4$–6). (b) Western blot analysis of 4HNE protein adduct expression in liver tissues at 6 and 12 hours after reperfusion or sham operation (β-actin is used as a loading control). (c, d) Representative sections of 4HNE staining and the numbers of 4HNE-positive cells in liver sections at 6 h after reperfusion or sham. PT: portal triads; CV: central veins. Scale bars: 50 μm. (e) The malondialdehyde (MDA) content was measured in liver tissues at 6 and 12 hours after reperfusion or sham operation. All data are shown as mean ± SEM ($n = 4$–6). $^{**}P < 0.01$, $^{*}P < 0.05$.

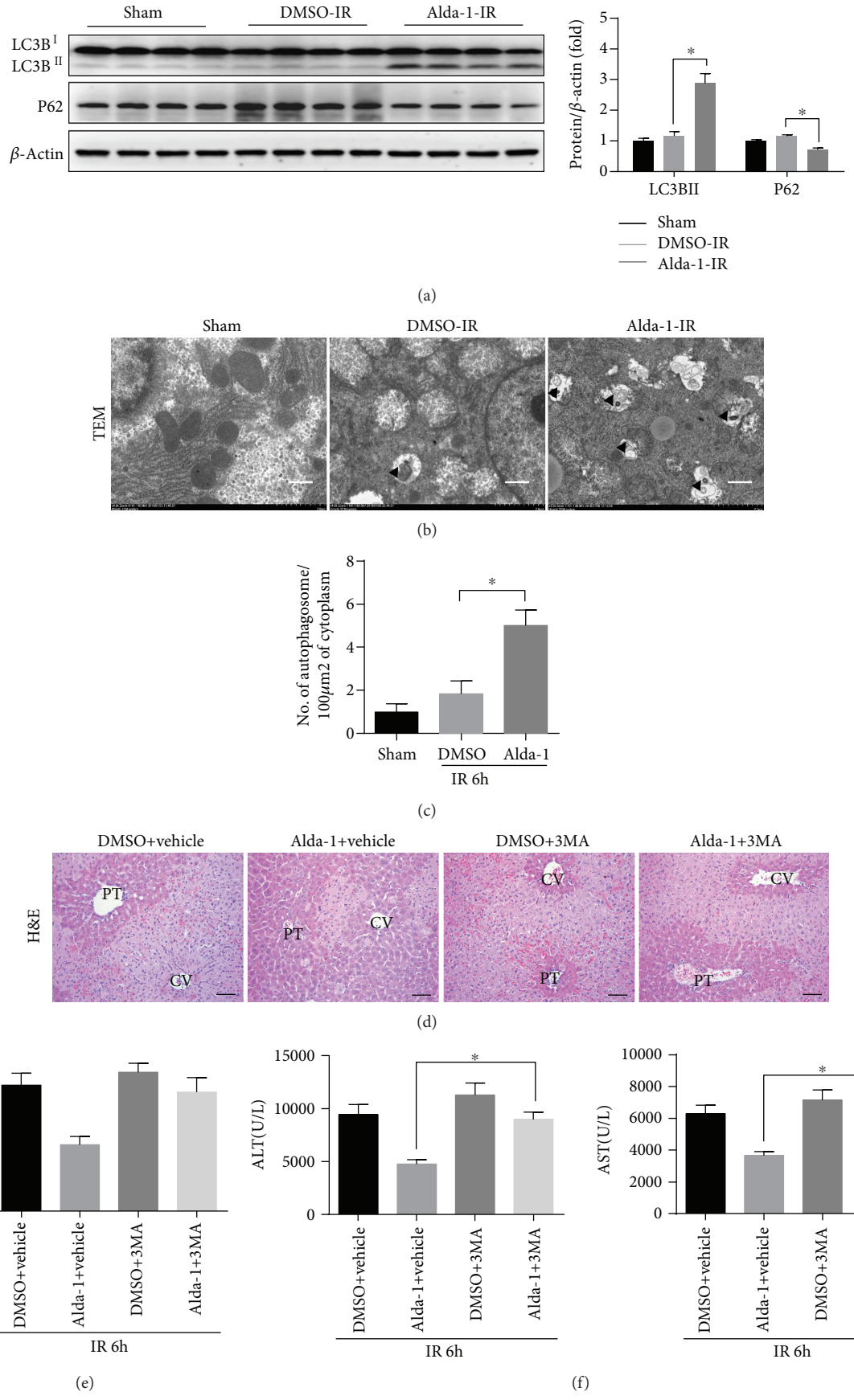

Figure 6: Continued.

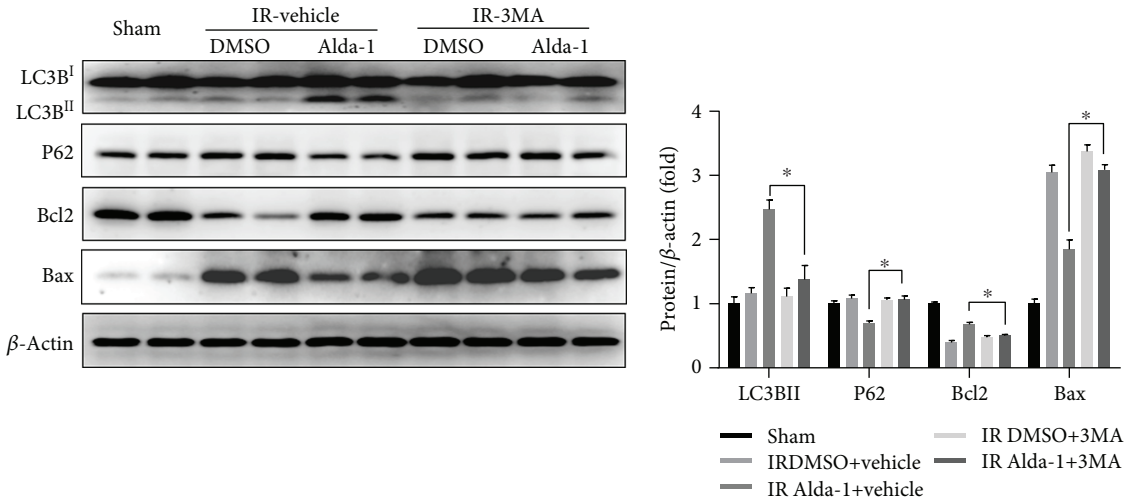

(g)

Figure 6: Autophagy is involved in ALDH2 activation-induced protection of mouse liver IRI. (a) Western blot analysis of LC3B and P62 expression in liver tissues at 6 hours after reperfusion or sham operation (β-actin is used as a loading control). (b, c) Representative transmission electron micrographs showing autophagosomes in the ischemic liver tissues at 6 h after reperfusion (black arrows denote autophagosomes) and the number of autophagosomes in per 100 μm^2 of the cytoplasm. PT: portal triads; CV: central veins. Scale bars: 50 μm. Scale bars: 1 μm. (d–g) Mice were treated with 3-methyladenine 1 h after Alda-1 or pretreated with DMSO and killed at 6 h after reperfusion. (d, e) Representative H&E-stained images and relative Suzuki's scores of the liver section. Scale bars: 50 μm. (f) Serum ALT/AST level. (g) Western blot analysis of LC3B, P62, Bcl2, and Bax expression in liver tissues (β-actin is used as a loading control). All data are shown as mean ± SEM ($n = 4$–6). $^*P < 0.05$.

inhibition also reversed the serum ALT/AST level decrease in Alda-1-treated mice (Figure 6(f)). Western blot assays showed that 3MA abrogated the Alda-1-induced expression increases in LC3BII and Bcl2 and decreases in P62 and Bax (Figure 6(g)). In addition, 3MA-mediated autophagy inhibition sensitize Alda-1-treated primary hepatocytes to H/R injury *in vitro* as indicated by decreased cell viability and increased LDH release levels (Supplementary Figures 3B and 3C). As we have previously demonstrated that rapamycin treatment protects the liver from IRI via both autophagy induction and mTORC2-Akt activation [29], we then test whether rapamycin treatment could further potentiate the hepatoprotective effects of Alda-1. We found that although either Alda-1 or rapamycin treatment decreased liver necrosis and serum ALT/ALT levels, no synergistic effects were observed in the case of cotreatment of Alda-1 and rapamycin (Supplementary Figures 4A–4C). Collectively, these results indicated that Alda-1 pretreatment plays a protective role in liver IRI through the enhancement of autophagy.

3.7. Alda-1-Induced Autophagy Enhancement during Liver IRI Is Mediated by AMPK Activation. Previous studies have shown that reactive aldehydes such as 4HNE impair the activation of AMPK signaling [30, 31]. Given that AMPK activation plays a protective role in liver IRI at least partly through the activation of the autophagy pathway [32, 33], we then tested whether the Alda-1-mediated hepatoprotection during liver IRI is attributed to AMPK activation. Western blot assays showed that, compared to sham and vehicle controls, Alda-1 pretreatment markedly increased the phosphorylation levels of AMPK in liver tissues after IRI (Figure 7(a)). Consistently, Alda-1 treatment also enhanced AMPK phosphorylation in primary hepatocytes after H/R challenge (Supplementary Figure 5A). To determine whether Alda-1-induced autophagy enhancement is dependent on AMPK activation, compound C (CC, a specific AMPK inhibitor) was employed to block AMPK activation during liver IRI. AMPK inhibition by CC blunted the hepatoprotection of Alda-1 during liver IRI as evidenced by increased hepatic necrosis areas and serum ALT/AST levels (Figures 7(b)–7(d)). In addition, Western blot showed that CC treatment resulted in a significant decrease in AMPK phosphorylation and Bcl2 and LC3BII expression and a marked increase in P62 and Bax expression (Figure 7(e)). Correspondingly, CC treatment significantly decreased cell viability and increased LDH release in primary hepatocytes treated with Alda-1 after H/R *in vitro* (Supplementary Figures 5B and 5C). Thus, these findings suggested that AMPK activation is necessary for Alda-1-mediated autophagy activation during liver IRI.

4. Discussion

In our present study, we demonstrated that Alda-1, an ALDH2 agonist, protects against liver IRI. In detail, Alda-1 treatment attenuated liver necrosis and hepatocyte apoptosis, reduced inflammatory responses, and inhibited mitochondrial dysfunction and ROS production during liver IRI. The underlying mechanisms of the protective role of Alda-1 were associated with the direct clearance of reactive aldehydes and the indirect autophagy enhancement which is induced by AMPK activation.

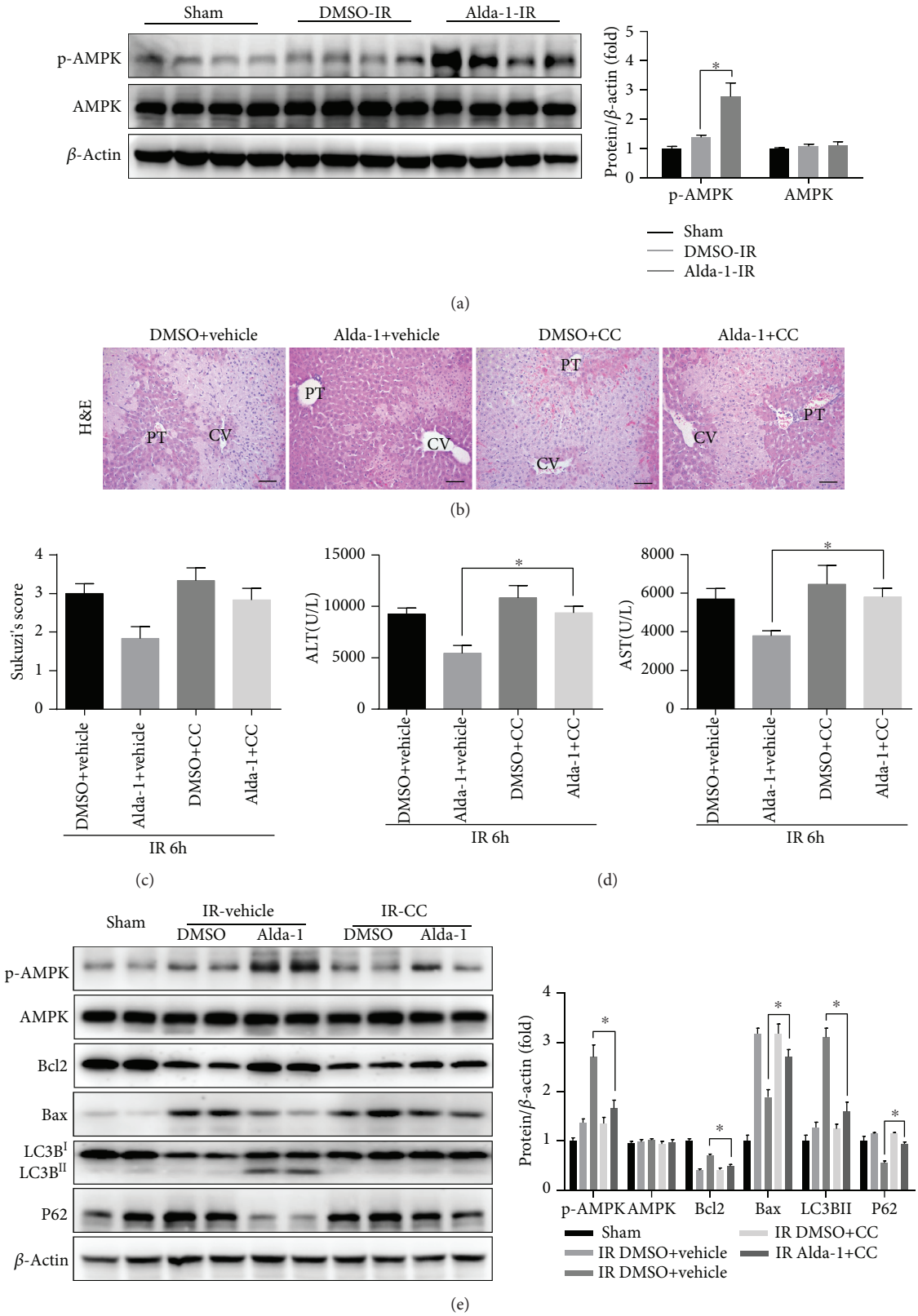

Figure 7: AMPK activation is involved in autophagy enhancement by Alda-1 pretreatment during liver IR. (a) Western blot analysis of p-AMPK and AMPK expression in liver tissues at 6 hours after reperfusion or sham operation (β-actin is used as a loading control). (b–d) Mice were treated with CC 1 h after Alda-1 or pretreated with DMSO and killed at 6 h after reperfusion. (b, c) Representative H&E-stained images and relative Suzuki's scores of the liver section. PT: portal triads; CV: central veins. Scale bars: 50 μm. Scale bars: 50 μm. (d) Serum ALT/AST level. (e) Western blot analysis of p-AMPK, AMPK, Bcl2 and Bax, LC3B, and P62 expression in liver tissues (β-actin is used as a loading control). All data are shown as mean ± SEM ($n = 4$–6). $^*P < 0.05$.

During IRI, increased ROS production is a major detrimental event to cause cell damage and even death, partly because ROS attacks various critical biological lipids, particularly membrane phospholipids, leading to the formation of reactive aldehydes, such as 4HNE and MDA, to further aggravate the injury [34]. Although multiple lines of evidence has demonstrated that ALDH2 is the major enzyme to detoxify those reactive aldehydes, the phenomenon that ALDH2 activity is usually inhibited during IRI makes it impossible to scavenge reactive aldehydes effectively [15, 16, 19–22], which consequently leads to massive accumulation of those toxic reactive aldehydes and cell damage. Therefore, activating ALDH2 is a conceivable approach to improve IRI. In fact, administration of Alda-1 has been demonstrated to improve IRI in many other organs except the liver [16, 19–22]. In the present study, we also demonstrated decreased ALDH2 activity in the mouse liver IRI model and administration of Alda-1 could significantly increase ALDH2 activity, which was independent of ALDH2 expression changes. Consequently, Alda-1-mediated enhancement of ALDH2 activity blocked the accumulation of 4HNE and MDA and improved the liver IRI.

In addition to causing cell damage and death, reactive aldehydes have also been reported to activate the NF-κB pathway linking to activation of inflammatory responses [35]; therefore, reactive aldehydes could induce inflammatory responses directly and indirectly. In the present study, we show that Alda-1 treatment could ameliorate hepatocyte apoptosis and sterile inflammation during liver IRI, which is consistent with previous reports showing that Alda-1 has both antiapoptosis and anti-inflammatory properties [19–22].

Autophagy is generally recognized as a cellular protective pathway in response to various intracellular or extracellular stimuli. Although the function of autophagy in IRI remains controversial, we and other groups have identified the protective role of autophagy during liver IRI [7–9, 29]. In the present study, we found autophagy enhancement after Alda-1 treatment with increased levels of LC3BII, P62 degradation, and autophagosomes. Apparently, the hepatoprotective role of Alda-1 was dependent on autophagy because 3MA-mediated autophagy inhibition greatly diminished the hepatoprotective effects of Alda-1 during liver IRI or *in vitro* H/R treatment. Interestingly, rapamycin-induced autophagy enhancement could not further augment Alda-1-mediated hepatoprotection, suggesting that Alda-1 and rapamycin do not work synergistically.

A recent study has shown that protein adducts of reactive aldehydes inhibit the activation of LKB resulting in impaired signaling activity of the LKB1/AMPK/mTOR pathway [30]. In addition, ALDH2 has been reported to protect myocardial function through an AMPK-dependent autophagy activation axis in an experimental diabetic cardiomyopathy model [28]. In the present study, we also found that Alda-1 treatment induced the activation of AMPK, whereas compound C-mediated AMPK inhibition greatly abrogated the protective role of Alda-1 and autophagy activation. Moreover, given the fact that 4HNE could directly target AMPK to inhibit its activity [31], we propose that Alda-1 treatment directly or indirectly activates AMPK resulting in autophagy activation during liver IRI.

Data Availability

The data used to support the findings of this study are available from the corresponding author upon request.

Conflicts of Interest

The authors have declared that they have no conflicts of interest.

Authors' Contributions

Meng Li and Min Xu contributed equally to this work.

Acknowledgments

This work was supported by the National Natural Science Foundation of China (81670562 to X. Kong, 81670598 to Q. Xia, and 31671453 to H. Wu), the Shanghai Municipal Education Commission—Gaofeng Clinical Medicine Grant Support (20171911 to X. Kong), a grant from the Committee of Science and Technology of Shanghai Municipal Government (16401970600-03 to X. Kong), and the National Key Research and Development Program of China (2017YFC0908100 to Q. Xia).

Supplementary Materials

Supplementary Figure 1: Alda-1 usage at different concentrations and times. Supplementary Figure 2: the expression of ALDH2 in liver IR. Supplementary Figure 3: autophagy enhancement in hepatocyte HR challenge. Supplementary Figure 4: combined use of rapamycin and Alda-1. Supplementary Figure 5: AMPK activation in hepatocyte HR challenge. *(Supplementary Materials)*

References

[1] Y. Zhai, H. Petrowsky, J. C. Hong, R. W. Busuttil, and J. W. Kupiec-Weglinski, "Ischaemia–reperfusion injury in liver transplantation—from bench to bedside," *Nature Reviews Gastroenterology & Hepatology*, vol. 10, no. 2, pp. 79–89, 2013.

[2] H. Jaeschke and B. L. Woolbright, "Current strategies to minimize hepatic ischemia-reperfusion injury by targeting reactive oxygen species," *Transplantation Reviews*, vol. 26, no. 2, pp. 103–114, 2012.

[3] A. J. Vardanian, R. W. Busuttil, and J. W. Kupiec-Weglinski, "Molecular mediators of liver ischemia and reperfusion injury: a brief review," *Molecular Medicine*, vol. 14, no. 5-6, pp. 337–345, 2008.

[4] T. Yorimitsu and D. J. Klionsky, "Autophagy: molecular machinery for self-eating," *Cell Death and Differentiation*, vol. 12, Supplement 2, pp. 1542–1552, 2005.

[5] P. E. Rautou, A. Mansouri, D. Lebrec, F. Durand, D. Valla, and R. Moreau, "Autophagy in liver diseases," *Journal of Hepatology*, vol. 53, no. 6, pp. 1123–1134, 2010.

[6] L. Murrow and J. Debnath, "Autophagy as a stress-response and quality-control mechanism: implications for cell injury and human disease," *Annual Review of Pathology*, vol. 8, no. 1, pp. 105–137, 2013.

[7] D. Xu, L. Chen, X. Chen et al., "The triterpenoid CDDO-imidazolide ameliorates mouse liver ischemia-reperfusion injury through activating the Nrf2/HO-1 pathway enhanced autophagy," *Cell Death & Disease*, vol. 8, no. 8, article e2983, 2017.

[8] J. Cardinal, P. Pan, and A. Tsung, "Protective role of cisplatin in ischemic liver injury through induction of autophagy," *Autophagy*, vol. 5, no. 8, pp. 1211-1212, 2009.

[9] A. Liu, H. Fang, W. Wei, O. Dirsch, and U. Dahmen, "Ischemic preconditioning protects against liver ischemia/reperfusion injury via heme oxygenase-1-mediated autophagy," *Critical Care Medicine*, vol. 42, no. 12, pp. e762–e771, 2014.

[10] K. M. Quesnelle, P. V. Bystrom, and L. H. Toledo-Pereyra, "Molecular responses to ischemia and reperfusion in the liver," *Archives of Toxicology*, vol. 89, no. 5, pp. 651–657, 2015.

[11] S. Haga, S. J. Remington, N. Morita, K. Terui, and M. Ozaki, "Hepatic ischemia induced immediate oxidative stress after reperfusion and determined the severity of the reperfusion-induced damage," *Antioxidants & Redox Signaling*, vol. 11, no. 10, pp. 2563–2572, 2009.

[12] M. Fukai, T. Hayashi, R. Yokota et al., "Lipid peroxidation during ischemia depends on ischemia time in warm ischemia and reperfusion of rat liver," *Free Radical Biology & Medicine*, vol. 38, no. 10, pp. 1372–1381, 2005.

[13] K. Uchida, "4-Hydroxy-2-nonenal: a product and mediator of oxidative stress," *Progress in Lipid Research*, vol. 42, no. 4, pp. 318–343, 2003.

[14] C. H. Chen, L. A. Cruz, and D. Mochly-Rosen, "Pharmacological recruitment of aldehyde dehydrogenase 3A1 (ALDH3A1) to assist ALDH2 in acetaldehyde and ethanol metabolism in vivo," *Proceedings of the National Academy of Sciences of the United States of America*, vol. 112, no. 10, pp. 3074–3079, 2015.

[15] K.–. H. Moon, B. L. Hood, P. Mukhopadhyay et al., "Oxidative inactivation of key mitochondrial proteins leads to dysfunction and injury in hepatic ischemia reperfusion," *Gastroenterology*, vol. 135, no. 4, pp. 1344–1357, 2008.

[16] C. H. Chen, G. R. Budas, E. N. Churchill, M. H. Disatnik, T. D. Hurley, and D. Mochly-Rosen, "Activation of aldehyde dehydrogenase-2 reduces ischemic damage to the heart," *Science*, vol. 321, no. 5895, pp. 1493–1495, 2008.

[17] S. Perez-Miller, H. Younus, R. Vanam, C. H. Chen, D. Mochly-Rosen, and T. D. Hurley, "Alda-1 is an agonist and chemical chaperone for the common human aldehyde dehydrogenase 2 variant," *Nature Structural & Molecular Biology*, vol. 17, no. 2, pp. 159–164, 2010.

[18] J. A. Belmont-Diaz, B. Yoval-Sanchez, L. F. Calleja-Castaneda, J. P. Pardo Vazquez, and J. S. Rodriguez-Zavala, "Alda-1 modulates the kinetic properties of mitochondrial aldehyde dehydrogenase (ALDH2)," *The FEBS Journal*, vol. 283, no. 19, pp. 3637–3650, 2016.

[19] S. H. Fu, H. F. Zhang, Z. B. Yang et al., "Alda-1 reduces cerebral ischemia/reperfusion injury in rat through clearance of reactive aldehydes," *Naunyn-Schmiedeberg's Archives of Pharmacology*, vol. 387, no. 1, pp. 87–94, 2014.

[20] J. Ding, Q. Zhang, Q. Luo et al., "Alda-1 attenuates lung ischemia-reperfusion injury by reducing 4-hydroxy-2-nonenal in alveolar epithelial cells," *Critical Care Medicine*, vol. 44, no. 7, pp. e544–e552, 2016.

[21] Z. Zhong, Q. Hu, Z. Fu et al., "Increased expression of aldehyde dehydrogenase 2 reduces renal cell apoptosis during ischemia/reperfusion injury after hypothermic machine perfusion," *Artificial Organs*, vol. 40, no. 6, pp. 596–603, 2016.

[22] Q. Zhu, G. He, J. Wang, Y. Wang, and W. Chen, "Pretreatment with the ALDH2 agonist Alda-1 reduces intestinal injury induced by ischaemia and reperfusion in mice," *Clinical Science*, vol. 131, no. 11, pp. 1123–1136, 2017.

[23] S. Suzuki, L. H. Toledo-Pereyra, F. J. Rodriguez, and D. Cejalvo, "Neutrophil infiltration as an important factor in liver ischemia and reperfusion injury. Modulating effects of FK506 and cyclosporine," *Transplantation*, vol. 55, no. 6, pp. 1265–1272, 1993.

[24] Y. Wen, D. Feng, H. Wu et al., "Defective initiation of liver regeneration in osteopontin-deficient mice after partial hepatectomy due to insufficient activation of IL-6/Stat3 pathway," *International Journal of Biological Sciences*, vol. 11, no. 10, pp. 1236–1247, 2015.

[25] P. Georgiev, F. Dahm, R. Graf, and P. A. Clavien, "Blocking the path to death: anti-apoptotic molecules in ischemia/reperfusion injury of the liver," *Current Pharmaceutical Design*, vol. 12, no. 23, pp. 2911–2921, 2006.

[26] J. Lutz, K. Thurmel, and U. Heemann, "Anti-inflammatory treatment strategies for ischemia/reperfusion injury in transplantation," *Journal of Inflammation*, vol. 7, no. 1, p. 27, 2010.

[27] R. Guo, X. Xu, S. A. Babcock, Y. Zhang, and J. Ren, "Aldehyde dedydrogenase-2 plays a beneficial role in ameliorating chronic alcohol-induced hepatic steatosis and inflammation through regulation of autophagy," *Journal of Hepatology*, vol. 62, no. 3, pp. 647–656, 2015.

[28] Y. Guo, W. Yu, D. Sun et al., "A novel protective mechanism for mitochondrial aldehyde dehydrogenase (ALDH2) in type i diabetes-induced cardiac dysfunction: role of AMPK-regulated autophagy," *Biochimica et Biophysica Acta (BBA) - Molecular Basis of Disease*, vol. 1852, no. 2, pp. 319–331, 2015.

[29] J. Zhu, T. Lu, S. Yue et al., "Rapamycin protection of livers from ischemia and reperfusion injury is dependent on both autophagy induction and mammalian target of rapamycin complex 2-Akt activation," *Transplantation*, vol. 99, no. 1, pp. 48–55, 2015.

[30] T. D. Calamaras, C. Lee, F. Lan, Y. Ido, D. A. Siwik, and W. S. Colucci, "The lipid peroxidation product 4-hydroxy-*trans*-2-nonenal causes protein synthesis in cardiac myocytes via activated mTORC1–p70S6K–RPS6 signaling," *Free Radical Biology & Medicine*, vol. 82, pp. 137–146, 2015.

[31] C. T. Shearn, D. S. Backos, D. J. Orlicky, R. L. Smathers-McCullough, and D. R. Petersen, "Identification of 5' AMP-activated kinase as a target of reactive aldehydes during chronic ingestion of high concentrations of ethanol," *The Journal of Biological Chemistry*, vol. 289, no. 22, pp. 15449–15462, 2014.

[32] M. Zhang, D. Yang, X. Gong et al., "Protective benefits of AMP-activated protein kinase in hepatic ischemia-reperfusion injury," *American Journal of Translational Research*, vol. 9, no. 3, pp. 823–829, 2017.

[33] S. Herzig and R. J. Shaw, "AMPK: guardian of metabolism and mitochondrial homeostasis," *Nature Reviews Molecular Cell Biology*, vol. 19, no. 2, pp. 121–135, 2018.

[34] F. J. Romero, F. Bosch-Morell, M. J. Romero et al., "Lipid peroxidation products and antioxidants in human disease," *Environmental Health Perspectives*, vol. 106, Supplement 5, pp. 1229–1234, 1998.

[35] M. Shoeb, N. H. Ansari, S. K. Srivastava, and K. V. Ramana, "4-Hydroxynonenal in the pathogenesis and progression of human diseases," *Current Medicinal Chemistry*, vol. 21, no. 2, pp. 230–237, 2014.

Hindawi
Journal of Immunology Research
Volume 2018, Article ID 8363265, 12 pages
https://doi.org/10.1155/2018/8363265

Research Article

Total HLA Class I Antigen Loss with the Downregulation of Antigen-Processing Machinery Components in Two Newly Established Sarcomatoid Hepatocellular Carcinoma Cell Lines

Wei-Yi Lei,[1,2,3] **Shih-Chieh Hsiung**,[4] **Shao-Hsuan Wen**,[5] **Chin-Hsuan Hsieh**,[4] **Chien-Lin Chen**,[1,2,3] **Christopher Glenn Wallace**,[6] **Chien-Chung Chang**,[5,7] **and Shuen-Kuei Liao**[8,9]

[1]*Institute of Medical Sciences, Tzu Chi University, Hualien, Taiwan*
[2]*College of Medicine, Tzu Chi University, Hualien, Taiwan*
[3]*Department of Medicine, Hualien Tzu Chi Hospital, Buddhist Tzu Chi Medical Foundation, Hualien, Taiwan*
[4]*Division of Urology, Department of Surgery, Chang Gung Memorial Hospital, Taoyuan, Taiwan*
[5]*Institute of Molecular and Cellular Biology, National Tsing Hua University, Hsinchu, Taiwan*
[6]*Department of Plastic and Reconstructive Surgery, Chang Gung Memorial Hospital, Taoyuan, Taiwan*
[7]*Department of Life Science, National Tsing Hua University, Hsinchu, Taiwan*
[8]*The Ph.D. Program for Cancer Biology and Drug Discovery, Taipei Medical University, Taipei City, Taiwan*
[9]*Vectorite Biomedica/U-Well Biopharma Inc., New Taipei City, Taiwan*

Correspondence should be addressed to Chien-Chung Chang; ccchang@life.nthu.edu.tw
and Shuen-Kuei Liao; liaosk@h.tmu.edu.tw

Received 27 January 2018; Revised 19 June 2018; Accepted 2 August 2018; Published 16 December 2018

Academic Editor: Xiaoni Kong

Limited information is currently available concerning HLA class I antigen abnormalities in sarcomatoid hepatocellular carcinoma (sHCC). Here, we have analyzed the growth characteristics and HLA class I antigen status of four sHCC cell lines (sHCC29, sHCC63, sHCC74, and SAR-HCV); the first three were newly established in this study. Among the four, sHCC29 showed the highest growth rate *in vitro* and tumorigenicity in NOD-SCID mice. Unlike sHCC74 and SAR-HCV, both sHCC29 and sHCC63 had no detectable surface HLA class I antigen expression, alongside undetected intracellular β_2-microglobulin (β_2m) and marked HLA class I heavy chain and selective antigen-processing machinery (APM) component downregulation. The loss of β_2m in sHCC29 and sHCC63 was caused by a >49 kb deletion across the *B2M* locus, while their downregulation of APM components was transcriptional, reversible by IFN-γ only in several components. β_2m was also undetected in the primary HCC lesions of the patients involved, indicating its *in vivo* relevance. We report for the first time HLA class I antigen loss with underlying *B2M* gene deficiency and APM defects in 50% (2 of 4) of the sHCC cell lines tested. These findings may have implications for a proper design of T cell immunotherapy for the treatment of sHCC patients.

1. Introduction

Hepatocellular carcinoma (HCC) is the 6th most common solid tumor and the third leading cause of cancer-related death worldwide [1, 2]. Although the role of hepatitis B virus (HBV) and HCV in hepatocarcinogenesis has been well documented, its precise mechanism remains largely unknown, especially for HCV-associated hepatocarcinogenesis. It has been reported that some liver tumors, including HCC, cholangiocarcinoma, and hepatocholangiocarcinoma, may undergo sarcomatous change [3], a phenomenon closely associated with epithelial-mesenchymal transition (EMT) and neoplastic progression [4, 5]. Notably, the primary liver sarcomatous carcinomas have been found to arise with or without cirrhosis pathology [6]. Although sarcomatous liver tumors are rare with only about 50 cases reported thus far

in the English medical literature [7–10], these sarcomatoid carcinomas are highly aggressive, characterized by a fast clinical course with a poor prognosis [10, 11]. No effective therapy is currently available for the treatment of this rare tumor subtype.

It has been known for some time that malignant cells can have impaired HLA class I antigen expression during the course of tumor progression [12–15]. HLA class I antigen downregulation or loss often occurs in tumor cells when the primary tumor breaks the basal membrane, invades the surrounding tissues, and/or begins to metastasize to regional lymph nodes or to distant organs with the latter occurring at higher frequencies [16, 17]. Since HLA class I antigens present tumor antigen-derived peptides to the host cytotoxic T lymphocytes (CTLs), altered or deficient HLA class I antigen expression by malignant cells constitutes an effective mechanism to escape HLA class I-restricted T cell antitumor surveillance. The clinical relevance of HLA class I antigen downregulation or loss in tumors has been indicated by its association with poor prognosis of several malignant diseases, including melanoma, breast cancer, and clear cell renal cell carcinoma [17]. In a therapeutic setting, the effector function of T cells could be dampened by the HLA class I antigen abnormalities in tumors, and this may pose an obstacle to therapeutic success. This possibility may explain the outcome of the recent T cell immune checkpoint blockade therapy of melanoma [18] and NSCLC [19], which is effective but with only 20–25% of response rate.

The HLA class I antigen status in tumor cells may represent a key variable for the efficacy of therapy that relies on CTLs to eliminate the tumor cells [20]. Primary HCCs have been reported to have sufficient levels of HLA class I antigens expressed [21, 22], yet currently, no information is available regarding the expression status of these molecules in the sarcomatoid subtype of HCC (sHCC) and its association with prognosis of the disease. Therefore, we herein established three sHCC cell lines derived from the surgically removed liver tumors of three patients with apparent sarcomatoid changes in the lesion; one is HCV-related while the other two are HBV-related. Together with a previously established sHCC cell line known as SAR-HCV [23], we have analyzed their HLA class I antigen expression and found that two of the four cell lines harbored a large deletion in the $\beta_2 m$ gene, associated with downregulation of several components in the HLA class I antigen presentation pathway.

2. Materials and Methods

2.1. The Patients. The clinical histories of patients from whom the three newly established sHCC cell lines originated are as follows.

2.1.1. Case 1 (sHCC29). A 58-year-old woman with history of liver cancer originating from chronic hepatitis B was admitted to Taipei Tzu Chi Hospital, Taiwan, in August 2010, with chief complaints of yellowish discoloration of the skin and tea-color urine for one week. She has received transcatheter arterial chemoembolisation (TACE) three months prior to admission to this hospital. Laboratory tests showed elevated serum total bilirubin (5.1 mg/dL), alpha-fetoprotein (182.7 ng/mL), and carbohydrate antigen 19-9 (70.5 U/mL) levels. The carcinoembryonic antigen (CEA) serum level was within the upper limit of normal. Computed tomography revealed a hypervascular mass in the liver hilum measuring 4×5 cm. The patient underwent left lobectomy, and pathology showed proliferation of spindle-shaped hepatocellular carcinoma cells. The patient has survived for 5 additional years without tumor recurrence as of this writing.

2.1.2. Case 2 (sHCC63). A 39-year-old man with a history of HBV-related cirrhosis was referred to Hualien Tzu Chi General Hospital, Taiwan, in May 2011, diagnosed as having liver cancer without any previous treatment for HCC. The alpha-fetoprotein serum level was 123.5 ng/mL. Both the carbohydrate antigen 19-9 and CEA serum levels were within the normal range. The combination of computed tomography with hepatic arteriography and arterial portography (CTHA/CTAP) showed a huge hypervascular tumor in the right lobe of the liver. The patient underwent liver resection. Histological examination revealed spindle-shaped sarcomatoid carcinoma cells with unclear trabecular and pseudoglandular structures. However, the tumor relapsed in the residual liver 5 months after surgery, and despite TACE therapy, the patient died one year later.

2.1.3. Case 3 (sHCC74). A 72-year-old woman was admitted to Hualien Tzu Chi General Hospital, Taiwan, and diagnosed as having liver cancer originating from chronic hepatitis C. The alpha-fetoprotein, carbohydrate antigen 19-9, and CEA serum levels were all within the upper limit of normal. Computed tomography showed a hypervascular tumor in the caudate lobe of the liver measuring 5×6 cm. She underwent segmentectomy, and pathology revealed spindle-shaped sarcomatoid carcinoma cells. One year after surgery, the tumors relapsed in the residual liver. The patient began with TACE therapy. Unfortunately, she died two years later.

2.2. Establishment of sHCC Cell Lines. Three sHCC cell lines were established from HCC tissues during surgery performed at Hualien Tzu Chi Hospital with patients' consent. The study has been approved by the Research Ethics Committee in Tzu Chi General Hospital (IRB 101–62). The three sHCC cell lines (sHCC29, sHCC63, and sHCC74) were established according to standard procedures. Essentially, the minced HCC tissues were pretreated with collagenase, washed, and cultivated on the mitomycin C-treated NIH/3T3 feeder layer for 4 to 6 passages to select the HCC cell lines. Homogenous HCC cell populations were obtained, and sustained proliferation was observed over 30 passages in culture *in vitro*. Cultured cell lines between 18 and 24 passages were used in the subsequent studies.

The fourth sHCC cell line known as SAR-HCV cell line was previously established from a malignant liver lesion of a 68-year-old male patient infected with HCV. Its initial characterization has been reported previously [23, 24].

2.3. Xenotransplantation of Four Established sHCC Cell Lines into Severe Combined Immunodeficiency Mice. Six-week-old female Non-Obese Diabetic (genetic background)/Severe

Combined Immunodeficiency (SCID) mice were purchased from BioLASCO, Taiwan Co. Ltd., Taipei, Taiwan. Tumorigenicity assays of the three cell lines (sHCC29, sHCC63, and sHCC74) were carried out in such mice in this study ($n = 5$/group). The experimental protocol was approved by the Animal Ethics Committee, Chang Gung University, Taoyuan, Taiwan. Single cell suspensions of the three cell lines were prepared from monolayer cultures by light trypsinization and washing in phosphate-buffered saline (PBS). Cells were then counted, and 10^7 cells/0.1 mL PBS were inoculated into the flank of each mouse. The animals were examined every 2 days to monitor the growth of tumors. The volume of palpable tumor nodules was calculated according to the formula volume$(\text{mm}^3) = 0.4 \times a \times b^2$, where ($a$) is the major diameter, and (b) is the minor diameter perpendicular to the major one.

2.4. IFN-γ. Recombinant human IFN-γ was purchased from R&D Systems, Inc. (Minneapolis, MN).

2.5. Monoclonal Antibodies (mAb) and Polyclonal Antibodies. The mAb W6/32, which recognizes β_2m-associated HLA-A, HLA-B, HLA-C, HLA-E, and HLA-G heavy chains [25, 26], was purchased from Thermo Fisher Scientific, Fremont, CA. The mAb TP25.99, which recognizes β_2m-free and β_2m-assciated HLA-A, HLA-B, and HLA-C heavy chains [27], the mAb B1.23.1, which recognizes β_2m-associated HLA-B, HLA-C heavy chains [28], the mAb HC10, which recognizes a determinant expressed on β_2m-free HLA-A10, HLA-A28, HLA-A29, HLA-A30, HLA-A31, HLA-A32, and HLA-A33 heavy chains and on all HLA-B and HLA-C heavy chains [29, 30], the mAb HCA2, which recognizes a determinant expressed on β_2m-free HLA-A (except HLA-A24), HLA-B7301 and HLA-G heavy chains [31], the β_2m-specific mAb L368 [32], the LMP-2-specific mAb SY-1 [33], the LMP7-specific mAb HB2 [34], the TAP1-specific mAb NOB1 [35], the TAP2-specific mAb NOB2, and the HLA-DR, HLA-DP, HLA-DQ-specific mAb LGII-612.14 [34] were previously produced and characterized. Fluorescein-isothiocyanate conjugated goat anti-mouse IgG antibodies were purchased from DAKO (Glostrup, Denmark).

2.6. Cytofluorometric Analysis. Cell surface and cytoplasmic staining with mAbs were conducted as described previously [34]. Purified normal mouse serum IgG or an isotype-matched mouse myeloma IgG was used as specific negative controls. Stained cells were analyzed by using a BD FACS-Verse™ flow cytometer (BD Biosciences, San Jose, CA). Results were expressed as % positively stained cells and as mean fluorescence intensity (MFI).

2.7. Reverse-Transcriptase-Polymerase Chain Reaction (RT-PCR) and Genomic PCR. Total RNA was isolated utilizing the TRIZOL reagent (Invitrogen, Carlsbad, CA) following the manufacturer's instructions. RT-PCR was performed with the primers for β_2m, *LMP2*, *LMP7*, *TAP1*, *TAP2*, and glyceraldehyde-3-phosphate dehydrogenase (*GAPDH*) as a loading control (Table 1). The following PCR conditions were used: 40 cycles at 95°C for 1 min, 60°C for 1.5 min, and 72°C for 2 min with a 10 min extension after the last cycle. Genomic DNA was isolated from sHCC cells utilizing the mammalian genomic DNA extraction mini-prep kit (Sigma, Dorset, England) according to the manufacturer's instructions. PCR was initially carried out using *B2M* gene-specific primers, forward 744F and reverse 468R, to amplify the promoter-to-intron 1 region. For determining the length of deletion in the gene, a panel of additional primers encompassing the *B2M* gene locus at 15q15 was designed based on NCBI GenBank Accession AC018901 (Supplementary Table 1) and used in PCR. The PCR products were fractionated on a 1% agarose gel (Roche, Indianapolis, IN) and visualized by ethidium bromide staining. For bands from RT-PCR, the density of bands was read by a densitometer, ChemiSmart 3000, equipped with the Bioprofil 1D++ software (Viber Lournat, Marne-la-Vallee, France). The relative level of transcript in each experimental group was estimated after normalization with the density of the resulting *GAPDH* band of the same experimental group.

Table 1: Primers used for RT-PCR analysis of β_2m and selected antigen-processing machinery component mRNA expression.

Gene	Nucleotide sequence (5′–3′)	Length (bp)
B2M	GGGCATTCCTGAAGCTGACA TGCGGCATCTTCAAACCTCC	424
LMP2	TTGTGATGGGTTCTGATTCCCG CAG AGCAATAGCGTCTGTGG	449
LMP7	TCGCCTTCAAGTTCCAGCATGG CAACCATCTTCCTTCAT GTGG	542
TAP1	TCTCCTCTCTTGGGGAGATG GAGACATGATGTTACCTGTCTG	273
TAP2	CTCCTCGTTGCCGGCTTCT TCAGCTCCCCTGTCTTAGTC	298
GAPDH	TTCATTGACCTCAACTACAT GAGGGGCCATCCACAGTCTT	469

2.8. Immunohistochemistry. Three-micron-thick affined formalin-fixed paraffin-embedded tumor blocks obtained from patients were processed in the Pathology Department, Tzu Chi General Hospital in Hualien, Taiwan. Prior to immunostaining, the deparaffinized slides were subjected to an antigen-retrieval process by dipping the slides in a breaker containing 0.01 M sodium citrate (pH 6.0) in a boiling state on a hot plate. Following a 20 min incubation, the breaker was removed from the hot plate and cooled down at room temperature for 20 min. Slides were washed once in PBS and stained with mAbs using avidin-biotin-peroxidase complex (ABC) method with the UltraVision Quanto Detection System HRP DAB kit (Lab Vision Corporation, Fremont, CA) according to the manufacturer's instructions.

3. Results

3.1. In Vitro Morphological and Growth Characteristics of sHCC Cell Lines. Typical fibroblastic morphology in a rather disorganized orientation was exhibited by each of the

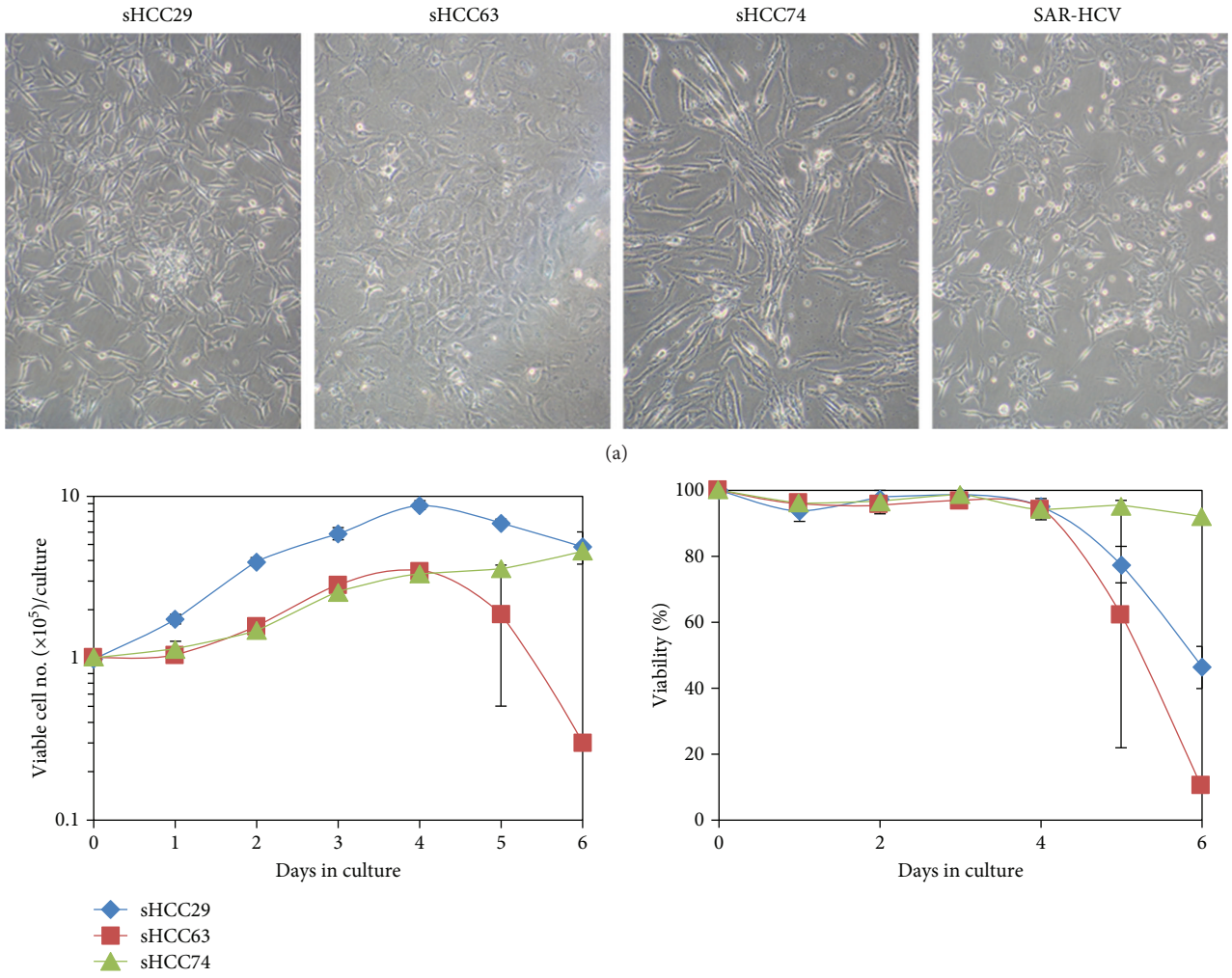

Cell line designation	Population doubling time (hr)	Saturation density (no. of cells/cm^2)	Time required for reaching saturation density (d)
sHCC29	21.1	11.9×10^4	4
sHCC63	43.6	4.7×10^4	4
sHCC74	61.7	4.4×10^4	6
SAR-HCV	22.6	11.5×10^4	5

(b)

Figure 1: *In vitro* live monolayer cell morphology and growth curves of the four sHCC cell lines. (a) Fibroblastic-like morphology is shown for each of the sHCC cell lines, sHCC29, sHCC63, sHCC74, and SAR-HCV, as they grow as monolayers. (b) Growth curve patterns of the first three sHCC are illustrated. The growth curve of SAR-HCV is not shown as it has been reported previously [23]. The population doubling time and time required for reaching saturation density in culture for each cell line based on the growth curve are listed in the attached table.

four sHCC cell lines when they were cultured *in vitro* as monolayers, although some subtle differences were noted among them (Figure 1(a)). For example, sHCC63 and sHCC74 showed longer cell bodies as compared with those of sHCC29 and SAR-HCV. In terms of growth characteristics, growth curves of the four cell lines are shown with somewhat different patterns (Figure 1(b)). sHCC29 and SAR-HCV had much shorter population doubling time (21.1 and 22.6 h *vs.* 43.6 and 61.7 h) and much higher saturation density (11.9×10^4 and 11.5×10^4 cells/cm^2 *vs.* 4.7×10^4 and 4.4×10^4 cells/cm^2), when compared with other two sHCC cell lines, sHCC63 and sHCC74 (table under Figure 1(b)). No viral DNA (HBV and/or HCV) was detected in the culture supernatants or cell extracts from any of the four sHCC cell lines by real-time PCR (data not shown).

3.2. Tumorigenicity in Immunodeficient Mice. Xenotransplantation abilities in NOD/SCID mice were tested by subcutaneous injection of 10^7 monodispersed cells harvested from sHCC29, sHCC63, and sHCC74 per mouse (Figure 2). Results showed that sHCC29 cells gave rise to

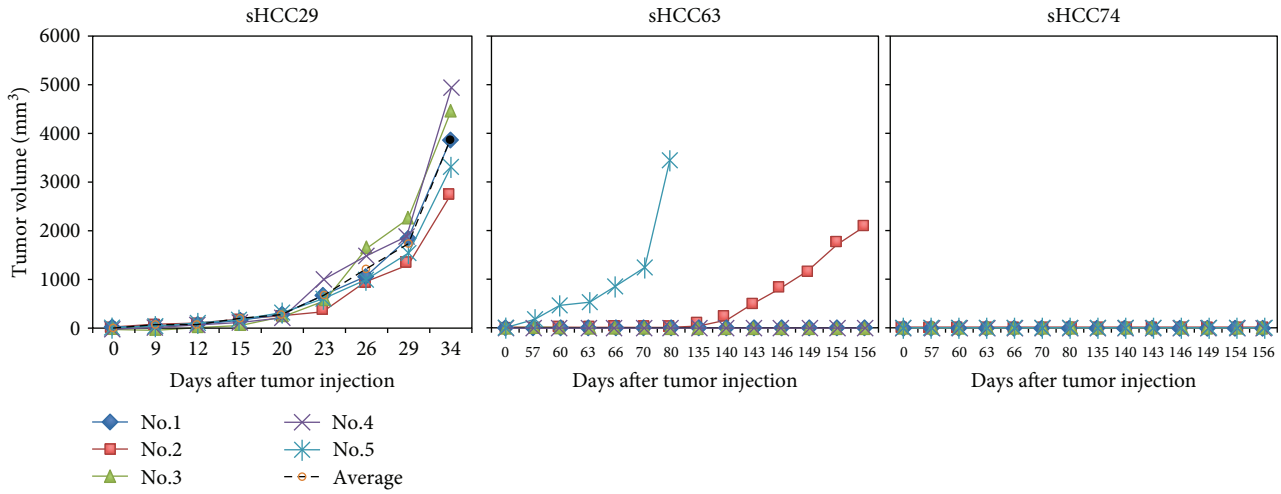

FIGURE 2: *In vivo* tumorigenicity of the three sHCC cell lines, sHCC29, sHCC63, and sHCC74, in NOD/SCID mice. Results on SAR-HCV are not shown, as they have been reported elsewhere [24].

solid tumors at the injection sites in 5/5 mice injected with a similar latent period (15 days); sHCC63 resulted in only 2/5 animals injected with quite different latent periods of 50 *vs.* 135 days, while injection of sHCC74 failed to develop any tumors during 156 days of observation following tumor injection at day 0. As for SAR-HCV, 4 out of 4 mice injected developed solid tumors at the injection sites but with a much longer average latent period of about 4 months [24], as compared with other 3 sHCC cell lines.

3.3. Lack of Surface HLA Class I Antigen and β_2m Expression and Downregulation of Several Antigen-Processing Machinery (APM) Components by the sHCC29 and sHCC63 Cell Lines. Among the four sHCC cell lines tested, only the cell lines sHCC29 and sHCC63 had no detectable surface HLA class I antigen expression as analyzed by cytofluorometry (Figures 3(a) and 3(b) in histogram and bar-type of expression, respectively). β_2m expression in sHCC29 and sHCC63 was undetectable and failed to be restored by incubation of cells with IFN-γ (300 U/mL, 48 h) *in vitro* (Figure 3(b)). Of note is that the expressions of surface HLA class I tested using both mAb W6/32 and mAb TP25.99 were identical, although the results obtained with the latter were not shown. In addition, the HLA class I heavy chain expression was markedly downregulated only in the two β_2m-negative cell lines. Among the analyzed APM components, TAP1 was expressed at a low frequency in the two β_2m-negative cell lines, and while LMP2 was abundantly expressed in all of three cell lines, LMP7 expression was detectable only at a very low percentage of sHCC63 cells (Figure 3(c)). These findings indicate that in sHCC29 and sHCC63 cells, β_2m loss was not the only defect underlying HLA class I antigen loss, since it was associated with additional APM defects. Notably, upregulation by IFN-γ (300 U/mL, 48 h) of HLA-A, -B, -C heavy chain expression was detectable only in sHCC63 cells.

3.4. Detection of a Large (>49 kb) Deletion of the β_2m Gene in the sHCC29 and sHCC63 Cell Lines. In addition to the failure of RT-PCR to detect β_2m cDNA (Figure 4(a)), genomic PCR also failed to detect the *B2M* promoter-to-intron 1 region (Figure 4(b)) in both sHCC29 and sHCC63 cells, compared to sHCC74 and SAR-HCV cells. These findings indicate a deletion of the *B2M* gene in the two β_2m-negative cell lines. To determine the length of this deletion, PCR analysis of their *B2M* locus utilizing a panel of 16 primer pairs encompassing the entire 15q15 region was performed. The results show that in both cell lines the deletion was at least 49 kb in length, with a 3′ breakpoint mapped approximately 22 kb (22,468 bp, nt 63,956) downstream of the *B2M* gene and a not-yet-identified 5′ breakpoint extending at least 27 kb (nt 14,771) upstream. These findings indicate that β_2m loss in both sHCC29 and sHCC63 cells was caused by a large deletion in the *B2M* gene that completely eliminated its coding sequence (Figure 4(c)).

3.5. Effect of IFN-γ on the β_2m, LMP2, LMP7, TAP1, and TAP2 Transcripts in the Three sHCC Cell Lines. Earlier, we have detected downregulation of several APM components at the protein level in the sHCC29 and sHCC63 cells. Here, we tested whether these abnormalities reflected downregulation at the transcriptional level reversible by IFN-γ, although this cytokine failed to do so at the protein level for most of the tested components (Figure 3). Figure 5 shows that the mRNA transcript levels of the tested APM components *LMP2*, *LMP7*, *TAP1*, and *TAP*2 were markedly lower in the sHCC29 and sHCC63 cells than those in the sHCC74 cells. Following treatment with IFN-γ (300 U/mL, 48 h), only *TAP1* mRNA expression in sHCC29 and only *TAP2* mRNA expression in sHCC63 cells were upregulated. Expression of the tested APM component mRNA in sHCC74 cells was abundant, and the level of expression was unaffected by IFN-γ (300 U/mL, 48 h).

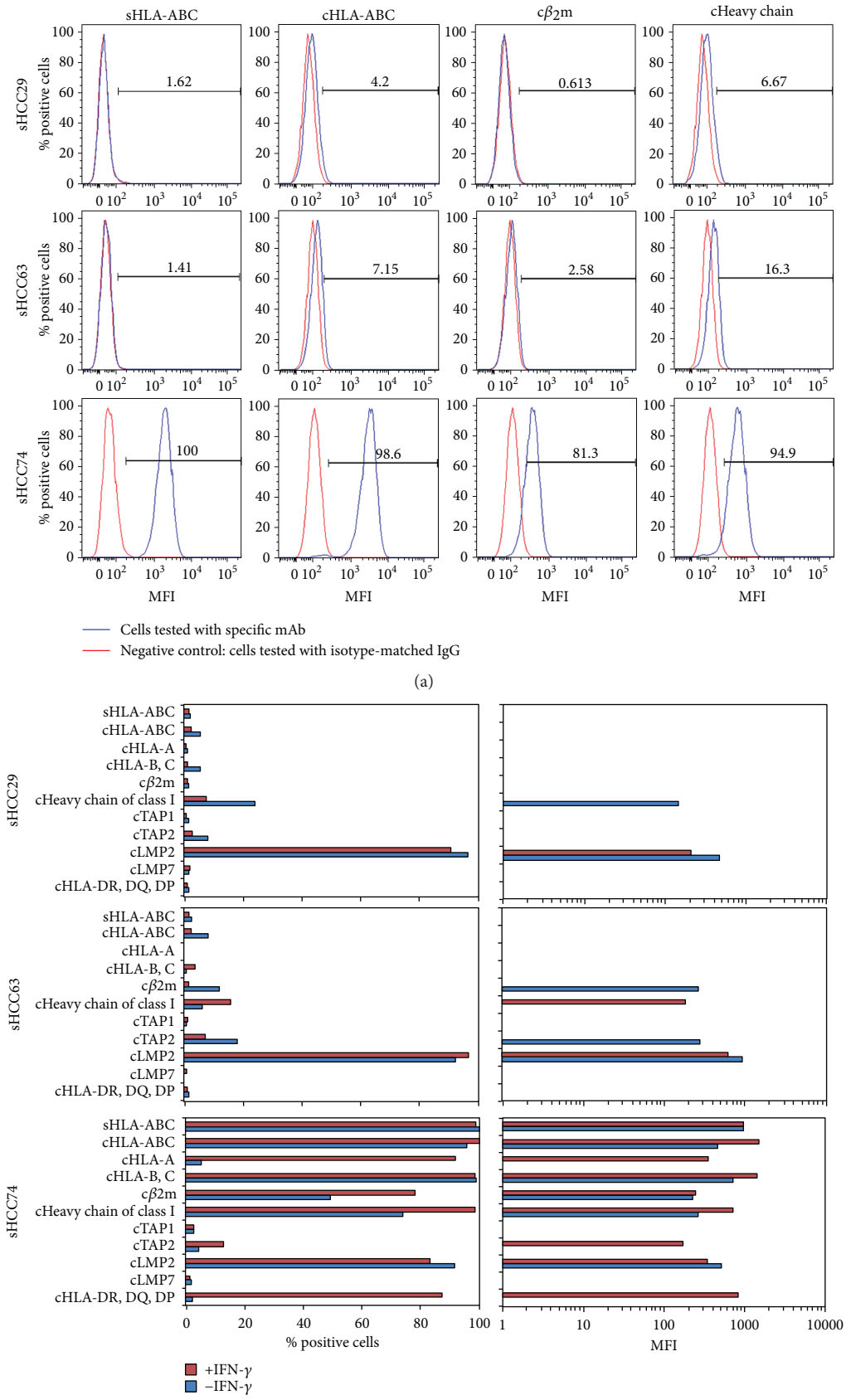

Figure 3: Continued.

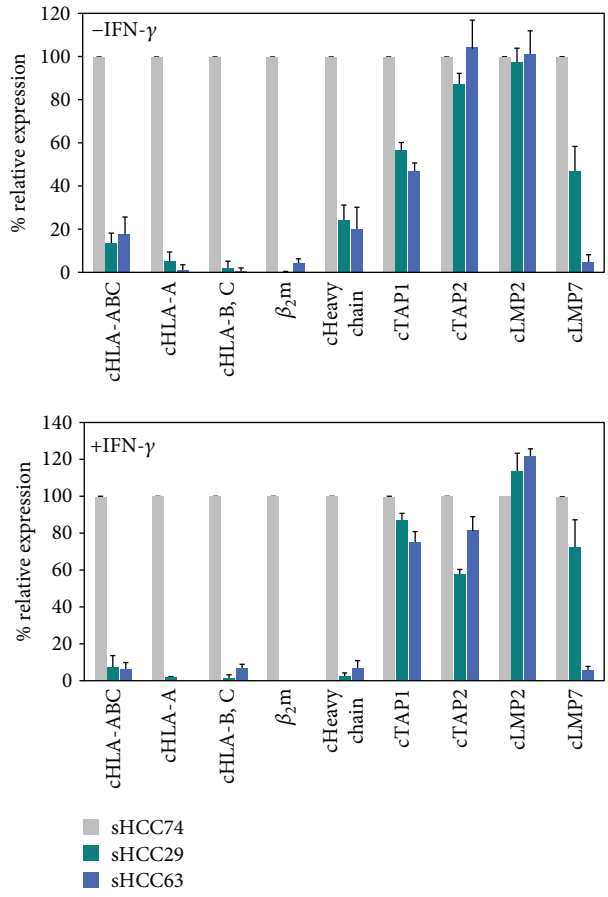

(c)

Figure 3: Differential expression of surface HLA class I antigens and various cytoplasmic antigens including β_2-microgobulin (β_2m), heavy chains, and selected antigen-processing machinery (APM) components in three newly established sHCC cell lines. (a) Surface HLA class I (sHLA-ABC) using mAb W6/32 and cytoplasmic HLA class I (cHLA-ABC) using mAb TP25.99, β_2m, and heavy chains (cHC) of the three sHCC cell lines were determined cytofluormetrically, and the results of a representative experiment were presented by histograms. (b) Cytoplasmic expression of additional HLA-A, HLA-B, -C allospecificities and APM components TAP1, TAP2, LMP2, and LMP7 were determined cytofluormetrically. The data are representative of three independent experiments. Symbols "s" and "c" at the prefix of indicated antigen stand for surface and cytoplasmic antigens, respectively. The results of cytofluorometric analysis are expressed as % positive cells on the left frame and mean fluorescence intensity (MFI) on the right frame. (c) Percent expression relative to sHCC74 of HLA class I allospecificities, heavy chains, β_2m, and selected APM components in sHCC29 and sHCC63 are shown. Results are expressed as percent MFI ± SD of three independent experiments. TAP: transporter associated with antigen processing; LMP: low-molecular-weight protein.

3.6. Phenotypic Expression of CD44 and CD24 on the Four sHCC Cell Lines. The differential or concurrent expression of CD44 and CD24 markers has been used for identification of cancer stem cells (CSCs) in a variety of human epithelial [36, 37] and sarcomatoid renal cell carcinoma [38] malignancies. No sHCC CSCs have yet been reported. Therefore, we sought to determine the phenotypic features of the four sHCC cell lines in terms of surface expression of CD44 and CD24. By cytofluorometric analysis, the two HLA class I-negative sHCC29 and sHCC63 cell lines exhibited a $CD44^-/CD24^-$ phenotype, whereas the other two HLA class I-positive sHCC74 and SAR-HCV cell lines showed $CD44^+/CD24^-$ phenotype (Figure 6(a)). These phenotypic differences between the two groups of cell lines were maintained stably, since there was no change in the differential CD44 and CD24 phenotype following the 5th, 13th, and 21st passages and even in cultures recovered from the respective xenografts (data not shown).

3.7. Lack of β_2m and HLA Class I Antigen Expression in the Patients' Sarcomatoid HCC Lesions from which the sHCC29 and sHCC63 Cell Lines Originated. To rule out the possibility that the lack of HLA class I antigen expression by cultured sHCC29 and sHCC63 cell lines was caused by *in vitro* artifacts associated with their *in vitro* culture conditions, the surgically removed lesions from which the cell lines were established were analyzed by immunohistochemistry for the expression of β_2m and HLA class I antigens (Figure 6(b)). The β_2m-specific mAb L368, the heavy chain-specific mAb HC-10, and HLA class I-specific mAb W6/32 all stained

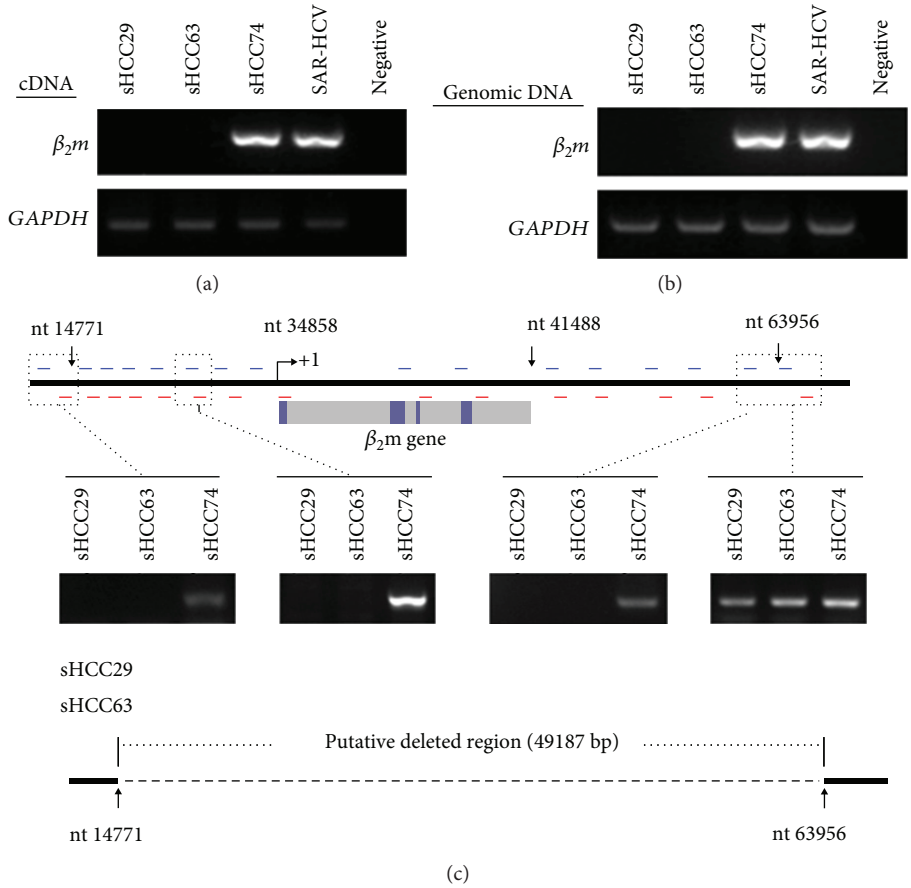

FIGURE 4: No detection of β_2m cDNA (a) and the *B2M* promoter-to-intron 1 region (b) in both sHCC29 and sHCC63 cells by RT-PCR and genomic PCR, respectively, as compared to sHCC74 and SAR-HCV cells. Schema illustrates the putative deleted region of the *B2M* gene in the two HLA class I-negative sHCC29 and sHCC63 cell lines (c). MFI: mean fluorescence intensity. See the text for detailed explanation.

positive with strong intensity on the cell surface and in the cytoplasm of the tumor lesion from which the HLA class I-positive sHCC74 cell line originated. In contrast, the cell surface HLA class I antigens were not detectable, and yet the cytoplasmic β_2m and HLA class I heavy chains were stained with moderate intensity in the tumor lesions from which the HLA class I-negative sHCC29 and sHCC63 cell lines were derived. The observed immunoreactivity was specific, as the control normal mouse serum or isotype-matched controls stained negative in all tested tumor sections. These findings support the *in vivo* relevance of β_2m loss and HLA class I heavy chain downregulation as detected in the sHCC29 and sHCC63 cell lines *in vitro*.

4. Discussion

In this study, we showed that two (sHCC29 and sHCC63) out of the four sHCC cell lines had undetectable surface HLA class I antigen expression which was IFN-γ-irreversible. The mechanism underlying this abnormality includes β_2m loss, which is caused by a >49 kb deletion at the *β2M* locus, and marked downregulation of HLA class I heavy chain, TAP1 and LMP7 expression. β_2m is known to be a subunit of HLA class I antigens critical to initiating HLA class I assembly in the endoplasmic reticulum for subsequent membrane transport, while TAP1 and LMP7 are directly or indirectly involved in the formation of an effective peptide-loading platform for HLA class I-β_2m-peptide complex stabilization. To the best of our knowledge, this combination of defects in the HLA class I antigen presentation pathway has never been described in any liver cancer types.

Previous studies have shown that the vast majority of *B2M* gene mutations detected in human malignant tumors are point mutations and microdeletions (a few bases) [39], except for a large (~6 kb) deletion identified in the melanoma cell line FO-1 [40]. Compared to this deletion that spans from the upstream regulatory region to part of exon 2 [40], the >49 kb deletion we identified in two sHCC cell lines extends well across the 15q15 *B2M* locus, which eliminates the entire *B2M* gene. Although we have mapped the 3′ breakpoint to ~22 kb downstream of the gene, we do not know at present how far beyond 27 kb upstream the 5′ breakpoint reaches in each of these two cell lines. In addition, whether this mutation was heterozygous or associated with loss of a wild-type copy remains unclear, although the latter has been reported in the majority of other tumor types with β_2m loss. Furthermore, it is intriguing as to why this *B2M* gene mutation was detected in the two sHCC cell

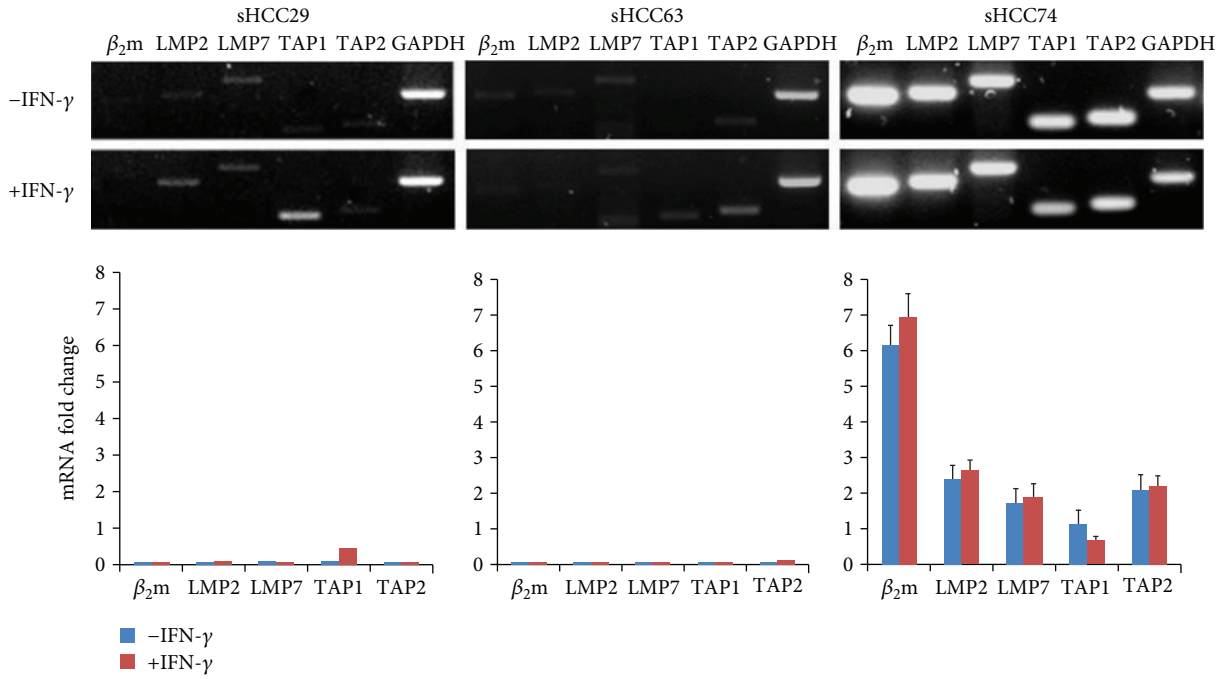

Figure 5: Differential expression of β_2m, *LMP2*, *LMP7*, *TAP1*, and *TAP2* mRNA in the three newly established sHCC cell lines cultured in the presence or absence of IFN-γ (300 U/mL, 48 h). Upper panel: agarose gel stained with ethidium bromide shows the electrophoresis of end point RT-PCR products for the tested mRNAs of the three sHCC cell lines. Lower panel: quantification of RT-PCR results from three independent experiments where relative mRNA expression of each gene was normalized to glyceraldehydes 3-phosphate dehydrogenase (*GAPDH*) and expressed as mean fold-changes ± SD. LMP: low-molecular-weight protein; TAP: transporter associated with antigen processing.

lines that were HBV-associated but not the other two that were HCV-associated. Whether this was a coincidence or a virus-specific phenomenon awaits further analysis of a larger panel of sHCC cell lines.

The combination of *B2M* gene mutation and HLA class I heavy chain or APM downregulation within a single tumor cell population has been described in melanoma [41]. In the present study, we found that both sHCC29 and sHCC63 cells had marked HLA-A, HLA-B, and HLA-C allospecificity, TAP1 and LMP7 downregulation. Notably, only in sHCC63 cells could the downregulated HLA class I heavy chains be slightly upregulated by IFN-γ. At variance with these findings, *TAP1* mRNA in sHCC29 cells and *TAP2* mRNA in sHCC63 cells were markedly upregulated, although the basal levels of the tested *TAP1*, *TAP2*, *LMP2*, and *LMP7* mRNA were quite low. Together, these results reflect regulatory defects possibly at different levels. First, *TAP1*, *TAP2*, *LMP2*, and *LMP7* genes may be insufficiently transcribed in sHCC cells in a coordinate fashion, in part because *TAP1* and *LMP2* genes are known to share a bidirectional promoter [42]. Second, some of the downregulated components detected may be under a posttranscriptional control, such as decreased mRNA stability. Third, a defect in the stabilization of multiprotein complex may exist when one or a few of these components are missing or in low quantities.

The two HLA class I-negative sHCC29 and sHCC63 cell lines have more robust *in vitro* growth characteristics and higher xenotransplantability into NOD/SCID mice than the HLA class I-positive sHCC74 cell line. These findings, however, were not associated with a cancer stem cell signature dictated by the $CD44^{High}/CD24^{Low}$ phenotype [43] because both sHCC29 and sHCC63 cells were $CD44^{-}/CD24^{-}$, whereas sHCC74 and SAR-HCV cells were $CD44^{+}/CD24^{-}$. Whether this is a feature unique of sHCC is currently not known. Moreover, the similar growth behavior between the HLA class I-positive SAR-HCV cells and the HLA class I-negative sHCC29 cells suggests that the HLA class I antigen status was independent of basic sHCC biology in the absence of host immunity. The only correlation we have identified thus far is between shorter doubling time *in vitro* and higher xenotransplantability in NOD/SCID mice, although more sHCC cell lines need to be analyzed.

From a therapeutic viewpoint, the lack of HLA class I-β_2m-peptide complex expression at the malignant cell surface will preclude the recognition and destruction by cognate CTLs in immuno-competent hosts [44, 45]. The lack of detection of β_2m in the sHCC tumor lesions from which the two HLA class I-negative cell lines originated indicates that CTLs were unlikely to control these tumor cells in patients [46]. Although not yet confirmed with a large panel of sHCC cell lines and the corresponding lesions because of their rarity, the 50% frequency of HLA class I antigen loss we have revealed in this cancer type strongly suggests a rationale for screening patients for their tumor lesion HLA class I antigen status before treating them with any type of T cell immunotherapy, including immune checkpoint blockade therapy that has recently been shown to be effective in treating

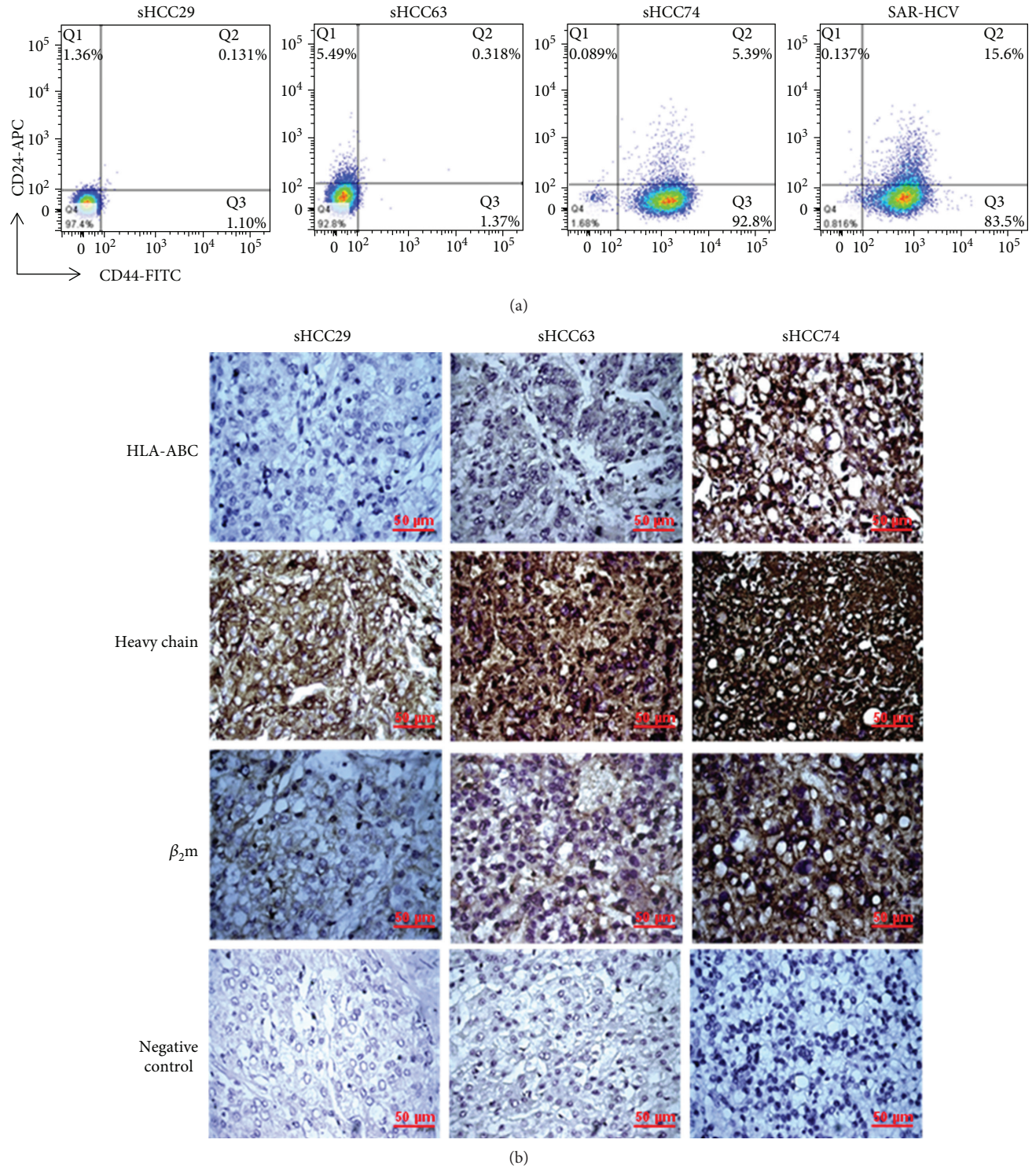

Figure 6: Two-color cytofluorometric analysis of the sHCC29, sHCC63, sHCC74, and SAR-HCV cell lines using mAbs to surface markers CD24 and CD44 conjugated with allophycoyanin (APC) and fluorescein isothioyanate (FITC), respectively (a). Immunohistochemical staining patterns of the tumor lesions from which the sHCC29, sHCC63, and sHCC74 cell lines were established using mAbs to HLA-ABC (with mAb W6/32), heavy chain (mAb HC-10), and β_2m (mAb L368). Isotype-matched Ig serves as the negative control (b).

some tumor types [18, 19]. With regard to patients with HLA class I-negative sHCC, their treatment options may include mAb-based targeted immunotherapy [47], NK [48] or cytokine-induced killer (CIK) [49] cell-based immunotherapy, and/or chimeric antigen receptor (CAR) T therapy [50]; all of which utilize an alternative approach other than those of the recognition of antigen through T cell receptors to elicit antitumor immunity in the patients.

Data Availability

The data used to support the findings of this study are available from the corresponding author upon request.

Conflicts of Interest

The authors declare no conflict of interest.

Acknowledgments

The authors wish to thank Miss Zi-Hua Chen and Miss I-Pu Chen for their technical assistance. Special thanks are expressed to Prof. Soldano Ferrone, University of Pittsburgh, PA, for providing us many monoclonal antibodies used in this study. This study was in part supported by the National Science Council of Taiwan (NSC94-2314-B-1282-064), Department of Health, Taiwan (DOH100-TD-C-111-008), and the Ministry of Science and Technology (Taiwan) (MOST 106-2320-B-007-001).

Supplementary Materials

Supplementary Table 1: additional β_2-microglobulin primers used for genomic PCR. *(Supplementary Materials)*

References

[1] D.-I. Tai, C.-H. Chen, T.-T. Chang et al., "Eight-year nationwide survival analysis in relatives of patients with hepatocellular carcinoma: role of viral infection," *Journal of Gastroenterology and Hepatology*, vol. 17, no. 6, pp. 682–689, 2002.

[2] D. M. Parkin, F. Bray, J. Ferlay, and P. Pisani, "Global cancer statistics, 2002," *CA: A Cancer Journal for Clinicians*, vol. 55, no. 2, pp. 74–108, 2005.

[3] K. G. Iskah, P. P. Antony, C. Niederau, and Y. Nakamura, "Mesenchymal tumors of the liver," in *WHO International Histological Classification of Tumours, Pathology and Genetics of the Tumours of the Digestive System*, R. H. Stanley and A. A. Lauri, Eds., pp. 191–198, IARC Press, Lyon, France, 2000.

[4] J. P. Thiery, "Epithelial–mesenchymal transitions in tumour progression," *Nature Reviews Cancer*, vol. 2, no. 6, pp. 442–454, 2002.

[5] S. Battaglia, N. Benzoubir, S. Nobilet et al., "Liver cancer-derived hepatitis C virus core proteins shift TGF-beta responses from tumor suppression to epithelial-mesenchymal transition," *PLoS One*, vol. 4, no. 2, article e4355, 2009.

[6] F. Giunchi, F. Vasuri, P. Baldin, F. Rosini, B. Corti, and A. D'Errico-Grigioni, "Primary liver sarcomatous carcinoma: report of two cases and review of the literature," *Pathology - Research and Practice*, vol. 209, no. 4, pp. 249–254, 2013.

[7] M. Kojiro, S. Sugihara, S. Kakizoe, O. Nakashima, and K. Kiyomatsu, "Hepatocellular carcinoma with sarcomatous change: a special reference to the relationship with anticancer therapy," *Cancer Chemotherapy and Pharmacology*, vol. 23, Supplement 1, pp. S4–S8, 1989.

[8] H. Nishi, K.-I. Taguchi, Y. Asayama et al., "Sarcomatous hepatocellular carcinoma: a special reference to ordinary hepatocellular carcinoma," *Journal of Gastroenterology and Hepatology*, vol. 18, no. 4, pp. 415–423, 2003.

[9] Y. Idobe-Fujii, N. Ogi, K. Hosho, M. Koda, Y. Murawaki, and Y. Horie, "Hepatocellular carcinoma with sarcomatous change arising after eradication of HCV via interferon therapy," *Clinical Imaging*, vol. 30, no. 6, pp. 416–419, 2006.

[10] X. M. Lao, D. Y. Chen, Y. Q. Zhang et al., "Primary carcinosarcoma of the liver: clinicopathologic features of 5 cases and a review of the literature," *The American Journal of Surgical Pathology*, vol. 31, no. 6, pp. 817–826, 2007.

[11] S. Yamada, N. Okumura, L. Wei et al., "Epithelial to mesenchymal transition is associated with shorter disease-free survival in hepatocellular carcinoma," *Annals of Surgical Oncology*, vol. 21, no. 12, pp. 3882–3890, 2014.

[12] S. Ferrone and F. M. Marincola, "Loss of HLA class I antigens by melanoma cells: molecular mechanisms, functional significance and clinial relevance," *Immunology Today*, vol. 16, no. 10, pp. 487–494, 1995.

[13] H. T. Khong and N. P. Restifo, "Natural selection of tumor variants in the generation of "tumor escape" phenotypes," *Nature Immunology*, vol. 3, no. 11, pp. 999–1005, 2002.

[14] A. Garcia-Lora, I. Algarra, and F. Garrido, "MHC class I antigens, immune surveillance, and tumor immune escape," *Journal of Cellular Physiology*, vol. 195, no. 3, pp. 346–355, 2003.

[15] D. Atkins, S. Ferrone, G. E. Schmahl, S. Störkel, and B. Seliger, "Down-regulation of HLA class I antigen processing molecules: an immune escape mechanism of renal cell carcinoma?," *The Journal of Urology*, vol. 171, no. 2, pp. 885–889, 2004.

[16] D. M. Parkin, F. Bray, J. Ferlay, and P. Pisani, "Estimating the world cancer burden: Globocan 2000," *International Journal of Cancer*, vol. 94, no. 2, pp. 153–156, 2001.

[17] A. J. Cochran, R. R. Huang, J. Lee, E. Itakura, S. P. L. Leong, and R. Essner, "Tumour–induced immune modulation of sentinel lymph nodes," *Nature Reviews Immunology*, vol. 6, no. 9, pp. 659–670, 2006.

[18] O. Hamid, C. Robert, A. Daud et al., "Safety and tumor responses with lambrolizumab (anti–PD-1) in melanoma," *The New England Journal of Medicine*, vol. 369, no. 2, pp. 134–144, 2013.

[19] B. C. Creelan, "Update on immune checkpoint inhibitors in lung cancer," *Cancer Control*, vol. 21, no. 1, pp. 80–89, 2014.

[20] P. Leone, E. C. Shin, F. Perosa, A. Vacca, F. Dammacco, and V. Racanelli, "MHC class I antigen processing and presenting machinery: organization, function, and defects in tumor cells," *Journal of the National Cancer Institute*, vol. 105, no. 16, pp. 1172–1187, 2013.

[21] A. A. Wadee, A. Paterson, K. A. Coplan, and S. G. Reddy, "HLA expression in hepatocellular carcinoma cell lines," *Clinical & Experimental Immunology*, vol. 97, no. 2, pp. 328–333, 1994.

[22] J. Huang, M. Y. Cai, and D. P. Wei, "HLA class I expression in primary hepatocellular carcinoma," *World Journal of Gastroenterology*, vol. 8, no. 4, pp. 654–657, 2002.

[23] D.-I. Tai, Y.-C. Shen, W.-H. Weng et al., "New sarcomatoid cancer cell line SAR-HCV established from a hepatitis C virus-related liver tumour lesion," *Anticancer Research*, vol. 31, no. 1, pp. 129–137, 2011.

[24] D.-I. Tai, Y.-C. Shen, C.-K. Chuang, and S.-K. Liao, "Human liver sarcomatoid carcinoma cell line that displays fibroblastic morphology and markers of mesenchymal, epithelial and neuroendocrine elements," *Proceedings of the American Association for Cancer Research*, vol. 41, p. 150, 2000.

[25] C. J. Barnstable, W. F. Bodmer, G. Brown et al., "Production of monoclonal antibodies to group A erythrocytes, HLA and other human cell surface antigens-new tools for genetic analysis," *Cell*, vol. 14, no. 1, pp. 9–20, 1978.

[26] C. W. Redman, A. J. McMichael, G. M. Stirrat, C. A. Sunderland, and A. Ting, "Class 1 major histocompatibility complex antigens on human extra-villous trophoblast," *Immunology*, vol. 52, no. 3, pp. 457–468, 1984.

[27] S. A. Desai, X. Wang, E. J. Noronha et al., "Structural relatedness of distinct determinants recognized by monoclonal antibody TP25.99 on β_2-microglobulin-associated and β_2-microglobulin-free HLA class I heavy chains," *The Journal of Immunology*, vol. 165, no. 6, pp. 3275–3283, 2000.

[28] N. Rebaï and B. Malissen, "Structural and genetic analyses of HLA class I molecules using monoclonal xenoantibodies," *Tissue Antigens*, vol. 22, no. 2, pp. 107–117, 1983.

[29] F. Perosa, G. Luccarelli, M. Prete, E. Favoino, S. Ferrone, and F. Dammacco, "β_2-microglobulin-free HLA class I heavy chain epitope mimicry by monoclonal antibody HC-10-specific peptide," *The Journal of Immunology*, vol. 171, no. 4, pp. 1918–1926, 2003.

[30] N. J. Stam, H. Spits, and H. L. Ploegh, "Monoclonal antibodies raised against denatured HLA-B locus heavy chains permit biochemical characterization of certain HLA-C locus products," *The Journal of Immunology*, vol. 137, no. 7, pp. 2299–2306, 1986.

[31] M. F. Sernee, H. L. Ploegh, and D. J. Schust, "Why certain antibodies cross-react with HLA- A and HLA-G: epitope mapping of two common MHC class I reagents," *Molecular Immunology*, vol. 35, no. 3, pp. 177–188, 1998.

[32] L. A. Lampson, C. A. Fisher, and J. P. Whelan, "Striking paucity of HLA-A, B, C and beta 2-microglobulin on human neuroblastoma cell lines," *The Journal of Immunology*, vol. 130, no. 5, pp. 2471–2478, 1983.

[33] N. Bandoh, T. Ogino, H. S. Cho et al., "Development and characterization of human constitutive proteasome and immunoproteasome subunit-specific monoclonal antibodies," *Tissue Antigens*, vol. 66, no. 3, pp. 185–194, 2005.

[34] X. Wang, M. Campoli, H. S. Cho et al., "A method to generate antigen-specific mAb capable of staining formalin-fixed, paraffin-embedded tissue sections," *Journal of Immunological Methods*, vol. 299, no. 1-2, pp. 139–151, 2005.

[35] T. Ogino, X. Wang, and S. Ferrone, "Modified flow cytometry and cell-ELISA methodology to detect HLA class I antigen processing machinery components in cytoplasm and endoplasmic reticulum," *Journal of Immunological Methods*, vol. 278, no. 1-2, pp. 33–44, 2003.

[36] H.-C. Chen, A. S.-B. Chou, Y.-C. Liu et al., "Induction of metastatic cancer stem cells from the NK/LAK-resistant floating, but not adherent, subset of the UP-LN1 carcinoma cell line by IFN-γ," *Laboratory Investigation*, vol. 91, no. 10, pp. 1502–1513, 2011.

[37] M. Al-Hajj, M. S. Wicha, A. Benito-Hernandez, S. J. Morrison, and M. F. Clarke, "Prospective identification of tumorigenic breast cancer cells," *Proceedings of the National Academy of Sciences of the United States of America*, vol. 100, no. 7, pp. 3983–3988, 2003.

[38] C.-H. Hsieh, S.-C. Hsiung, C.-T. Yeh et al., "Differential expression of CD44 and CD24 markers discriminates the epitheliod from the fibroblastoid subset in a sarcomatoid renal carcinoma cell line: evidence suggesting the existence of cancer stem cells in both subsets as studied with sorted cells," *Oncotarget*, vol. 8, no. 9, pp. 15593–15609, 2017.

[39] M. Bernal, F. Ruiz-Cabello, A. Concha, A. Paschen, and F. Garrido, "Implication of the β_2-microglobulin gene in the generation of tumor escape phenotypes," *Cancer Immunology, Immunotherapy*, vol. 61, no. 9, pp. 1359–1371, 2012.

[40] C. M. D'Urso, Z. G. Wang, Y. Cao, R. Tatake, R. A. Zeff, and S. Ferrone, "Lack of HLA class I antigen expression by cultured melanoma cells FO-1 due to a defect in B2m gene expression," *The Journal of Clinical Investigation*, vol. 87, no. 1, pp. 284–292, 1991.

[41] C. C. Chang, M. Campoli, N. P. Restifo, X. Wang, and S. Ferrone, "Immune selection of hot-spot β_2-*microglobulin* gene mutations, HLA-A2 allospecificity loss, and antigen-processing machinery component down-regulation in melanoma cells derived from recurrent metastases following immunotherapy," *The Journal of Immunology*, vol. 174, no. 3, pp. 1462–1471, 2005.

[42] K. L. Wright, L. C. White, A. Kelly, S. Beck, J. Trowsdale, and J. P. Ting, "Coordinate regulation of the human TAP1 and LMP2 genes from a shared bidirectional promoter," *Journal of Experimental Medicine*, vol. 181, no. 4, pp. 1459–1471, 1995.

[43] A. Jaggupilli and E. Elkord, "Significance of CD44 and CD24 as cancer stem cell markers: an enduring ambiguity," *Clinical & Developmental Immunology*, vol. 2012, article 708036, 11 pages, 2012.

[44] M.-S. Wu, C.-H. Li, J. G. Ruppert, and C.-C. Chang, "Cytokeratin 8-MHC class I interactions: a potential novel immune escape phenotype by a lymph node metastatic carcinoma cell line," *Biochemical and Biophysical Research Communications*, vol. 441, no. 3, pp. 618–623, 2013.

[45] C. C. Chang, G. Pirozzi, S. H. Wen et al., "Multiple structural and epigenetic defects in the human leukocyte antigen class I antigen presentation pathway in a recurrent metastatic melanoma following immunotherapy," *Journal of Biological Chemistry*, vol. 290, no. 44, pp. 26562–26575, 2015.

[46] P. Thor Straten and F. Garrido, "Targetless T cells in cancer immunotherapy," *Journal for ImmunoTherapy of Cancer*, vol. 4, no. 1, p. 23, 2016.

[47] P. Cater, "Improving the efficacy of antibody-based cancer therapies," *Nature Reviews Cancer*, vol. 1, no. 2, pp. 118–129, 2001.

[48] S. K. Grossenbacher, R. J. Canter, and W. J. Murphy, "Natural killer cell immunotherapy to target stem-like tumor cells," *Journal for ImmunoTherapy of Cancer*, vol. 4, no. 1, p. 19, 2016.

[49] F. Wei, X.-X. Rong, R.-Y. Xie et al., "Cytokine-induced killer cells efficiently kill stem-like cancer cells of nasopharyngeal carcinoma via the NKG2D-ligands recognition," *Oncotarget*, vol. 6, no. 33, pp. 35023–35039, 2015.

[50] G. Lipowska-Bhalla, D. E. Gilham, R. E. Hawkins, and D. G. Rothwell, "Targeted immunotherapy of cancer with CAR T cells: achievements and challenges," *Cancer Immunology, Immunotherapy*, vol. 61, no. 7, pp. 953–962, 2012.

Hindawi
Journal of Immunology Research
Volume 2018, Article ID 7283703, 10 pages
https://doi.org/10.1155/2018/7283703

Research Article

Mesenchymal Stem Cells Ameliorate Hepatic Ischemia/Reperfusion Injury via Inhibition of Neutrophil Recruitment

Shihui Li,[1] **Xu Zheng**,[2] **Hui Li**,[1] **Jun Zheng**,[1] **Xiaolong Chen**,[1] **Wei Liu**,[3] **Yan Tai**,[3] **Yingcai Zhang**,[1] **Genshu Wang**,[1] **and Yang Yang**[1]

[1]*Department of Hepatic Surgery and Liver transplantation Center of the Third Affiliated Hospital, Organ Transplantation Institute, Sun Yat-sen University, Organ Transplantation Research Center of Guangdong Province, Guangzhou, Guangdong 510630, China*
[2]*Clinical Immunology Laboratory, Department of Rheumatology & Immunology, The First Affiliated Hospital of USTC, Hefei, Anhui 230001, China*
[3]*Guangdong Provincial Key Laboratory of Liver Disease Research, The Third Affiliated Hospital, Sun Yat-sen University, Guangzhou, Guangdong 510630, China*

Correspondence should be addressed to Genshu Wang; wgsh168@163.com and Yang Yang; yyysysu@126.com

Received 13 May 2018; Revised 23 September 2018; Accepted 18 October 2018; Published 3 December 2018

Guest Editor: Dechun Feng

Ischemia/reperfusion injury (IRI) remains a major problem in organ transplantation, which represents the main cause of graft dysfunction posttransplantation. Hepatic IRI is characterized by an excessive inflammatory response within the liver. Mesenchymal stem cells (MSCs) have been shown to be immunomodulatory cells and have the therapeutic action on IRI in several organs. However, the mechanism of regulatory effect of MSCs on IRI remains unclear. In the present study, we examined the impact of MSCs on hepatic inflammatory response such as neutrophil influx and liver damage in a rat model of 70% hepatic IRI. Treatment with MSCs protected rat against hepatic IRI, with significantly decreased serum levels of liver enzymes, attenuated hepatic neutrophil infiltration, reduced expression of apoptosis-associated proteins, and ameliorated liver pathological injury. MSCs also significantly enhanced the intracellular activation of p38 MAPK phosphorylation, which led to decreased expression of CXCR2 on the surface of neutrophils. In addition, MSCs significantly diminished neutrophil chemoattractant CXCL2 production by inhibiting NF-κB p65 phosphorylation in macrophages. These results demonstrate that MSCs significantly ameliorate hepatic IRI predominantly through its inhibitory effect on hepatic neutrophil migration and infiltration.

1. Introduction

Liver transplantation is one of the most efficient life-saving treatments for various end-stage hepatic diseases [1]. However, hepatic IRI remains a major problem in this clinical setting. IRI affects liver viability that usually leads to delayed recovery or even loss of graft function in liver transplantation [2]. Moreover, IRI directly correlates to graft rejection, which causes up to 10% of early transplant failures and also leads to a higher incidence of chronic rejection [3]. Hepatic IRI also plays a critical role in donor shortage due to the higher sensitivity to IRI of clinical marginal liver donors.

During hepatic IRI, liver damages are caused largely during the reperfusion period, when an excessive innate immune response is triggered by blood reperfusion [4]. The mechanisms of reperfusion-induced pathological and functional alterations are not fully understood and under intensive investigation [5]. The results of previous studies are complicated, but all showed that significant inflammatory components are involved. Neutrophils are considered central factors in the events leading to injury after reperfusion [6].

MSCs exert a variety of immune-regulatory functions on cells within both adaptive and innate immunity, which make MSC therapy more efficient than single-agent drug therapies [7]. MSCs could suppress proliferation and functions of effector T cell [8] and enhance generation of regulatory T cells [9]. MSCs also inhibit B cell, natural killer cells, and dendritic cell activation and proliferation [10–12]. In addition, MSCs could induce a shift from proinflammatory M1 to anti-inflammatory M2 macrophages [13]. Studies have rarely

investigated the protective effects of MSCs in hepatic IRI and related mechanism of the beneficial effect of MSCs on ischemia reperfusion-injured tissues. None of them has investigated the interactions between MSCs and neutrophils during hepatic IRI, in spite of the key role of neutrophils in innate immune response-mediated tissue damage after reperfusion

In this study, we focus on the effects of MSCs on neutrophils which exert protective role on neutrophil-mediated tissue damage during hepatic IRI.

2. Materials and Methods

2.1. Ethics Statements. Male Sprague-Dawley (SD) rats weighing 80–100 g and 200–250 g from the Laboratory Animal Center of Sun Yat-sen University (Guangzhou, China) were used for all experiments. All animal experiments were carried out in accordance with the National Institutes of Health Guide for the Care and Use of Laboratory Animals (NIH Publication No. 8023, revised 1978). All of the experimental procedures were approved by the Sun Yat-sen University Ethics Committee.

2.2. Model of Hepatic Ischemia/Reperfusion Injury. The hepatic artery and portal vein to the left lateral and median lobes of male SD rats weighing 200–250 g were clamped for 60 min by clamp after being anesthetized. Reperfusion was initiated by removing the clamp. A total of 3×10^5 MSCs at passages 3–5 suspended in 1 mL PBS or 1 mL PBS were injected via the portal vein, respectively, in the MSC + IRI group and the PBS group immediately after the removal of the clamp. The animals in the sham group underwent the same anesthesia, laparotomy, and injection procedures, except the interruption of blood supply to the liver lobes.

2.3. Isolation and Characterization of Rat MSCs. Rat MSCs were prepared from rat bone marrow cells as we previously described [14]. Briefly, bone marrow cells flushed from the femurs of male SD rats were collected and cultured in Dulbecco modified Eagle medium (DMEM; Gibco, Rockville, MD) supplemented with 10% fetal calf serum (FCS; Gibco), 2 ng/mL basic fibroblast growth factor (b-FGF; Gibco), and 1% penicillin/streptomycin (P/S; Gibco), at 200,000 cells/cm^2 at 37°C in 5% CO_2. The nonadherent cells were removed after 24 hours, and the adherent cells were harvested by trypsinization (0.05% trypsin) when reaching 80% confluence. The immunophenotypes of these cells were persistently positive for CD29, CD44, and CD90 but negative for CD34, CD45, and CD11b for more than three passages. To determine their multilineage differentiation potential, MSCs at passages 3–5 were subjected to adipogenesis differentiation and osteogenesis differentiation media (Gibco) according to the manufacturer's instructions.

2.4. Isolation of Neutrophils. Blood was collected from male SD rats and diluted in 1 × HBSS (Hanks balanced salt solution; Gibco) at 1 : 1 ratio and layered over Percoll plus (GE Healthcare) in a centrifuge tube. The red cell pellet that contains the neutrophils and erythrocytes was collected and suspended in 5 mL HBSS after centrifugation. Erythrocytes were removed by hypotonic lysis using ACK Lysis Buffer (TBD sciences, Tianjing). Purified neutrophils were suspended in HBSS and were kept on ice until needed.

2.5. Coculture Experiment. Neutrophils or macrophages were placed in the lower chamber and stimulated for 12 h with 10 ng/mL of LPS in the presence or absence of MSCs in the upper chamber at a 10 : 1 ratio by using the transwell system (0.3 mm pore size membrane; Corning, Cambridge, MA).

2.6. Flow Cytometry. For phenotypic analysis of the cell surface marker expression, cells were harvested, then incubated with respective fluorescent antibodies for 30 minutes at 4°C, washed twice, and resuspended in 300 μL PBS. For intracellular staining, cells were fixed by formaldehyde and permeabilized by ice-cold methanol before immunostaining. Fluorescent antibodies included phycoerythrin- (PE-) conjugated anti-rat CD29, CD44, CD90, CD34, CD45, and CD11b (eBioscience, San Diego, CA), allophycocyanin- (APC-) conjugated anti-rat CXCR2 (R&D Systems, Minneapolis, MN), Alexa fluor 647-conjugated anti-rat phospho-p38 MAPK, and phospho-NF-κB p65 (Cell Signaling Technology, Danvers, MA). The results were processed using FlowJo software (Tree Star, Inc).

2.7. Analysis of Relative Gene Expression Using Real-Time Quantitative Reverse Transcription PCR. Real-time quantitative reverse transcription PCR (qRT-PCR) analysis was performed 12 h after the liver or cells were treated. Total RNA was isolated using Trizol reagent (Invitrogen, Carlsbad, CA) according to the manufacturer's instructions. Total RNA (1 mg) extracted from each sample was reverse transcribed to cDNA in a 20 μL reaction mixture using an RT reagent kit (Roche) according to the manufacturer's directions. Real-time qRT-PCR was performed for the candidate genes and for GAPDH as the internal control. Quantitative real-time PCR was performed in a Light Cycler Real-Time PCR machine using Roche Fast Start Universal SYBR Green Master (Rox). The primers are shown in Table 1. The specificity of the PCR products was verified by melting curve analysis. Each sample was analyzed in triplicate.

2.8. Western Blot Analysis. Equal amounts of protein from each sample were separated by 12% SDS-PAGE and transferred to PVDF membranes (Millipore, Boston, MA). The proteins were then incubated overnight at 4°C with primary antibodies against rat Bad, Fas, Cleaved caspase 3, phospho-p38 MAPK, and β-actin (Cell Signaling Technology); following a 30 min wash, the membranes were incubated with a secondary antibody conjugated to HRP for 1 h at room temperature. After being washed for 30 min, the membranes were visualized by enhanced chemiluminescence (ECL; Millipore, Billerica, MA) and recorded by FluorChem M (Protein Simple, San Jose, California).

2.9. Measurement of Inflammatory Cytokines and Chemokine. The concentration of IL-2, IL-4, IL-6, IL-10, and CXCL2 in the liver and cell culture supernatants was quantitatively measured by enzyme-linked immunosorbent assay (ELISA) (EIAab Science), according to the manufacturer's instructions.

Table 1: Gene names and primer sequences used for quantitative RT-PCR.

Gene name	Primers used	
	Sense (5′ to 3′)	Antisense (5′ to 3′)
IL2	GCAGGCCACAGAATTGAAAC	CCAGCGTCTTCCAAGTGAA
IL4	GTCACTGACTGTAGAGAGCTATTG	CTGTCGTTACATCCGTGGATAC
IL6	GAAGTTAGAGTCACAGAAGGAGTG	GTTTGCCGAGTAGACCTCATAG
IL10	AGTGGAGCAGGTGAAGAATG	GAGTGTCACGTAGGCTTCTATG
CD11b	GAGCACCATCTGGGACATAAA	GGCATCAGAGTCCACATCAA
CD18	CCAGTAACGTAGTCCAGCTTATC	CATAGGTGACTTTCAGGGTGTC
CCL2	GTCTCAGCCAGATGCAGTTAAT	CTGCTGGTGATTCTCTTGTAGTT
CCL17	GTGCTGCCTGGACTACTT	CTTCCCTGGACAGTCTCAAA
CCL19	GCCTTCCGCTACCTTCTTATC	GTCTTCGGATGATGCGTTCT
CCL21	GGCCGTCCCTTTCTTCTATG	AGTCCTGCTGTCTCCTTCT
CCL27	CTCCAACAAGCCAGAGACTAAG	CTCCAACAAGCCAGAGACTAAG
CXCL1	GCACCCAAACCGAAGTCATA	GGGACACCCTTTAGCATCTTT
CXCL2	GACAGAAGTCATAGCCACTCTT	GCCTTGCCTTTGTTCAGTATC
CXCL6	GCTCAAGCTGCTCCTTTCT	GCAGGGATCACCTCCAAATTA
CXCL10	AAGCGGTGAGCCAAAGAA	CAGGAGAAACAGGGACAGTTAG
CXCL12	GGGAAGGGAAACGGAGAAAG	CTCACCACACACACATCACTAA
CXCL13	CCAAGCTCCAGTGAGTAAGAAA	AAGATTCCGAGCAGGGATTAAG
GAPDH	ACTCCCATTCTTCCACCTTTG	CCCTGTTGCTGTAGCCATATT

In order to detect the inflammatory cytokines and chemokine in the liver, the homogenate made from the liver tissue was mixed with precooled PBS (100 mg/500 μL), and the supernatant was collected after centrifugation (500g, 5 min) for further ELISA testing.

2.10. Histopathology and Immunohistochemistry. The harvested liver tissues were fixed in 4% paraformaldehyde, embedded in paraffin, cut into 4 μm sections, and stained with hematoxylin and eosin. For immunohistochemistry, endogenous peroxidases, nonspecific binding sites were blocked using 0.3% H_2O_2 and Goat Serum, respectively. Then, sections were incubated with an anti-rat MPO Ab at 4°C overnight. Subsequently, the Catalyzed Signal Amplification System (DAKO, K1500) was used for staining. Then, the slides were counterstained with hematoxylin. Liver sections were evaluated blindly by counting labeled cells in 10 high-power fields.

2.11. TUNEL Stain. TUNEL stain was performed to detect the apoptosis of liver tissue sections by using TUNEL kit (KeyGEN, China) according to the instructions. Apoptotic cells were observed under fluorescence microscope, and the nuclei of the positive cells were presented as bright green.

2.12. Prussian Blue Staining of MSCs Labeled with SPIO. MSCs were labeled with Ferumoxytol (Southeast University, Nanjing, China), as previously described [15]. Briefly, polyamine poly-l-lysine (PLL) (Sigma, USA) was used as the transfection agent. PLL (10.0 μg/mL) was mixed with Ferumoxytol (500 μg/mL) for 60 min at room temperature on a rotating shaker. MSCs of passages 3–5 were cultured with the medium that contained the Ferumoxytol-PLL complex (50 μg/mL Ferumoxytol) for 24 h. After being incubated with the Ferumoxytol-PLL complex, the MSCs were washed three times to remove excessive contrast agent. For Prussian blue staining, which indicates the presence of iron, the coverslip samples were fixed with 4% paraformaldehyde for 30 min, washed, incubated for another 30 min with 2% potassium ferrocyanide in 6% hydrochloric acid, washed again, and counterstained with nuclear fast red.

2.13. Statistical Analysis. All values are expressed as the mean ± SD. Data were analyzed with an unpaired two-tailed Student's *t*-test. $P < 0.05$ was considered statistically significant.

3. Results

3.1. Characterization of Rat MSCs. Rat MSCs at passage 3 were analyzed for the expression of cell surface molecules by flow cytometry. The MSCs expressed CD29, CD44, and CD90 but did not express hematopoietic cell markers such as CD45, CD34, and CD11b (Figure 1(a)) which have been previously reported.

In addition, the differentiation capacity of MSCs was also examined. Rat MSCs could be differentiated into osteoblasts and adipocytes, which represent classical mesenchymal lineage cells (Figure 1(b)).

3.2. MSCs Reduce the Release of Liver Enzymes and Improve the Histopathologic Changes of the Livers in IRI. To investigate the protective effect of MSCs in rat liver IRI model, we measured serum ALT (Figure 2(a)) and AST (Figure 2(b)) after 12 h of I/R. ALT and AST levels in rats treated with MSCs were significantly reduced compared to those in rats

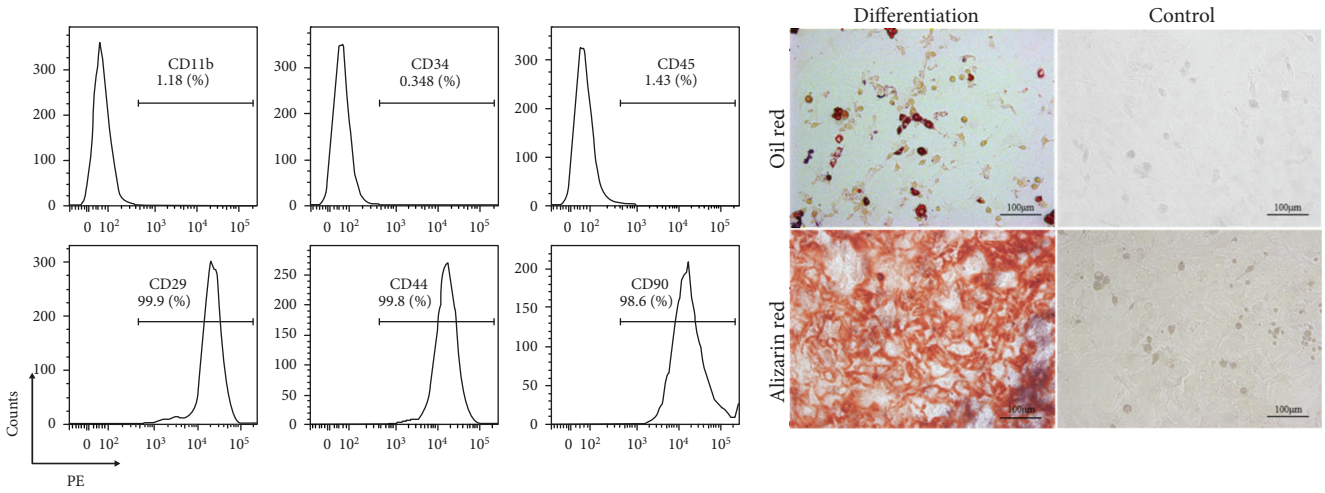

Figure 1: Characterization of rat bone marrow derived-MSCs. (a) Immunophenotype of rat MSCs. Cells were harvested at passage 3, labeled with the antibodies specific for the indicated surface antigens or negative controls, and analyzed by flow cytometry. The numbers in the panels represent the mean fluorescence intensity of the cells expressing each marker. (b) Rat MSCs at passage 3 that were induced to differentiate into adipocytes and osteoblasts. Cells stain positive for oil with oil red staining and for calcium with alizarin red solution, respectively. Original magnification, ×200.

treated with PBS injections. At the same time, decreased expression levels of various proapoptotic proteins in IRI liver lobes including Cleaved caspase-3, Bad, and Fas were found in response to MSC treatment compared to the control group (Figure 2(c)). In addition, the histopathologic injury of the liver including portal inflammation, hepatocyte swelling, cytoplasm rarefaction, and coagulative necrosis was alleviated in the MSC-treated group. After 12 h of reperfusion, the IRI + PBS group had significantly more inflammatory cell accumulation (solid black triangles) in the portal area compared to the IRI + MSC group. The count of swelling hepatocyte (solid black arrows) in the IRI + PBS group is much more than that in the IRI + MSC group, as well as the degree of cytoplasm rarefaction. The IRI + PBS group also had markedly higher hepatocellular necrosis (hollow arrows) and acidophilic degeneration (hollow triangles) compared to the IRI + MSC group (Figure 2(d)). Furthermore, the TUNEL stain of the liver showed that the number of apoptosis cells (bright green) in the MSC treatment group was rarer than that in the IRI + PBS group (Figure 2(e)).

3.3. MSCs Affect Cytokine Expression and Reduce Neutrophil Infiltration. Following I/R injury, there were significant increases in proinflammatory cytokines IL-2, IL-4, and IL-6 and chemokine CXCL2 at both mRNA (Figure 3(a)) and protein (Figure 3(b)) levels in the liver. Treatment with MSCs markedly attenuated I/R-stimulated CXCL2 and proinflammatory cytokine aforementioned expression in the liver. Furthermore, the immunohistochemical analysis showed distinct neutrophil infiltration compared to the sham group, and the cell infiltration decreased significantly after MSC therapy (Figures 3(c) and 3(d)). The change of levels of the CD11b/CD18 mRNA also indicated that MSC injection could reduce neutrophil infiltration (Figures 3(e) and 3(f)).

3.4. MSCs Accumulated in the Injured Liver Lobes in the Model of Hepatic IRI. MSCs were known to migrate or dock preferentially to injured sites [16]. This phenomenon could facilitate the paracrine of MSCs considered a principal mechanism in MSC therapy [17]. Thus, we labeled MSCs with SPIO and tracked the accumulation of MSCs at 24 h, 72 h, and 2 w postinjection in the model of hepatic IRI. SPIO-labeled MSCs stained with Prussian blue showed blue particles in the cytoplasm in contrast with unlabeled cells in which no blue particles were observed, and the labeling ratio was approximately 100% (Figure 4(a)). The signal intensity of the injured liver lobe increased on the T2 sequence in both the IRI + PBS group and the IRI + MSC group that implied the degree of inflammation of the lobes, but the signal of the IRI + MSC group was significantly lower than that of the IRI + PBS group after 72 h, which means MSC injection could protect the liver during IRI. In the IRI + MSC-SPIO group, in which MSCs were labeled with SPIO, the signal intensity of IRI lobes was significantly lower than that of others 72 h after reperfusion indicated the recruitment of MSCs in these areas. In addition, the signal intensity gradually approached close to normal on day 14 (Figure 4(b)).

3.5. MSCs Attenuate Neutrophil Recruitment via Downregulation of CXCR2. To study the mechanism(s) underlying the decrease of infiltration of neutrophils in IRI liver, we examined the surface expression of CXCR2, an important chemokine receptor that mediates neutrophil recruitment. As shown in Figures 5(a) and 5(b), MSC treatment significantly downregulated the surface expression of CXCR2 on neutrophils. Further, we found that the inhibitory effect on CXCR2 expression was caused by enhanced intracellular activation of p38 MAPK phosphorylation (Figures 5(c) and 5(d)) and has been blocked by p38 MAPK inhibitor (Figure 5(e)).

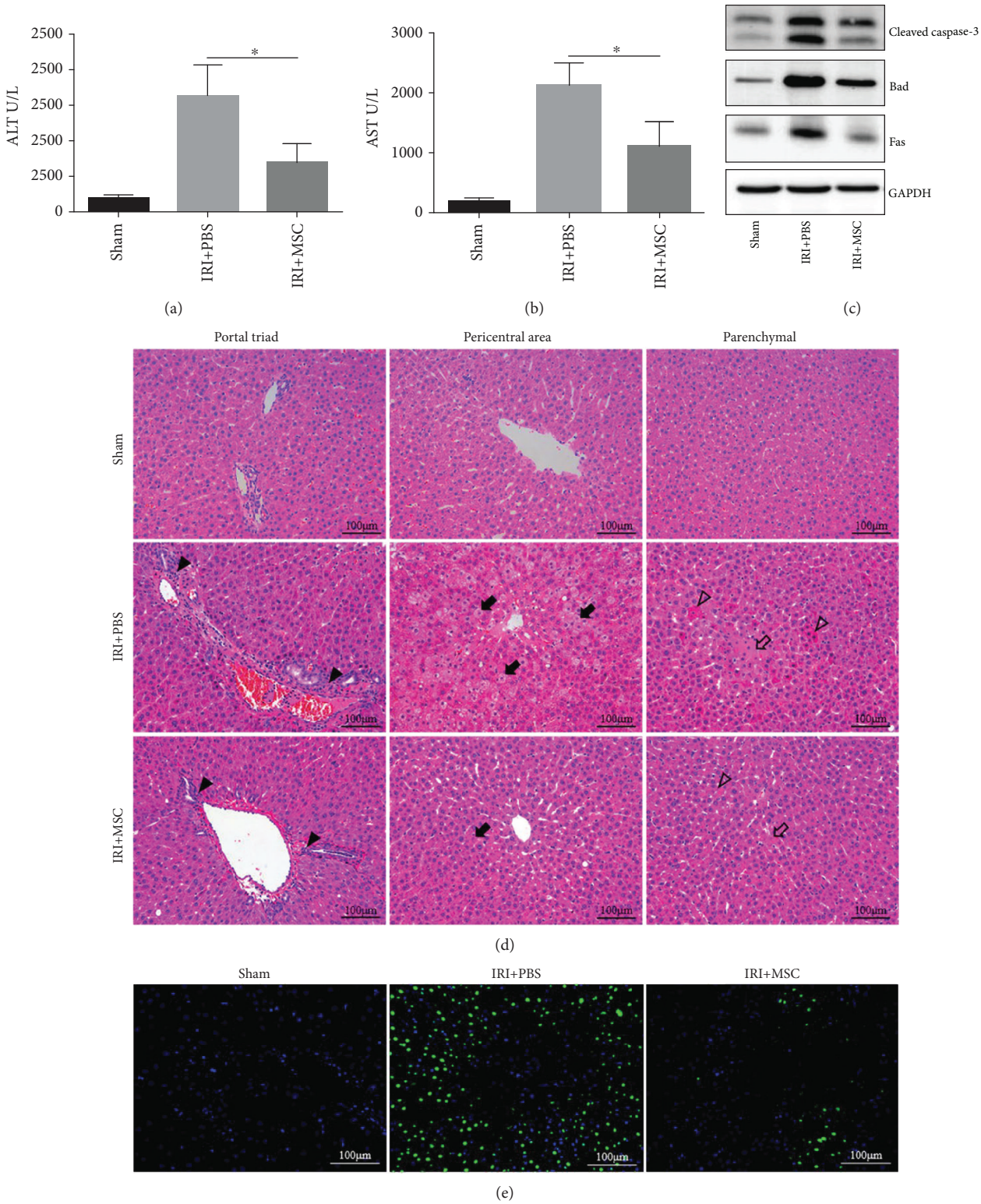

Figure 2: Rat MSCs reduced the release of liver enzymes and improved the histopathologic changes of livers in IRI. Male SD rats were randomized into sham, IRI + PBS, and IRI + MSC groups. Samples of each group were collected 12 h postreperfusion. (a, b) As markers for hepatic injury, serum levels of ALT and AST were determined. (c) The expression levels of various proapoptotic proteins including Cleaved caspase-3, Bad, and Fas in the I/R liver lobes were determined by Western blot analysis. (d) Representative images of hematoxylin and eosin-stained sections of liver tissues were shown. Inflammatory cell accumulation (solid black triangles), hepatocellular swelling (solid black arrows), necrosis (hollow arrows), and acidophilic degeneration (hollow triangles) were observed. (e) TUNEL staining of apoptosis cells (bright green) in liver tissues. Data are mean ± SD; $^{*}p < 0.05$. Original magnification, ×200.

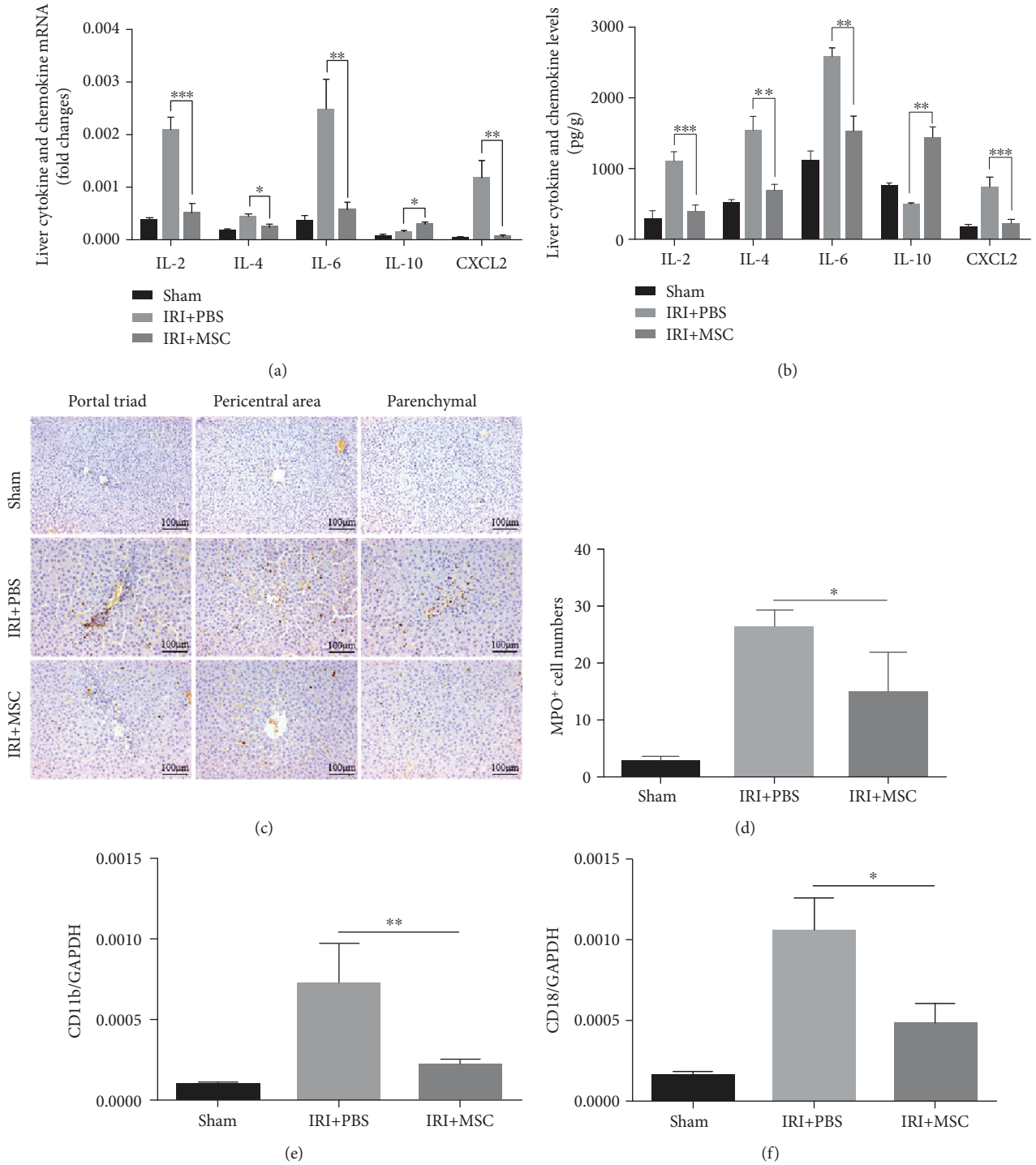

Figure 3: MSCs affect cytokine expression and reduce neutrophil infiltration. (a, e, f) The relative mRNA levels of IL-2, IL-4, IL-6, IL-10, CXCL2, CD11b, and CD18 genes in I/R lobes were detected by qRT-PCR. Data were normalized to glyceraldehyde-3-phosphate dehydrogenase gene expression. (b) The concentration of IL-2, IL-4, IL-6, IL-10, and CXCL2 in I/R lobes was measured by ELISA. (c) Representative images of immunohistochemistry-stained sections of MPO^+ cells of liver tissues were shown. (d) The mean frequency of hepatic MPO^+ cells in 10 high-power fields was calculated. Data are mean ± SD. $^*p < 0.05$, $^{**}p < 0.01$, $^{***}p < 0.001$. Original magnification, ×200.

3.6. MSCs Inhibit Macrophage CXCL2 Expression via Attenuation of NF-κB p65 Phosphorylation. As shown in Figure 5(f), the CXCL2 mRNA expression level was almost 30 times higher in I/R injured liver lobes and exhibited the most significant change among the tested chemokines. Injection of MSCs significantly attenuated CXCL2 mRNA expression (Figure 3(a)) and protein production (Figure 3(b)). In vitro, these changes of CXCL2 expression (Figure 5(g)) were

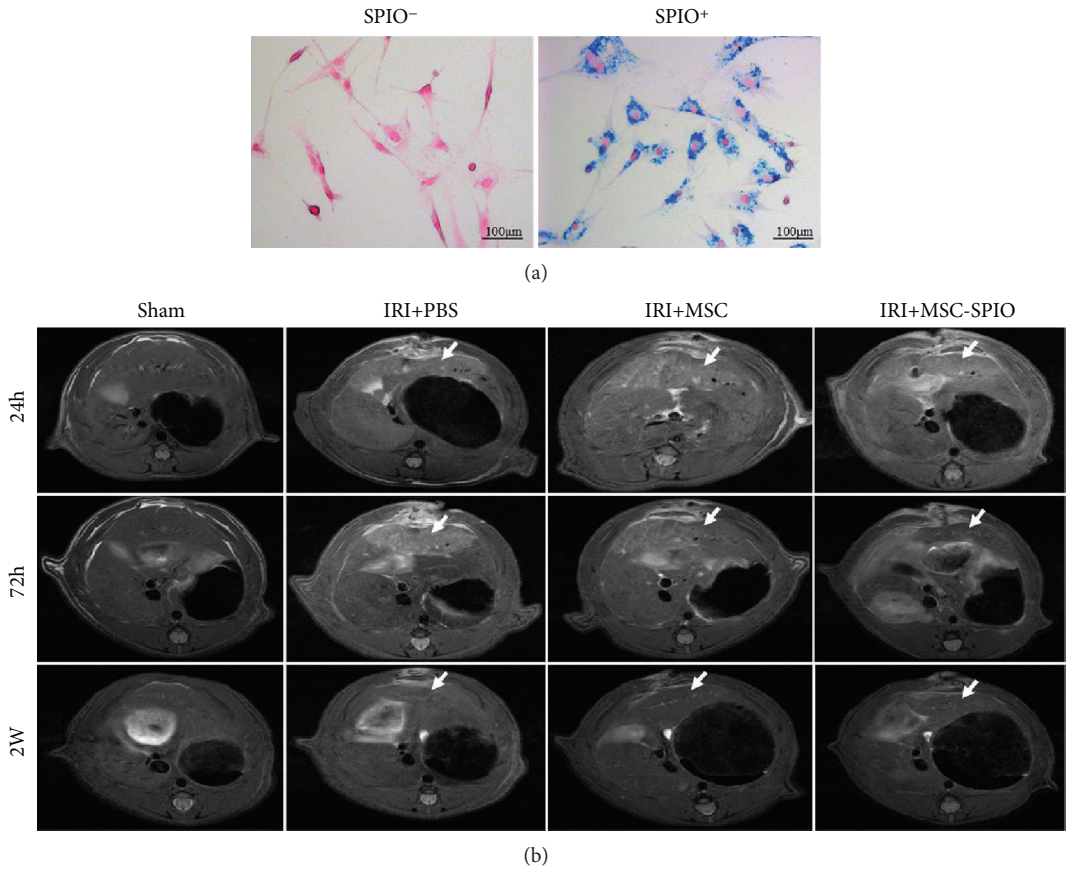

Figure 4: MSCs accumulated in injured liver lobes in the model of hepatic IRI. (a) SPIO-labeled MSCs were positive for Prussian blue staining. Blue particles were observed in the cytoplasm of $SPIO^+$ cells. (b) Male SD rats were randomized into sham, IRI + PBS, IRI + MSC, and IRI + MSC-SPIO groups. Representative images of MRI scanning on the T2 sequence of I/R lobes in each group were shown after 24 h, 72 h, and 2 w of reperfusion. The liver lobes experienced IRI were pointed out by white arrows. Original magnification, ×200.

correlated with the phosphorylation of NF-κB p65 in macrophages. MSCs inhibited the activation of NF-κB p65 of macrophages (Figure 5(h)).

4. Discussion

Hepatic IRI occurs in diverse clinical situations, such as hepatic resection, liver transplantation, shock, and trauma. In particular, in liver transplantation, IRI is the main cause of morbidity and mortality due to graft rejection [18]. Previous studies have shown that liver damage is mainly caused during reperfusion period, and neutrophils are considered central factors in the events leading to injury after reperfusion [19]. MSCs represent a promising candidate for liver cell therapy because of their immunomodulation of both adaptive and innate immunity [20]. So far, few studies have examined the effects of MSCs on hepatic IRI [21]. In this study, we investigate the roles of MSCs on hepatic inflammatory response, neutrophil recruitment, and liver tissue damage in a rat model of partial hepatic IRI. We reported that injected MSCs accumulated in damaged liver lobes and effectively protected rat against hepatic IRI, with significantly decreased serum levels of liver enzymes, attenuated hepatic neutrophil infiltration, reduced expression of apoptosis-associated proteins, and ameliorated liver pathological changes. We further demonstrated that MSCs significantly inhibited IRI-stimulated overexpression and release of neutrophil chemoattractant CXCL2 through attenuation of NF-κB p65 activation and substantially attenuated neutrophil chemotaxis via downregulation of CXCR2 expression by increasing of p38 MAPK phosphorylation in neutrophils.

As shown in previous studies, hepatic IRI should be considered as an innate immunity-dominated inflammation response [22]. Liver damage is driven by a complex set of leukocytes, including natural killer cells, natural killer T cells, dendritic cells, neutrophils, and eosinophils. Neutrophils, the largest circulating fraction of leukocytes, arrive at the injury site first and play the crucial role in liver injury. It has been reported that the extent of neutrophil sequestration in patients with ischemic or alcoholic liver disease correlates strongly with disease severity [23], while depletion of neutrophils before hepatic insult can limit tissue injury in animal experiments [24]. In the present study, after 12 h of reperfusion in the IRI rats, histopathologic examination showed markedly hepatocellular injury including swelling, apoptosis, and necrosis, which was consistent with high levels of AST and ALT in the serum. The pathology was observed by the concurrent recruitment of neutrophils in the liver. Treatment

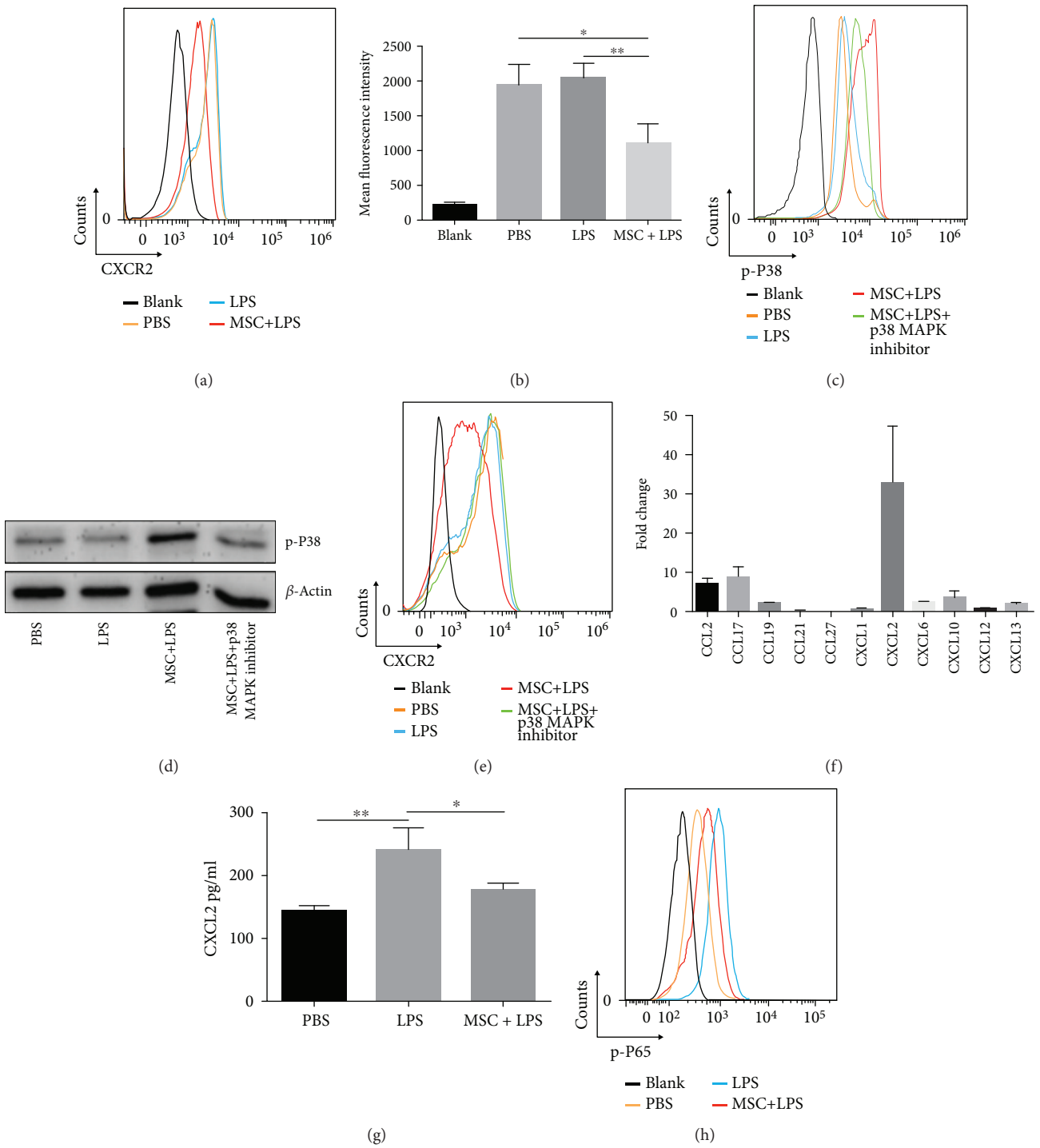

Figure 5: MSCs attenuate neutrophil recruitment via hindering CXCL2/CXCR2 signaling. (a, e) Surface expression of CXCR2 on neutrophils was detected by flow cytometry analysis. (b) The mean fluorescence intensity of CXCR2 on the surface of neutrophils was recorded. (c) The levels of p38 MAPK phosphorylation in neutrophils were detected by flow cytometry analysis, and (d) the consequences were verified by Western blot analysis. (f) The expression levels of mRNA of various chemokines involved in hepatic IRI were analyzed by qRT-PCR. Fold change represents the expression of each chemokine in I/R liver lobes 12 h postreperfusion compared with normal liver. (g) Macrophages were cultured in the presence or absence of MSCs for 12 h. The concentration of CXCL2 in the supernatant was measured by ELISA. (h) The levels of NF-κB p65 phosphorylation in macrophages were detected by flow cytometry analysis. Data are mean ± SD. $^{*}p < 0.05$, $^{**}p < 0.01$, $^{***}p < 0.001$. p-P38: phospho-p38 MAPK; p-P65: phospho-NF-κB p65.

with MSCs significantly attenuated I/R-induced influx of neutrophils into the liver, thus ameliorating liver injury. We further confirmed the MSC homing phenomenon by using MRI tracking technology. As with similar other studies [25–27], MSCs docked preferentially to injured sites. In consideration of the paracrine and regeneration mechanism of MSCs in cell therapy, their ability of trafficking to particular tissues deserves further research [28].

We next examined the underlying mechanisms by which MSCs attenuate neutrophil accumulation in the I/R liver. As mentioned, CXCR2 signaling is an important chemokine axis that regulates neutrophil release from the bone marrow [29] and recruitment from the circulation into the site of inflammation [30]. Depletion of CXCR2 on neutrophils could significantly alleviate organ inflammation due to the reduction of neutrophil infiltration [31]. We found that MSC treatment significantly downregulates CXCR2 expression on neutrophils, thus attenuating neutrophil chemotaxis toward the I/R liver lobe. It has been shown that the chemoattractant CXCL2 plays a key role in neutrophil recruitment. The expression of CXCL2 protein in the ischemic lobes was increased hundred- to thousandfold over control [32]. Furthermore, the expression of CXCL2 was much earlier than neutrophil accumulation, which suggests that CXCL2 may be involved in the initial recruitment of neutrophils to the ischemic lobe [33]. Our findings are lined with previous studies that I/R resulted in markedly increased CXCL2 expression in the liver at both mRNA and protein levels. Interestingly, the MSC treatment significantly reduced I/R-stimulated CXCL2 production. Taking into account both of the impacts, MSCs attenuate neutrophil chemotaxis by hindering CXCL2/CXCR2 signaling.

Prior to neutrophil infiltration, the hypoxic-ischemic damage of resident liver cells during ischemic phase results in the release of endogenous molecules named danger-associated molecular patterns (DAMPs), which can be recognized by pattern recognition receptors expressed on innate immune cells thus causing neutrophil gathering [34]. Toll-like receptors (TLRs) play important roles among these DAMP receptors including retinoic acid-inducible gene I-like receptors, nucleotide-binding oligomerization domain-like receptors, and C-type lectin receptors. Notably, the activation of MAPK and NF-κB signaling pathways was enrolled during the recognition of DAMPs [35]. Previous studies showed that the increase of phosphorylation levels of the p38 MAPK was related to neutrophil chemotaxis [36]. In this study, we found activation of p38 MAPK phosphorylation in neutrophils upon treatment with MSCs, which led to decreased expression of CXCR2 on the cell surface. Furthermore, the inhibitory effect of MSCs on CXCR2 expression can be blocked by p38 MAPK inhibitor. Macrophages were considered the main source of CXCL2 in liver injury [37]. We then examined the effect of MSCs on NF-κB p65 and MARK p38 activation in macrophages. MSCs substantially inhibited NF-κB p65 phosphorylation, thereby attenuating CXCL2 expression and production in macrophages. These results suggest a synergy between the affection of MSCs on neutrophils and macrophages to alleviate hepatic IRI.

In conclusion, we have demonstrated that MSCs may represent a potential therapeutic strategy to alleviate hepatic ischemia/reperfusion injuries. The effects of MSCs were found, for the first time, due to the inhibition ability of neutrophil chemotaxis via NF-κB p65 and MAPK p38 signaling pathways. The results of this study offer a new insight into the mechanisms responsible for MSC-mediated inhibition, a protective manner, which may promote the future clinical application of MSCs in liver transplantation.

Data Availability

The data used to support the findings of this study are included within the article.

Conflicts of Interest

The authors declare that they have no competing interests.

Authors' Contributions

Shihui Li and Xu Zheng contributed equally to this work.

Acknowledgments

This work was supported by the National Natural Science Foundation of China (81170422, 81300365, 81370575, 81570593, and 81870447) and the Guangdong Natural Science Foundation (2015A030312013 and 2017A020215178). The authors confirm that the funding did not lead to any conflict of interests regarding the publication of this manuscript. The authors sincerely thank Yiping Wang, PhD, from the University of Sydney, for editing the English text of a draft of this manuscript.

References

[1] W. R. Kim, J. R. Lake, J. M. Smith et al., "OPTN/SRTR 2013 annual data report: liver," *American Journal of Transplantation*, vol. 15, Supplement 2, pp. 1–28, 2015.

[2] F. Serracino-Inglott, N. A. Habib, and R. T. Mathie, "Hepatic ischemia-reperfusion injury," *American Journal of Surgery*, vol. 181, no. 2, pp. 160–166, 2001.

[3] R. Busuttil and K. Tanaka, "The utility of marginal donors in liver transplantation," *Liver Transplantation*, vol. 9, no. 7, pp. 651–663, 2003.

[4] R. F. Saidi and S. K. H. Kenari, "Liver ischemia/reperfusion injury: an overview," *Journal of Investigative Surgery*, vol. 27, no. 6, pp. 366–379, 2014.

[5] M. Cannistra, M. Ruggiero, A. Zullo et al., "Hepatic ischemia reperfusion injury: a systematic review of literature and the role of current drugs and biomarkers," *International Journal of Surgery*, vol. 33, pp. S57–S70, 2016.

[6] M. Honda, T. Takeichi, K. Asonuma, K. Tanaka, M. Kusunoki, and Y. Inomata, "Intravital imaging of neutrophil recruitment in hepatic ischemia-reperfusion injury in mice," *Transplantation*, vol. 95, no. 4, pp. 551–558, 2013.

[7] P. Rowart, P. Erpicum, O. Detry et al., "Mesenchymal stromal cell therapy in ischemia/reperfusion injury," *Journal of Immunology Research*, vol. 2015, Article ID 602597, 8 pages, 2015.

[8] K. Akiyama, C. Chen, D. Wang et al., "Mesenchymal-stem-cell-induced immunoregulation involves FAS-ligand-/FAS-mediated T cell apoptosis," *Cell Stem Cell*, vol. 10, no. 5, pp. 544–555, 2012.

[9] L. C. Davies, N. Heldring, N. Kadri, and K. Le Blanc, "Mesenchymal stromal cell secretion of programmed death-1 ligands regulates T cell mediated immunosuppression," *Stem Cells*, vol. 35, no. 3, pp. 766–776, 2017.

[10] A. Corcione, F. Benvenuto, E. Ferretti et al., "Human mesenchymal stem cells modulate B-cell functions," *Blood*, vol. 107, no. 1, pp. 367–372, 2006.

[11] Y. Liu, Z. Yin, R. Zhang et al., "MSCs inhibit bone marrow-derived DC maturation and function through the release of TSG-6," *Biochemical and Biophysical Research Communications*, vol. 450, no. 4, pp. 1409–1415, 2014.

[12] P. A. Sotiropoulou, S. A. Perez, A. D. Gritzapis, C. N. Baxevanis, and M. Papamichail, "Interactions between human mesenchymal stem cells and natural killer cells," *Stem Cells*, vol. 24, no. 1, pp. 74–85, 2006.

[13] J. Maggini, G. Mirkin, I. Bognanni et al., "Mouse bone marrow-derived mesenchymal stromal cells turn activated macrophages into a regulatory-like profile," *PLoS One*, vol. 5, no. 2, article e9252, 2010.

[14] G. Pan, Y. Yang, J. Zhang et al., "Bone marrow mesenchymal stem cells ameliorate hepatic ischemia/reperfusion injuries via inactivation of the MEK/ERK signaling pathway in rats," *The Journal of Surgical Research*, vol. 178, no. 2, pp. 935–948, 2012.

[15] A. S. Arbab, L. A. Bashaw, B. R. Miller et al., "Characterization of biophysical and metabolic properties of cells labeled with superparamagnetic iron oxide nanoparticles and transfection agent for cellular MR imaging," *Radiology*, vol. 229, no. 3, pp. 838–846, 2003.

[16] L. da Silva Meirelles, A. I. Caplan, and N. B. Nardi, "In search of the in vivo identity of mesenchymal stem cells," *Stem Cells*, vol. 26, no. 9, pp. 2287–2299, 2008.

[17] L. Da Silva Meirelles, A. M. Fontes, D. T. Covas, and A. I. Caplan, "Mechanisms involved in the therapeutic properties of mesenchymal stem cells," *Cytokine & Growth Factor Reviews*, vol. 20, no. 5-6, pp. 419–427, 2009.

[18] B. Andria, A. Bracco, C. Attanasio et al., "Biliverdin protects against liver ischemia reperfusion injury in swine," *PLoS One*, vol. 8, no. 7, article e69972, 2013.

[19] S. Hashimoto, M. Honda, T. Takeichi et al., "Intravital imaging of neutrophil recruitment in intestinal ischemia-reperfusion injury," *Biochemical and Biophysical Research Communications*, vol. 495, no. 3, pp. 2296–2302, 2018.

[20] J. Colmenero and P. Sancho-Bru, "Mesenchymal stromal cells for immunomodulatory cell therapy in liver transplantation: One step at a time," *Journal of Hepatology*, vol. 67, no. 1, pp. 7–9, 2017.

[21] J. Gracia-Sancho, A. Casillas-Ramirez, and C. Peralta, "Molecular pathways in protecting the liver from ischaemia/reperfusion injury: a 2015 update," *Clinical Science*, vol. 129, no. 4, pp. 345–362, 2015.

[22] H. Ji, X. Shen, F. Gao et al., "Programmed death-1/B7-H1 negative costimulation protects mouse liver against ischemia and reperfusion injury," *Hepatology*, vol. 52, no. 4, pp. 1380–1389, 2010.

[23] J. J. Maher, M. K. Scott, J. M. Saito, and M. C. Burton, "Adenovirus-mediated expression of cytokine-induced neutrophil chemoattractant in rat liver induces a neutrophilic hepatitis," *Hepatology*, vol. 25, no. 3, pp. 624–630, 1997.

[24] J. A. Hewett, A. E. Schultze, S. Vancise, and R. A. Roth, "Neutrophil depletion protects against liver injury from bacterial endotoxin," *Laboratory Investigation*, vol. 66, no. 3, pp. 347–361, 1992.

[25] X. L. Shi, J. Y. Gu, B. Han, H. Y. Xu, L. Fang, and Y. T. Ding, "Magnetically labeled mesenchymal stem cells after autologous transplantation into acutely injured liver," *World Journal of Gastroenterology*, vol. 16, no. 29, pp. 3674–3679, 2010.

[26] T. H. Kim, J. K. Kim, W. Shim, S. Y. Kim, T. J. Park, and J. Y. Jung, "Tracking of transplanted mesenchymal stem cells labeled with fluorescent magnetic nanoparticle in liver cirrhosis rat model with 3-T MRI," *Magnetic Resonance Imaging*, vol. 28, no. 7, pp. 1004–1013, 2010.

[27] F. Defresne, T. Tondreau, X. Stéphenne et al., "Biodistribution of adult derived human liver stem cells following intraportal infusion in a 17-year-old patient with glycogenosis type 1A," *Nuclear Medicine and Biology*, vol. 41, no. 4, pp. 371–375, 2014.

[28] J. M. Karp and G. S. Leng Teo, "Mesenchymal stem cell homing: the devil is in the details," *Cell Stem Cell*, vol. 4, no. 3, pp. 206–216, 2009.

[29] K. J. Eash, A. M. Greenbaum, P. K. Gopalan, and D. C. Link, "CXCR2 and CXCR4 antagonistically regulate neutrophil trafficking from murine bone marrow," *The Journal of Clinical Investigation*, vol. 120, no. 7, pp. 2423–2431, 2010.

[30] F. Rios-Santos, J. C. Alves-Filho, F. O. Souto et al., "Down-regulation of CXCR2 on neutrophils in severe sepsis is mediated by inducible nitric oxide synthase-derived nitric oxide," *American Journal of Respiratory and Critical Care Medicine*, vol. 175, no. 5, pp. 490–497, 2007.

[31] C. W. Steele, S. A. Karim, M. Foth et al., "CXCR2 inhibition suppresses acute and chronic pancreatic inflammation," *The Journal of Pathology*, vol. 237, no. 1, pp. 85–97, 2015.

[32] G. C. Wilson, S. Kuboki, C. M. Freeman et al., "CXC chemokines function as a rheostat for hepatocyte proliferation and liver regeneration," *PLoS One*, vol. 10, no. 3, article e0120092, 2015.

[33] A. B. Lentsch, H. Yoshidome, W. G. Cheadle, F. N. Miller, and M. J. Edwards, "Chemokine involvement in hepatic ischemia/reperfusion injury in mice: roles for macrophage inflammatory protein-2 and Kupffer cells," *Hepatology*, vol. 27, no. 2, pp. 507–512, 1998.

[34] B. Mcdonald, K. Pittman, G. B. Menezes et al., "Intravascular danger signals guide neutrophils to sites of sterile inflammation," *Science*, vol. 330, no. 6002, pp. 362–366, 2010.

[35] Y. C. Lu, W. C. Yeh, and P. S. Ohashi, "LPS/TLR4 signal transduction pathway," *Cytokine*, vol. 42, no. 2, pp. 145–151, 2008.

[36] X. Xu, S. Zheng, Y. Xiong et al., "Adenosine effectively restores endotoxin-induced inhibition of human neutrophil chemotaxis via A1 receptor-p38 pathway," *Inflammation Research*, vol. 66, no. 4, pp. 353–364, 2017.

[37] C. C. Qin, Y. N. Liu, Y. Hu, Y. Yang, and Z. Chen, "Macrophage inflammatory protein-2 as mediator of inflammation in acute liver injury," *World Journal of Gastroenterology*, vol. 23, no. 17, pp. 3043–3052, 2017.

Hindawi
Journal of Immunology Research
Volume 2018, Article ID 1509851, 7 pages
https://doi.org/10.1155/2018/1509851

Research Article

RIPK3-Mediated Necroptosis and Neutrophil Infiltration Are Associated with Poor Prognosis in Patients with Alcoholic Cirrhosis

Zhenzhen Zhang,[1,2] Guomin Xie,[3] Li Liang,[4] Hui Liu,[5] Jing Pan,[1] Hao Cheng,[1] Hua Wang,[6] Aijuan Qu,[3] and Yan Wang[1]

[1]*Department of Infectious Diseases, Peking University First Hospital, Beijing 100034, China*
[2]*Xiamen Branch, Zhongshan Hospital, Fudan University, Xiamen 361015, China*
[3]*Department of Physiology and Pathophysiology, School of Basic Medical Sciences, Capital Medical University, Key Laboratory of Remodeling-Related Cardiovascular Diseases, Ministry of Education, Beijing Key Laboratory of Metabolic Disturbance-Related Cardiovascular Disease, Beijing 100069, China*
[4]*Department of Pathology, Peking University First Hospital, Beijing 100034, China*
[5]*Department of Pathology, Beijing Youan Hospital, Capital Medical University, Beijing 100069, China*
[6]*Department of Oncology, The First Affiliated Hospital, Institute for Liver Diseases of Anhui Medical University, Hefei 230032, China*

Correspondence should be addressed to Yan Wang; wangyanwang@bjmu.edu.cn

Received 8 June 2018; Revised 17 September 2018; Accepted 23 September 2018; Published 25 November 2018

Guest Editor: Feng Li

Alcoholic cirrhosis is an end-stage liver disease with impaired survival and often requires liver transplantation. Recent data suggests that receptor-interacting protein kinase-3- (RIPK3-) mediated necroptosis plays an important role in alcoholic cirrhosis. Additionally, neutrophil infiltration is the most characteristic pathologic hallmark of alcoholic hepatitis. Whether RIPK3 level is correlated with neutrophil infiltration or poor prognosis in alcoholic cirrhotic patients is still unknown. We aimed to determine the correlation of RIPK3 and neutrophil infiltration with the prognosis in the end-stage alcoholic cirrhotic patients. A total of 20 alcoholic cirrhotic patients subjected to liver transplantation and 5 normal liver samples from control patients were retrospectively enrolled in this study. Neutrophil infiltration and necroptosis were assessed by immunohistochemical staining for myeloperoxidase (MPO) and RIPK3, respectively. The noninvasive score system (model for end-stage liver disease (MELD)) and histological score systems (Ishak, Knodell, and ALD grading and ALD stage) were used to evaluate the prognosis. Neutrophil infiltration was aggravated in patients with a high MELD score (≥32) in the liver. The MPO and RIPK3 levels in the liver were positively related to the Ishak score. The RIPK3 was also significantly and positively related to the Knodell score. In conclusion, RIPK3-mediated necroptosis and neutrophil-mediated alcoholic liver inflammatory response are highly correlated with poor prognosis in patients with end-stage alcoholic cirrhosis. RIPK3 and MPO might serve as potential predictors for poor prognosis in alcoholic cirrhotic patients.

1. Introduction

Alcoholic cirrhosis is the end-stage serious liver disease with high morbidity and mortality and is the leading cause of liver transplantation [1–3]. Prognostic models can be used to assess the severity and survival of the disease and can be useful as a medical decision-making tool to guide patient care. However, the early detection and evaluation of this severe disease have not been fully elucidated.

The most widely used noninvasive predictor of poor prognosis in alcoholic liver cirrhosis is the model for end-stage liver disease (MELD) scoring systems [4]. While for specific predictors, histologic scoring system is the main method [5, 6]. The ALD grading and staging schema were

first proposed for alcoholic liver disease [7], then recently the alcoholic hepatitis histologic score (AHHS), proposed for alcoholic hepatitis (AH) [8]. And the Ishak score [9] and Knodell score [10] were recognized predictors for chronic hepatitis. However, these scoring systems are based on clinical, biochemical, and histological features and do not take into consideration the molecular pathogenesis of the disease. Thus, identification of pathogenesis-related factors indicating poor prognosis in patients with alcoholic cirrhosis is necessary for early prevention and treatment.

The pathogenesis of alcoholic cirrhosis is characterized by inflammation, fibrosis, and damaged cellular membranes incapable of detoxification ending in scaring and necrosis [11–13]. Recently, it has been reported that necroptosis, i.e., programmed cell necrosis, plays an important role in alcoholic cirrhosis [14, 15]. Receptor-interacting protein kinase 3 (RIPK3) is a key component of the necrosome [16, 17] and was reported to be activated in the livers of mouse models after chronic ethanol feeding as well as in the livers of ALD patients [18]. Furthermore, RIP3-knockout mice could prevent ethanol-induced liver injury and inflammation [18]. RIPK3 has been shown to interact with RIPK1 in kinase activation [19]. However, in some circumstances, RIPK3 serves its necrotic role independent of RIPK1 in viral infection [20], in TNF-α mediated shock [21], and also in ethanol-induced liver injury [18]. Whether the expression of RIPK3 is related to a poor prognosis in alcoholic cirrhosis is hitherto unknown.

Neutrophil infiltration is another pathologic hallmark for alcoholic cirrhotic liver [22]. Our previous studies demonstrate that neutrophil infiltration plays a major role in alcoholic liver disease of murine models [23, 24]. Neutrophil depletion by a pharmacological agent (anti-Ly6G antibody) ameliorates alcoholic liver injury [23]. It is also reported that the expression of CXC chemokines recruiting the neutrophil infiltration in the liver is associated with the prognosis of patients with alcoholic hepatitis [25], although several studies have indicated that programmed cell death may trigger inflammation in liver diseases of murine models [16], such as viral infection [20], systemic inflammatory response syndrome or sepsis [26], drug-induced liver injury [27], and alcoholic liver disease [18, 28]. However, whether RIPK3 level is correlated with neutrophil infiltration in alcoholic cirrhotic patients is still unknown.

In the present study, we aimed to determine the correlation between RIPK3 with the degree of neutrophil infiltration in the liver and the related prognosis in the end-stage alcoholic cirrhotic patients. Our results showed that RIPK3-mediated necroptosis and neutrophil-mediated alcoholic liver inflammatory response are highly correlated with poor prognosis in end-stage alcoholic cirrhotic patients. RIPK3 and MPO may serve as potential predictors for poor prognosis in patients with alcoholic cirrhosis.

2. Materials and Methods

2.1. Patients. In this retrospective study, a total of 20 diagnosed alcoholic cirrhotic patients (stage 3 to 4 fibrosis according to clinical practice guidelines [3, 29]) and 5 healthy controls were analyzed during liver transplantation from the Liver Tissue Cell Distribution System, University of Minnesota (Minneapolis, MN), between 2006 and 2011 [30]. Patients with concomitant other causes of liver disease, including chronic hepatitis B, chronic hepatitis C, hepatocellular carcinoma and nonalcoholic fatty liver disease, autoimmune liver disease, and drug-induced liver injury, were excluded.

2.2. Data Collection. Clinical and biochemical parameters at the time of liver transplantation were carefully collected from the medical records. The MELD scores were calculated. Then the patients were divided into two groups based on a MELD score greater than or less than 32 [31]. The liver tissue was fixed in 10% formalin and paraffin-embedded for histological evaluation. All patients provided written consent, and the protocol was approved by the clinical research ethics committee of the Liver Tissue Cell Distribution System, University of Minnesota (Minneapolis, MN), and executed according to the Declaration of Helsinki.

2.3. Histological Assessment. Deparaffinized liver sections (5 μm thick) were stained with hematoxylin and eosin (H&E) and immunohistochemical staining for MPO, RIPK1, RIPK3, and pMLKL using the DAB kit (Gene Tech, China) according to the manufacturer's protocol. The primary antibodies used were anti-myeloperoxidase (MPO) (Biocare Medical, Concord, CA), anti-RIPK3 (WuXi App Tec, China), anti-RIPK1 (Cell Signaling, USA), and pMLKL (Abcam, USA). Terminal deoxynucleotidyl transferase-mediated deoxyuridine triphosphate nick-end labeling (TUNEL) staining was performed with an ApopTag Peroxidase In Situ Cell Death Detection Kit (Roche, Mannheim, GER). All slides were evaluated by two pathologists blinded to patient clinical information. MPO- and RIPK3-positive cells were quantified randomly from 5 fields at 100x magnification per patient using Image J software 1.46r (NIH, USA). The corresponding histological features of ALD grading and staging schema [7], Ishak score [9], Knodell score/histology activity index [10], and alcoholic hepatitis histologic score (AHHS) [8] were numerically evaluated.

2.4. Statistical Analysis. The statistical analyses were performed between the two groups. All data were treated as continuous variables. For the data conformed to the normal distribution, the average and standard error of the mean (SEM) were displayed using Student's t-test. For nonnormality, the median and interquartile ranges were analyzed and compared using Wilcoxon rank-sum (Mann–Whitney) tests. The correlation analysis was using Pearson's correlation test. All calculations were performed using SPSS 23.0 (IBM, Armonk, NY), and $P < 0.05$ was considered significant.

3. Results

3.1. Neutrophil Infiltration Is a Hallmark of Alcoholic Cirrhosis. Inflammatory infiltration is one of the hallmarks for alcoholic cirrhosis [23, 24]. To confirm whether neutrophil infiltration contributes to this process, H&E staining and IHC staining for MPO were performed. As shown by

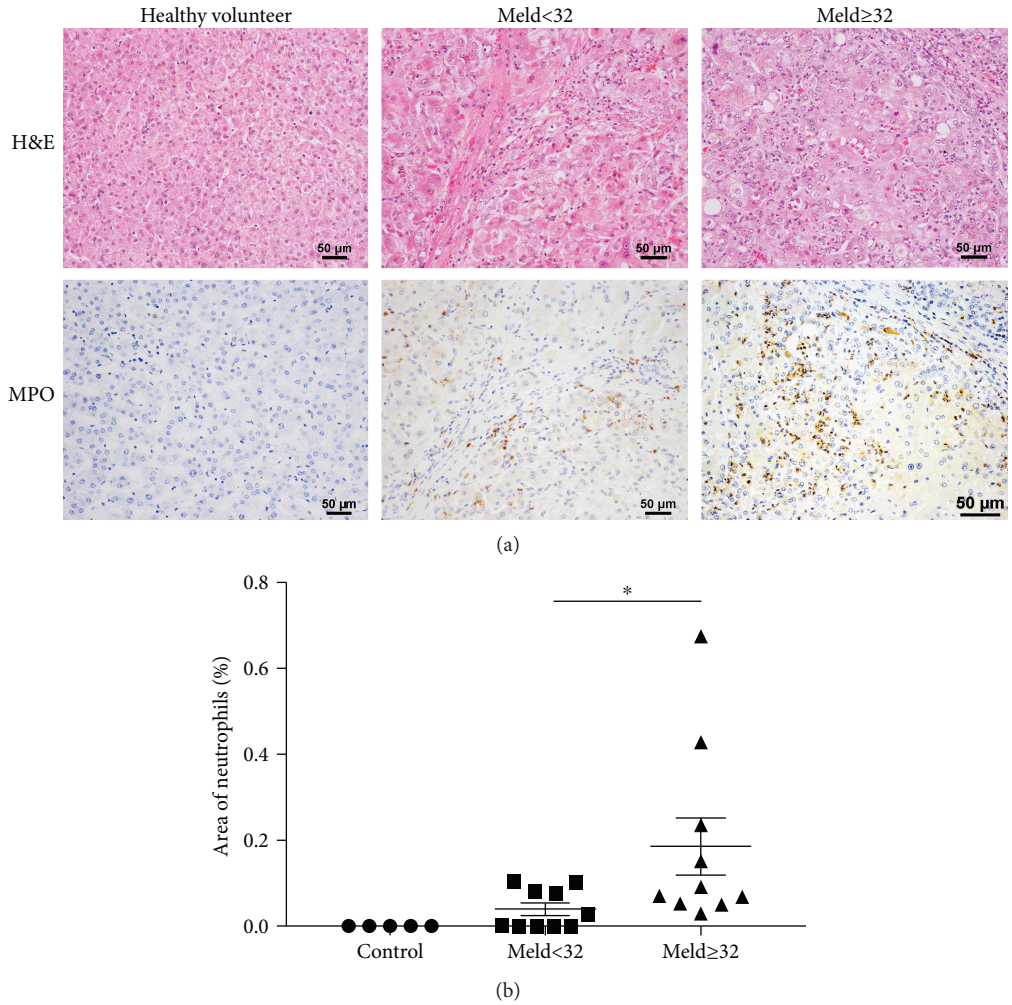

Figure 1: Hepatic neutrophil infiltration is a hallmark of alcoholic cirrhosis. Representative images of H&E staining (a) and immunohistochemistry (IHC) of MPO (b) were examined in patients with end-stage alcoholic cirrhosis and healthy controls. Data were represented as the means ± SEM. $^{*}P < 0.05$.

H&E staining in Figure 1(a), there were obvious inflammatory foci around the necrotic area in the liver of cirrhosis patients but not in healthy volunteers. IHC staining for the neutrophil marker MPO demonstrated that the inflammatory foci were mainly MPO-positive neutrophils (Figure 1(b)). This is consistent with previous studies [11, 23–25, 32] indicating that neutrophil infiltration plays an important role in alcohol-induced liver injury.

3.2. RIPK3, But Not RIPK1, Is Highly Expressed in Patients with Alcoholic Cirrhosis. Alcoholic cirrhosis is associated with necrotic hepatocyte cell death, called necroptosis [14], which is regulated by RIP1-RIP3-MLKL- (mixed lineage kinase domain-like protein-) mediated necrotic cascade, but the role of RIPK1 and RIPK3 in the pathogeneses of alcoholic liver cirrhosis is largely unknown. To further investigate whether RIPK1 or RIPK3 mediates the pathogeneses of alcoholic liver cirrhosis, IHC analyses of RIPK1 and RIPK3 in patients with alcoholic cirrhosis were examined. As shown in Figure 2, very strong RIPK3 staining but not RIPK1 was found in the necrotic area, indicating that RIPK3, but not RIPK1, was involved in alcoholic liver cirrhosis, consistent with previous studies showing RIPK3 is mediated in the mouse model of ethanol-induced liver injury and progression of ALD patients [27]. Furthermore, phospho-mixed lineage kinase-like protein (p-MLKL) a downstream molecule of RIPK3 in necroptosis pathway was also activated in the necrotic area in patients with alcoholic cirrhosis. Finally, the increased cell death in alcoholic cirrhotic patients was further confirmed by TUNEL staining.

3.3. Neutrophil Infiltration and the level of RIPK3 Are Associated with Poor Prognosis Based on MELD over 32. To explore whether the neutrophil infiltration or the level of RIPK3 can predict prognosis according to MELD over 32 or not, patient clinical parameters are measured to assess liver function on the day of enrollment to liver transplantation and the prognosis scores of histologic parameters according to MELD greater or less than 32 are summarized in Table 1. The results revealed that patients with MELD

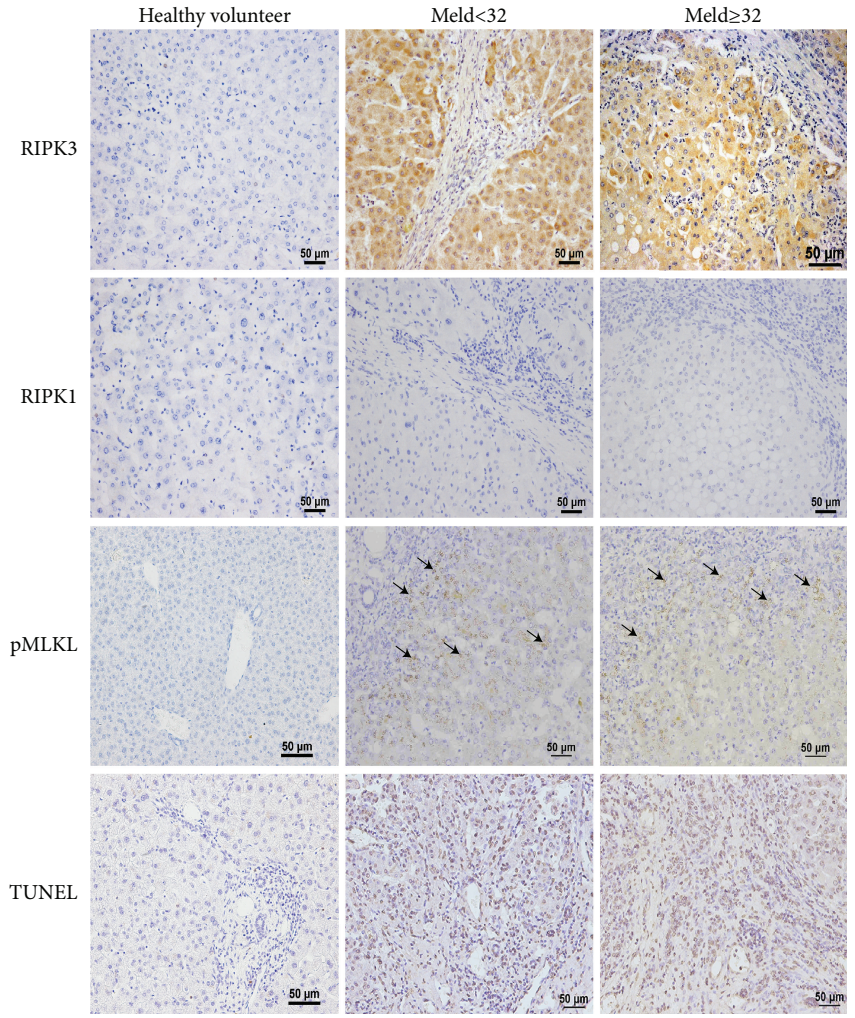

Figure 2: RIPK3, but not RIPK1, is highly expressed in patients with alcoholic cirrhosis. Representative images of immunohistochemistry (IHC) of RIPK1, RIPK3, pMLKL, and TUNEL staining were examined in patients with end-stage alcoholic cirrhotic patients and healthy controls. $n = 20$.

Table 1: Comparative analysis of patients with MELD greater or less than 32.

	MELD ≥ 32 ($n = 10$)	MELD < 32 ($n = 10$)	t/Z value	P value
MPO (%)	0.0806 (0.05195, 0.2874)	0.0151 (0.00, 0.08675)	−2.125	0.034*
RIPK3 (%)	4.7367 (1.7054, 6.2929)	2.0914 (1.4491, 4.7188)	−0.735	0.462
Ishak score	6.75 (5.125, 9.000)	4.00 (3.25, 5.75)	−1.847	0.065
Ishak fibrosis score	6.00 (6.00, 6.00)	6.00 (5.5, 6.0)	−0.860	0.390
Knodell score	11.3 ± 2.7305	9.222 ± 2.1667	−1.823	0.086
AHHS score	6.70 ± 1.11056	6.3889 ± 1.21906	−0.582	0.568
ALD grading	6.90 ± 2.3781	5.556 ± 1.5899	−1.431	0.171
ALD stage	6.00 (5.00, 6.00)	6.00 (5.00, 6.00)	−0.159	0.874

MPO: myeloperoxidase; RIPK3: receptor-interacting protein kinase3; MELD: model for end-stage liver disease; AHHS: alcoholic hepatitis histologic score. *$p < 0.05$.

score over than 32 were associated with upregulation of the levels of MPO, indicating they can be used as indicators of poor prognosis.

3.4. Neutrophil Infiltration and the Expression of RIPK3 Are Associated with Poor Prognosis Based on Histologic Parameters. To further investigate the relationship between

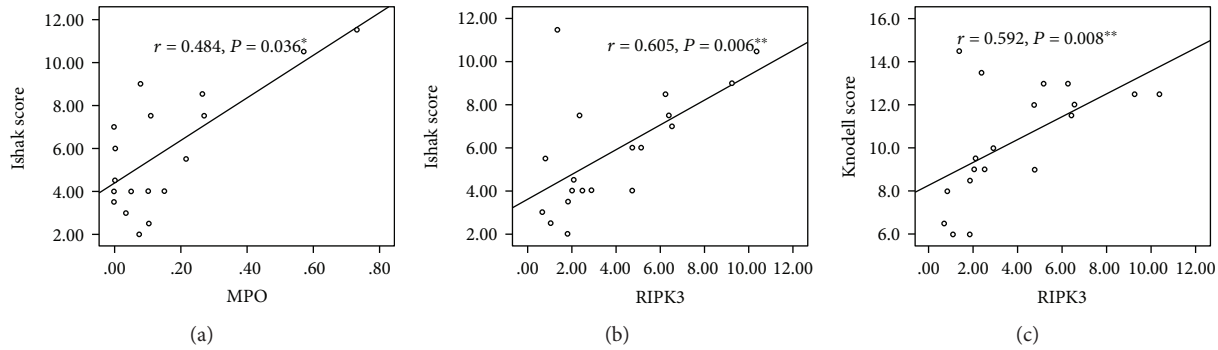

Figure 3: Correlation between RIPK3 and MPO with histological scoring systems. The correlation analyses of RIPK3 and MPO with histological scoring systems were examined at those alcoholic cirrhotic patients. Data were represented as the means ± SEM. $^{*}P < 0.05$ and $^{**}P < 0.01$.

RIPK3 expression, neutrophil infiltration, and histologic parameters, correlation analysis was performed. The prognostic histological score systems, including Ishak score [9], Knodell score [10], ALD grading and staging schema [7], and alcoholic hepatitis histologic score (AHHS) [8], were analyzed by two pathologists. As shown in Figure 3, significant correlations were observed between the Ishak score and the area of MPO and RIPK3 staining in patients' livers ($r = 0.484$ and $P = 0.036$ and $r = 0.605$ and $P = 0.006$, respectively). Importantly, the RIPK3 was also significantly and positively related to the Knodell score ($r = 0.592$, $P = 0.008$).

4. Discussion

The current study investigated the relationship between RIPK3-mediated necroptosis and neutrophil-mediated alcoholic liver inflammation with disease prognosis. The results demonstrated that MELD (a widely recognized noninvasive predictor of disease outcome) and histological prognostic scores (the invasive predictor) were well correlated to the levels of neutrophil infiltration and the expression of RIPK3. Importantly, RIPK3 and MPO may act as factors to predict poor outcomes in patients with alcoholic cirrhosis.

One of the most intriguing features in alcoholic cirrhosis is the remarkable hepatic neutrophil infiltration. Neutrophil infiltration has played an important role in promoting the development of alcoholic cirrhosis in murine models [23, 24, 32]. Either pharmacological inhibition or genetic deletion of E-selectin [23], an important adhesion molecule for neutrophil migration, or CXCL1 [24], a key chemokine in neutrophil recruitment, can prevent mice from ethanol-induced hepatic neutrophil infiltration. Therefore, there is an urgent need for further translational studies using human samples to identify neutrophil targets for therapy. Here, the pathogenic role of neutrophil infiltration was shown in alcoholic cirrhotic patients.

Another essential finding from this study is the meaningful confirmation of RIPK3 but not RIPK1 as being significantly upregulated in human livers. RIPK1 and RIPK3 are recently discovered proteins that regulate caspase-independent programmed cell death, called necroptosis [16, 17, 33]. RIPK3 is strongly expressed in the alcoholic cirrhotic patients in our study, and the pMLKL, which is a substrate for RIPK3 kinase activity [16, 17], was also activated in the necrotic area. Roychowdhury et al. first reported elevated RIPK3 expression in ethanol-induced liver injury murine models and in human ALD samples independent of RIPK1. A deficiency of RIPK3 extremely reduced the severity of ethanol-induced liver injury, but not for RIPK1-specific inhibitor [18]. This mechanism is used because of impaired hepatic proteasome function failing to produce RIPK3, as pharmacological inhibition or genetic disruption of proteasome accumulates RIPK3. However, another study also showed that RIPK1 decreased Gao-binge-induced neutrophil infiltration [34]. It remains a controversial issue whether RIPK1 or RIPK3 is correlated with neutrophil infiltration and needs to be further studied. Our study showed that RIPK3 but not RIPK1 was activated in patients with alcoholic cirrhosis. Further studies using liver-specific RIPK3 KO and RIPK1 KO mice should be conducted to confirm these results.

To show the prognostic value of neutrophil infiltration and RIPK3 in patients with alcoholic cirrhosis, the noninvasive prognostic score MELD and the invasive histological scoring system were evaluated. The MELD score is a recognized prognosis predictor in liver cirrhosis, especially for those waiting for liver transplantation [31, 35]. The results of our study show that neutrophil infiltration was upregulated in the group with a MELD score greater than 32, indicating neutrophil infiltration may represent poor prognosis in alcoholic cirrhosis. This is consistent with previous findings that neutrophil infiltration may promote the development of alcoholic cirrhosis [23, 24, 32].

On the other hand, the histological scoring systems predicting ALD have not been uniform. Yip and Burt first recommended a grading and staging scoring system for the assessment of histological severity of ALD in 2006 [7]. It was verified recently that even the early or compensated ALD should be evaluated as a predictor of long-term mortality [36]. Altamirano et al. proposed an AHHS scoring system using AH to predicting patients' outcomes [8]. However, this study excluded the other spectrum of ALD except for AH, and whether AHHS applies to those patients remains unknown. The patients in our study all had end-stage alcoholic cirrhosis, and the results of our study between the

relationship of the AHHS score and clinical parameters, MPO, or RIPK3 were not significant, suggesting the AHHS score may not be suitable for alcoholic cirrhosis. This should be further validated by a more prospective study.

The Knodell score and Ishak score are frequently used in chronic hepatitis, particularly HCV [9, 10]. The position of fibrosis differs between HCV and ALD, because HCV begins with a periportal distribution of fibrosis and extending to the portal center, whereas ALD starts with central expansion [29]. This means that there will be more fibrosis in ALD patients than HCV patients in the early stage of the disease. However, because patients in our study all have end-stage alcoholic cirrhosis (fibrosis score more than 4), which eliminated this difference, so the Ishak score and Knodell score were used to assess the patient histological features. The results show that MPO and RIPK3 correlated to the Ishak score and RIPK3 correlated to the Knodell score, suggesting MPO and RIPK3 may be good prognostic factors for the patients' outcome based on histological parameters.

Furthermore, the following limitations of this study need to be considered. Firstly, this is a retrospective study observing patient prognostic indicators and the sample size is limited due to the difficulty in obtaining samples. Further prospective studies containing larger samples should be performed to confirm this finding. Second, all the patients underwent liver transplantation; therefore, disease mortality could not be directly evaluated, so prognostic indicators were analyzed relative to prognostic MELD models and histologic parameters. Clearly, these findings should be confirmed in further prospective studies analyzing the mortality during hospitalization and the medium and long-term (admission, 30 days to 3 months, or 6 months, respectively) outcome and compare the different scores with analytic parameters or others.

5. Conclusions

The present study demonstrates that RIPK3 and neutrophil infiltration in patients with alcoholic cirrhosis can be used to predict poor disease prognosis based noninvasive predictors MELD and invasive histological scoring systems.

Data Availability

The data used to support the findings of this study are available from the corresponding author upon request.

Conflicts of Interest

The authors declare that there is no conflict of interest regarding the publication of this paper.

Authors' Contributions

Zhenzhen Zhang and Guomin Xie are first authors with an equal contribution.

Acknowledgments

This work was supported in part by the National Natural Science Foundation of China (81300312 and 81870417 to YW; 81302157 and 81370521 to AQ) and the Natural Hepatitis Protection and Treatment Foundation grant, CFHPC (20132028 to YW). We thank the lab of liver diseases, NIAAA, for kindly providing patients' liver sections.

References

[1] D. Goldberg, I. C. Ditah, K. Saeian et al., "Changes in the prevalence of hepatitis C virus infection, nonalcoholic steatohepatitis, and alcoholic liver disease among patients with cirrhosis or liver failure on the waitlist for liver transplantation," *Gastroenterology*, vol. 152, no. 5, pp. 1090–1099.e1, 2017.

[2] Z. Younossi and L. Henry, "Contribution of alcoholic and nonalcoholic fatty liver disease to the burden of liver-related morbidity and mortality," *Gastroenterology*, vol. 150, no. 8, pp. 1778–1785, 2016.

[3] European Association for the Study of the Liver, "EASL clinical practical guidelines: management of alcoholic liver disease," *Journal of Hepatology*, vol. 57, no. 2, pp. 399–420, 2012.

[4] W. Dunn, L. H. Jamil, L. S. Brown et al., "MELD accurately predicts mortality in patients with alcoholic hepatitis," *Hepatology*, vol. 41, no. 2, pp. 353–358, 2005.

[5] R. P. Mookerjee, C. Lackner, R. Stauber et al., "The role of liver biopsy in the diagnosis and prognosis of patients with acute deterioration of alcoholic cirrhosis," *Journal of Hepatology*, vol. 55, no. 5, pp. 1103–1111, 2011.

[6] A. Katoonizadeh, W. Laleman, C. Verslype et al., "Early features of acute-on-chronic alcoholic liver failure: a prospective cohort study," *Gut*, vol. 59, no. 11, pp. 1561–1569, 2010.

[7] W. W. Yip and A. D. Burt, "Alcoholic liver disease," *Seminars in Diagnostic Pathology*, vol. 23, no. 3-4, pp. 149–160, 2006.

[8] J. Altamirano, R. Miquel, A. Katoonizadeh et al., "A histologic scoring system for prognosis of patients with alcoholic hepatitis," *Gastroenterology*, vol. 146, no. 5, pp. 1231–1239.e6, 2014.

[9] Z. D. Goodman, "Grading and staging systems for inflammation and fibrosis in chronic liver diseases," *Journal of Hepatology*, vol. 47, no. 4, pp. 598–607, 2007.

[10] R. G. Knodell, K. G. Ishak, W. C. Black et al., "Formulation and application of a numerical scoring system for assessing histological activity in asymptomatic chronic active hepatitis," *Hepatology*, vol. 1, no. 5, pp. 431–435, 1981.

[11] A. Louvet and P. Mathurin, "Alcoholic liver disease: mechanisms of injury and targeted treatment," *Nature Reviews Gastroenterology & Hepatology*, vol. 12, no. 4, pp. 231–242, 2015.

[12] S. L. Friedman, "Preface. Hepatic fibrosis: pathogenesis, diagnosis, and emerging therapies," *Clin Liver Dis*, vol. 12, no. 4, pp. xiii–xxiv, 2008.

[13] T. Luedde, N. Kaplowitz, and R. F. Schwabe, "Cell death and cell death responses in liver disease: mechanisms and clinical relevance," *Gastroenterology*, vol. 147, no. 4, pp. 765–783.e4, 2014.

[14] S. Wang, P. Pacher, R. C. de Lisle, H. Huang, and W.-X. Ding, "A mechanistic review of cell death in alcohol-induced

liver injury," *Alcoholism: Clinical and Experimental Research*, vol. 40, no. 6, pp. 1215–1223, 2016.

[15] M. A. Barnes, S. Roychowdhury, and L. E. Nagy, "Innate immunity and cell death in alcoholic liver disease: role of cytochrome P4502E1," *Redox Biology*, vol. 2, pp. 929–935, 2014.

[16] M. Pasparakis and P. Vandenabeele, "Necroptosis and its role in inflammation," *Nature*, vol. 517, no. 7534, pp. 311–320, 2015.

[17] A. Kaczmarek, P. Vandenabeele, and D. V. Krysko, "Necroptosis: the release of damage-associated molecular patterns and its physiological relevance," *Immunity*, vol. 38, no. 2, pp. 209–223, 2013.

[18] S. Roychowdhury, M. R. McMullen, S. G. Pisano, X. Liu, and L. E. Nagy, "Absence of receptor interacting protein kinase 3 prevents ethanol-induced liver injury," *Hepatology*, vol. 57, no. 5, pp. 1773–1783, 2013.

[19] J. Li, T. McQuade, A. B. Siemer et al., "The RIP1/RIP3 necrosome forms a functional amyloid signaling complex required for programmed necrosis," *Cell*, vol. 150, no. 2, pp. 339–350, 2012.

[20] J. W. Upton, W. J. Kaiser, and E. S. Mocarski, "Virus inhibition of RIP3-dependent necrosis," *Cell Host & Microbe*, vol. 7, no. 4, pp. 302–313, 2010.

[21] A. Linkermann, J. H. Bräsen, F. De Zen et al., "Dichotomy between RIP1- and RIP3-mediated necroptosis in tumor necrosis factor-α-induced shock," *Molecular Medicine*, vol. 18, no. 1, pp. 577–586, 2012.

[22] V. Wieser, P. Tymoszuk, T. E. Adolph et al., "Lipocalin 2 drives neutrophilic inflammation in alcoholic liver disease," *Journal of Hepatology*, vol. 64, no. 4, pp. 872–880, 2016.

[23] A. Bertola, O. Park, and B. Gao, "Chronic plus binge ethanol feeding synergistically induces neutrophil infiltration and liver injury in mice: a critical role for E-selectin," *Hepatology*, vol. 58, no. 5, pp. 1814–1823, 2013.

[24] B. Chang, M. J. Xu, Z. Zhou et al., "Short- or long-term high-fat diet feeding plus acute ethanol binge synergistically induce acute liver injury in mice: an important role for CXCL1," *Hepatology*, vol. 62, no. 4, pp. 1070–1085, 2015.

[25] M. Dominguez, R. Miquel, J. Colmenero et al., "Hepatic expression of CXC chemokines predicts portal hypertension and survival in patients with alcoholic hepatitis," *Gastroenterology*, vol. 136, no. 5, pp. 1639–1650, 2009.

[26] L. Duprez, N. Takahashi, F. van Hauwermeiren et al., "RIP kinase-dependent necrosis drives lethal systemic inflammatory response syndrome," *Immunity*, vol. 35, no. 6, pp. 908–918, 2011.

[27] A. Ramachandran, M. R. McGill, Y. Xie, H. M. Ni, W. X. Ding, and H. Jaeschke, "Receptor interacting protein kinase 3 is a critical early mediator of acetaminophen-induced hepatocyte necrosis in mice," *Hepatology*, vol. 58, no. 6, pp. 2099–2108, 2013.

[28] L. E. Nagy, W. X. Ding, G. Cresci, P. Saikia, and V. H. Shah, "Linking pathogenic mechanisms of alcoholic liver disease with clinical phenotypes," *Gastroenterology*, vol. 150, no. 8, pp. 1756–1768, 2016.

[29] D. C. Rockey, S. H. Caldwell, Z. D. Goodman, R. C. Nelson, and A. D. Smith, "Liver biopsy," *Hepatology*, vol. 49, no. 3, pp. 1017–1044, 2009.

[30] Y. Wang, D. Feng, H. Wang et al., "*STAT4* knockout mice are more susceptible to concanavalin A–induced T-cell hepatitis," *The American Journal of Pathology*, vol. 184, no. 6, pp. 1785–1794, 2014.

[31] R. Wiesner, E. Edwards, R. Freeman et al., "Model for end-stage liver disease (MELD) and allocation of donor livers," *Gastroenterology*, vol. 124, no. 1, pp. 91–96, 2003.

[32] H. Jaeschke, "Neutrophil-mediated tissue injury in alcoholic hepatitis," *Alcohol*, vol. 27, no. 1, pp. 23–27, 2002.

[33] M. Najjar, D. Saleh, M. Zelic et al., "RIPK1 and RIPK3 kinases promote cell-death-independent inflammation by toll-like receptor 4," *Immunity*, vol. 45, no. 1, pp. 46–59, 2016.

[34] S. Wang, H. M. Ni, K. Dorko et al., "Increased hepatic receptor interacting protein kinase 3 expression due to impaired proteasomal functions contributes to alcohol-induced steatosis and liver injury," *Oncotarget*, vol. 7, no. 14, pp. 17681–17698, 2016.

[35] D. M. Heuman, S. G. Abou-Assi, A. Habib et al., "Persistent ascites and low serum sodium identify patients with cirrhosis and low MELD scores who are at high risk for early death," *Hepatology*, vol. 40, no. 4, pp. 802–810, 2004.

[36] C. Lackner, W. Spindelboeck, J. Haybaeck et al., "Histological parameters and alcohol abstinence determine long-term prognosis in patients with alcoholic liver disease," *Journal of Hepatology*, vol. 66, no. 3, pp. 610–618, 2017.

Hindawi
Journal of Immunology Research
Volume 2018, Article ID 5241526, 12 pages
https://doi.org/10.1155/2018/5241526

Research Article

Enhanced Regeneration and Hepatoprotective Effects of Interleukin 22 Fusion Protein on a Predamaged Liver Undergoing Partial Hepatectomy

Heng Zhou,[1,2,3] **Guomin Xie**,[2,3] **Yudi Mao**,[1] **Ke Zhou**,[2,3] **Ruixue Ren**,[3,4] **Qihong Zhao**,[5] **Hua Wang**,[3,4] **and Shi Yin**[1]

[1]*Department of Geriatrics, Anhui Provincial Hospital, Anhui Medical University, Hefei 230001, China*
[2]*School of Pharmacy, Anhui Medical University, Hefei 230032, China*
[3]*Institute for Liver Disease, Anhui Medical University, Hefei 230032, China*
[4]*Department of Oncology, The First Affiliated Hospital of Anhui Medical University, Hefei 230032, China*
[5]*Department of Food and Nutrition Hygiene, School of Public Health, Anhui Medical University, Hefei 230032, China*

Correspondence should be addressed to Hua Wang; wanghua@ahmu.edu.cn and Shi Yin; yinshi@ahmu.edu.cn

Received 27 April 2018; Accepted 29 August 2018; Published 31 October 2018

Academic Editor: YinYing Lu

Liver ischemia-reperfusion injury (IRI) and regeneration deficiency are two major challenges for surgery patients with chronic liver disease. As a survival factor for hepatocytes, interleukin 22 (IL-22) plays an important role in hepatoprotection and the promotion of regeneration after hepatectomy. In this study, we aim to investigate the roles of an interleukin 22 fusion protein (IL-22-FP) in mice with a predamaged liver after a two-third partial hepatectomy (PHx). Predamaged livers in mice were induced by concanavalin A (ConA)/carbon tetrachloride (CCl4) following PHx with or without IL-22-FP treatment. A hepatic IRI mouse model was also used to determine the hepatoprotective effects of IL-22-FP. In the ConA/CCl4 model, IL-22-FP treatment alleviated liver injury and accelerated hepatocyte proliferation. Administration of IL-22-FP activated the hepatic signal transducer and activator of transcription 3 (STAT3) and upregulated the expression of many mitogenic proteins. IL-22-FP treatment prior to IRI effectively reduced liver damage through decreased aminotransferase and improved liver histology. In conclusion, IL-22-FP promotes liver regeneration in mice with predamaged livers following PHx and alleviates IRI-induced liver injury. Our study suggests that IL-22-FP may represent a promising therapeutic drug against regeneration deficiency and liver IRI in patients who have undergone PHx.

1. Introduction

IL-22 is an emerging CD4+ Th cytokine produced by activated T cells, such as T helper 22 (Th22) cells, Th17 cells, and NK cells [1–4]. As a member of the IL-10 cytokine family, IL-22 plays a role in a variety of tissues and organs by binding to the receptors IL-10R2 and IL-22R1; IL-10R2 is expressed in many types of cells, but the expression of IL-22R1 is limited to epithelial cells in the skin, pancreas, liver, gut, and lung [5–8].

IL-22 plays an important role in protection against damage, strengthening of innate immunity and enhancement of regeneration [8–10]. IL-22 plays important roles in various human and animal liver diseases, such as acute liver injury, viral hepatitis, liver fibrosis, hepatocellular carcinoma (HCC), and alcoholic liver disease [11–19]. Studies from professor Bin Gao have shown that IL-22 is released when T cells are activated and then protects against liver damage caused by a variety of toxins, such as ConA or CCl4, via activation of the STAT3 pathway [20, 21]. IL-22 has been shown to be a significant mediator of the inflammatory response caused by HBV and HCV. In HBV patients, hepatic expression of IL-22 was elevated compared with healthy individuals and the degree of increase was related to the grade of inflammation [22–26]. Compared with normal controls, the expression of numerous genes associated

with the IL-22 pathway was significantly upregulated in HBV-infected liver tissues [24]. IL-22 ameliorates liver fibrogenesis by inducing hepatic stellate cell senescence, and it stimulates liver cancer development through activation of the STAT3 pathway [16, 17, 19].

Liver regeneration is a complex process and is closely related to a wide variety of cytokines, hormones, and growth factors [27]. It is generally accepted that serum levels of lipopolysaccharide (LPS) will be upregulated after partial hepatectomy (PHx), which stimulates the Kupffer cells to produce IL-6 and tumor necrosis factor alpha (TNF-α). IL-6 targets hepatocytes, triggering activation of the STAT3 pathway, and ultimately promotes hepatocyte survival and proliferation [27–29]. It is an indisputable fact that IL-22 contributes to liver regeneration after PHx. Researchers have found that the serum IL-22 and hepatic IL-22 receptor mRNA levels were significantly upregulated after PHx in mice. Some studies have shown that the promotive properties of IL-22 on liver regeneration after PHx are likely due to interactions with TGF-α and IL-6 [30–32]. In addition, IL-22 plays a protective role in liver ischemia-reperfusion injury (IRI) [33]. After treatment with IL-22, the serum aspartate aminotransferase (AST) level decreased but the expression of IL-22R1 in damaged hepatocytes increased, which significantly alleviates IR-triggered hepatocellular damage and decreases IR-related liver inflammation [33]. As mentioned, liver regeneration deficiency and liver injury are still the two major stumbling blocks for patients after PHx, although the liver is a unique organ that has the ability to regenerate after injury or resection. IL-22 has been reported to contribute to liver regeneration after hepatectomy and protect the liver against IRI, and this corresponds to the two problems patients experience after PHx. Therefore, treatment utilizing IL-22 is expected to become a potential therapeutic approach for patients post-PHx.

The majority of clinical patients who receive PHx have a predamaged liver condition caused by various liver diseases and thus obviously decreased liver regeneration ability. However, at present, most of the evidence that supports IL-22 promotion of liver regeneration is from a PHx model without other injuries. In this article, we used ConA and CCl4 to induce liver injury in mice, to investigate the effect of IL-22 on liver regeneration after PHx under these conditions. In addition, currently, almost all the IL-22 used in rodent PHx models is recombinant human interleukin 22 (rh-IL-22). The half-life of rh-IL-22 (expressed in *Escherichia coli*) in animals is less than 2 h, and therefore, repeated administration in a short time is inevitable when rh-IL-22 is used as a therapeutic drug. IL-22-FP, the IL-22 used in this article, is manufactured in Chinese hamster ovary (CHO) cells and has a double molecular structure of IL-22 (an IL-22 dimer, Figure 1). As a recombinant fusion protein, IL-22-FP is composed of human IL-22 and human IgG2-Fc. IL-22-FP has a longer half-life and more easily achieves a stable blood concentration compared to rh-IL-22 [34]. In this article, we are committed to investigating the effects and mechanisms of IL-22-FP on liver protection and regeneration in mice with a predamaged liver condition following PHx, in the hope of providing a new therapeutic means for treatment of clinical patients who undergo liver surgery.

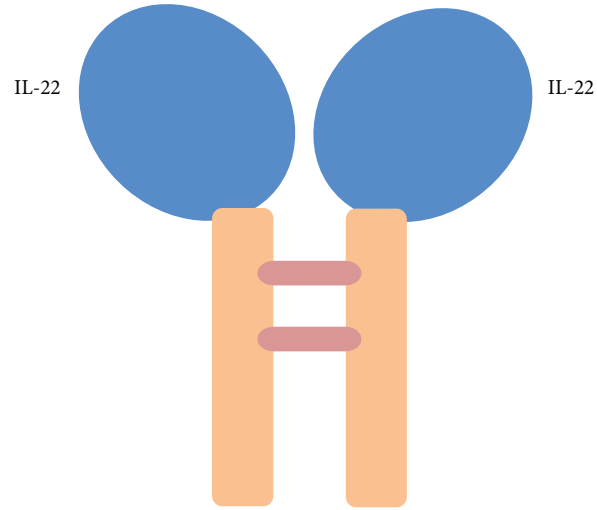

Figure 1: Structure of IL-22-FP. IL-22-FP is manufactured in Chinese hamster ovary (CHO) cells and has a double molecular structure of IL-22 (an IL-22 dimer). As a recombinant fusion protein, IL-22-FP is composed of human IL-22 and human IgG2-Fc.

2. Materials and Methods

2.1. Materials. Male C57BL/6 (8 to 10 wk old) mice used in the experiments were purchased from the Shanghai Lab Animal/Research Center (Shanghai, China). ConA was obtained from Sigma (MO, USA), and CCl4 was obtained from Sinopharm Chemical Reagent Co. Ltd (Shanghai, China). IL-22-FP was provided by GENERON Corporation Ltd. (Shanghai, China); recombinant human interleukin 22 (rh-IL-22) was obtained from Sino Biological Inc. (Beijing, China). Anti-CyclinB1 antibody was purchased from Abcam (Shanghai, China). Other antibodies used in this article, including anti-STAT3, anti-phospho-STAT3 (Tyr^{705}), and proliferating cell nuclear antigen (PCNA) antibodies, were purchased from Cell Signaling Technology (Beverly, MA, USA).

2.2. Two-Third PHx Model. We performed PHx as previously described [30, 32]. In brief, male C57BL/6 mice were maintained under specific pathogen-free conditions and they had access to water and food freely before each experiment. A midline incision was created, after the mice were anesthetized with ether gas, and the left lateral and median lobes of the liver were freed. Then using a 3-0 silk suture to ligate the blood vessels at the root of the median and left lateral hepatic lobes, the ligated hepatic lobes were resected.

2.3. ConA Model. In this model, mice were randomly divided into four groups: the ConA group, PHx group, ConA + PHx group, and ConA + PHx + IL-22-FP group. ConA was administered with a single intravenous injection at 18 μg/g mice body weight, and 4 days later, the PHx was performed. The PHx group mice received identical volumes

of phosphate-buffered saline (PBS) in the same way. For the ConA + PHx + IL-22-FP group mice, IL-22-FP was injected intravenously (iv) 30 min before PHx at 0.125 μg/g body weight, and other group animals received an identical volume of PBS in the same manner. Mice were euthanized at different time points (32 h, 40 h, 48 h, and 1 wk) following surgery (each group has 4 mice at each time point), and the liver tissue and serum samples were obtained for subsequent examination.

2.4. CCl4 Model. Similar to the ConA model, mice were divided into 4 groups in this model: the CCl4 group, PHx group, CCl4 + PHx group, and CCl4 + PHx + IL-22-FP group. Mice received an intraperitoneal (ip) injection of 10% CCl4 solution (volume of CCl4: volume of olive oil = 1: 9) at 1 μl/g body weight three times a week for 4 wk, while the PHx group mice were administered with only olive oil. As with the ConA model, IL-22-FP was injected intravenously at 0.125 μg/g body weight 30 min before PHx, and other group mice were injected with PBS. Mice were euthanized at the same time points (32 h, 40 h, 48 h, and 1 wk) and in the same way as the ConA model mice (each group has 4 mice at each time point).

2.5. Hepatic IRI Model. The hepatic IRI model that we used has been previously described [35, 36]. In brief, male C57BL/6 mice (8–10 wk of age) were anesthetized with chloral hydrate (ip) before a midline incision was created. With full exposure of the structure where it is connected with the portal triad and the median and left liver lobes (including the portal vein, hepatic artery, and bile duct), a vascular atraumatic clamp was used to blocked it for 90 min, and then the clamp was removed, and the liver was reperfused. Mice were euthanized at 6, 24, and 48 h postreperfusion (each group has 4 mice at each time point). Mice were randomly divided into 4 groups: the sham group, IRI group, IRI + rh-IL-22 group, and IRI + IL-22-FP group. The sham group mice received only a midline incision. For IRI + rh-IL-22 group and IRI + IL-22-FP group mice, IL-22 (rh-IL-22 or IL-22-FP) was injected (iv) 30 min before ischemia/reperfusion surgery at 0.125 μg/g body weight, and other mice were treated with PBS.

2.6. Liver Weight/Body Weight Ratios (LW/BW). Mice were euthanized by overdose of anesthesia at 32 h, 40 h, 48 h, and 1 wk after PHx (ConA model and CCl4 model) or at 6, 24, and 48 h postreperfusion (IRI model). The liver and body weights of each mouse were measured, and the liver weight/body weight ratio (LW/BW) was determined to assess the degree of liver regeneration.

2.7. Analysis of Liver Injury. Serum aspartate aminotransferase (AST) and alanine aminotransferase (ALT) levels were measured using a standard autobiochemical analyzer (Beckman Coulter AU5800, USA) to assess the degree of liver damage. Liver tissue was fixed with formalin and embedded in paraffin, and the paraffin-embedded liver tissue was cut into sections and stained with hematoxylin and eosin (HE) for histological examination.

2.8. BrdU Staining and Analysis. Mice received an intraperitoneal injection of 5-bromo-2′-deoxyuridine (Sigma, Germany) at 50 μg/g body weight 2 h prior to euthanasia. Liver specimens were collected to process for BrdU staining with a BrdU in situ detection kit (BD Bioscience, San Jose, CA, USA). $BrdU^+$ hepatocytes are regenerated hepatocytes. The number of $BrdU^+$ hepatocytes and total hepatocytes in 4–6 microscope fields (200x) was determined, and the $BrdU^+$ hepatocyte/total hepatocyte ratio was calculated; this ratio directly reflected the degree of hepatocyte regeneration.

2.9. Western Blots. Proteins were extracted from hepatic tissue for Western blot analysis. The protein concentration was detected with a BCA protein assay kit (Beyotime Biotechnology, Shanghai, China), and the absorbance value of the protein was measured with a microplate reader (BioTek Instruments, USA). The protein samples were separated by SDS-PAGE and transferred to PVDF membranes. The membranes were incubated with primary antibodies including antibodies against PCNA (1 : 1000), CyclinB1 (1 : 2000), p-STAT3 (1 : 1000), and STAT3 (1 : 2000) at 4°C overnight before being incubated with horseradish peroxidase-conjugated secondary antibodies (1 : 5000 dilution) at 4°C for 4 h. Protein bands were visualized with a SuperSignal West Pico Trial Kit (Thermo Scientific, Rockford, USA).

2.10. Statistical Analysis. All parametric data are expressed as the mean ± SD. SPSS software was used for statistical analysis. One-way ANOVA was applied to compare differences between groups. $p < 0.05$ was the threshold for statistical significance. The data were analyzed with GraphPad Prism software.

3. Results

3.1. Enhanced Liver Regeneration after PHx in IL-22-FP-Treated Mice in the ConA Model. In the ConA model, we divided mice into 4 groups: the ConA group, PHx group, ConA + PHx group, and ConA + PHx + IL-22-FP group, with the specific circumstances described above. After euthanasia, we weighed the liver and body of the mice and LW/BW ratios were calculated to reflect the rate of liver regeneration. The LW/BW ratios at different time points (32 h, 40 h, 48 h, and 1 wk) post-PHx are shown in Figure 2(a). Compared with the ConA + PHx group, the LW/BW ratios of the ConA + PHx + IL-22-FP group were significantly increased at 32 h ($^{***}p < 0.001$), 40 h ($^{*}p < 0.05$), and 48 h ($^{*}p < 0.05$) after PHx. Similarly, this ratio in the ConA + PHx + IL-22-FP group was also higher than that in the PHx group at 32 h ($^{***}p < 0.001$) and 40 h ($^{*}p < 0.05$) but this difference was not particularly evident at 48 h. The difference in the ratio of these 3 groups (PHx, ConA + PHx, and ConA + PHx + IL-22-FP) was smaller at 1 wk after PHx.

A portion of the liver tissue was preserved in formalin for BrdU staining (Figure 2(b)). The $BrdU^+$ hepatocyte/total hepatocyte ratio was calculated (Figure 2(c)). At 32 h ($^{*}p < 0.05$) and 40 h ($^{**}p < 0.01$), this ratio in the ConA + PHx + IL-22-FP group was significantly higher than

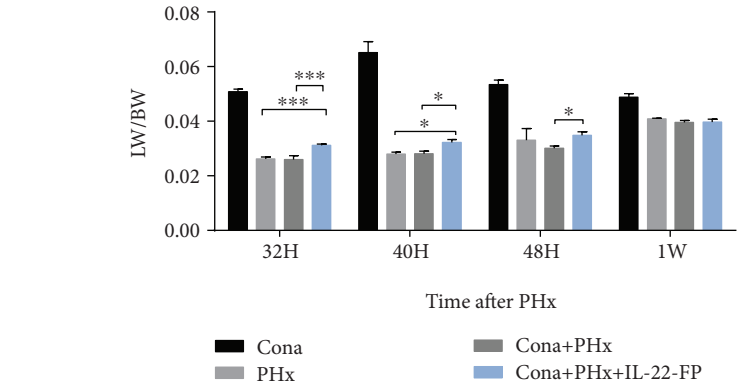

(a)

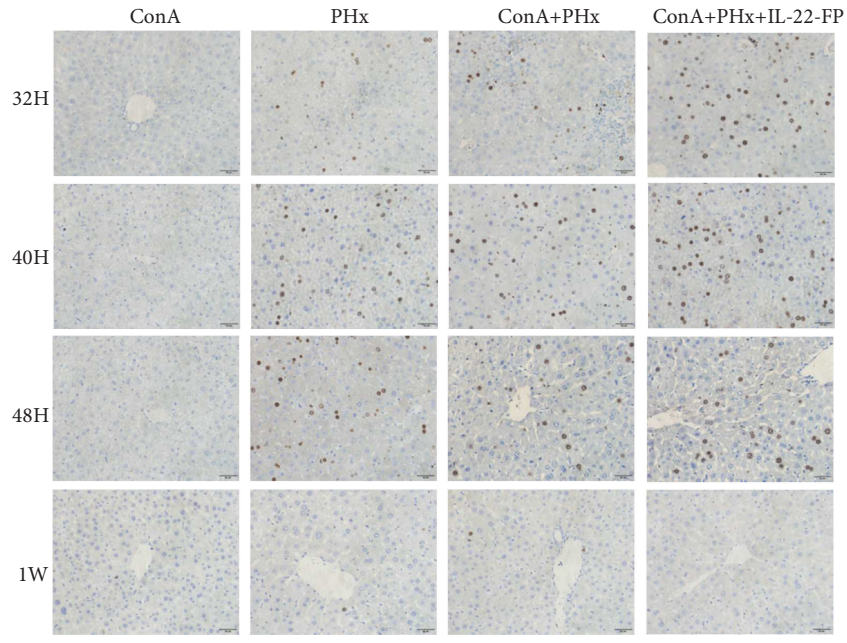

(b)

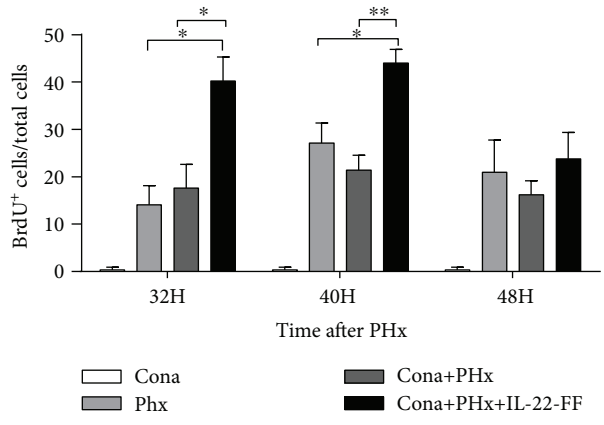

(c)

Figure 2: IL-22-FP enhances liver regeneration in a ConA model after PHx. C57BL/6 mice (8 to 10 wk old) were randomly divided into 4 groups: the ConA group, PHx group, ConA + PHx group, and ConA + PHx + IL-22-FP group. Each group of mice was treated as described in Materials and Methods. (a) The liver weight/body weight ratio (LW/BW) of each group at 32 h, 40 h, 48 h, and 1 wk post-PHx; $n = 4$ for each group. (b) Bromodeoxyuridine (BrdU) staining of mouse liver at 32 h, 40 h, 48 h, and 1 wk post-PHx (400x magnification). (c) $BrdU^+$ hepatocyte/total hepatocyte ratios of 4 groups of mice at 32, 40, and 48 h post-PHx. Pictures were taken at 400x magnification; $n = 4$ for each group. $^*p < 0.05$, $^{**}p < 0.01$, and $^{***}p < 0.001$.

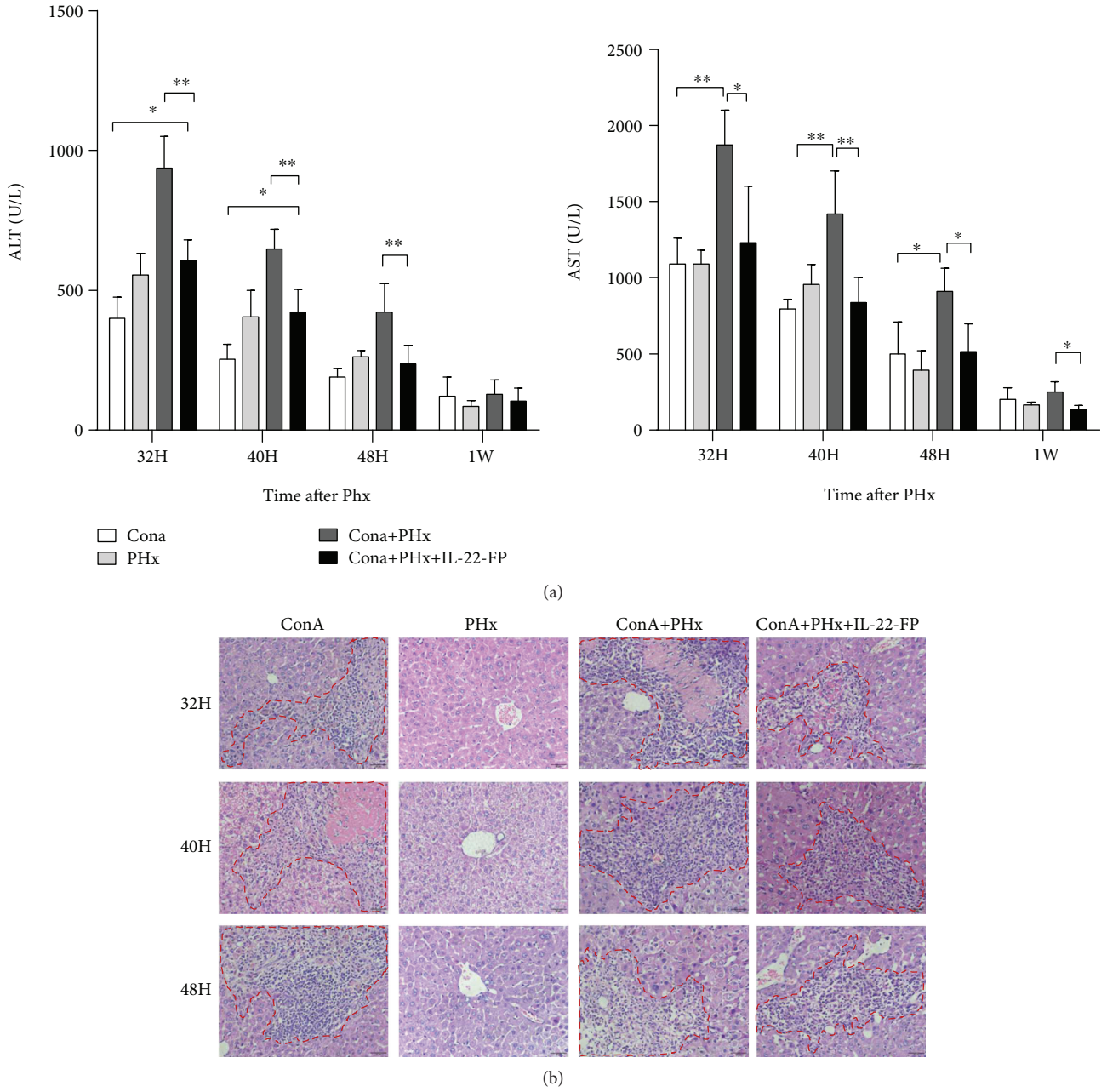

Figure 3: Hepatoprotective effects of IL-22-FP in a ConA model. Mice were grouped and treated as described in Figure 1. (a) At different time points (32 h, 40 h, 48 h, and 1 wk) post-PHx, mice serum samples were collected to detect ALT and AST levels; $n = 4$ for each group. (b) Mice were euthanized at different time points (32 h, 40 h, and 48 h) post-PHx, and liver tissues were stained with hematoxylin and eosin (HE). Pictures were taken at 400x magnification. $^{*}p < 0.05$ and $^{**}p < 0.01$.

that in the ConA + PHx group, while this difference at 48 h was small. The number of $BrdU^{+}$ hepatocytes was relatively higher in the ConA + PHx + IL-22-FP group than in the PHx group at 32 h ($^{*}p < 0.05$) and 40 h ($^{*}p < 0.05$) post-PHx.

3.2. Hepatoprotective Effect of IL-22-FP after PHx in the ConA Model. Grouping and modeling were performed as described in Materials and Methods. Serum ALT and AST levels in the ConA model were measured via biochemical analysis. As illustrated in Figure 3(a), the serum ALT levels in the ConA + PHx group were higher than those in the ConA + PHx + IL-22-FP group at 32 h ($^{**}p < 0.01$), 40 h ($^{**}p < 0.01$), and 48 h ($^{**}p < 0.01$) post-PHx. However, this difference was not statistically significant at 1 wk after PHx. Unlike the ALT levels, serum AST levels were significantly greater in the ConA + PHx group than in the ConA + PHx + IL-22-FP group at all observation time points.

Compared with the ConA + PHx + IL-22-FP group mice, the ConA + PHx group mice appeared to suffer from more severe hepatic injury, more extensive tissue necrosis and inflammatory cell infiltration was found in the ConA + PHx group at 32, 40, and 48 h post-PHx (Figure 3(b)).

3.3. Enhanced Liver Regeneration after PHx in IL-22-FP-Treated Mice in the CCl4 Model. Mice were randomly divided into 4 groups: the CCl4 group, PHx group, CCl4 + PHx group, and CCl4 + PHx + IL-22-FP group. Different groups of mice were treated as mentioned in Materials and Methods. As shown in Figure 4(a), in the CCl4 + PHx group, the LW/BW ratio of the CCl4 + PHx + IL-22-FP group was increased obviously at 32 h ($^{*}p < 0.05$) and 40 h ($^{*}p < 0.05$) after PHx. At 32 ($^{*}p < 0.05$), 40 ($^{**}p < 0.01$), and 48 h ($^{*}p < 0.05$), the LW/BW ratio of the CCl4 + PHx + IL-22-FP group was significantly higher than that of the PHx group. There was no obvious difference in this ratio between the CCl4 + PHx + IL-22-FP group and other groups at 1 wk post-PHx.

Mice were euthanized at 32 h, 40 h, 48 h, and 1 wk after PHx, and the results of BrdU staining in the liver are shown in Figure 4(b). We counted the $BrdU^{+}$ hepatocyte/total hepatocyte ratios at different time points in each group (Figure 4(c)). As expected, in the CCl4 + PHx + IL-22-FP group, the number of $BrdU^{+}$ hepatocytes under the same high-magnification microscope at different time points (32 h, 40 h, and 48 h) was significantly higher than those in the CCl4 + PHx group and the PHx group. As shown in Figure 4(b), almost no $BrdU^{+}$ hepatocytes were found in any of the groups at 1 wk post-PHx.

3.4. Hepatoprotective Effect of IL-22-FP in the IRI Model. Male C57BL/6 mice were randomly divided into 4 groups: the sham group, IRI group, IRI + rh-IL-22 group, and IRI + IL-22-FP group. The last three groups of mice received 90 min of liver ischemia followed by reperfusion at different time points (6, 24, and 48 h), and the details are described above. As illustrated in Figure 5(a), in mice treated with IL-22 (the IRI + rh-IL-22 group and the IRI + IL-22-FP group), the serum ALT and AST levels at all observation time points were significantly reduced and the effect of IL-22-FP was more obvious than that of rh-IL-22 in reducing the ALT and AST levels at 48 h postreperfusion ($^{*}p < 0.05$).

Liver tissues were stained with hematoxylin and eosin. Necrosis of liver tissue was even worse in the IRI group and the IRI + rh-IL-22 group compared with the IRI + IL-22-FP group at 48 h postreperfusion (Figure 5(b)).

3.5. Effects of IL-22-FP on PCNA, CyclinB1, and p-STAT3 Activation after PHx. The expression of PCNA protein in ConA model mice at 40 h post-PHx was detected with Western blotting. As illustrated in Figures 6(a) and 6(b), the activation of PCNA in the ConA + PHx + IL-22-FP group was significantly increased compared with that in the ConA group ($^{***}p < 0.001$), PHx group ($^{***}p < 0.001$), and ConA + PHx group ($^{**}p < 0.01$). This result indicates that IL-22-FP promoted the expression of PCNA protein after PHx.

As shown in Figures 6(c) and 6(d), the activation of CyclinB1, PCNA, STAT3, and p-STAT3 was obviously increased in the CCl4 + PHx + IL-22-FP group compared with the other groups at 40 h post-PHx in the CCl4 model; it was difficult to observe the expression of p-STAT3 in the CCl4 group.

4. Discussion

Partial hepatectomy is still the best available treatment for HCC patients. For a normal liver, the maximum resection rate is 70–75%; when this ratio is exceeded, the patient is likely to experience acute liver failure due to insufficient regeneration of the remnant liver. For patients with liver disease/liver injury pre-PHx, the resection rate is greatly reduced, which severely restricts the use of surgery and the treatment of patients. In this article, we confirmed the hepatoprotective and proregenerative characteristics of IL-22-FP in mice with a predamaged liver condition (caused by ConA/CCl4) and who had undergone PHx. We also confirmed the hepatoprotective effect of IL-22-FP on liver IRI, and this protective effect was stronger than that of rh-IL-22. These properties of IL-22-FP indicate that it is likely a potential therapeutic approach for liver surgery patients.

The hepatoprotective effects of IL-22 in various animal and human liver diseases have been investigated [9, 20, 37, 38]. In 2004, professor Bin Gao's team confirmed that IL-22 mRNA and protein expression was significantly increased in T cell-mediated hepatitis caused by ConA. Blocking IL-22 with neutralizing antibodies worsened the liver damage induced by ConA through reduction in the transduction and activation of the STAT3 pathway, and this type of damage was reduced with administration of recombinant IL-22 [21]. In the same year, this team further confirmed that hydrodynamic gene delivery of IL-22 protects the liver from the damage caused by ConA and CCl4 [20]. In addition, many researchers have confirmed that IL-22 plays a protective role in hepatic injury caused by a variety of toxins such as D-galactosamine (D-GalN) and acetaminophen (APAP) [9, 12, 13, 39]. Unfortunately, at present, the exact mechanism of the hepatoprotective effects of IL-22 is still not very clear. Some researchers propose that this protective role of IL-22 may be related to the expression of IL-22-induced antiapoptotic (such as Bcl-2 and Bcl-xL) and mitogenic (such as c-myc and CyclinD1) proteins after activation of the STAT3 pathway [21]. As the results of our experiments also demonstrate, IL-22-FP protects the liver from serious injury caused by ConA and CCl4 and this has a strong relationship with activation of the STAT3 pathway.

The results of many experiments have confirmed that IL-22 contributes to hepatic regeneration [30–32]. Hepatic IL-22Rα mRNA and serum IL-22 levels are significantly increased after PHx, and anti-IL-22 antibody administered before hepatectomy can significantly reduce liver regeneration, although treatment with exogenous IL-22 before partial hepatectomy has no effect on hepatocyte proliferation [30]. Further research found that the role of IL-22 in promoting liver regeneration was achieved by increasing hepatocyte proliferation and hepatocyte migration [31]. Moreover, IL-22 promotion of liver regeneration in mice with liver disease (caused by ConA) after PHx has been confirmed [32]. Our findings indicate that IL-22-FP enhances liver regeneration in mice with a predamaged liver condition that have undergone PHx. It is generally accepted that

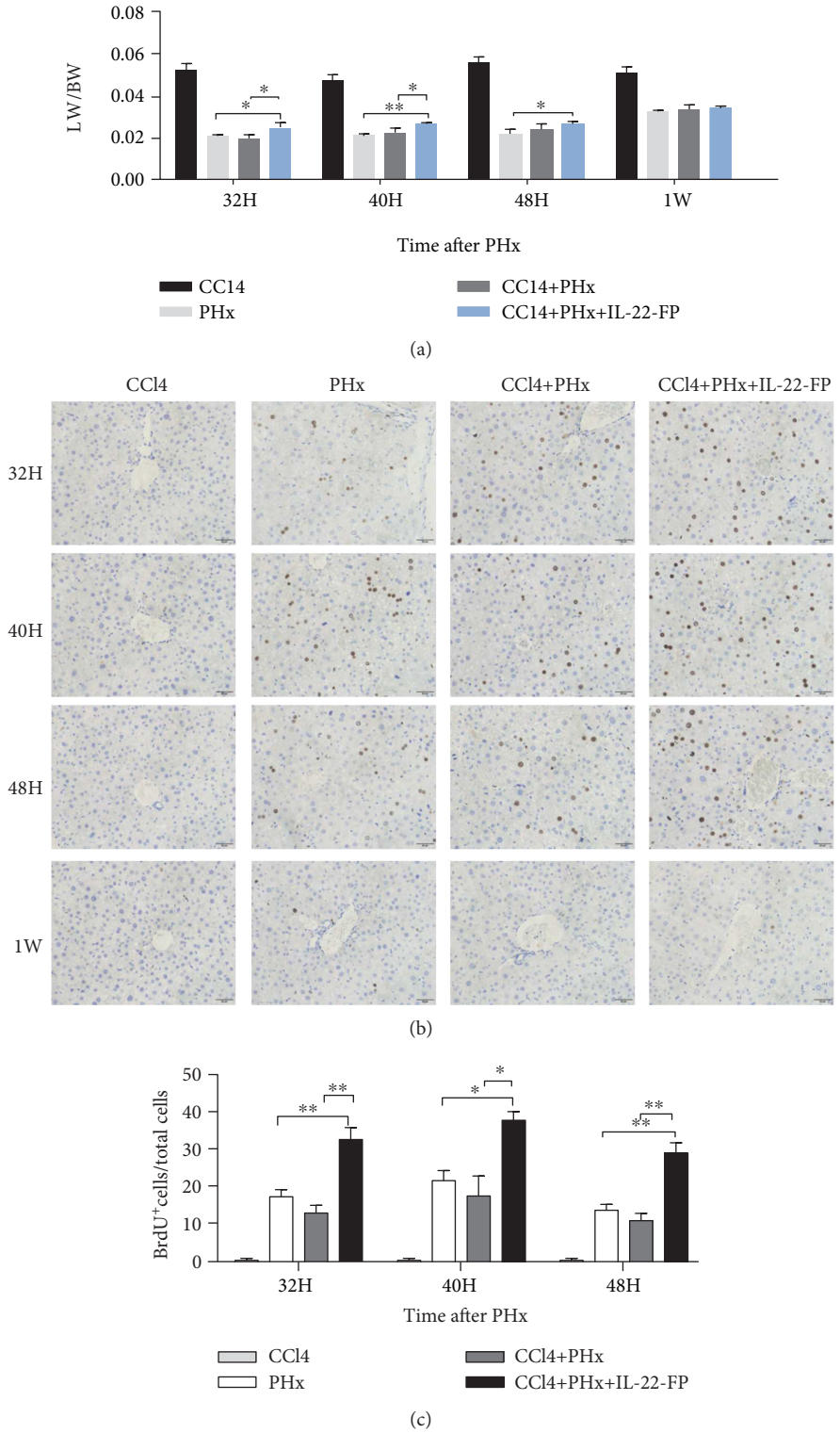

Figure 4: IL-22-FP promotes liver regeneration in a CCl4 model after PHx. Male C57BL/6 mice (8 to 10 wk old) were randomly divided into four groups: the CCl4 group, PHx group, CCl4 + PHx group, and CCl4 + PHx + IL-22-FP group. Mice in different groups were treated as described in Materials and Methods. (a) Liver weight/body weight ratios of different group mice at 32 h, 40 h, 48 h, and 1 wk post-PHx; $n = 4$ for each group. (b) BrdU staining of residual liver in four groups of mice at 32, 40, and 48 h post-PHx (400x magnification). (c) $BrdU^+$ hepatocyte/total hepatocyte ratios of four groups at different time points (32, 40, and 48 h) post-PHx. Pictures were taken at 400x magnification; $n = 4$ for each group. $^*p < 0.05$ and $^{**}p < 0.01$.

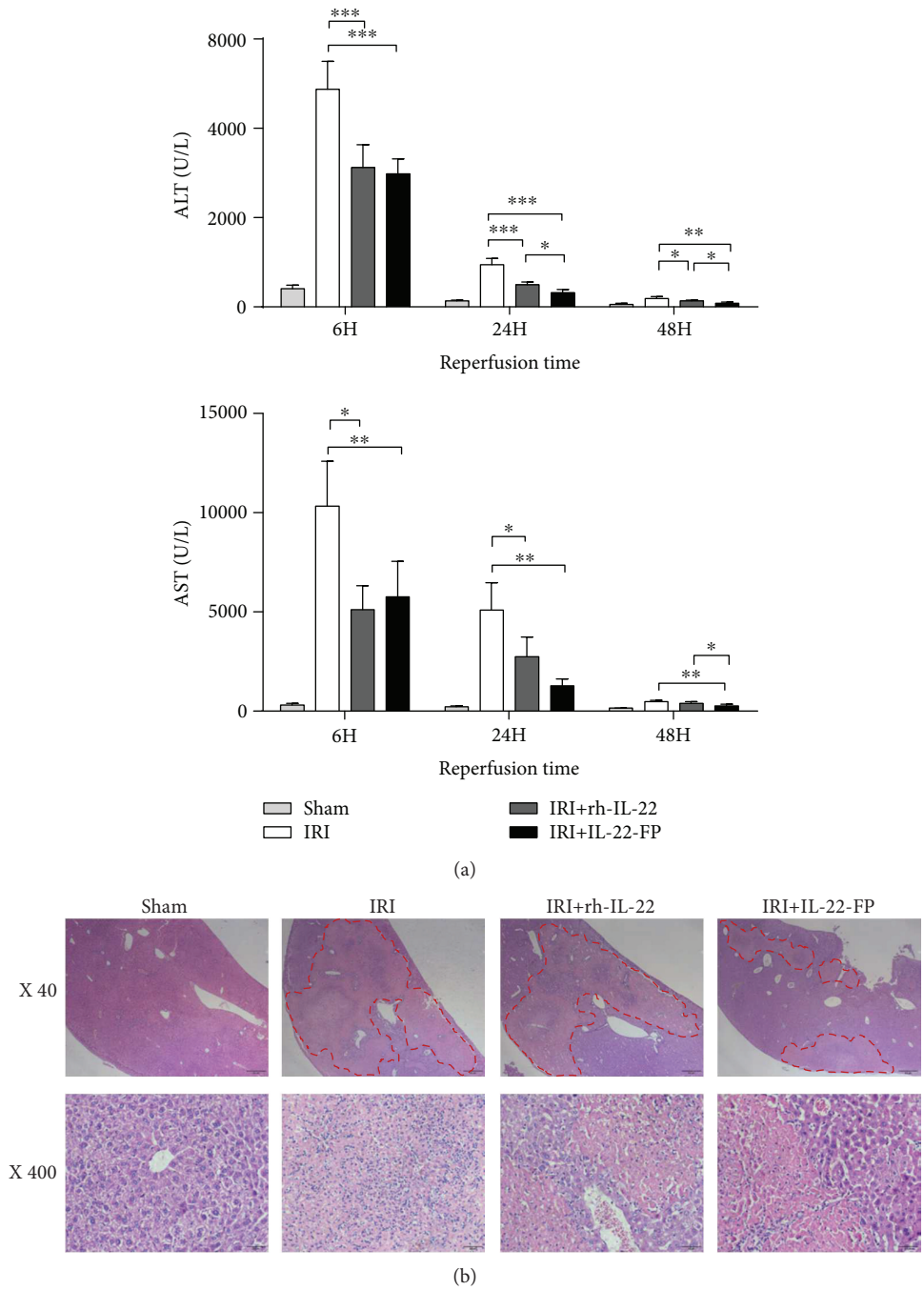

Figure 5: The protective effect of IL-22-FP on the liver in an IRI model. Male C57BL/6 mice (8 to 10 wk old) were randomly divided into 4 groups: the sham group, IRI group, IRI + rh-IL-22 group, and IRI + IL-22-FP group. The different groups of mice were treated as described above. (a) Serum ALT and AST levels in four groups of mice at 6, 24, and 48 h postreperfusion; $n = 4$ for each group. (b) Hematoxylin and eosin staining of liver tissue to display necrosis in liver sections at 48 h postreperfusion (40x or 400x magnification). $^{*}p < 0.05$ and $^{**}p < 0.01$.

treatment with IL-22 induces activation of STAT3, which then promotes the expression of a variety of cell cycle proteins, eventually promoting hepatocyte proliferation [30–32]. Our research results (Figures 6(a) and 6(c)) suggested that STAT3 was activated significantly in the liver of mice treated with IL-22-FP compared with the other three groups. Activated STAT3 induces the expression of cell cycle proteins (e.g., CyclinB1 and CyclinD1) and increases the expression of PCNA protein significantly in the liver to eventually promotes the proliferation of hepatocytes. These findings suggest that IL-22 is an inducer of STAT3 activation in hepatocytes and activated STAT3 is a contributing factor to the regeneration of hepatocytes. Therefore, IL-22 promotes liver regeneration through the STAT3 pathway.

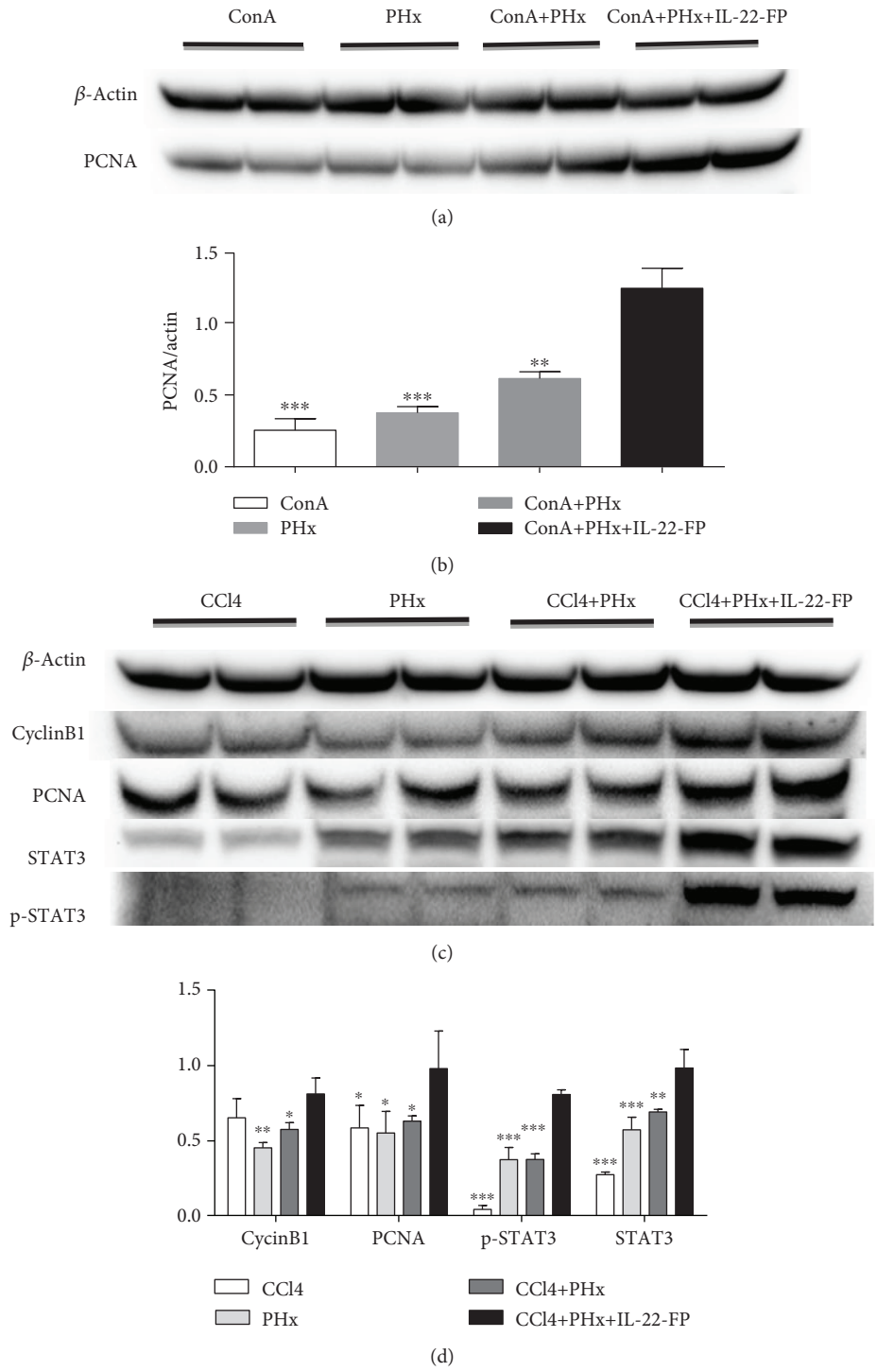

Figure 6: Effects of IL-22-FP on PCNA, CyclinB1, STAT3, and p-STAT3 activation after PHx. After euthanasia, the residual mouse liver was frozen for Western blot analysis. (a, b) PCNA expression was obviously increased in the ConA + PHx + IL-22-FP group compared with that in the other three groups at 40 h post-PHx in the ConA model. $^{**}p < 0.01$ and $^{***}p < 0.001$. (c, d) Expression of CyclinB1, PCNA, and p-STAT3 was obviously increased in the CCl4 + PHx + IL-22-FP group compared with that in the other three groups at 40 h post-PHx in the CCl4 model (all statistics were compared with the CCl4 + PHx + IL-22-FP group). $^{*}p < 0.05$, $^{**}p < 0.01$, and $^{***}p < 0.001$.

Liver IRI is one of the major complications in liver resection and liver transplantation [40, 41]. At the onset of reperfusion, an imbalance between nitric oxide levels and endothelin leads to failure of liver microcirculation. Nuclear factor-κB in the liver is activated to promote a combination of proinflammatory cytokines and adhesion molecules, which promotes neutrophil recruitment and oxygen-derived free radical production, further contributing to hepatocyte injury [42, 43]. Paul et al. discovered that IL-22 plays an important role in ischemia-reperfusion-induced

liver injury. IL-22 was detected at 24 h postreperfusion, and IL-22R1 expression significantly increased at 6 h postreperfusion in wild-type mice. IL-22 protects the liver against IRI, decreases serum AST levels, alleviates cardinal histological features caused by ischemia-reperfusion, and diminishes leukocyte sequestration [8, 33]. Administration of IL-22-FP significantly decreased serum AST levels at 6, 24, and 48 h postreperfusion (Figure 5(a)). Notably, the application of IL-22-FP led to a more pronounced reduction in AST levels at 48 h postreperfusion compared with rh-IL-22. The hepatoprotective mechanism of IL-22 in IRI is still incompletely understood. One view is that this effect of IL-22 is related to regulation of the inflammatory response [33]. Damaged hepatocytes increased the expression of IL-22-R1 after treatment with IL-22 and IL-22 combined with IL-22-R1, thereby stimulating downstream signaling pathways to promote hepatocyte survival or regeneration [33].

In the liver, only hepatic cells express the IL-22 receptor; immune cells have no IL-22 receptor, and therefore, IL-22 does not target immune cells. Because of this, we have reason to speculate that local or short-term treatment with IL-22 will protect the liver and promote hepatic regeneration without causing excessive inflammation in the liver [44, 45]. Most patients who undergo liver resection have different types of liver disease, and thus, we used ConA and CCl4 to induce liver damage in mice to imitate human liver disease. As our experimental data have shown, IL-22-FP has a significant role in liver protection and enhancing hepatocyte regeneration and these two aspects exactly correspond to the two key problems clinical patients experience after PHx. IL-22-FP ameliorates the liver damage and enhances the proliferation of residual liver cells. In conclusion, IL-22-FP has great potential for treatment of patients with liver disease that have undergone PHx.

Data Availability

The data used to support the findings of this study have been deposited in the Figshare repository (doi:10.6084/m9.figshare.6287198).

Ethical Approval

Our animal experiments were approved by the biomedical ethics committee of the Medical University of Anhui. There are no studies with human participants performed in this article.

Conflicts of Interest

The authors declare that there is no conflict of interest regarding the publication of this article.

Authors' Contributions

Heng Zhou participated in the design of the research study, operated the research, analyzed the data, made the graph, and wrote the manuscript. Hua Wang and Shi Yin designed the research, contributed to the analysis of the data, and helped in writing the manuscript. Hua Wang and Shi Yin provided the fund of the study. Guomin Xie, Yudi Mao, Ke Zhou, and Ruixue Ren contributed to performing the research; they were also involved in the data analysis, graph making, and manuscript writing. Qihong Zhao designed the study and analyzed the data. It is worth mentioning that Qihong Zhao has provided us with the laboratory for the research.

Acknowledgments

This work was supported by the National Natural Science Foundation of China (grant numbers 81100311 and 81470879/H0318 to S Yin; grant number 81522009/H0317 to H Wang). The interleukin 22 fusion protein (IL-22-FP) used in this article was provided by GENERON Corporation Ltd. (Shanghai).

References

[1] D. B. B. Trivella, J. R. Ferreira-Júnior, L. Dumoutier, J.-C. Renauld, and I. Polikarpov, "Structure and function of interleukin-22 and other members of the interleukin-10 family," *Cellular and Molecular Life Sciences*, vol. 67, no. 17, pp. 2909–2935, 2010.

[2] J. A. Dudakov, A. M. Hanash, and M. R. M. van den Brink, "Interleukin-22: immunobiology and pathology," *Annual Review of Immunology*, vol. 33, no. 1, pp. 747–785, 2015.

[3] R. Sabat, W. Ouyang, and K. Wolk, "Therapeutic opportunities of the IL-22-IL-22R1 system," *Nature Reviews Drug Discovery*, vol. 13, no. 1, pp. 21–38, 2014.

[4] C. Lim and R. Savan, "The role of the IL-22/IL-22R1 axis in cancer," *Cytokine & Growth Factor Reviews*, vol. 25, no. 3, pp. 257–271, 2014.

[5] H. Mühl, P. Scheiermann, M. Bachmann, L. Härdle, A. Heinrichs, and J. Pfeilschifter, "IL-22 in tissue-protective therapy," *British Journal of Pharmacology*, vol. 169, no. 4, pp. 761–771, 2013.

[6] O. B. Parks, D. A. Pociask, Z. Hodzic, J. K. Kolls, and M. Good, "Interleukin-22 signaling in the regulation of intestinal health and disease," *Frontiers in Cell and Development Biology*, vol. 3, p. 85, 2016.

[7] O. Park, H. Wang, H. Weng et al., "In vivo consequences of liver-specific interleukin-22 expression in mice: implications for human liver disease progression," *Hepatology*, vol. 54, no. 1, pp. 252–261, 2011.

[8] C. X. Pan, J. Tang, X. Y. Wang, F. R. Wu, J. F. Ge, and F. H. Chen, "Role of interleukin-22 in liver diseases," *Inflammation Research*, vol. 63, no. 7, pp. 519–525, 2014.

[9] W. W. Xing, M. J. Zou, S. Liu et al., "Hepatoprotective effects of IL-22 on fulminant hepatic failure induced by d-galactosamine and lipopolysaccharide in mice," *Cytokine*, vol. 56, no. 2, pp. 174–179, 2011.

[10] R. Lai, X. Xiang, R. Mo et al., "Protective effect of Th22 cells and intrahepatic IL-22 in drug induced hepatocellular injury," *Journal of Hepatology*, vol. 63, no. 1, pp. 148–155, 2015.

[11] L. A. Zenewicz, G. D. Yancopoulos, D. M. Valenzuela, A. J. Murphy, M. Karow, and R. A. Flavell, "Interleukin-22 but not interleukin-17 provides protection to hepatocytes during acute liver inflammation," *Immunity*, vol. 27, no. 4, pp. 647–659, 2007.

[12] P. Scheiermann, M. Bachmann, I. Goren, B. Zwissler, J. Pfeilschifter, and H. Mühl, "Application of interleukin-22 mediates protection in experimental acetaminophen-induced acute liver injury," *The American Journal of Pathology*, vol. 182, no. 4, pp. 1107–1113, 2013.

[13] T. H. Ashour, "Therapy with interleukin-22 alleviates hepatic injury and hemostasis dysregulation in rat model of acute liver failure," *Advances in Hematology*, vol. 2014, Article ID 705290, 7 pages, 2014.

[14] S. H. Ki, O. Park, M. Zheng et al., "Interleukin-22 treatment ameliorates alcoholic liver injury in a murine model of chronic-binge ethanol feeding: role of signal transducer and activator of transcription 3," *Hepatology*, vol. 52, no. 4, pp. 1291–1300, 2010.

[15] M. Saalim, S. Resham, S. Manzoor et al., "IL-22: a promising candidate to inhibit viral-induced liver disease progression and hepatocellular carcinoma," *Tumour Biology*, vol. 37, no. 1, pp. 105–114, 2016.

[16] D. H. Lu, X. Y. Guo, S. Y. Qin et al., "Interleukin-22 ameliorates liver fibrogenesis by attenuating hepatic stellate cell activation and downregulating the levels of inflammatory cytokines," *World Journal of Gastroenterology*, vol. 21, no. 5, pp. 1531–1545, 2015.

[17] X. Kong, D. Feng, H. Wang et al., "Interleukin-22 induces hepatic stellate cell senescence and restricts liver fibrosis in mice," *Hepatology*, vol. 56, no. 3, pp. 1150–1159, 2012.

[18] X. Kong, D. Feng, S. Mathews, and B. Gao, "Hepatoprotective and anti-fibrotic functions of interleukin-22: therapeutic potential for the treatment of alcoholic liver disease," *Journal of Gastroenterology and Hepatology*, vol. 28, Supplement 1, pp. 56–60, 2013.

[19] R. Jiang, Z. Tan, L. Deng et al., "Interleukin-22 promotes human hepatocellular carcinoma by activation of STAT3," *Hepatology*, vol. 54, no. 3, pp. 900–909, 2011.

[20] H. Pan, F. Hong, S. Radaeva, and B. Gao, "Hydrodynamic gene delivery of interleukin-22 protects the mouse liver from concanavalin A-, carbon tetrachloride-, and Fas ligand-induced injury via activation of STAT3," *Cellular & Molecular Immunology*, vol. 1, no. 1, pp. 43–49, 2004.

[21] S. Radaeva, R. Sun, H. N. Pan, F. Hong, and B. Gao, "Interleukin 22 (IL-22) plays a protective role in T cell-mediated murine hepatitis: IL-22 is a survival factor for hepatocytes via STAT3 activation," *Hepatology*, vol. 39, no. 5, pp. 1332–1342, 2004.

[22] Y. Zhang, M. A. Cobleigh, J.–. Q. Lian et al., "A proinflammatory role for interleukin-22 in the immune response to hepatitis B virus," *Gastroenterology*, vol. 141, no. 5, pp. 1897–1906, 2011.

[23] W. Gao, Y. C. Fan, J. Y. Zhang, and M. H. Zheng, "Emerging role of interleukin 22 in hepatitis B virus infection: a double-edged sword," *Journal of Clinical and Translational Hepatology*, vol. 1, no. 2, pp. 103–108, 2013.

[24] J. Zhao, Z. Zhang, Y. Luan et al., "Pathological functions of interleukin-22 in chronic liver inflammation and fibrosis with hepatitis B virus infection by promoting T helper 17 cell recruitment," *Hepatology*, vol. 59, no. 4, pp. 1331–1342, 2014.

[25] J. Dambacher, F. Beigel, K. Zitzmann et al., "The role of interleukin-22 in hepatitis C virus infection," *Cytokine*, vol. 41, no. 3, pp. 209–216, 2008.

[26] D. Feng, X. Kong, H. Weng et al., "Interleukin-22 promotes proliferation of liver stem/progenitor cells in mice and patients with chronic hepatitis B virus infection," *Gastroenterology*, vol. 143, no. 1, pp. 188–198.e7, 2012.

[27] C. Jia, "Advances in the regulation of liver regeneration," *Expert Review of Gastroenterology & Hepatology*, vol. 5, no. 1, pp. 105–121, 2014.

[28] G. K. Michalopoulos, "Liver regeneration after partial hepatectomy: critical analysis of mechanistic dilemmas," *The American Journal of Pathology*, vol. 176, no. 1, pp. 2–13, 2010.

[29] H. Wang, O. Park, F. Lafdil et al., "Interplay of hepatic and myeloid signal transducer and activator of transcription 3 in facilitating liver regeneration via tempering innate immunity," *Hepatology*, vol. 51, no. 4, pp. 1354–1362, 2010.

[30] X. Ren, B. Hu, and L. M. Colletti, "IL-22 is involved in liver regeneration after hepatectomy," *American Journal of Physiology. Gastrointestinal and Liver Physiology*, vol. 298, no. 1, pp. G74–G80, 2010.

[31] S. Brand, J. Dambacher, F. Beigel et al., "IL-22-mediated liver cell regeneration is abrogated by SOCS-1/3 overexpression in vitro," *American Journal of Physiology. Gastrointestinal and Liver Physiology*, vol. 292, no. 4, pp. G1019–G1028, 2007.

[32] Y. M. Zhang, Z. R. Liu, Z. L. Cui et al., "Interleukin-22 contributes to liver regeneration in mice with concanavalin A-induced hepatitis after hepatectomy," *World Journal of Gastroenterology*, vol. 22, no. 6, pp. 2081–2091, 2016.

[33] P. J. Chestovich, Y. Uchida, W. Chang et al., "Interleukin-22: implications for liver ischemia-reperfusion injury," *Transplantation*, vol. 93, no. 5, pp. 485–492, 2012.

[34] K. Y. Tang, J. Lickliter, Z. H. Huang et al., "Safety, pharmacokinetics, and biomarkers of F-652, a recombinant human interleukin-22 dimer, in healthy subjects," *Cellular & Molecular Immunology*, 2018.

[35] E. Eggenhofer, M. Sabet-Rashedi, M. Lantow et al., "RORγt$^+$ IL-22-producing NKp46$^+$ cells protect from hepatic ischemia reperfusion injury in mice," *Journal of Hepatology*, vol. 64, no. 1, pp. 128–134, 2016.

[36] J. Yu, Z. Feng, L. Tan, L. Pu, and L. Kong, "Interleukin-11 protects mouse liver from warm ischemia/reperfusion (WI/Rp) injury," *Clinics and Research in Hepatology and Gastroenterology*, vol. 40, no. 5, pp. 562–570, 2016.

[37] H. Abe, A. Kimura, S. Tsuruta et al., "Aryl hydrocarbon receptor plays protective roles in ConA-induced hepatic injury by both suppressing IFN-γ expression and inducing IL-22," *International Immunology*, vol. 26, no. 3, pp. 129–137, 2014.

[38] C. Wahl, U. M. Wegenka, F. Leithauser, R. Schirmbeck, and J. Reimann, "IL-22-dependent attenuation of T cell-dependent (ConA) hepatitis in herpes virus entry mediator deficiency," *The Journal of Immunology*, vol. 182, no. 8, pp. 4521–4528, 2009.

[39] D. Feng, Y. Wang, H. Wang et al., "Acute and chronic effects of IL-22 on acetaminophen-induced liver injury," *Journal of Immunology*, vol. 193, no. 5, pp. 2512–2518, 2014.

[40] Y. Chen, L. Lv, H. Pi et al., "Dihydromyricetin protects against liver ischemia/reperfusion induced apoptosis via activation of FOXO3a-mediated autophagy," *Oncotarget*, vol. 7, no. 47, pp. 76508–76522, 2016.

[41] G. Pasut, A. Panisello, E. Folch-Puy et al., "Polyethylene glycols: an effective strategy for limiting liver ischemia reperfusion injury," *World Journal of Gastroenterology*, vol. 22, no. 28, pp. 6501–6508, 2016.

[42] F. Serracino-Inglott, N. A. Habib, and R. T. Mathie, "Hepatic ischemia-reperfusion injury," *American Journal of Surgery*, vol. 181, no. 2, pp. 160–166, 2001.

[43] K. Weigand, S. Brost, N. Steinebrunner, M. Büchler, P. Schemmer, and M. Müller, "Ischemia/reperfusion injury in liver surgery and transplantation: pathophysiology," *HPB Surgery*, vol. 2012, Article ID 176723, 8 pages, 2012.

[44] B. Gao, "Interplay of interleukin-22 and its binding protein in controlling liver scarring," *Hepatology*, vol. 61, no. 4, pp. 1121–1123, 2015.

[45] O. Park, S. H. Ki, M. Xu et al., "Biologically active, high levels of interleukin-22 inhibit hepatic gluconeogenesis but do not affect obesity and its metabolic consequences," *Cell & Bioscience*, vol. 5, no. 1, p. 25, 2015.

Hindawi
Journal of Immunology Research
Volume 2018, Article ID 3917032, 9 pages
https://doi.org/10.1155/2018/3917032

Research Article

Complement System as a Target for Therapies to Control Liver Regeneration/Damage in Acute Liver Failure Induced by Viral Hepatitis

Juliana Gil Melgaço,[1] **Carlos Eduardo Veloso**,[2] **Lúcio Filgueiras Pacheco-Moreira**,[3] **Claudia Lamarca Vitral**,[4] **and Marcelo Alves Pinto**[1]

[1]*Laboratório de Desenvolvimento Tecnológico em Virologia, Instituto Oswaldo Cruz, Fundação Oswaldo Cruz, Rio de Janeiro, Brazil*
[2]*Departamento de Patologia, Instituto Nacional do Câncer, Rio de Janeiro, Brazil*
[3]*Hospital Federal de Bonsucesso, Rio de Janeiro, Brazil*
[4]*Departamento de Microbiologia e Parasitologia, Instituto Biomédico, Universidade Federal Fluminense, Niterói, Brazil*

Correspondence should be addressed to Juliana Gil Melgaço; juliana.melgaco@gmail.com
and Marcelo Alves Pinto; marcelop@ioc.fiocruz.br

Received 12 May 2018; Accepted 28 August 2018; Published 8 October 2018

Academic Editor: Dechun Feng

The complement system plays an important role in innate immunity inducing liver diseases as well as signaling immune cell activation in local inflammation regulating immunomodulatory effects such as liver damage and/or liver regeneration. Our aim is to evaluate the role of complement components in acute liver failure (ALF) caused by viral hepatitis, involving virus-induced ALF in human subjects using peripheral blood, samples of liver tissues, and ex vivo assays. Our findings displayed low levels of C3a in plasma samples with high frequency of C3a, C5a, and C5b/9 deposition in liver parenchyma. Meanwhile, laboratory assays using HepG2 (hepatocyte cell line) showed susceptibility to plasma samples from ALF patients impairing *in vitro* cell proliferation and an increase in apoptotic events submitting plasma samples to heat inactivation. In summary, our data suggest that the complement system may be involved in liver dysfunction in viral-induced acute liver failure cases using ex vivo assays. In extension to our findings, we provide insights into future studies using animal models for viral-induced ALF, as well as other associated soluble components, which need further investigation.

1. Introduction

Acute liver failure (ALF) is a complex and rare clinical syndrome characterized by the development of severe liver dysfunction, promoted by extensive death of functional cells. The mortality rate is close to 80%, and liver transplantation [1–4] is the only treatment modality available to this date. ALF can be induced by viral infections and toxicity promoted by drug abuse or alcoholism. In Brazil, viral infections are responsible for the majority of ALF cases, including viral hepatitis viruses such as hepatitis A virus (HAV) and hepatitis B virus (HBV), as well as coinfections related to hepatitis C virus (HCV), HIV, Epstein-Barr virus, and CMV [5–7].

Inflammatory response is strongly associated with liver diseases, and activation can trigger liver damage with aggressive hepatocyte loss [8]. In ALF, extensive liver injury can be caused by a variety of molecules of the innate immune system, and the complement system plays an important role in this process [9, 10]. The complement system is the major component of innate immunity; its protective function starts with a cascade of proteases and soluble factors that activates the immune system, stimulating microbial clearance [11]. Nevertheless, the function of the complement system is associated with processes of development, degeneration, and regeneration of multiple organs [12–14]. Anaphylatoxins C3a and C5a present potential chemoattractant activity to amplify immune cell recruitment such as macrophages

Table 1: Characteristics of the study population.

Subjects	Samples	Age	Gender	ALT	AST	INR	Encephalopathy	Outcome	Diagnostic	Etiology
1	HS1	29	F	14	21	1	None	NA	Healthy	None
2	HS2	27	M	16	22	1	None	NA	Healthy	None
3	HS3	29	F	13	19	1.1	None	NA	Healthy	None
4	HS4	26	M	23	33	0.9	None	NA	Healthy	None
5	HS5	46	F	18	26	0.8	None	NA	Healthy	None
6	HS6	31	F	11	15	0.9	None	NA	Healthy	None
7	HS9	26	F	16	25	0.9	None	NA	Healthy	None
8	HS10	33	F	13	18	1.1	None	NA	Healthy	None
9	ALF1	5	F	326	331	6.7	IV	Survival	Acute liver failure	HAV
10	ALF2	14	M	877	1790	4.32	IV	Death	Acute liver failure	HAV
11	ALF3	7	M	1562	5611	2.55	III	Death	Acute liver failure	HAV
12	ALF4	14	M	313	330	8.64	IV	Death	Acute liver failure	HAV
13	ALF5	1	F	668	171	6.38	II	Death	Acute liver failure	HAV
14	ALF6	24	M	964	762	3.3	II	Death	Acute liver failure	HBV
15	ALF7	31	F	314	562	2.1	II	Survival	Acute liver failure	HBV
16	ALF8	17	M	200	120	1.7	II	Survival	Acute liver failure	HAV

Legend: HS: healthy subjects; ALF: acute liver failure patients; HAV: hepatitis A virus; HBV: hepatitis B virus; F: female; M: male; NA: not applicable.

and neutrophils into the liver parenchyma [15]; quickly, C5a is converted to C5aDesArg *in vivo*, leading to local inflammation [16]. Following the complement cascade, C5b with C6–C9 forms the "membrane attack complex" (MAC), capable of lysing infected cells and pathogens [17, 18].

A susceptible cell culture system and animal models are important to improve knowledge of viral liver pathogenesis and promising therapies. However, useful viral-induced ALF animal models are not simple; in addition, the diversity of liver cell lines is used to study therapy interventions and also to understand mechanisms related to liver diseases, such as viral hepatitis [19, 20]. Here, we assessed the toxicological effects of the complement system in the peripheral blood of patients during acute liver failure.

2. Materials and Methods

2.1. Study Population and Samples. Blood samples ($n = 8$) and liver samples ($n = 6$) from ALF patients and blood samples ($n = 10$) and liver samples ($n = 1$) from healthy subjects (HS) were collected at the Liver Clinic/Hospital Federal de Bonsucesso, Rio de Janeiro, Brazil, between February 2004 and November 2013.

Inclusion criteria included the presence of coagulopathy (INR ≥ 1.5) and encephalopathy score above II, according to O'Grady et al. [21] and as described previously [7, 22, 23]. Clinical details of the study population are shown in Table 1.

Screening to investigate the etiological agent involved in ALF cases as well as in samples of healthy donors was performed for HAV, HBV, and HCV detection and also for other infectious and autoimmune disorders as described by Melgaço et al. [7].

The adopted protocol performed complied with relevant laws and institutional guidelines according to the ethical standards of the Declaration of Helsinki approved by the Institutional Review Board of Fiocruz (#222/03).

2.2. Laboratory Assays

2.2.1. Detection of C3a Levels in Peripheral Blood Circulation. Blood samples (9 mL) were centrifuged ($200 \times g$/10 min) to separate plasma from other products. Plasma samples were aliquoted and stored at −70°C until laboratory assays. Initially, plasma samples were divided into two groups: in the first one, plasma was thawed at room temperature (RT) overnight and in the second one, plasma was thawed at RT overnight and submitted to temperature complement inactivation by heating at 57°C for 30 min. To detect C3a levels in plasma samples, a commercial kit was used according to the manufacturer's instructions (eBioscience, cat #BMS2089TEN, San Diego, CA, USA).

2.2.2. Detection of Anaphylatoxins and Membrane Attack Complex (MAC) in Liver Tissue Samples. Liver samples were obtained at the time of transplantation and stored in liquid nitrogen until immunofluorescence assays, sectioned at 5 μm, and stained with antibodies to membrane attack complex C5b/9 (clone: aE11, Santa Cruz cat #SC-58935, Brazil); the C3a component (clone: K13/16, Santa Cruz cat #SC-47688, Brazil) and C5a component (clone: 2952, Santa Cruz cat #SC-52634, Brazil) were applied to the sections at a dilution of 1 : 50 for 1 hour at 37°C. After incubation, sections were washed in phosphate-buffered saline (pH = 7.2) and incubated with the secondary antibody Alexia Fluor 488® (Abcam cat #AB-150113, USA) at a dilution of 1 : 1000. Photomicrographs were taken in a confocal microscope FV10i-O (Olympus, Japan) using FV10-ASW software. Calculation of marked areas was carried out using the software ImageJ (https://imagej.net/ImageJ).

2.2.3. In Vitro Evaluation of ALF Soluble Components. Hepatocellular carcinoma lineage (HepG2, ATCC® number: HB-8065™) was chosen to evaluate ex vivo effects of ALF

soluble components from plasma samples, since they are a well-established model for hepatocyte metabolism that under specific culture conditions maintains normal cell functions [24, 25]. HepG2 cultures were maintained in RPMI1640 (pH 7.4) (Gibco, USA) supplemented with 10% fetal bovine serum (FBS) (Gibco, USA) and 2 mM L-glutamine (Merck, Germany) in 75 cm^2 bottles at 37°C in a CO_2 humidified incubator. The medium was changed twice weekly, and passages were performed using trypsinization solution (0.2% and 0.02% versene in RPMI1640 medium). HepG2 confluency was regularly checked. The plasma of healthy subjects and ALF plasma samples were added to HepG2 cultures to assess the hypothesis of their toxicological effects. HepG2 cultures in a confluent monolayer were kept for 24 hours at 37°C in 24-well plates (5×10^4cells/well). Then, different concentrations of plasma samples (complement heat-inactivated and noninactivated) diluted in RPMI1640 (0.1%, 1%, and 10%) were added to HepG2 cultures and incubated for 48 hours. Then, to assess viability, HepG2 cultures were labeled using 5 μM of fluorescent vital dye cell trace in RPMI1640 (CFSE-FITC, Invitrogen®, USA). Negative proliferation percentage using CFSE-FITC was quantified by flow cytometry. Positive control of the absence of cell proliferation was carried out using colchicine at 10 μM [26]. Negative control was performed adding RPMI1640 with 10% fetal bovine serum (FBS) heat-inactivated (57°C, 30 min) in HepG2 culture.

Levels of liver enzymes (ALT and AST) in supernatant of cell cultures were quantified to assess cellular damage and apoptosis caused by ALF plasma samples (Diasys®, Germany); HAV and HBV viral load quantification was performed by real-time PCR [27, 28]. HepG2 cells were incubated with α-CD95-FITC (annexin V, clone DX2, BD Pharmingen, USA). In this assay, HepG2 cells were also kept for 48 h, and positive control was assessed using ascorbic acid (AA) (70 μM) for a 48 h incubation [29]. Blockage of membrane pores was achieved using specific phosphate saline solution (5% of 0.1 M BSA) and not fixed, according to the previous description [30].

After incubation, cells were analyzed by flow cytometry in both assays, 20,000 live cells were analyzed using a FACS-Calibur™ flow cytometer with four fluorescence channels (FL1-530/30, FL2-585/42, FL3-670LP, and FL4-661/16), and off-line analysis was performed using FlowJo software (version 10.0.5) (FlowJo, LLC data analysis software, USA).

2.2.4. Statistical Analysis. Statistical analyses were performed using Kruskal-Wallis and Dunn's multiple comparison test. $^*p \leq 0.05$, $^{**}p \leq 0.01$, and $^{***}p \leq 0.001$. All statistical analyses were performed using GraphPad Prism software version 7.

3. Results

3.1. The Lowest C3a Levels Detected in ALF Plasma Samples. Plasma samples from ALF patients and healthy subjects were submitted to C3a detection assays. Comparatively, Figure 1 shows superior levels of C3a detected among healthy donors (both heat-inactivated and noninactivated samples) even after thermal treatment ($p = 0.0419$).

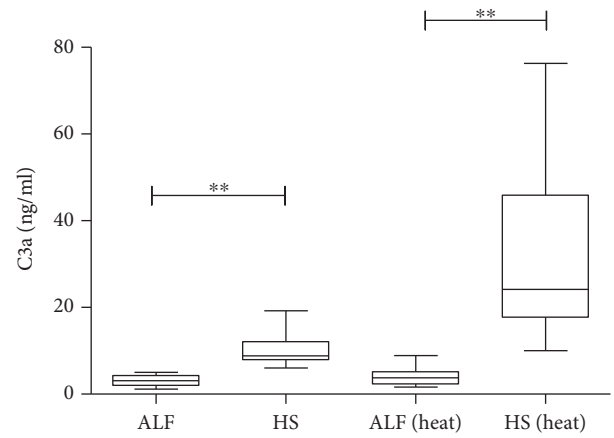

Figure 1: Soluble component C3a of complement system characterization of plasma samples from acute liver failure patients (ALF) and healthy subjects (HS) under heat inactivation (heat) and without heat inactivation.

3.2. Complement System Was Detected in Liver Samples from ALF Patients. Comparatively, a significant high percentage of C3a, C5a, and C5b/9 in labeled liver cells from ALF patients (Figure 2) was detected in tissue sections.

3.3. ALF Plasma Samples Induce Antiproliferative Activity and Apoptosis of In Vitro HepG2 Expansion. Impairment of *in vitro* HepG2 expansion in the presence of 10% heat-inactivated (EC50, $p = 0.0034$) and noninactivated ALF plasma samples (EC50, $p = 0.0153$) was observed despite reduced circulation of C3a in ALF patients, similar to what was detected in positive controls (colchicine) (Figure 3). Results are presented in a 10% concentration of plasma samples diluted in RPMI1640 media.

To evaluate membrane damage in HepG2 cultures, alanine and aspartate aminotransferase levels (ALT and AST) in supernatant after ALF plasma exposure were measured and no changes in AST levels were found (data not shown). ALT levels were significantly higher in heat-inactivated ALF plasma than in plasma of healthy subjects and noninactivated ALF plasma, as displayed in Figure 4(a). In addition, we also explored the viral load of hepatitis A virus (HAV) and hepatitis B virus (HBV) in plasma samples used in cell cultures before and after thermal inactivation and on supernatant after ALF plasma exposure. No significant changes in viral load were found before and after thermal inactivation ($p > 0.05$), as well as after HepG2 exposure to ALF plasma samples ($p > 0.05$) (Table 2).

Subsequently, by extending our analysis to annexin V, the median percentage of apoptotic cells expressing annexin V was significantly high in the presence of 10% heat- and non-inactivated ALF plasma samples compared with that of HS samples (Figure 4(b)).

4. Discussion

The complement system activation occurs in viral liver diseases [31–35]. Despite preventive measures, some viral liver

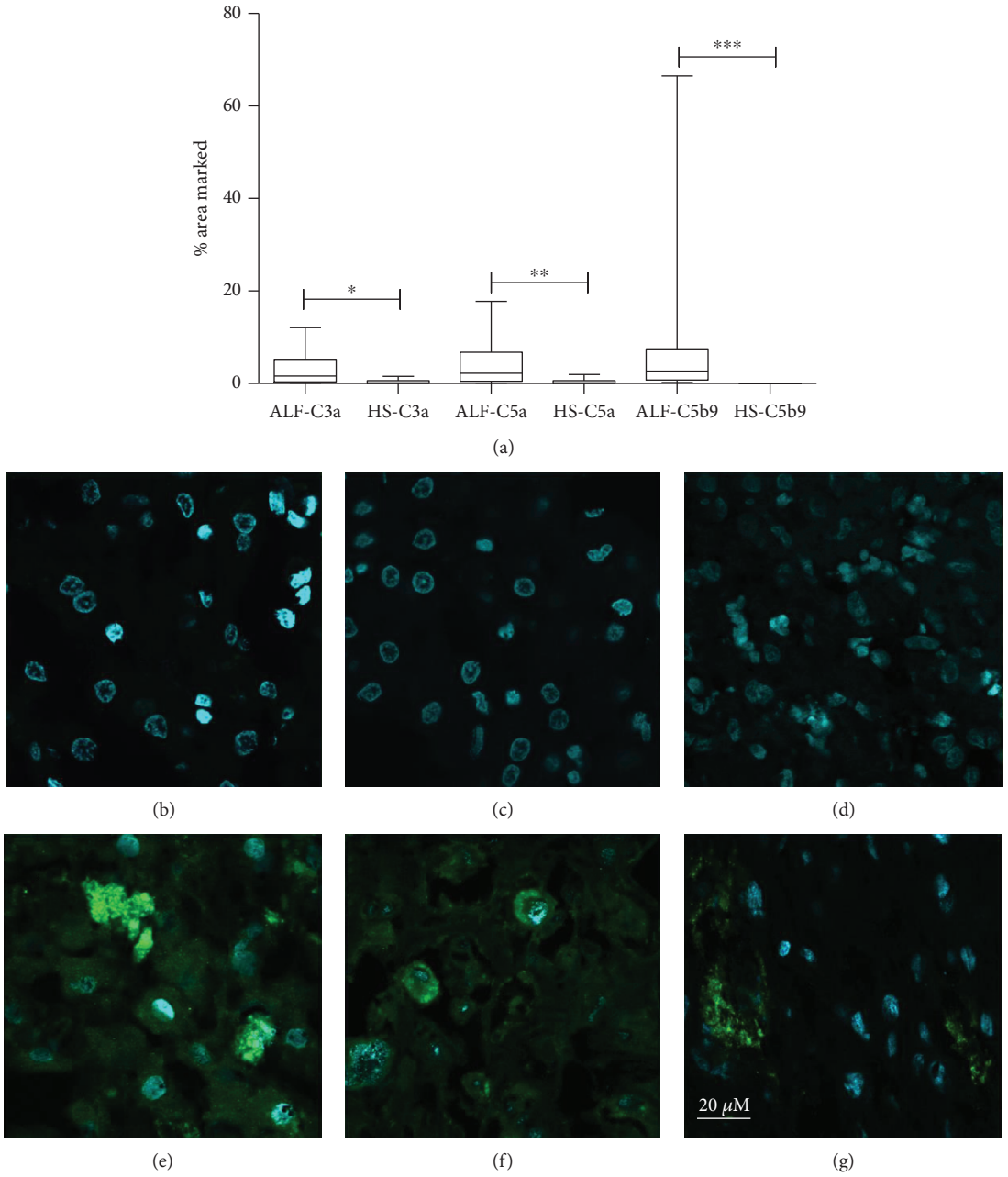

Figure 2: Liver deposit of anaphylatoxins C3a, C5a, and C5b/9 (MAC): (a) percentage of the area marked with anaphylatoxins in healthy subjects (HS) and acute liver failure (ALF) samples of liver tissue; (b–g) immunofluorescence assay (IFA) of liver samples tested for αC3a (b, e), αC5a (c, f), and αC5b/9 (d, g); the yellow underlined figures are from healthy subjects (b, c, d); the red underlined figures are from acute liver failure patients (e, f, g). Confocal microscopy zoom was of 400-fold.

diseases are widespread in developing countries causing acute hepatitis and its worst outcome is acute liver failure [33, 36]. Here, we confirmed the early impact of ALF plasma samples on HepG2 proliferation and viability, mimicking ALF liver environment. Some studies established the effects of the complement system on liver regeneration; however, the effective involvement of the components in viral liver injury and regeneration is still unknown [14, 18].

Our findings displayed a striking loss of C3 levels in peripheral blood from ALF patients, followed by high deposition of complement system components, such as C3a, C5a, and C5b-9 (MAC) in the liver parenchyma (liver explant) at the time of transplantation. C3 is a major component of the complement cascade, present at the early stage of liver inflammation [37], and C3 can regulate efflux and metabolism of steroid lipids in hepatocyte proliferation [18, 38]. In our previous report, plasmatic elevation titers of systemic inflammatory mediators (TNF-α, IL-6, IL-8, IL-10, IFNγ, and total mtDNA) were demonstrated in ALF patients [7, 22, 23, 39]. Similarly, other authors described the synergic

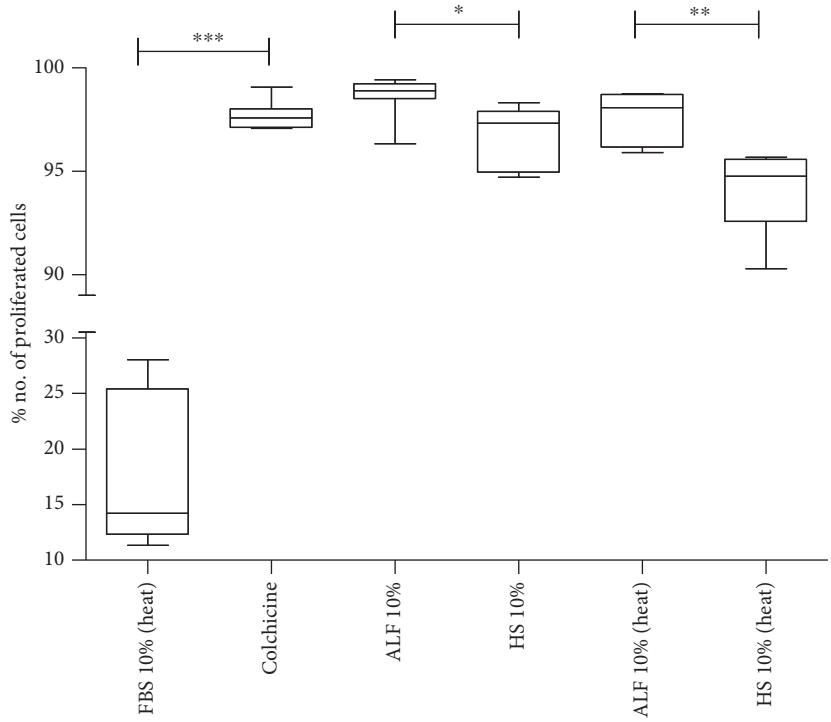

Figure 3: Effect of plasma (10%) from acute liver failure patients (ALF) and healthy subjects (HS) on HepG2 proliferation. Abbreviations: heat: heat-inactivated; ALF 10% vs. ALF 10% (heat), $p = 0.0489$.

effect of IL-1 beta and IL-6 on C3 mRNA transcription and C3 secretion in rat hepatocytes [40] since hepatocytes and Kupffer cells constitutively express receptors for C3 and C5a [40, 41].

In this study, viral-induced ALF patients with reduced C3a levels were associated with critical and progressive clinical conditions (donor shortage) and liver dysfunction. Similarly, nonviral etiologies [42, 43], LPS/D-GaIN-induced ALF [9], and chronic hepatitis cases [44, 45] could be justified by protein aggregates mediated by vitronectin or clusterin (complement regulatory proteins) [46], limited to the measurement of the complement components [45]. Displacement of the complement system from peripheral to central compartments in viral-induced ALF patients was already described in ALF animal models [15, 18] which were not exactly similar between animal and human studies [47]. Additionally, this study highlights that reduced levels of C3a in plasma from viral-induced ALF patients could not stimulate division of healthy hepatocytes since C3a biosynthesis depends on the normal liver function [32] as discussed by other authors in mouse models [15]. Hepatic deposition of components found in higher percentage in ALF liver samples could also suggest attempts for liver regeneration [18, 38, 48], which were not successful [10]. Despite the decrease in C3a levels in the plasma, its function cannot be ignored since it can trigger several cellular communications with different functionalities [13, 49]. On the other hand, lower C3a plasma levels and liver deposition can be a signal of liver "immunological storm" inducing hepatic damage [9, 32, 44, 45]. Those contradictory aspects discussed here raise the need for further investigation to understand the immune system in ALF syndrome.

Surprisingly, we observed a significant increase in C3a levels when plasma samples from healthy subjects were heat-inactivated. Contradictorily, some studies demonstrated that heat may influence [50] or not [51] immunoassay results, also associated with antibodies' interaction with protein activity after heating [50–52]. In our protocol, heat inactivation was performed at 57°C for 30 minutes; some studies described that complete inactivation of complement components in human serum can be effective for 30–60 minutes at 57°C [52, 53]. However, Moore and colleagues showed that C3b remained detectable and functional in decreased levels after heat inactivation of human sera [52].

Relevant weaknesses were identified in this study such as (i) soluble plasma components (endotoxin, hormones, bile acid, and other proteins); (ii) the reduced number of patients enrolled in this study related to the reduced number of liver transplants now occurring in Rio de Janeiro, Brazil; and (iii) scarce cases of ALF syndrome (0.5–1% of acute hepatitis cases [5, 7]).

In addition, we observed that *in vitro* HepG2 proliferation exposed to heat- or noninactivated plasma samples from ALF patients was significantly reduced, confirming our hypothesis related to the impairment of replicative capacity of resident hepatocytes. Intriguingly, during the early stages of liver damage, inflammatory cytokines induce healthy hepatocyte division [54]; however, during liver failure, its regenerative process is inadequate to match rapid, confluent loss of hepatocyte mass and function [8, 10].

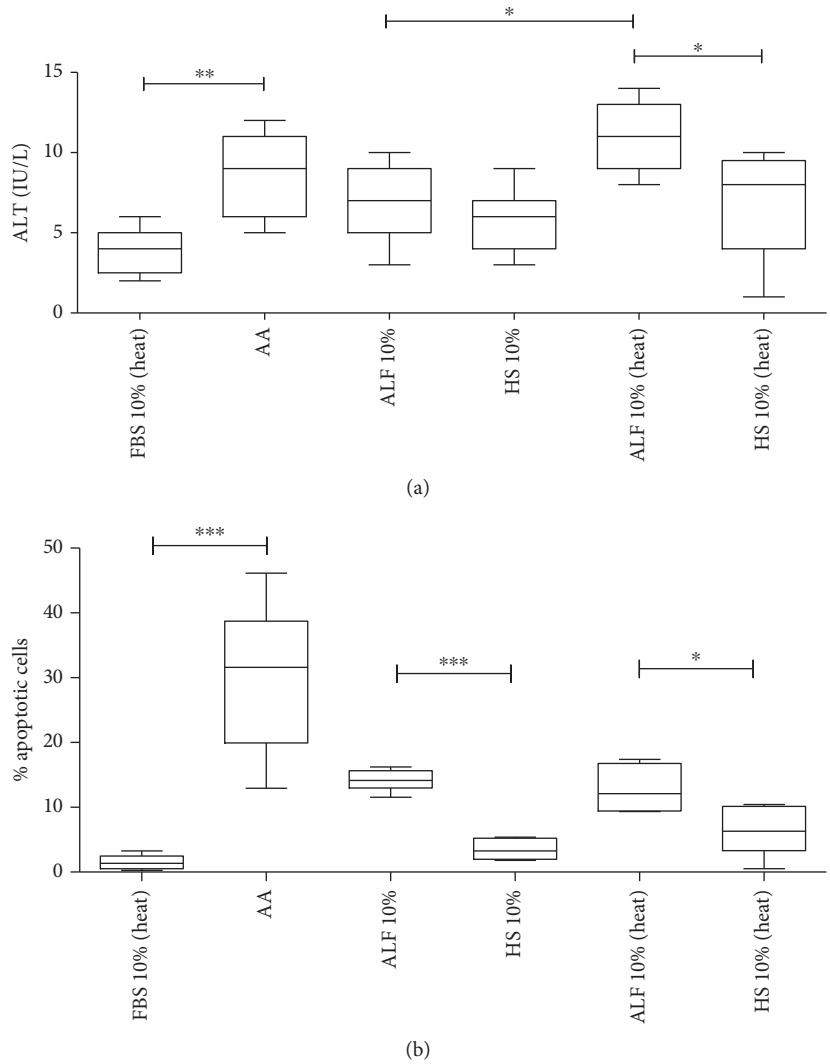

Figure 4: Effect of plasma (10%) from acute liver failure patients (ALF) and healthy subjects (HS) on a HepG2 cell line. (a) Measurement of *in vitro* alanine aminotransferase (ALT): FBS 10% (heat) vs. ALF 10%, $p = 0.0265$; FBS 10% (heat) vs. ALF 10% (heat), $p = 0.0014$. (b) Apoptosis evaluation. Abbreviations: FBS: fetal bovine serum; AA: ascorbic acid; heat: heat-inactivated.

Table 2: Viral load obtained from plasma samples and HepG2 cell culture after ALF plasma exposure before and after heat inactivation.

Viral hepatitis	Viral load on plasma samples	Viral load on plasma samples (heat-inactivated)	Viral load on supernatant from HepG2 cells	Viral load on supernatant from HepG2 cells (heat-inactivated)	Plasma samples vs. plasma samples (heat-inactivated) (p value)	Viral load on supernatant from HepG2 cells vs. viral load on supernatant from HepG2 cells (heat-inactivated) (p value)
A	3.27 ± 0.43	2.58 ± 0.53	3.24 ± 0.81	2.48 ± 0.48	0.062	0.250
B	3.97 ± 0.32	3.73 ± 0.45	3.64 ± 0.32	3.28 ± 0.41	0.120	0.094

Legend: viral load data was expressed as $\log_{10}$ copies/mL and mean ± SE.

Impairment of *in vitro* cell expansion could trigger the apoptotic process with massive loss of liver cells in ALF leading to interruption of liver regeneration, as observed in our findings (Figures 3 and 4) and described by others [43, 55, 56]. Other studies also showed plasma effects on hepatocyte cell lines affecting metabolism [57, 58]. In addition, heat inactivation may not be enough to abrogate the function of the complement system in ALF [52]. Also, biochemical thermal alterations in the complement and other components together can trigger an apoptotic event and/or may affect HepG2 cell proliferation [13, 49, 57, 58].

The viral load is another relevant variable that affects HepG2 proliferation. No significant changes were found in the viral load before and after ALF exposure. After heat

inactivation, a slight decrease in the viral load was observed (Table 2), as described by others [59]. Probably, viable particles were not present in those samples, since plasma samples with no more than 4 $\log_{10}$ copies/mL were selected for this study, and HepG2 cell lines were not susceptible to HBV or HAV replication [60–62].

Our results raise the possibility of C3 as a target for new therapeutic approaches based on C3 function in hepatocytes for liver regeneration attempts. Although we cannot predict possible influence efficacy in this type of therapy, the knowledge of C3 effects on immortalized human hepatocyte cell lines could be useful to assess hepatocyte regeneration. It is noteworthy that other components (phosphate, creatinine, bile acid, and reactive oxygen species, among others) need further investigation since soluble factors are associated with fulminant hepatitis outcome [63–66]. However, we are studying an *in vitro* system using human samples to assess the role of primary complement component (C3a) in liver environment simulation.

Finally, lower levels of complement C3 in viral-induced ALF followed by a high frequency of C3a, C5a, and C5b/9 deposition in the dysfunctional liver parenchyma combined with higher HepG2 susceptibility suggest that therapies targeting the complement pathway should be further investigated to control liver regeneration/damage in fulminant hepatitis caused by viral hepatitis. Animal models should be the next very useful step to monitor ALF therapy since knockout studies using anticomplement antibodies, small interfering RNAs, and recombinant complement protein may be useful to evaluate the function of complements on cell proliferation and apoptosis.

Data Availability

The data used to support the findings of this study are included within the article.

Conflicts of Interest

All authors present no conflict of interests.

Acknowledgments

We would like to thank the study population from Hospital Federal de Bonsucesso and the physicians who contributed to this study. We are also thankful for the technical support from Fundação Oswaldo Cruz and Instituto Nacional do Câncer, especially to Andrea Henriques Pons from flow cytometry platform, as well as to Matheus A. Rajão and João Paulo de Biaso Viola from confocal microscopy platform. This work was supported by the Fundação de Amparo à Pesquisa do Estado do Rio de Janeiro (Grant #6526/110.848/2013) and Brazilian National Council for Research and Development (Grant #308951/2010-7).

References

[1] H. S. Lee, G. H. Choi, D. J. Joo et al., "Prognostic value of model for end-stage liver disease scores in patients with fulminant hepatic failure," *Transplantation Proceedings*, vol. 45, no. 8, pp. 2992–2994, 2013.

[2] W. M. Lee, "Acute liver failure," *Seminars in Respiratory and Critical Care Medicine*, vol. 33, no. 1, pp. 36–45, 2012.

[3] J. Wendon, J. Cordoba, A. Dhawan et al., "EASL clinical practical guidelines on the management of acute (fulminant) liver failure," *Journal of Hepatology*, vol. 66, no. 5, pp. 1047–1081, 2017.

[4] T. Whitehouse and J. Wendon, "Acute liver failure," *Best Practice & Research. Clinical Gastroenterology*, vol. 27, no. 5, pp. 757–769, 2013.

[5] D. C. Santos, J. M. Martinho, L. F. Pacheco-Moreira et al., "Fulminant hepatitis failure in adults and children from a public hospital in Rio de Janeiro, Brazil," *Brazilian Journal of Infectious Diseases*, vol. 13, no. 5, pp. 323–329, 2009.

[6] S. Jayakumar, R. Chowdhury, C. Ye, and C. J. Karvellas, "Fulminant viral hepatitis," *Critical Care Clinics*, vol. 29, no. 3, pp. 677–697, 2013.

[7] J. G. Melgaço, F. M. Soriani, P. H. Sucupira et al., "Changes in cellular proliferation and plasma products are associated with liver failure," *World Journal of Hepatology*, vol. 8, no. 32, pp. 1370–1383, 2016.

[8] C. Brenner, L. Galluzzi, O. Kepp, and G. Kroemer, "Decoding cell death signals in liver inflammation," *Journal of Hepatology*, vol. 59, no. 3, pp. 583–594, 2013.

[9] S. Sun, Y. Guo, G. Zhao et al., "Complement and the alternative pathway play an important role in LPS/D-GalN-induced fulminant hepatic failure," *PLoS One*, vol. 6, no. 11, article e26838, 2011.

[10] Z. Wu, M. Han, T. Chen, W. Yan, and Q. Ning, "Acute liver failure: mechanisms of immune-mediated liver injury," *Liver International*, vol. 30, no. 6, pp. 782–794, 2010.

[11] D. Ricklin, G. Hajishengallis, K. Yang, and J. D. Lambris, "Complement: a key system for immune surveillance and homeostasis," *Nature Immunology*, vol. 11, no. 9, pp. 785–797, 2010.

[12] M. M. Markiewski and J. D. Lambris, "The role of complement in inflammatory diseases from behind the scenes into the spotlight," *The American Journal of Pathology*, vol. 171, no. 3, pp. 715–727, 2007.

[13] P. F. Zipfel and C. Skerka, "Complement regulators and inhibitory proteins," *Nature Reviews. Immunology*, vol. 9, no. 10, pp. 729–740, 2009.

[14] J. Phieler, R. Garcia-Martin, J. D. Lambris, and T. Chavakis, "The role of the complement system in metabolic organs and metabolic diseases," *Seminars in Immunology*, vol. 25, no. 1, pp. 47–53, 2013.

[15] G. L. Xu, J. Chen, F. Yang, G. Q. Li, L. X. Zheng, and Y. Z. Wu, "C5a/C5aR pathway is essential for the pathogenesis of murine viral fulminant hepatitis by way of potentiating Fgl2/fibroleukin expression," *Hepatology*, vol. 60, no. 1, pp. 114–124, 2014.

[16] E. S. Reis, H. Chen, G. Sfyroera et al., "C5a receptor-dependent cell activation by physiological concentrations of desarginated C5a: insights from a novel label-free cellular assay," *The Journal of Immunology*, vol. 189, no. 10, pp. 4797–4805, 2012.

[17] C. Gaboriaud, N. M. Thielens, L. A. Gregory, V. Rossi, J. C. Fontecilla-Camps, and G. J. Arlaud, "Structure and activation of the C1 complex of complement: unraveling the puzzle," *Trends in Immunology*, vol. 25, no. 7, pp. 368–373, 2004.

[18] J. S. Min, R. A. DeAngelis, E. S. Reis et al., "Systems analysis of the complement-induced priming phase of liver regeneration," *The Journal of Immunology*, vol. 197, no. 6, pp. 2500–2508, 2016.

[19] M. Song, Y. Sun, J. Tian et al., "Silencing retinoid X receptor alpha expression enhances early-stage hepatitis B virus infection in cell cultures," *Journal of Virology*, vol. 92, no. 8, 2018.

[20] R. Nakatake, M. Kaibori, Y. Nakamura et al., "Third-generation oncolytic herpes simplex virus inhibits the growth of liver tumors in mice," *Cancer Science*, vol. 109, no. 3, pp. 600–610, 2018.

[21] J. G. O'Grady, G. J. Alexander, K. M. Hayllar, and R. Williams, "Early indicators of prognosis in fulminant hepatic failure," *Gastroenterology*, vol. 97, no. 2, pp. 439–445, 1989.

[22] D. C. dos Santos, J. M. da Silva Gomes Martinho, L. F. Pacheco-Moreira et al., "Eosinophils involved in fulminant hepatic failure are associated with high interleukin-6 expression and absence of interleukin-5 in liver and peripheral blood," *Liver International*, vol. 29, no. 4, pp. 544–551, 2009.

[23] D. C. dos Santos, P. C. Neves, E. L. Azeredo et al., "Activated lymphocytes and high liver expression of IFN-γ are associated with fulminant hepatic failure in patients," *Liver International*, vol. 32, no. 1, pp. 147–157, 2012.

[24] I. Jiménez, P. Aracena, M. E. Letelier, P. Navarro, and H. Speisky, "Chronic exposure of HepG2 cells to excess copper results in depletion of glutathione and induction of metallothionein," *Toxicology In Vitro*, vol. 16, no. 2, pp. 167–175, 2002.

[25] M. R. Flórez, M. Costas-Rodríguez, C. Grootaert, J. Van Camp, and F. Vanhaecke, "Cu isotope fractionation response to oxidative stress in a hepatic cell line studied using multi-collector ICP-mass spectrometry," *Analytical and Bioanalytical Chemistry*, vol. 410, no. 9, pp. 2385–2394, 2018.

[26] K. Kowalczyk, A. Błauż, W. M. Ciszewski, A. Wieczorek, B. Rychlik, and D. Plażuk, "Colchicine metallocenyl bioconjugates showing high antiproliferative activities against cancer cell lines," *Dalton Transactions*, vol. 46, no. 48, pp. 17041–17052, 2017.

[27] V. S. De Paula, L. Diniz-Mendes, L. M. Villar et al., "Hepatitis A virus in environmental water samples from the Amazon Basin," *Water Research*, vol. 41, no. 6, pp. 1169–1176, 2007.

[28] S. D. Pas and H. G. Niesters, "Detection of HBV DNA using real time analysis," *Journal of Clinical Virology*, vol. 25, no. 1, pp. 93-94, 2002.

[29] E. Yurtcu, O. D. Iseri, and F. I. Sahin, "Effects of ascorbic acid and β-carotene on HepG2 human hepatocellular carcinoma cell line," *Molecular Biology Reports*, vol. 38, no. 7, pp. 4265–4272, 2011.

[30] R. C. Duhamel and D. A. Johnson, "Use of nonfat dry milk to block nonspecific nuclear and membrane staining by avidin conjugates," *The Journal of Histochemistry & Cytochemistry*, vol. 33, no. 7, pp. 711–714, 1985.

[31] C. G. Antoniades, P. A. Berry, J. A. Wendon, and D. Vergani, "The importance of immune dysfunction in determining outcome in acute liver failure," *Journal of Hepatology*, vol. 49, no. 5, pp. 845–861, 2008.

[32] X. Qin and B. Gao, "The complement system in liver diseases," *Cellular & Molecular Immunology*, vol. 3, no. 5, pp. 333–340, 2006.

[33] H. S. Shin, S. P. Kim, S. H. Han et al., "Prognostic indicators for acute liver failure development and mortality in patients with hepatitis a: consecutive case analysis," *Yonsei Medical Journal*, vol. 55, no. 4, pp. 953–959, 2014.

[34] H. Lin, Q. Zhang, X. Li, Y. Wu, Y. Liu, and Y. Hu, "Identification of key candidate genes and pathways in hepatitis B virus-associated acute liver failure by bioinformatical analysis," *Medicine*, vol. 97, no. 5, article e9687, 2018.

[35] M. L. Chang, C. J. Kuo, H. C. Huang, Y. Y. Chu, and C. T. Chiu, "Association between leptin and complement in hepatitis C patients with viral clearance: homeostasis of metabolism and immunity," *PLoS One*, vol. 11, no. 11, article e0166712, 2016.

[36] J. J. Zhang, Y. C. Fan, Z. H. Zhang et al., "Methylation of suppressor of cytokine signalling 1 gene promoter is associated with acute-on-chronic hepatitis B liver failure," *Journal of Viral Hepatitis*, vol. 22, no. 3, pp. 307–317, 2014.

[37] A. El-Shamy, A. D. Branch, T. D. Schiano, and P. D. Gorevic, "The complement system and C1q in chronic hepatitis C virus infection and mixed cryoglobulinemia," *Frontiers in Immunology*, vol. 9, p. 1001, 2018.

[38] M. J. Rutkowski, M. E. Sughrue, A. J. Kane, B. J. Ahn, S. Fang, and A. T. Parsa, "The complement cascade as a mediator of tissue growth and regeneration," *Inflammation Research*, vol. 59, no. 11, pp. 897–905, 2010.

[39] P. E. Marques, S. S. Amaral, D. A. Pires et al., "Chemokines and mitochondrial products activate neutrophils to amplify organ injury during mouse acute liver failure," *Hepatology*, vol. 56, no. 5, pp. 1971–1982, 2012.

[40] J. M. Stapp, V. Sjoelund, H. A. Lassiter, R. C. Feldhoff, and P. W. Feldhoff, "Recombinant rat IL-1beta and IL-6 synergistically enhance C3 mRNA levels and complement component C3 secretion by H-35 rat hepatoma cells," *Cytokine*, vol. 30, no. 2, pp. 78–85, 2005.

[41] M. Daveau, M. Benard, M. Scotte et al., "Expression of a functional C5a receptor in regenerating hepatocytes and its involvement in a proliferative signaling pathway in rat," *Journal of Immunology*, vol. 173, no. 5, pp. 3418–3424, 2004.

[42] M. D. Leise, J. J. Poterucha, and J. A. Talwalkar, "Drug-induced liver injury," *Mayo Clinic Proceedings*, vol. 89, no. 1, pp. 95–106, 2014.

[43] S. S. Rensen, Y. Slaats, A. Driessen et al., "Activation of the complement system in human nonalcoholic fatty liver disease," *Hepatology*, vol. 50, no. 6, pp. 1809–1817, 2009.

[44] F. T. Ozer, A. Barut, A. Inal, and A. Hacibektaşoğlu, "Complement C3 and C4 levels in serum from acute viral hepatitis," *Mikrobiyoloji Bülteni*, vol. 26, no. 4, pp. 314–319, 1992.

[45] B. N. Pham, J. F. Mosnier, F. Durand et al., "Immunostaining for membrane attack complex of complement is related to cell necrosis in fulminant and acute hepatitis," *Gastroenterology*, vol. 108, no. 2, pp. 495–504, 1995.

[46] A. K. Chauhan and T. L. Moore, "Presence of plasma complement regulatory proteins clusterin (Apo J) and vitronectin (S40) on circulating immune complexes (CIC)," *Clinical and Experimental Immunology*, vol. 145, no. 3, pp. 398–406, 2006.

[47] D. Wieland, M. Hofmann, and R. Thimme, "Overcoming CD8 + T-cell exhaustion in viral hepatitis: lessons from the mouse model and clinical perspectives," *Digestive Diseases*, vol. 35, no. 4, pp. 334–338, 2017.

[48] J. A. Cienfuegos, F. Rotellar, J. Baixauli, F. Martínez-Regueira, F. Pardo, and J. L. Hernández-Lizoáin, "Liver regeneration–the best kept secret. A model of tissue injury response," *Revista*

Española de Enfermedades Digestivas, vol. 106, no. 3, pp. 171–194, 2014.

[49] R. R. Buchner, T. E. Hugli, J. A. Ember, and E. L. Morgan, "Expression of functional receptors for human C5a anaphylatoxin (CD88) on the human hepatocellular carcinoma cell line HepG2. Stimulation of acute-phase protein-specific mRNA and protein synthesis by human C5a anaphylatoxin," *The Journal of Immunology*, vol. 155, no. 1, pp. 308–315, 1995.

[50] E. Güven, K. Duus, M. C. Lydolph, C. S. Jørgensen, I. Laursen, and G. Houen, "Non-specific binding in solid phase immunoassays for autoantibodies correlates with inflammation markers," *Journal of Immunological Methods*, vol. 403, no. 1-2, pp. 26–36, 2014.

[51] A. Samuelson, M. Glimåker, E. Skoog, J. Cello, and M. Forsgren, "Diagnosis of enteroviral meningitis with IgG-EIA using heat-treated virions and synthetic peptides as antigens," *Journal of Medical Virology*, vol. 40, no. 4, pp. 271–277, 1993.

[52] M. A. Moore, Z. W. Hakki, R. L. Gregory, L. E. Gfell, W. K. Kim-Park, and M. J. Kowolik, "Influence of heat inactivation of human serum on the opsonization of *Streptococcus mutans*," *Annals of the New York Academy of Sciences*, vol. 832, no. 1, pp. 383–393, 1997.

[53] R. D. Soltis, D. Hasz, M. J. Morris, and I. D. Wilson, "The effect of heat inactivation of serum on aggregation of immunoglobulins," *Immunology*, vol. 36, no. 1, pp. 37–45, 1979.

[54] S. M. Fouraschen, Q. Pan, P. E. de Ruiter et al., "Secreted factors of human liver-derived mesenchymal stem cells promote liver regeneration early after partial hepatectomy," *Stem Cells and Development*, vol. 21, no. 13, pp. 2410–2419, 2012.

[55] H. Bantel and K. Schulze-Osthoff, "Mechanisms of cell death in acute liver failure," *Frontiers in Physiology*, vol. 3, p. 79, 2012.

[56] M. Maes, M. Vinken, and H. Jaeschke, "Experimental models of hepatotoxicity related to acute liver failure," *Toxicology and Applied Pharmacology*, vol. 290, pp. 86–97, 2016.

[57] R. Saich, C. Selden, M. Rees, and H. Hodgson, "Characterization of pro-apoptotic effect of liver failure plasma on primary human hepatocytes and its modulation by molecular adsorbent recirculation system therapy," *Artificial Organs*, vol. 31, no. 9, pp. 732–742, 2007.

[58] W. B. Du, X. P. Pan, X. P. Yu et al., "Effects of plasma from patients with acute on chronic liver failure on function of cytochrome P450 in immortalized human hepatocytes," *Hepatobiliary & Pancreatic Diseases International*, vol. 9, no. 6, pp. 611–614, 2010.

[59] D. A. Peterson, L. G. Wolfe, E. P. Larkin, and F. W. Deinhardt, "Thermal treatment and infectivity of hepatitis A virus in human feces," *Journal of Medical Virology*, vol. 2, no. 3, pp. 201–206, 1978.

[60] H. Nishitsuji, K. Harada, S. Ujino et al., "Investigating the hepatitis B virus life cycle using engineered reporter hepatitis B viruses," *Cancer Science*, vol. 109, no. 1, pp. 241–249, 2018.

[61] P. Gripon, S. Rumin, S. Urban et al., "Infection of a human hepatoma cell line by hepatitis B virus," *Proceedings of the National Academy of Sciences of the United States of America*, vol. 99, no. 24, pp. 15655–15660, 2002.

[62] A. M. Gaspar, C. L. Vitral, C. F. Yoshida, and H. G. Schatzmayr, "Primary isolation of a Brazilian strain of hepatitis A virus (HAF-203) and growth in a primate cell line (FRhK-4)," *Brazilian Journal of Medical and Biological Research*, vol. 25, no. 7, pp. 697–705, 1992.

[63] R. C. Zangar, N. Bollinger, T. J. Weber, R. M. Tan, L. M. Markillie, and N. J. Karin, "Reactive oxygen species alter autocrine and paracrine signaling," *Free Radical Biology & Medicine*, vol. 51, no. 11, pp. 2041–2047, 2011.

[64] S. Sarwar, A. A. Khan, A. Alam et al., "Predictors of fatal outcome in fulminant hepatic failure," *Journal of the College of Physicians and Surgeons–Pakistan*, vol. 16, no. 2, pp. 112–116, 2006.

[65] M. McMillin, G. Frampton, S. Grant et al., "Bile acid-mediated sphingosine-1-phosphate receptor 2 signaling promotes neuroinflammation during hepatic encephalopathy in mice," *Frontiers in Cellular Neuroscience*, vol. 11, p. 191, 2017.

[66] G. S. Herbert, K. B. Prussing, A. L. Simpson et al., "Early trends in serum phosphate and creatinine levels are associated with mortality following major hepatectomy," *HPB*, vol. 17, no. 12, pp. 1058–1065, 2015.

Hindawi
Journal of Immunology Research
Volume 2018, Article ID 1206737, 8 pages
https://doi.org/10.1155/2018/1206737

Review Article

Natural Killer Cells in Liver Disease and Hepatocellular Carcinoma and the NK Cell-Based Immunotherapy

Pingyi Liu, Lingling Chen, and Haiyan Zhang

Laboratory of Department of Hematology, Yishui Central Hospital of Linyi, Linyi, China

Correspondence should be addressed to Pingyi Liu; 471271309@qq.com

Received 19 June 2018; Accepted 16 August 2018; Published 4 September 2018

Academic Editor: Patrice Petit

Nature killer (NK) cells play a critical role in host innate and adaptive immune defense against viral infections and tumors. NK cells are enriched in liver hematopoietic cells with unique NK repertories and functions to safeguard liver cells against hepatitis virus infection or malignancy transformation. However, accumulating evidences were found that the NK cells were modulated by liver diseases and liver cancers including hepatocellular carcinoma (HCC) and showed impaired functions failing to activate the elimination of the viral-infected cells or tumor cells and were further involved in the pathogenesis of liver injury and inflammation. The full characterization of circulation and intrahepatic NK cell phenotype and function in liver disease and liver cancer has not only provided new insight into the disease pathogenesis but has also discovered new targets for developing new NK cell-based therapeutic strategies. This review will discuss and summarize the NK cell phenotypic and functional changes in liver disease and HCC, and the NK cell-based immunotherapy approaches and progresses for cancers including HCC will also be reviewed.

1. Introduction

Liver is a vital organ in human; however, many people suffered from liver disease and liver cancers, such as hepatocellular carcinoma (HCC) which is one of the leading causes of cancer-related death worldwide [1]. The incidence of several major types of cancer, such as lung cancer, colon cancer, and prostate cancer, decreased in recent decade. In contrast, the incidence of HCC increased year by year [1]. In addition, the mortality rate of HCC is similar to the incidence rate which indicates that effective treatments for HCC are lacking in clinic [2, 3]. The major risk factors causing HCC include chronic viral infection, alcohol-related cirrhosis, and nonalcoholic steatohepatitis (NASH) [4]. Chronic hepatitis B virus (HBV) and hepatitis C virus (HCV) infections account for most of HCC cases worldwide [4, 5]; however, NASH will likely become a leading cause of HCC in the future, as the successful HBV vaccination and effective anti-HCV drugs will significantly reduce the number of chronic viral hepatitis patient in the near future [6–8].

In recent decades, accumulating evidences supported that the liver is also an immunological organ with predominant innate immunity [9–11]. The liver is enriched with innate immune cells including Kupffer cells, nature killer (NK) cells, NK T cells, and $\gamma\delta$ T cells. These cells are critical in host defense against invading pathogens, liver injury and repair, and tumor development [11]. NK cells have been originally described as innate immune cells that are involved in the first line of immune defense against viral infections and tumors. In human, NK cells are phenotypically defined as $CD3^{-}CD56^{+}$ large granular lymphocytes. Recently, a population of liver-resident NK cells was defined as $CD49a^{+}DX5^{-}$ NK cells in mice. These cells originated from T hepatic hematopoietic progenitors and showed memory-like properties [12, 13]. The counterpart of these liver-resident NK cells was also characterized in human [14, 15]. The functions of NK cells are strictly regulated by the balance of activating receptors and inhibitory receptors interacting with target cells. These receptors can bind to specific ligands; for example, the major histocompatibility complex class (MHC-1) is expressed on healthy hepatocytes, which interacts with inhibitory receptors on NK cells and prevents the activation of NK cells. NK cells can directly eradicate infected cells or tumor cells lacking of MHC-1

molecule expression [16]. Once MHC-1 is downregulated by viral infection or tumorigenesis on the hepatocytes, the NK cells will loss the inhibitory signal controlled by the interaction of the NK inhibitory receptor with the MHC-1 complex, and the NK cells will be activated to kill infected hepatocytes. In the liver, the percentage of NK cells in total lymphocytes is around 5 times higher than the percentage in peripheral blood (PB) or spleen; thus, the NK cells were considered to play a very important role in the prevention of HCC and therefore were considered a potential cell therapy resource for the treatment of HCC [17].

In this review, we will summarize the phenotypes and functions of NK cells in chronic viral hepatitis, alcoholic liver disease, NASH, and HCC, and the progresses in NK cell-based immunotherapy for cancers but not limited to HCC are also reviewed.

2. NK Cells in Chronic Viral Hepatitis

Chronic viral hepatitis including HBV and HCV is the leading cause for the development of liver cirrhosis and subsequent HCC. HBV and HCV are pathogen replicate and grow inside of hepatocytes which alter the surface molecule for the interaction with NK cells. NK cells are critical in the early immune response for the clearance of virus. In chronic HBV and HCV patients, the percentage of circulating PB NK cells was lower than that in healthy controls [18–21]. In addition, the production of proinflammatory cytokines such as interferon gamma (IFN-γ) and tumor necrosis factor-α (TNF-α) by NK cells was decreased in chronic HBV and HCV patients [18, 19, 22]. However, the impact of chronic viral infection on the cytolytic activity of NK cells was controversial. Several reports showed that NK cytolytic effector function was not changed [18, 20], while other researchers observed impaired NK cytolytic activity [23–25]. The differences between these studies were probably due to the lack of standardized protocol and reagents as well as the heterogeneity of patients. The phenotype of NK cells between HBV and HCV patients was different, and NK cells showed an increase in the activating receptor NKG2D expression and a decrease in inhibitory receptor expression phenotype in chronic HCV patients, while in chronic HBV patients, the percentage of activating NKG2C$^+$ NK cells increased and the inhibitory receptor expression was normal [18]. The reduced percentage and impaired function of NK cells in chronic viral hepatitis patients were believed to contribute to the disease progression and the transformation of HCC.

3. NK Cells in Alcoholic Liver Disease

Alcoholic liver disease is caused by alcohol abuse and also considered a major cause for cirrhosis and HCC, and around half of liver cirrhosis was related to alcohol [26]. NK cells were shown to play a critical role in resolving fibrosis by directly killing activated hepatic stellate cells (HSCs) and inducing HSC apoptosis by the production of IFN-γ [27]. However, chronic exposure to alcohol reduced the expression of NKG2D, tumor necrosis factor-related apoptosis-inducing ligand (TRAIL), and IFN-γ on NK cells, which subsequently abrogated the antifibrotic effects of NK cells [28, 29]. In addition, the suppression of NK cell activation by chronic alcohol consumption was supported by several studies [30–32]. The elevation of NKG2D, granzyme B, perforin, Fas ligand (FasL), TRAIL, and IFN-γ expression in NK cells by poly I:C stimulation was blocked in ethanol diet-fed mice [30]. More evidence and further study are needed to confirm whether the impairment of NK cell function by chronic alcohol consumption contributes to the development of alcohol-related HCC.

4. NK Cells in NASH

Although the incidence of chronic viral hepatitis decreases benefiting from the vaccinations and the advanced clinical therapies, the incidence of HCC gradually increases in developed countries. The nonalcoholic fatty liver disease (NAFLD) and NASH become two of the leading causes of HCC. However, there were only very limited studies about the role of NK cells in the pathogenesis of NAFLD and NASH. Less circulating PB NK cells and cytotoxic ability were found in patients with obesity than in healthy controls [33]. In contrast, another report showed that NK cell-derived mediators such as NKG2D and TRAIL mRNA levels were increased in NASH patients [34]. In a recent study, DX5$^+$ NKp46$^+$ NK cells were found to be increased in a NASH mouse model. Moreover, these NKp46$^+$ NK cells regulate M1/M2 polarization of liver macrophages and inhibit the development of liver fibrosis in the NASH model [35]. So, how the dysregulation of NK cells in NASH contributes to HCC development is still largely unknown.

5. NK Cells and HCC

As we discussed above, NK cells are enriched in healthy liver, and they play critical roles in the surveillance of HCC. Similar to chronic viral hepatitis, the number of peripheral NK cells, especially CD56^{dim}CD16$^+$ NK cells, dramatically reduced in HCC patients [36, 37]. The NK cell number in the liver tumor area was also less than the NK cell number in the nontumor area and showed impaired cytotoxic ability as well as IFN-γ production [36, 38]. Moreover, the number of infiltrating and CD56$^+$ NK cells positively correlated with HCC cancer cell apoptosis and patient survival [39, 40]. Several mechanisms had been proposed to explain the defect of the NK cell number and function in HCC; for example, infiltrated monocytes/macrophages in the peritumoral area induced rapid activation of NK cells. These activated NK cells then became exhausted and eventually died which was mediated by the CD48/2B4 interactions [38]. Myeloid-derived suppressor cells (MDSCs) may also interact with NK cells in HCC patients. MDSCs from HCC patients directly inhibited cytotoxicity and cytokine production of NK cells in a contact-dependent manner [41]. In addition, fibroblasts derived from HCC triggered NK cell dysfunction which was mediated by indoleamine 2,3-dioxygenase (IDO) and prostaglandin E2 (PGE2) produced by the HCC cells, and these two natural immunosuppressants downregulate activating NK

receptors [42]. Taken together, multiple mechanisms were involved in the NK cell malfunction, resulting in the development of HCC, and the lack of the NK cell number and the defects in function of NK cells facilitated the escape of tumor cells from immune surveillance.

6. NK Cell-Based Immunotherapy for Cancer

As we discussed above, NK cells, as a type of innate immune cell, are rapidly mobilized and serve as the first-line immune responders against viral-infected cells and tumor cells; however, the NK cells usually become inhibited in many cancers including HCC. Studies have been performed to explore NK cell-based immunotherapy for cancers. These approaches include either endogenous stimulation of the NK cells in patients, such as administration of cytokines to activate NK cells in cancer patients and treatment of the patients with antibodies that target the NK inhibitor receptor or checkpoint protein to activate NK cells or agonist of NK cell activating receptors, or adoptive NK cell transfer to the cancer patients. The therapeutic effects and progresses of these approaches will be reviewed in this article.

6.1. Cytokine Treatment to Increase the Cytotoxicity of NK Cells. Interleukin-2 (IL-2) was the first FDA-approved cytokine to boost cytotoxicity of NK cells [43]. However, IL-2 can act not only on NK cells but also on T cells including regulatory T cells (Tregs) which may inhibit NK cell function. Depletion of Tregs improved NK cell proliferation and outcome in acute myeloid leukemia (AML) therapy [44]. Several strategies were used to improve the efficiency of IL-2, including a modified IL-2 called "super-2" which can activate NK cells and cytotoxic CD8 T cells but not Tregs [45]. The fusion protein of IL-2 and NKG2D ligand only activated on NKG2D-expressing NK cells but on T cells [46].

Interleukin-15 (IL-15) is another cytokine to boost NK activity and increase cytotoxicity of both NK cells and $CD8^+$ T cells without activating Tregs [47]. IL-15 treatment significantly increased the number of NK cells in both mouse model and human patients [48, 49]. Several IL-15 fusion proteins or modified IL-15 have been developed to increase their stability and efficiency [50–52]. The clinical trials for the antitumor effect of IL-15, modified IL-15, and IL-15 fusion proteins are ongoing.

6.2. Antibodies to Modulate the NK Cytotoxic Function. Killer cell immunoglobulin-like receptors (KIRs) are expressed on NK cells and a minority of T cells [53]. KIRs bind with MHC-1 molecules to control the cytotoxic function of these immune cells. NK cells express both inhibitory KIR and activating KIR. The balance between the NK KIR inhibitory signal and KIR activating signal defines the NK effector function. Tumor cell-derived MHC-1 or class I-like molecules usually bind to KIR to inhibit NK cell activation [54]. Antibodies against inhibitory KIR showed promising effects on promoting NK cell cytotoxicity in mouse models [55]. However, the clinical trial did not show favorable effects of the KIR2D (an activating KIR receptor) antibody IPH2101 in multiple myeloma (MM) patients [56]. The lack of efficiency of the KIR2D antibody IPH2101 was probably due to the depletion of KIR2D-expressing NK cells by the antibody. The combination of lenalidomide, an immunomodulatory drug that can activate NK cells, with IPH2101 showed promising beneficial effects on MM patients in a phase I clinical trial [57].

Another NK receptor target to improve the cytotoxic function of NK cells is NKG2A. NKG2A is expressed in NK and $CD8^+$ T cells as an inhibitor receptor. The heterodimer of NKG2A and CD94 can bind to HLA-E which is usually upregulated in tumor cells [54]; therefore, the tumor cells escaped the NK by this inhibitory signal. An antibody targeting NKG2A showed increased NK cell cytotoxicity and reduced disease progression in human primary leukemia or Epstein-Barr virus cell line-infused mouse model [58]. The clinical trial is ongoing to evaluate its safety and efficiency for cancer therapy.

Programmed cell death protein 1 (PD-1) is a well-known immune checkpoint of T cells. It is a cell surface receptor; the integration with its ligand on target cells suppresses the T cell activation and plays an important role in downregulating the immune system. Recently, the PD-1 receptor is found to be highly expressed on PB and tumor-infiltrating NK cells from patients with multiple myeloma (MM) and with digestive cancers including esophageal, colorectal, biliary, gastric, and liver cancers [59]. In the digestive cancer study, the investigators showed that PD-1 upregulation on NK cells correlated with poorer disease outcome in esophageal and liver cancers. In both the MM study and the digestive cancer study, PD-1-blocking antibody could increase the NK cytotoxic function in vitro targeting the tumor cell line or primary cancer cells. Moreover, the PD-1 antibodies inhibited the tumor growth in a xenograft mouse model [59]. These findings suggested that PD-1 blockade might be an efficient strategy in NK cell-based tumor immunotherapy.

In a recent study, Zhang et al. have found that the checkpoint inhibitory receptor TIGIT ("T cell immunoglobulin and immunoreceptor tyrosine-based inhibitory motif domain") was highly expressed on the exhausted tumor-(colorectal cancer) associated infiltrating NK cells. Monoclonal antibody-mediated blockade alone which targets TIGIT or in combination with the antibody against the PD-1 ligand PD-L1 increased the antitumor activity of both NK cells and T cells in preclinical mouse models and efficiently delays tumor growth [60]. Therapeutic strategies combining multiple blocking antibodies to treat cancer patients with NK cell exhaustion may improve the therapeutic efficacy, although the side effect of the antibody treatment needs to be carefully evaluated.

6.3. Agonist of NK Cell Activating Receptors. NK cells express a variety of activating receptors that play critical roles in regulating NK cell function. Major activating receptors on NK cells were well studied such as NKG2D, NKp30, NKp44, NKp46, and NKp80 [61]. Induction of NK cell activation to release cytokines or direct kill target cells requires combinatorial activating receptor synergy [62]. Activating receptor downregulation is observed in cancer patients and was correlated with poor disease outcomes [63–66]. It is believed that

the tumor cells express a high soluble amount of activation receptor ligand that induced the downregulation of activation receptors on NK cells in the patients [66–68]. Modulating NK cell activating receptor expression by neutralizing their soluble ligand secreted by tumor cells in patients is a potential clinical therapeutic strategy.

6.4. Adoptive Transfer of NK Cells. NK cell adoptive transfer therapy requires the NK ex vivo expansion, in vivo long persistence, maximal in vivo activity, and NK cell killing specificity. The source of NK cells for adoptive transfer therapy can be autologous or allogeneic PB NK cells, stem cell-derived NK cells, and NK cell lines such as NK-92 and KHYG-1. Fresh or expanded NK cells derived from patients (autologous) failed to show improved clinical outcome in several types of cancers [69, 70]. The reason was that these transferred NK cells remained in circulation rather than in tumor tissue [69]. In contrast, NK cells derived from a healthy donor (allogeneic) showed a positive response in AML patients [71], and the following studies also showed encouraging results by using haploidentical NK cells for both elderly and pediatric AML patients [72–74]. The clinical efficacy of the allogeneic NK cell adoptive immunotherapy to treat solid tumors has also been evaluated by several groups [75–77]. Lin et al. had reported that percutaneous cryoablation combined with allogeneic NK adoptive transfer significantly increased the median progression-free survival of advanced HCC patients [75]. And multiple allogeneic NK cell infusion was associated with better prognosis in advanced cancers, including advanced HCC [75] and stage III pancreatic cancer [76]. Allogeneic NK cell immunotherapy for advanced non-small-cell lung cancer also showed a significant benefit in clinic [77]. The successful allogeneic NK cell adoptive transfer therapy may depend on the protocol for isolation and expansion and the purity of NK cells [78–80].

To increase the killing specificity and efficiency of NK cell-based immunotherapy, several genetic modification approaches have been developed. The genetic modification for NK cells was not as easy as that for other immune cells such as T cells due to the resistance to retroviral infection. Several strategies were explored to improve the efficiency for transfection in NK cells [81, 82]. The introduction of CD16a, IL-15, and IL-2 in NK cells may increase the proliferation, activation, and cytotoxicity of NK cells [83–85]. Recently, the successful application of the chimeric antigen receptor (CAR) in T cells was adopted in NK cells to increase the specificity and efficiency of NK cell immunotherapy. Compared with CAR-T cells, CAR-NK cells were short lived, which reduced the risk for autoimmunity and tumor transformation. The cytokines released from NK cells such as IFN-γ and granulocyte-macrophage colony-stimulating factor (GM-CSF) were safer than the cytokine storm in CAR-T cell therapy [86]. As we mentioned above, due to the difficulties in expansion and transduction of primary NK cells, the only FDA-approved cell line for use in clinical trials, NK-92, was considered an ideal NK cell source for CAR-NK cell therapy [87–89]. ErbB2/HER2-specific CAR-NK-92 cells showed very encouraging efficiency in target therapy of glioblastoma in an animal model [90]. CD19-specific CAR-NK-92 cells were sufficient to lyse $CD19^+$ B-precursor leukemia cell lines as well as lymphoblasts from leukemia patients [91, 92]. In a preclinical study, CD5 CAR-NK-92 cells shows consistent, specific, and potent antitumor activity against T cell leukemia and lymphoma cell lines and primary tumor cells [93]. For the HCC, the first report was published very recently; glypican-3- (GPC3-) specific CAR-NK-92 cells showed potent antitumor activities in multiple HCC xenografts with both high and low GPC3 expressions. As expected, the GPC3 CAR-NK-92 cells did not show cytotoxicity to GFP3-negative HCC cells [94]. Currently, 9 clinical trials are ongoing to evaluate the safety and efficiency of CAR-NK cells, of which 7 trials are used for leukemia or lymphoma and 2 trials are for solid tumor. In the current preclinical study, some other NK sources are under investigation [95], such as the NK cells derived from hematopoietic progenitor cells [96] or from cord blood, and expanded in vitro with the aAPC K562-based system [97].

7. Summary

NK cells have been discovered for more than 40 years [98]; however, how to manipulate NK cells for the therapy of diseases remains elusive. The impairment of the function of NK cells was observed in many types of liver diseases including chronic viral hepatitis, alcoholic and nonalcoholic steatohepatitis, and HCC. Several approaches have been developed to boost the activity of NK cells for therapeutic purpose, but most of these studies are still in a preclinical stage. With the success of ex vivo genetic modification of T cells in the therapy of leukemia, it is promising that the similar strategy, as wells as other approaches to regulate the balance between activating and inhibitory receptors in NK cells, might also lead to the successful treatment for various liver diseases including HCC.

Disclosure

Pingyi Liu and Lingling Chen are the co-first authors.

Conflicts of Interest

The authors declare that they have no conflicts of interest.

References

[1] R. L. Siegel, K. D. Miller, and A. Jemal, "Cancer statistics, 2017," *CA: A Cancer Journal for Clinicians*, vol. 67, no. 1, pp. 7–30, 2017.

[2] J. Bruix, G. J. Gores, and V. Mazzaferro, "Hepatocellular carcinoma: clinical frontiers and perspectives," *Gut*, vol. 63, no. 5, pp. 844–855, 2014.

[3] A. Forner, J. M. Llovet, and J. Bruix, "Hepatocellular carcinoma," *The Lancet*, vol. 379, no. 9822, pp. 1245–1255, 2012.

[4] M. C. Wallace, D. Preen, G. P. Jeffrey, and L. A. Adams, "The evolving epidemiology of hepatocellular carcinoma: a global perspective," *Expert Review of Gastroenterology & Hepatology*, vol. 9, no. 6, pp. 765–779, 2015.

[5] H. B. El-Serag, "Epidemiology of viral hepatitis and hepatocellular carcinoma," *Gastroenterology*, vol. 142, no. 6, pp. 1264–1273.e1, 2012.

[6] S. Locarnini, A. Hatzakis, D. S. Chen, and A. Lok, "Strategies to control hepatitis B: public policy, epidemiology, vaccine and drugs," *Journal of Hepatology*, vol. 62, no. 1, pp. S76–S86, 2015.

[7] N. Alkhouri, E. Lawitz, and F. Poordad, "Novel treatments for chronic hepatitis C: closing the remaining gaps," *Current Opinion in Pharmacology*, vol. 37, pp. 107–111, 2017.

[8] C. Margini and J. F. Dufour, "The story of HCC in NAFLD: from epidemiology, across pathogenesis, to prevention and treatment," *Liver International*, vol. 36, no. 3, pp. 317–324, 2016.

[9] V. Racanelli and B. Rehermann, "The liver as an immunological organ," *Hepatology*, vol. 43, Supplement 1, pp. S54–S62, 2006.

[10] C. N. Jenne and P. Kubes, "Immune surveillance by the liver," *Nature Immunology*, vol. 14, no. 10, pp. 996–1006, 2013.

[11] B. Gao, W. I. Jeong, and Z. Tian, "Liver: an organ with predominant innate immunity," *Hepatology*, vol. 47, no. 2, pp. 729–736, 2008.

[12] H. Peng, X. Jiang, Y. Chen et al., "Liver-resident NK cells confer adaptive immunity in skin-contact inflammation," *Journal of Clinical Investigation*, vol. 123, no. 4, pp. 1444–1456, 2013.

[13] L. H. Zhang, J. H. Shin, M. D. Haggadone, and J. B. Sunwoo, "The aryl hydrocarbon receptor is required for the maintenance of liver-resident natural killer cells," *The Journal of Experimental Medicine*, vol. 213, no. 11, pp. 2249–2257, 2016.

[14] L. Tang, H. Peng, J. Zhou et al., "Differential phenotypic and functional properties of liver-resident NK cells and mucosal ILC1s," *Journal of Autoimmunity*, vol. 67, pp. 29–35, 2016.

[15] K. Hudspeth, M. Donadon, M. Cimino et al., "Human liver-resident $CD56^{bright}/CD16^{neg}$ NK cells are retained within hepatic sinusoids via the engagement of CCR5 and CXCR6 pathways," *Journal of Autoimmunity*, vol. 66, pp. 40–50, 2016.

[16] M. G. Morvan and L. L. Lanier, "NK cells and cancer: you can teach innate cells new tricks," *Nature Reviews Cancer*, vol. 16, no. 1, pp. 7–19, 2016.

[17] H. Sun, C. Sun, Z. Tian, and W. Xiao, "NK cells in immunotolerant organs," *Cellular & Molecular Immunology*, vol. 10, no. 3, pp. 202–212, 2013.

[18] B. Oliviero, S. Varchetta, E. Paudice et al., "Natural killer cell functional dichotomy in chronic hepatitis B and chronic hepatitis C virus infections," *Gastroenterology*, vol. 137, no. 3, pp. 1151–1160.e7, 2009.

[19] O. Dessouki, Y. Kamiya, H. Nagahama et al., "Chronic hepatitis C viral infection reduces NK cell frequency and suppresses cytokine secretion: reversion by anti-viral treatment," *Biochemical and Biophysical Research Communications*, vol. 393, no. 2, pp. 331–337, 2010.

[20] C. Morishima, D. M. Paschal, C. C. Wang et al., "Decreased NK cell frequency in chronic hepatitis C does not affect *ex vivo* cytolytic killing," *Hepatology*, vol. 43, no. 3, pp. 573–580, 2006.

[21] P. Bonorino, M. Ramzan, X. Camous et al., "Fine characterization of intrahepatic NK cells expressing natural killer receptors in chronic hepatitis B and C," *Journal of Hepatology*, vol. 51, no. 3, pp. 458–467, 2009.

[22] G. Ahlenstiel, R. H. Titerence, C. Koh et al., "Natural killer cells are polarized toward cytotoxicity in chronic hepatitis C in an interferon-alfa–dependent manner," *Gastroenterology*, vol. 138, no. 1, pp. 325–335.e2, 2010.

[23] J. Corado, F. Toro, H. Rivera, N. E. Bianco, L. Deibis, and J. B. De Sanctis, "Impairment of natural killer (NK) cytotoxic activity in hepatitis C virus (HCV) infection," *Clinical and Experimental Immunology*, vol. 109, no. 3, pp. 451–457, 1997.

[24] G. Pár, D. Rukavina, E. R. Podack et al., "Decrease in CD3-negative-$CD8dim^{+}$ and Vδ2/Vγ9 TcR+ peripheral blood lymphocyte counts, low perforin expression and the impairment of natural killer cell activity is associated with chronic hepatitis C virus infection," *Journal of Hepatology*, vol. 37, no. 4, pp. 514–522, 2002.

[25] J. Nattermann, G. Feldmann, G. Ahlenstiel, B. Langhans, T. Sauerbruch, and U. Spengler, "Surface expression and cytolytic function of natural killer cell receptors is altered in chronic hepatitis C," *Gut*, vol. 55, no. 6, pp. 869–877, 2006.

[26] B. Gao and R. Bataller, "Alcoholic liver disease: pathogenesis and new therapeutic targets," *Gastroenterology*, vol. 141, no. 5, pp. 1572–1585, 2011.

[27] S. Radaeva, R. Sun, B. Jaruga, V. T. Nguyen, Z. Tian, and B. Gao, "Natural killer cells ameliorate liver fibrosis by killing activated stellate cells in NKG2D-dependent and tumor necrosis factor–related apoptosis-inducing ligand–dependent manners," *Gastroenterology*, vol. 130, no. 2, pp. 435–452, 2006.

[28] W. I. Jeong, O. Park, and B. Gao, "Abrogation of the antifibrotic effects of natural killer cells/interferon-γ contributes to alcohol acceleration of liver fibrosis," *Gastroenterology*, vol. 134, no. 1, pp. 248–258, 2008.

[29] H. S. Yi, Y. S. Lee, J. S. Byun et al., "Alcohol dehydrogenase III exacerbates liver fibrosis by enhancing stellate cell activation and suppressing natural killer cells in mice," *Hepatology*, vol. 60, no. 3, pp. 1044–1053, 2014.

[30] H. N. Pan, R. Sun, B. Jaruga, F. Hong, W. H. Kim, and B. Gao, "Chronic ethanol consumption inhibits hepatic natural killer cell activity and accelerates murine cytomegalovirus-induced hepatitis," *Alcoholism: Clinical and Experimental Research*, vol. 30, no. 9, pp. 1615–1623, 2006.

[31] S. Støy, A. Dige, T. D. Sandahl et al., "Cytotoxic T lymphocytes and natural killer cells display impaired cytotoxic functions and reduced activation in patients with alcoholic hepatitis," *American Journal of Physiology-Gastrointestinal and Liver Physiology*, vol. 308, no. 4, pp. G269–G276, 2015.

[32] K. Cui, G. Yan, X. Zheng et al., "Suppression of natural killer cell activity by regulatory NKT10 cells aggravates alcoholic hepatosteatosis," *Frontiers in Immunology*, vol. 8, article 1414, 2017.

[33] D. O'Shea, T. J. Cawood, C. O'Farrelly, and L. Lynch, "Natural killer cells in obesity: impaired function and increased susceptibility to the effects of cigarette smoke," *PLoS One*, vol. 5, no. 1, article e8660, 2010.

[34] A. Kahraman, M. Schlattjan, P. Kocabayoglu et al., "Major histocompatibility complex class I–related chains A and B (MIC A/B): a novel role in nonalcoholic steatohepatitis," *Hepatology*, vol. 51, no. 1, pp. 92–102, 2010.

[35] A. C. Tosello-Trampont, P. Krueger, S. Narayanan, S. G. Landes, N. Leitinger, and Y. S. Hahn, "$NKp46^{+}$ natural killer cells attenuate metabolism-induced hepatic fibrosis by regulating macrophage activation in mice," *Hepatology*, vol. 63, no. 3, pp. 799–812, 2016.

[36] L. Cai, Z. Zhang, L. Zhou et al., "Functional impairment in circulating and intrahepatic NK cells and relative mechanism in hepatocellular carcinoma patients," *Clinical Immunology*, vol. 129, no. 3, pp. 428–437, 2008.

[37] A. Fathy, M. M. Eldin, L. Metwally, M. Eida, and M. Abdel-Rehim, "Diminished absolute counts of CD56dim and CD56bright natural killer cells in peripheral blood from Egyptian patients with hepatocellular carcinoma," *The Egyptian Journal of Immunology*, vol. 16, no. 2, pp. 17–25, 2009.

[38] Y. Wu, D. M. Kuang, W. D. Pan et al., "Monocyte/macrophage-elicited natural killer cell dysfunction in hepatocellular carcinoma is mediated by CD48/2B4 interactions," *Hepatology*, vol. 57, no. 3, pp. 1107–1116, 2013.

[39] V. Chew, J. Chen, D. Lee et al., "Chemokine-driven lymphocyte infiltration: an early intratumoural event determining long-term survival in resectable hepatocellular carcinoma," *Gut*, vol. 61, no. 3, pp. 427–438, 2012.

[40] V. Chew, C. Tow, M. Teo et al., "Inflammatory tumour microenvironment is associated with superior survival in hepatocellular carcinoma patients," *Journal of Hepatology*, vol. 52, no. 3, pp. 370–379, 2010.

[41] B. Hoechst, T. Voigtlaender, L. Ormandy et al., "Myeloid derived suppressor cells inhibit natural killer cells in patients with hepatocellular carcinoma via the NKp30 receptor," *Hepatology*, vol. 50, no. 3, pp. 799–807, 2009.

[42] T. Li, Y. Yang, X. Hua et al., "Hepatocellular carcinoma-associated fibroblasts trigger NK cell dysfunction via PGE2 and IDO," *Cancer Letters*, vol. 318, no. 2, pp. 154–161, 2012.

[43] L. J. Burns, D. J. Weisdorf, T. E. DeFor et al., "IL-2-based immunotherapy after autologous transplantation for lymphoma and breast cancer induces immune activation and cytokine release: a phase I/II trial," *Bone Marrow Transplantation*, vol. 32, no. 2, pp. 177–186, 2003.

[44] V. Bachanova, S. Cooley, T. E. Defor et al., "Clearance of acute myeloid leukemia by haploidentical natural killer cells is improved using IL-2 diphtheria toxin fusion protein," *Blood*, vol. 123, no. 25, pp. 3855–3863, 2014.

[45] A. M. Levin, D. L. Bates, A. M. Ring et al., "Exploiting a natural conformational switch to engineer an interleukin-2 'superkine'," *Nature*, vol. 484, no. 7395, pp. 529–533, 2012.

[46] R. Ghasemi, E. Lazear, X. Wang et al., "Selective targeting of IL-2 to NKG2D bearing cells for improved immunotherapy," *Nature Communications*, vol. 7, article 12878, 2016.

[47] A. H. Pillet, J. Thèze, and T. Rose, "Interleukin (IL)-2 and IL-15 have different effects on human natural killer lymphocytes," *Human Immunology*, vol. 72, no. 11, pp. 1013–1017, 2011.

[48] K. C. Conlon, E. Lugli, H. C. Welles et al., "Redistribution, hyperproliferation, activation of natural killer cells and CD8 T cells, and cytokine production during first-in-human clinical trial of recombinant human interleukin-15 in patients with cancer," *Journal of Clinical Oncology*, vol. 33, no. 1, pp. 74–82, 2015.

[49] M. A. Cooper, J. E. Bush, T. A. Fehniger et al., "In vivo evidence for a dependence on interleukin 15 for survival of natural killer cells," *Blood*, vol. 100, no. 10, pp. 3633–3638, 2002.

[50] M. Thaysen-Andersen, E. Chertova, C. Bergamaschi et al., "Recombinant human heterodimeric IL-15 complex displays extensive and reproducible *N*- and *O*-linked glycosylation," *Glycoconjugate Journal*, vol. 33, no. 3, pp. 417–433, 2016.

[51] Y. Chen, B. Chen, T. Yang et al., "Human fused NKG2D–IL-15 protein controls xenografted human gastric cancer through the recruitment and activation of NK cells," *Cellular & Molecular Immunology*, vol. 14, no. 3, pp. 293–307, 2017.

[52] M. Rosario, B. Liu, L. Kong et al., "The IL-15-based ALT-803 complex enhances FcγRIIIa-triggered NK cell responses and *in vivo* clearance of B cell lymphomas," *Clinical Cancer Research*, vol. 22, no. 3, pp. 596–608, 2016.

[53] E. Alari-Pahissa, C. Grandclement, B. Jeevan-Raj, and W. Held, "Inhibitory receptor-mediated regulation of natural killer cells," *Critical Reviews in Immunology*, vol. 34, no. 6, pp. 455–465, 2014.

[54] L. Martinet and M. J. Smyth, "Balancing natural killer cell activation through paired receptors," *Nature Reviews Immunology*, vol. 15, no. 4, pp. 243–254, 2015.

[55] F. Romagne, P. Andre, P. Spee et al., "Preclinical characterization of 1-7F9, a novel human anti-KIR receptor therapeutic antibody that augments natural killer-mediated killing of tumor cells," *Blood*, vol. 114, no. 13, pp. 2667–2677, 2009.

[56] N. Korde, M. Carlsten, M. J. Lee et al., "A phase II trial of pan-KIR2D blockade with IPH2101 in smoldering multiple myeloma," *Haematologica*, vol. 99, no. 6, pp. e81–e83, 2014.

[57] D. M. Benson Jr, A. D. Cohen, S. Jagannath et al., "A phase I trial of the anti-KIR antibody IPH2101 and lenalidomide in patients with relapsed/refractory multiple myeloma," *Clinical Cancer Research*, vol. 21, no. 18, pp. 4055–4061, 2015.

[58] L. Ruggeri, E. Urbani, P. Andre et al., "Effects of anti-NKG2A antibody administration on leukemia and normal hematopoietic cells," *Haematologica*, vol. 101, no. 5, pp. 626–633, 2016.

[59] Y. Liu, Y. Cheng, Y. Xu et al., "Increased expression of programmed cell death protein 1 on NK cells inhibits NK-cell-mediated anti-tumor function and indicates poor prognosis in digestive cancers," *Oncogene*, vol. 36, no. 44, pp. 6143–6153, 2017.

[60] Q. Zhang, J. Bi, X. Zheng et al., "Blockade of the checkpoint receptor TIGIT prevents NK cell exhaustion and elicits potent anti-tumor immunity," *Nature Immunology*, vol. 19, no. 7, pp. 723–732, 2018.

[61] R. W. Johnstone, A. J. Frew, and M. J. Smyth, "The TRAIL apoptotic pathway in cancer onset, progression and therapy," *Nature Reviews Cancer*, vol. 8, no. 10, pp. 782–798, 2008.

[62] E. O. Long, H. Sik Kim, D. Liu, M. E. Peterson, and S. Rajagopalan, "Controlling natural killer cell responses: integration of signals for activation and inhibition," *Annual Review of Immunology*, vol. 31, no. 1, pp. 227–258, 2013.

[63] T. Garcia-Iglesias, A. del Toro-Arreola, B. Albarran-Somoza et al., "Low NKp30, NKp46 and NKG2D expression and reduced cytotoxic activity on NK cells in cervical cancer and precursor lesions," *BMC Cancer*, vol. 9, no. 1, p. 186, 2009.

[64] C. Kellner, T. Maurer, D. Hallack et al., "Mimicking an induced self phenotype by coating lymphomas with the NKp30 ligand B7-H6 promotes NK cell cytotoxicity," *The Journal of Immunology*, vol. 189, no. 10, pp. 5037–5046, 2012.

[65] N. F. Delahaye, S. Rusakiewicz, I. Martins et al., "Alternatively spliced NKp30 isoforms affect the prognosis of gastrointestinal stromal tumors," *Nature Medicine*, vol. 17, no. 6, pp. 700–707, 2011.

[66] M. Semeraro, S. Rusakiewicz, V. Minard-Colin et al., "Clinical impact of the NKp30/B7-H6 axis in high-risk neuroblastoma patients," *Science Translational Medicine*, vol. 7, no. 283, article 283ra55, 2015.

[67] V. Groh, J. Wu, C. Yee, and T. Spies, "Tumour-derived soluble MIC ligands impair expression of NKG2D and T-cell activation," *Nature*, vol. 419, no. 6908, pp. 734–738, 2002.

[68] B. K. Kaiser, D. Yim, I. T. Chow et al., "Disulphide-isomerase-enabled shedding of tumour-associated NKG2D ligands," *Nature*, vol. 447, no. 7143, pp. 482–486, 2007.

[69] M. R. Parkhurst, J. P. Riley, M. E. Dudley, and S. A. Rosenberg, "Adoptive transfer of autologous natural killer cells leads to high levels of circulating natural killer cells but does not mediate tumor regression," *Clinical Cancer Research*, vol. 17, no. 19, pp. 6287–6297, 2011.

[70] N. Sakamoto, T. Ishikawa, S. Kokura et al., "Phase I clinical trial of autologous NK cell therapy using novel expansion method in patients with advanced digestive cancer," *Journal of Translational Medicine*, vol. 13, no. 1, p. 277, 2015.

[71] L. Ruggeri, M. Capanni, E. Urbani et al., "Effectiveness of donor natural killer cell alloreactivity in mismatched hematopoietic transplants," *Science*, vol. 295, no. 5562, pp. 2097–2100, 2002.

[72] A. Curti, L. Ruggeri, A. D'Addio et al., "Successful transfer of alloreactive haploidentical KIR ligand-mismatched natural killer cells after infusion in elderly high risk acute myeloid leukemia patients," *Blood*, vol. 118, no. 12, pp. 3273–3279, 2011.

[73] J. S. Miller, Y. Soignier, A. Panoskaltsis-Mortari et al., "Successful adoptive transfer and in vivo expansion of human haploidentical NK cells in patients with cancer," *Blood*, vol. 105, no. 8, pp. 3051–3057, 2005.

[74] J. E. Rubnitz, H. Inaba, R. C. Ribeiro et al., "NKAML: a pilot study to determine the safety and feasibility of haploidentical natural killer cell transplantation in childhood acute myeloid leukemia," *Journal of Clinical Oncology*, vol. 28, no. 6, pp. 955–959, 2010.

[75] M. Lin, S. Liang, X. Wang et al., "Cryoablation combined with allogenic natural killer cell immunotherapy improves the curative effect in patients with advanced hepatocellular cancer," *Oncotarget*, vol. 8, no. 47, pp. 81967–81977, 2017.

[76] M. Lin, M. Alnaggar, S. Liang et al., "An important discovery on combination of irreversible electroporation and allogeneic natural killer cell immunotherapy for unresectable pancreatic cancer," *Oncotarget*, vol. 8, no. 60, pp. 101795–101807, 2017.

[77] M. Lin, S. Z. Liang, X. H. Wang et al., "Clinical efficacy of percutaneous cryoablation combined with allogenic NK cell immunotherapy for advanced non-small cell lung cancer," *Immunologic Research*, vol. 65, no. 4, pp. 880–887, 2017.

[78] A. Bishara, D. de Santis, C. C. Witt et al., "The beneficial role of inhibitory *KIR* genes of HLA class I NK epitopes in haploidentically mismatched stem cell allografts may be masked by residual donor-alloreactive T cells causing GVHD," *Tissue Antigens*, vol. 63, no. 3, pp. 204–211, 2004.

[79] S. M. Davies, L. Ruggieri, T. DeFor et al., "Evaluation of KIR ligand incompatibility in mismatched unrelated donor hematopoietic transplants. Killer immunoglobulin-like receptor," *Blood*, vol. 100, no. 10, pp. 3825–3827, 2002.

[80] D. A. Knorr, V. Bachanova, M. R. Verneris, and J. S. Miller, "Clinical utility of natural killer cells in cancer therapy and transplantation," *Seminars in Immunology*, vol. 26, no. 2, pp. 161–172, 2014.

[81] T. Sutlu, S. Nystrom, M. Gilljam, B. Stellan, S. E. Applequist, and E. Alici, "Inhibition of intracellular antiviral defense mechanisms augments lentiviral transduction of human natural killer cells: implications for gene therapy," *Human Gene Therapy*, vol. 23, no. 10, pp. 1090–1100, 2012.

[82] V. F. van Tendeloo, P. Ponsaerts, F. Lardon et al., "Highly efficient gene delivery by mRNA electroporation in human hematopoietic cells: superiority to lipofection and passive pulsing of mRNA and to electroporation of plasmid cDNA for tumor antigen loading of dendritic cells," *Blood*, vol. 98, no. 1, pp. 49–56, 2001.

[83] B. Clémenceau, R. Vivien, C. Pellat, M. Foss, G. Thibault, and H. Vié, "The human natural killer cytotoxic cell line NK-92, once armed with a murine CD16 receptor, represents a convenient cellular tool for the screening of mouse mAbs according to their ADCC potential," *MAbs*, vol. 5, no. 4, pp. 587–594, 2013.

[84] C. Sahm, K. Schonfeld, and W. S. Wels, "Expression of IL-15 in NK cells results in rapid enrichment and selective cytotoxicity of gene-modified effectors that carry a tumor-specific antigen receptor," *Cancer Immunology, Immunotherapy*, vol. 61, no. 9, pp. 1451–1461, 2012.

[85] S. Nagashima, R. Mailliard, Y. Kashii et al., "Stable transduction of the interleukin-2 gene into human natural killer cell lines and their phenotypic and functional characterization in vitro and in vivo," *Blood*, vol. 91, no. 10, pp. 3850–3861, 1998.

[86] H. Klingemann, "Are natural killer cells superior CAR drivers?," *Oncoimmunology*, vol. 3, no. 4, article e28147, 2014.

[87] G. Suck, M. Odendahl, P. Nowakowska et al., "NK-92: an 'off-the-shelf therapeutic' for adoptive natural killer cell-based cancer immunotherapy," *Cancer Immunology, Immunotherapy*, vol. 65, no. 4, pp. 485–492, 2016.

[88] C. Zhang, P. Oberoi, S. Oelsner et al., "Chimeric antigen receptor-engineered NK-92 cells: an off-the-shelf cellular therapeutic for targeted elimination of cancer cells and induction of protective antitumor immunity," *Frontiers in Immunology*, vol. 8, p. 533, 2017.

[89] P. Nowakowska, A. Romanski, N. Miller et al., "Clinical grade manufacturing of genetically modified, CAR-expressing NK-92 cells for the treatment of ErbB2-positive malignancies," *Cancer Immunology, Immunotherapy*, vol. 67, no. 1, pp. 25–38, 2018.

[90] C. Zhang, M. C. Burger, L. Jennewein et al., "ErbB2/HER2-specific NK cells for targeted therapy of glioblastoma," *Journal of the National Cancer Institute*, vol. 108, no. 5, 2016.

[91] A. Romanski, C. Uherek, G. Bug et al., "CD19-CAR engineered NK-92 cells are sufficient to overcome NK cell resistance in B-cell malignancies," *Journal of Cellular and Molecular Medicine*, vol. 20, no. 7, pp. 1287–1294, 2016.

[92] S. Oelsner, M. E. Friede, C. Zhang et al., "Continuously expanding CAR NK-92 cells display selective cytotoxicity against B-cell leukemia and lymphoma," *Cytotherapy*, vol. 19, no. 2, pp. 235–249, 2017.

[93] K. H. Chen, M. Wada, K. G. Pinz et al., "Preclinical targeting of aggressive T-cell malignancies using anti-CD5 chimeric antigen receptor," *Leukemia*, vol. 31, no. 10, pp. 2151–2160, 2017.

[94] M. Yu, H. Luo, M. Fan et al., "Development of GPC3-specific chimeric antigen receptor-engineered natural killer cells for the treatment of hepatocellular carcinoma," *Molecular Therapy*, vol. 26, no. 2, pp. 366–378, 2018.

[95] K. Rezvani, R. Rouce, E. Liu, and E. Shpall, "Engineering natural killer cells for cancer immunotherapy," *Molecular Therapy*, vol. 25, no. 8, pp. 1769–1781, 2017.

[96] E. Lowe, L. C. Truscott, and S. N. De Oliveira, "In vitro generation of human NK cells expressing chimeric antigen receptor through differentiation of gene-modified hematopoietic stem cells," *Methods in Molecular Biology*, vol. 1441, pp. 241–251, 2016.

[97] E. Liu, Y. Tong, G. Dotti et al., "Cord blood NK cells engineered to express IL-15 and a CD19-targeted CAR show long-term persistence and potent antitumor activity," *Leukemia*, vol. 32, no. 2, pp. 520–531, 2018.

[98] R. B. Herberman, M. E. Nunn, H. T. Holden, and D. H. Lavrin, "Natural cytotoxic reactivity of mouse lymphoid cells against syngeneic and allogeneic tumors. II. Characterization of effector cells," *International Journal of Cancer*, vol. 16, no. 2, pp. 230–239, 1975.

Hindawi
Journal of Immunology Research
Volume 2018, Article ID 9832467, 10 pages
https://doi.org/10.1155/2018/9832467

Research Article

Construction and Characterization of Adenovirus Vectors Encoding Aspartate-β-Hydroxylase to Preliminary Application in Immunotherapy of Hepatocellular Carcinoma

Yujiao Zhou,[1] **Feifei Liu**,[2] **Chengmin Li**,[3] **Guo Shi**,[4] **Xiaolei Xu**,[1] **Xue Luo**,[1] **Yuanling Zhang**,[1] **Jingjie Fu**,[1] **Aizhong Zeng**,[1] **and Limin Chen**[5]

[1]*Department of Infectious Disease, The First Affiliated Hospital of Chongqing Medical University, Chongqing 400016, China*
[2]*Department of Infectious Disease, The People's Hospital of Deyang City, Deyang, Sichuan Province 618000, China*
[3]*Department of Infectious Disease, The Chongqing Fuling Center Hospital, Chongqing 400016, China*
[4]*Department of General Surgery, The First Affiliated Hospital of Chongqing Medical University, Chongqing 400016, China*
[5]*Toronto General Research Institute, University of Toronto, Toronto, ON, Canada*

Correspondence should be addressed to Aizhong Zeng; aizhong9@sina.com

Received 25 January 2018; Accepted 30 May 2018; Published 15 July 2018

Academic Editor: Feng Li

Dendritic cells (DCs) harboring tumor-associated antigen are supposed to be a potential immunotherapy for hepatocellular carcinoma (HCC). Aspartate-β-hydroxylase (AAH), an overexpressed tumor-associated cell surface protein, is considered as a promising biomarker and therapeutic target for HCC. In this study, we constructed adenovirus vector encoding AAH gene by gateway recombinant cloning technology and preliminarily explored the antitumor effects of DC vaccines harboring AAH. Firstly, the total AAH mRNA was extracted from human HCC tissues; the cDNA was amplified by RT-PCR, verified, and sequenced after TA cloning. Gateway technology was used and the obtained 18T-AAH was used as a substrate, to yield the final expression vector Ad-AAH-IRES2-EGFP. Secondly, bone marrow-derived DCs were infected by Ad-AAH-IRES2-EGFP to yield AAH-DC vaccines. Matured DCs were demonstrated by increased expression of CD11c, CD80, and MHC-II costimulatory molecules. A dramatically cell-killing effect of T lymphocytes coculturing with AAH-DCs on HepG2 HCC cell line was demonstrated by CCK-8 and FCM assays in vitro. More importantly, in an animal experiment, the lysis effect of cytotoxic T lymphocytes (CTLs) on HepG2 cells in the AAH-DC group was stronger than that in the control groups. In conclusion, the gateway recombinant cloning technology is a powerful method of constructing adenovirus vector, and the product Ad-AAH-IRES2-EGFP may present as a potential candidate for DC-based immunotherapy of HCC.

1. Introduction

Hepatocellular carcinoma (HCC) is a common malignant tumor, and despite curable strategies such as resection or liver transplantation, patients with advanced HCC continue to present a poor outcome [1, 2]. Although sorafenib has been shown to improve survival of advanced HCC patients, it ultimately failed to show any improvement in outcomes for the treatment of HCC in randomized studies. The clinical trials of new drugs including lenvatinib, regorafenib, and pembrolizumab have shown promise; however, more convictive clinical evidences are still needed [3]. Therefore, there is a clear need for new therapeutic approaches for HCC.

Aspartate-β-hydroxylase (AAH) is a highly conserved type II transmembrane protein and a kind of α-ketoglutarate-dependent dioxygenase. Currently, AAH has been found highly expressed in a variety of human malignancies including HCC, cholangiocellular carcinoma, and breast, pancreatic, and non-small lung cancer [4–7]; however, it is rarely expressed in normal tissues and lowly expressed in tumor-adjacent tissues [4]. Previous researches have demonstrated that overexpression of AAH strikingly increases

Table 1: PCR primer sequences of the AAH gene for DNA ligating.

Primer name	Sequence (5′→3′)	Amplification fragments
AAH-F	ATCATCCTCGAGGCCACCATGGCCCAGCGTAAGAATGCCAAG	2277 bp
AAH-R	ATCATCGGATCCCTAAATTGCTGGAAGGCTGCGTCTCTGCT	

Table 2: PCR primers for AAH and IRES2-EGFP fusion.

Primer name	Sequence (5′→3′)
attB1-AAH	GGGGACAAGTTTGTACAAAAAAGCAGGCTTCGCCACCATGGCCCAGCGTAAGAATGCCAAGAGC
IRES2-AAH-2277R	GTTAGGGGGGGGGGAGGGAGAGGGGCCTAAattGCTGGAAGGCTGCGTCTCTGCT
AAH-IRES2-1F	AGCAGAGACGCAGCCTTCCAGCAattTAGGCCCCTCTCCCTCCCCCCCCCCTAAC
attB2-EGFP	GGGGACCACTTTGTACAAGAAAGCTGGGTCTTACTTGTACAGCTCGTCCATGCCGAGAGTG

motility and invasiveness of HCC cell lines [8]. Xian et al. [9] reported that AAH overexpression was detected in 150 of 161 patients with HCC, and higher expression levels of AAH correlated significantly with the presence of intrahepatic metastasis and the progression of histological grades. Another clinical study showed that overexpression of AAH is associated with worse clinical outcomes in HCC patients after surgery [10]. The research of Aihara et al. [11] has demonstrated that small molecule inhibitors of AAH produce antitumor effect in HCC. As a conclusion, AAH could be considered as a prognostic maker and therapeutic target for HCC.

After forty years of research, it is generally realized that dendritic cells (DCs), the most powerful professional antigen-presenting cells, are the center part of the immune system, because of their ability to control both immune tolerance and immunity. The application of DCs loaded with tumor-associated antigen (TAA) is supposed to be a promising approach in the prophylaxis and therapy of malignant tumors. The prophylactic and therapeutic effect of DC-mediated tumor vaccines has been successfully confirmed in mouse models. Besides, the history of application of therapeutic DC vaccines in cancer patients has been more than a decade. To date, several new-type DC vaccines have successfully gained entry to phase III clinical trials; however, the most appropriate indication for these vaccines is melanoma [12]. Delivering TAA into DCs in vitro needs the help of vectors. Diverse tools including cytoplasmic transduction peptide delivery system, microbial components, plasmids, and virus have been developed [13–16]. In this study, our aim was to construct a novel adenovirus (Ad) vector encoding AAH gene and to preliminarily explore the potential antitumor activity of DCs loaded with AAH against HCC.

2. Materials and Methods

2.1. Primer Designing and Polymerase Chain Reaction (PCR) Amplification of DNA Fragments. Primers (Table 1) were synthesized according to the human AAH gene sequence (GenBank accession number 004318) and obtained commercially from the manufacturer (Invitrogen, USA, HG1606160040). Total mRNA was extracted from human HCC tissues (supplied by the Hepatobiliary Surgery Department of the First Affiliated Hospital of Chongqing Medical University). PCR amplification system included 5x PrimeSTAR® GXL Buffer 10 μl, dNTP mixture 1 μl, forward primer 0.5 μl, reverse primer 0.5 μl, PrimeSTAR GXL for RT-PCR 2 μl, DNA 2 μl, and RNase-free dH_2O 34 μl. PCR amplification conditions were as follows: 98°C for 10s; 68°C for 15 s; 68°C for 2 min, 30 cycles; and 4°C for 3 min. Subsequently, PCR products were cloned into pMD18-T vector using a TA cloning kit (Takara, Japan, R023A) and sequenced. The plasmid 18T-AAH obtained by TA cloning would be used as templates for the following PCR amplification.

2.2. Construction of Ad Vectors by Gateway Technology. Firstly, 18T-AAH and plasmid internal ribozyme entry site-2/enhanced green fluorescent protein (pIRES2-EGFP) were used as templates, respectively; the products attB1-AAH and attB2-IRES2-EGFP were amplified by PCR. Secondly, the objective DNA fragments flanked by attB sites were obtained by PCR amplification using the primers shown in Table 2. Finally, recombinant Ad vector encoding AAH was produced by gateway technology according to the manufacturer's instruction (Takara, Japan, R023A). Briefly, in the BP reaction, PCR products before-mentioned were inserted into the donor vector with the attP sites (Figure 1(a)) yielding the shuttle vector, containing the gene of interest flanked by the attL sites. Then, in the LR reaction, the shuttle vector was integrated into the destination vector (pAd CMV/V5-DEST) (Figure 1(b)) containing the attR sites producing the final expression constructs (Ad-AAH-IRES2-EGFP). The brief flow chart was shown in Figures 1(c) and 1(d). The final products were also transformed into competent *E. coli* DH5α and positively selected by DNA sequencing.

2.3. Ad Packaging and Amplification. The recombinant plasmid Ad-AAH-IRES2-EGFP was linearized by PacI and delivered into HEK293 cells for Ad packaging and amplification. HEK293 cells were seeded at 4.5×10^5 cells per well into a 6-well plate with DMEM media containing 10% fetal bovine serum (FBS) (Gibco, USA, 10099141) and 1% penicillin streptomycin at 37°C in a humidified atmosphere of 5% CO_2. The infection process was accomplished according to

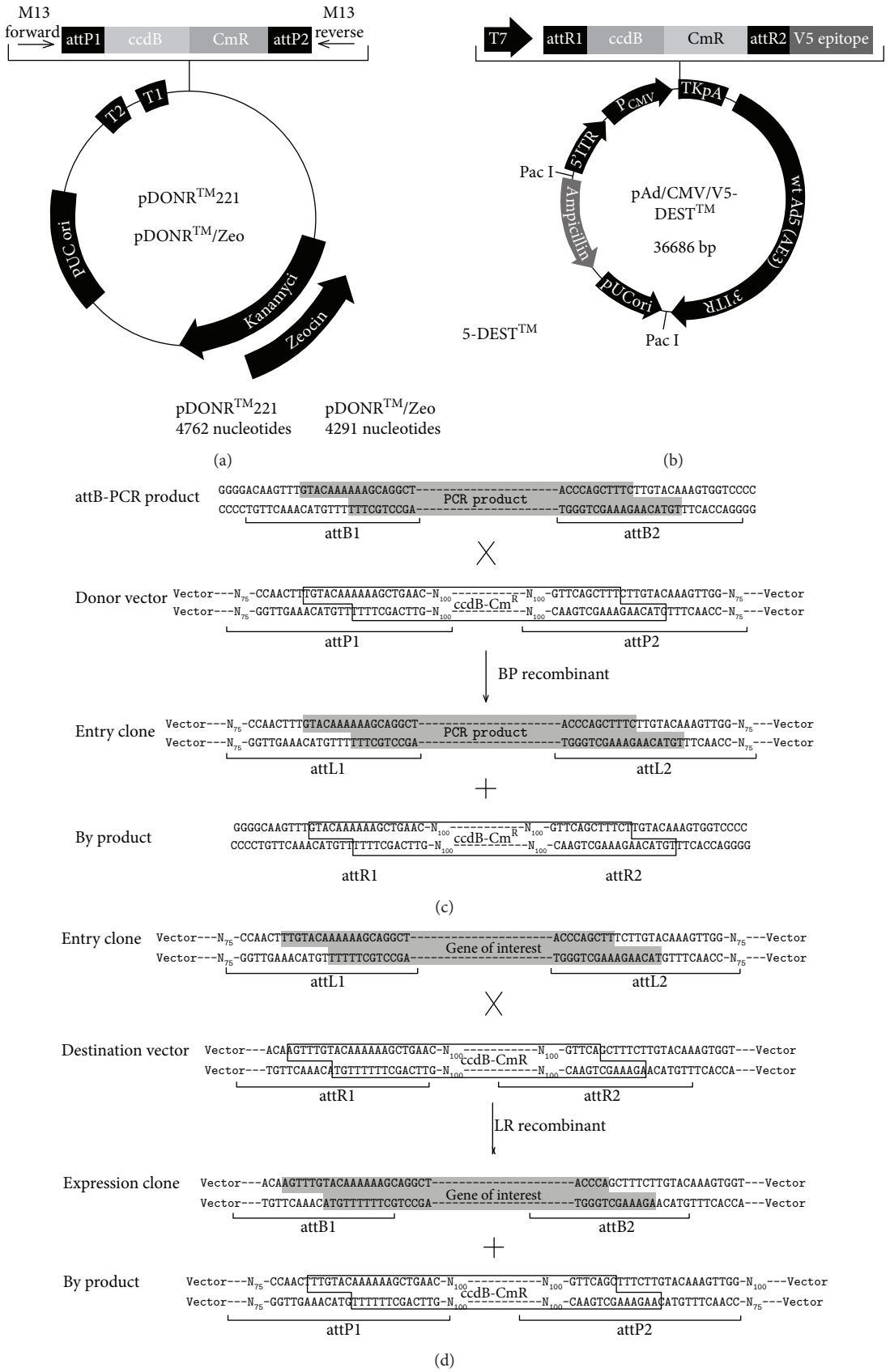

Figure 1: Images of vectors and brief flow chart of gateway cloning method. (a) Donor vector pDONR221. (b) Destination vector pAd CMV/V5-DEST. (c) The BP recombinant (attB × attP → attL × attR). (d) The LR recombinant (attL × attR → attB × attP).

the instruction of Lipofectamine 2000 transfection handbook (Invitrogen, USA). Postinfected HEK293 cells represented a significant cytopathic effect (CPE) at day 8 and were cracked by repeated freezing and thawing between 37°C and −80°C for three times aiming to release the viral particles. The supernatants containing virus was collected and stored at −80°C. The titer of Ad-AAH-IRES2-EGFP was detected by immunoassay. In brief, HEK293 cells were seeded into a 24-well plate at a concentration of 3×10^5 cells/well. Subsequently, the virus was diluted at a dilution range from 10^{-2} to 10^{-6} by DMEM medium and infected HEK293 cells, respectively. After 48 h incubation, AAH polyclonal antibody (1 : 1000, Proteintech, USA, 271391) was added into each well. The infected cells represented an obvious brown color after 3,3′-diaminobenzidine solution dyeing, then the titer was calculated by the formula: (mean positi ve cells/per field) × (fields/per well)/(volume of virus × dilut ion ratio).

2.4. Construction of AAH-DC Vaccine. In brief, the bone marrow was flushed from the femurs, and the tibias of C57BL/6 mice were depleted of erythrocytes with lysis buffer. The cells obtained were cultured in a 6-well plate with RPMI-1640 media containing 10%FBS, 10 ng/ml recombinant murine GM-CSF (PeproTech, USA, 081455), and 10 ng/ml recombinant murine IL-4 (PeproTech, USA, 081449). Half of the media were replaced with fresh cytokine-containing (rmGM-CSF and rmIL-4) media at a one-day interval. On days 5 and 6, 10 ng/ml recombinant murine TNF-α (PeproTech, USA, 061454) was added to the media. On day 7, nonadherent cells were harvested, resuspended in sterile phosphate-buffered saline (PBS), and seeded onto a 12-well plate at a density of 5×10^5 cells/well. Ad-AAH-IRES2-EGFP was added to the well at a multiplicity of infection (MOI) of 200. After 48 hours of incubation, AAH-loaded DCs were obtained. DCs incubated with empty vector Ad-IRES2-EGFP (supplied by the manufacturer) or alone served as the control.

The phenotype analysis of maturated DCs was identified by flow cytometry (FCM). At 36 h postinfection, DCs were collected and adjusted into a concentration of 1×10^6/ml in 0.2 ml PBS. Cells were cocultured with anti-mouse CD11c-PerCP-Cy5.5 (eBioscience, USA, 450114), CD80-PE (eBioscience, USA, 120801), and MHC-II-APC antibodies (eBioscience, USA, 175321) at 4°C for 30 min. The cells were then washed twice with PBS buffer; the expression of mature markers of DCs was analyzed using FCM.

2.5. Cell-Killing Effect In Vitro. At first, splenic T cells derived from C57BL/6 mice were cultured in a 6-well plate at 1×10^6 cells/well with complete RPMI-1640 media, then cocultured with AAH-DC vaccines, GFP-DC vaccines, and blank DC vaccines at a ratio of 1 : 20, respectively. The three kinds of mix-cultured cells were severally harvested after 72 hours of incubation and used as the effector cells.

The human HCC cell line HepG2, highly expressing AAH, was maintained in DMEM medium supplemented with 10% FBS. The cellular proliferation activity was detected by cell counting kit-8 (CCK-8) (Genview, USA, GK3607) assay. Briefly, HepG2 cells were used as the target cells, cultured in a 96-well plate at 3×10^3 cells per well, and mixed with effector cells obtained from each of groups abovementioned at effector-to-target (E/T) ratios of 40 : 1, 20 : 1, 10 : 1, or 5 : 1. After 24 hours of cocultivation, the supernatants were removed and the adherent cells were gently washed once by sterile PBS buffer. The CCK-8 solution was added to all the wells according to the directions of the manufacturer. The OD value was detected at 450 nm by applying a microplate reader. HepG2 cells alone were used as the blank control group.

On the other hand, HepG2 cells were seeded in a 6-well plate at 1×10^5 cells/well, cocultured with different kinds of effector cells aforementioned at a ratio of 40 : 1. HepG2 cells alone were also used as control. After 24 hours of incubation, the supernatants were removed. The four groups of target cells were harvested, dissociated with 0.25% trypsin, and resuspended in Annexin V-FITC/PI binding buffer. The cellular apoptosis rate of target cells was detected by FCM.

2.6. Lactate Dehydrogenase (LDH) Release Assay. 6~8-week-old female C57BL/6 mice, purchased from the Animal Experimental Center of Chongqing Medical University, were maintained under individual ventilated cage (IVC) conditions, fed standard chow, and supplied with sterilized water. All the procedures were approved by the Ethics Committee of the First Affiliated Hospital of Chongqing Medical University. All the mice were in deep anesthesia by diethyl ether and euthanized by high concentration of CO_2 inhalation. C57BL/6 mice were randomly divided into five groups (3 mice/group): (1) AAH-DC group, the mice were immunized by subcutaneous injection with 1×10^6 AAH-DCs in 0.1 ml PBS; (2) GFP-DC group, the mice were immunized by subcutaneous injection with 1×10^6 GFP-DCs in 0.1 ml PBS; (3) DC group, the mice were subcutaneously injected with 1×10^6 noninfected DCs in 0.1 ml PBS; (4) PBS group, the mice were subcutaneously injected with 0.1 ml sterile PBS; and (5) AAH group, Ad-AAH-IRES2-EGFP alone in a volume of 0.1 ml was used to perform the immunization. The injection was given three times at a 7-day interval. The splenic T cells derived from C57BL/6 mice of each group were, respectively, acquired after the last immunization.

Cytotoxic function of the T cells was determined according to LDH Cytotoxicity Assay Kit (Beyotime, China, 092017170925). All steps were performed following the manufacturer's instructions. Briefly, the activated T lymphocytes, obtained after coculturing with 25 μg/ml mitomycin-C-treated HepG2 cells and 5 ng/ml recombinant murine IL-2 (Peprotech, USA, 0608108) for 72 hours, were regarded as the effector cells. HepG2 cells were used as target cells, seeded on a 96-well plate at a density of 4×10^3 cells/well, and cocultured with effector cells at the E/T ratios of 50 : 1, 100 : 1, 200 : 1, and 400 : 1 in a total volume of 200 μl/well for 24 hours of incubation. The spontaneous release of LDH by target cells or effector cells was assayed by incubation of target cells or effector cells alone, respectively. The maximum release of LDH was determined by mixing the target cells with lysis solution. The supernatants were measured by LDH working solution, and absorbance was detected at

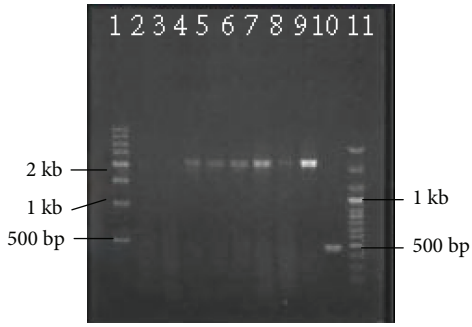

Figure 2: Agarose gel electrophoresis of gradient PCR products. The total AAH mRNA was extracted from surgically resected HCC tissues; the PCR products were amplified with the use of commercially obtained primers and validated by 0.8% agarose gel electrophoresis. Lane 1: 500 bp marker; lane 11: 100 bp marker; lanes 3–9: gradient AAH PCR products, respectively, representing annealing temperature: 56°C, 58°C, 60°C, 62°C, 64°C, 66°C, 68°C; lane 2: negative control group; lane 10: positive control group, 462 bp.

490 nm using a microplate reader. The cellular lysis rate was calculated as the following formula: cytotoxicity (%) = [OD (experimental) − OD (effector spontaneous) − OD (target spontaneous)]/[OD (target maximum) − OD (target spontaneous)] × 100.

2.7. Statistical Analysis. The results were expressed as means ± SD and analyzed with SPSS 21.0 statistical software package (SPSS Inc., Chicago, IL, USA). Data was analyzed by one-way analysis of variance (ANOVA) followed by a LSD t-test when comparing more than two groups. $P < 0.05$ was considered significant.

3. Results

3.1. Amplification of AAH Gene by PCR. The DNA fragment of the AAH gene was amplified by reverse transcription polymerase chain reaction (RT-PCR). The expected band size was of 2270 bp. According to gradient PCR, 68°C was found as the optimum annealing temperature (Figure 2).

3.2. Identification of Ad Vector Encoding AAH. The recombinant Ad vector encoding AAH identified by PCR and DNA sequencing was selected and packaged into HEK293 cells. After 13 days of conventional cultivation, infected HEK293 cells showed significant CPE and clear green fluorescence (Figure 3(a)). The titer of Ad-AAH-IRES2-EGFP was detected as 5.0×10^9 ifu/ml according to the immunoassay aforementioned. Western blot results as shown in Figure 3(b) revealed that the positive expression of AAH protein (~86 kD) was detected in HEK293 cells infected by Ad-AAH-IRES2-EGFP; no expression was found in control groups.

3.3. Identification of DC Vaccines. The expression of green fluorescent protein in DCs was observed by inverted fluorescence microscope (Figure 4(a)), indicating that recombinant Ad vector harboring AAH could effectively infect DCs. The expression of AAH protein in postinfected DCs was also measured by western blot. As shown in Figure 4(b), AAH protein was obviously expressed in the AAH-DC group, while there was no expression in other groups. In addition, compared to GFP-DCs or blank DCs, a significant increased expression of CD11c, CD80, and MHC-II in AAH-DCs was found by FCM analysis (Figures 4(c) and 4(d)).

3.4. CTL Activity. According to the results of the CCK-8 experiment (Figure 5(a)), the proliferation activity of HepG2 cells was gradually decreasing following with the increasing E/T ratio. At each E/T ratio, the proliferation of HepG2 cells in the AAH-DC-CTL group was lower than that in the control groups. On the other hand, FCM analysis revealed that the apoptosis rate of target cells in the AAH-DC-CTL group (21.68 ± 0.24%) was higher than that in the GFP-DC-CTL group (13.93 ± 1.73%), DC-CTL group (9.09 ± 1.07%), and HepG2 alone group (3.10 ± 1.20%); the differences were statistically significant ($F = 237.641$, $P = 0.001$) (Figure 5(b)). In addition, we prepared an LDH release assay to evaluate the cytotoxic activity of CTLs. The results showed that the lysis rate of target cells in the AAH-DC group at E/T ratios of 50 : 1, 100 : 1, 200 : 1, and 400 : 1 was 29.40 ± 7.46%, 32.83 ± 7.76%, 50.63 ± 6.28%, and 56.80 ± 8.12%, respectively. Meanwhile, the highest lysis rate of the AAH-DC group at an E/T ratio of 400 : 1 was significantly higher than that of the GFP-DC group (39.30 ± 3.72%), DC group (14.53 ± 5.40%), PBS group (12.43 ± 6.87%), and AAH group (44.80 ± 4.45%) (Figure 5(c)). Although the percentage of cytotoxicity in the AAH group was higher than that in the GFP-DC group, DC group, and PBS group, it is still lower than that in the AAH-DC group, indicating that DCs harboring AAH gene were prone to induce a stronger CTL immune response in vivo.

4. Discussion

The success of cancer immunotherapy relies on the existence of a high sensitive and high specific TAA. Currently, with respect to HCC, a number of TAAs have been identified: α-fetoprotein (AFP), New York esophageal squamous cell carcinoma-1 (NY-ESO-1), melanoma antigen gene (MAGE) family, glypican-3 (GPC3), and so on [17]. T cell responses targeting those TAAs in HCC patients can be generally observed; however, the subsequent clinical outcomes are not very satisfactory [18]. The AAH gene is also well characterized in HCC, which has been described in detail earlier in the article. Noda et al. [19] reported that immunization of rats with AAH-loaded DCs generated cytotoxicity against intrahepatic cholangiocarcinoma produced by hepatic injection of BDEneu-CL24 cells, which was probably associated with increased $CD3^+$ T lymphocyte infiltration into the tumors. Similarly, Shimoda and colleagues [20] found the prophylactic and therapeutic function of AAH-loaded DCs in a HCC-bearing BALB/c mice model. So far, inducible cellular immunity against AAH in murine models has found that AAH could be a promising immunotherapeutic target of HCC, but there are few reports regarding clinical trials of vaccine that employ this antigen; consequently, the efficiency of human's T cell responses specific for AAH is still unknown. In the study by Tomimaru et al. [21], synthesized

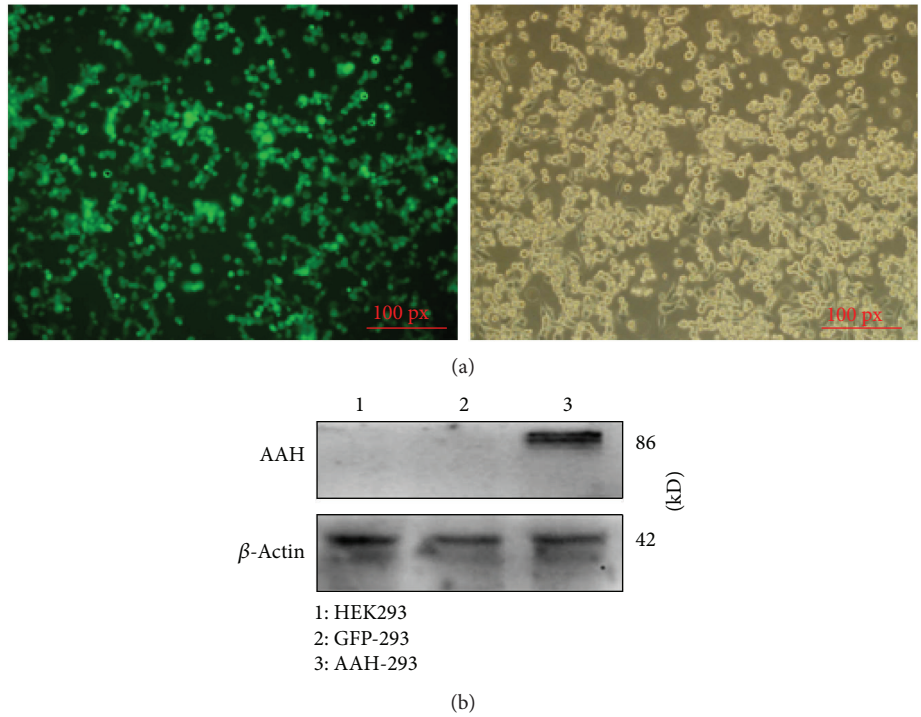

Figure 3: Expression of AAH in HEK293 cells after infection. (a) The fluorescent (①) and visible (②) photograph of HEK293 cells infected by Ad-AAH-IRES2-EGFP at 13 d postinfection (100x). (b) The expression of AAH protein in HEK293 cells at 48 h postinfection by western blot.

HLA class I- and class II-restricted AAH peptides were found to be significantly immunogenic. In addition, both $CD4^+$ and $CD8^+$ T cells purified from the peripheral blood mononuclear cells of HCC patients were found to be activated by AAH protein-loaded DCs, and the inducement function of AAH protein-loaded DCs was remarkably stronger than that of AFP-loaded DCs [20]. To sum up, all the related researches suggest that AAH-loaded DC vaccine may represent as a novel candidate for the immunotherapy of HCC.

Constructing a stable delivering system carrying AAH gene is the first step to further explore the function of AAH-loaded DCs. In this study, we chose Ad as the optimal vector for the following reasons: (1) Ad possesses a strong ability of infection with respect to many different kinds of cells; (2) recombinant Ad could induce cellular immune response and/or humoral immune response; and (3) it infects host cells without insertion mutation, comparatively more safely [22, 23]. As a result, Ad is more likely to be chosen in clinical trials of gene therapy compared with other kinds of vectors. Here, we introduced a gateway recombinant cloning technology, a highly efficient and accurate cloning method, to construct a new-type recombinant Ad vector encoding AAH gene. Unlike conventional cloning technology, the gateway technology provides an accurate way on the basis of bacteriophage-λ to transfer DNA fragments between cloning vectors and allows precise cloning without altering the coding sequence in both donor and destination vectors because of the presence of *ccd*B gene [24, 25]. Furthermore, the gateway technology performs an effective cloning of objective DNA fragments in a single step, yielding destination vectors rapidly with the absence of restriction enzymes and ligases [26]. As a consequence, we highly appreciate the potential of gateway technology for constructing recombinant Ad vector. In this study, pAd CMV/V5-DEST, a 2nd-generation Ad vector, was selected as the destination vector. In the BP reaction, the attB-flanked PCR products were inserted into the donor vector containing the attP sites. Then, the entry clone with the attL sites and pAd CMV/V5-DEST with the attR sites reacted with each other to yield the final expression clone. The whole process was simple and convenient, required much less time, and greatly saved cost. The destination protein was found to have steadily expressed, as demonstrated by the positive expression of AAH protein in postinfected HEK293 cells after 13 days of infection. It was noteworthy that the ability of such recombinant Ad, stably expressing AAH protein, could make it be more beneficial to consistently produce antigens so as to effectively induce immune response in the body.

Ad has a broad spectrum of infection. Not only HEK293 cells but also DCs could be highly effectively infected by Ad in vitro. DCs infected by recombinant Ad vector harboring AAH gene were found to have matured because increased expressions of CD11c, CD80, and MHC-II on the surface of AAH-DCs were detected. It is well known that "mature" DCs have a more powerful ability of antigen presenting than "immature" DCs, which is achieved by a mechanism known as cross-presentation. In the present study, the expression of AAH protein in DCs was successfully detected after 24–72 hours of infection (data not supply), implying that DC vaccine carrying AAH antigen was successfully constructed. Proliferation and apoptosis are two important properties of tumor cells. The abilities of inhibiting proliferation and prompting apoptosis were often used to define whether the antitumor method is effective or not. The antitumor

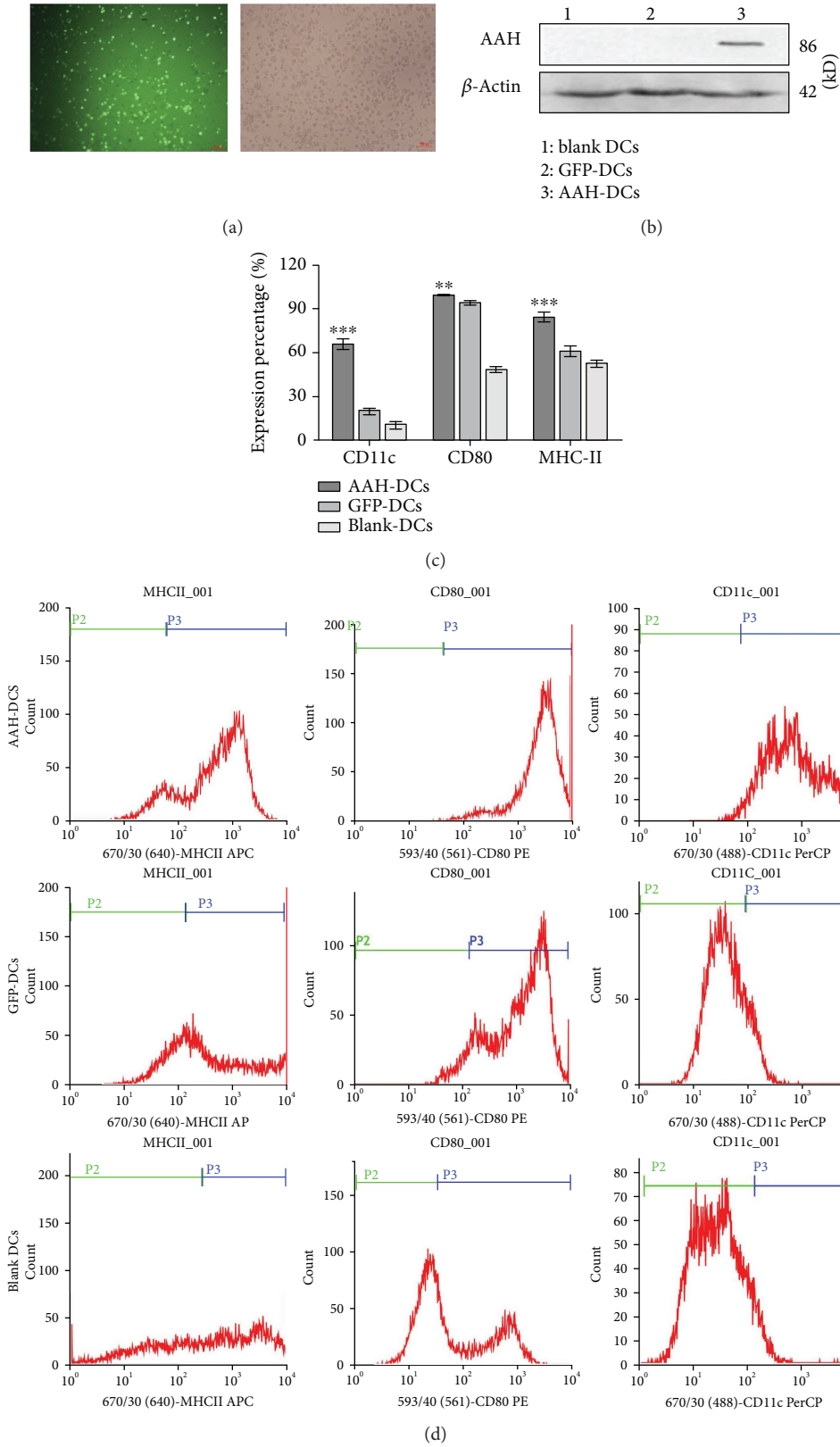

FIGURE 4: Expression of the AAH gene in dendritic cell (DC) vaccines. (a) The fluorescent (①) and visible (②) images of DCs infected by Ad-AAH-IRES2-EGFP at a MOI of 200 after 36 h infection (100x). (b) Expression of AAH protein in DC vaccines by western blot. (c) The expression percentage of typical phenotypes of mature DCs by FCM analysis. Compared to the GFP-DC group or blank DC group, the maturation markers of DCs in the AAH-DC group were significantly highly expressed; $^{***}P < 0.001$, $^{**}P < 0.01$. (d) The typical phenotypes of DCs by FCM.

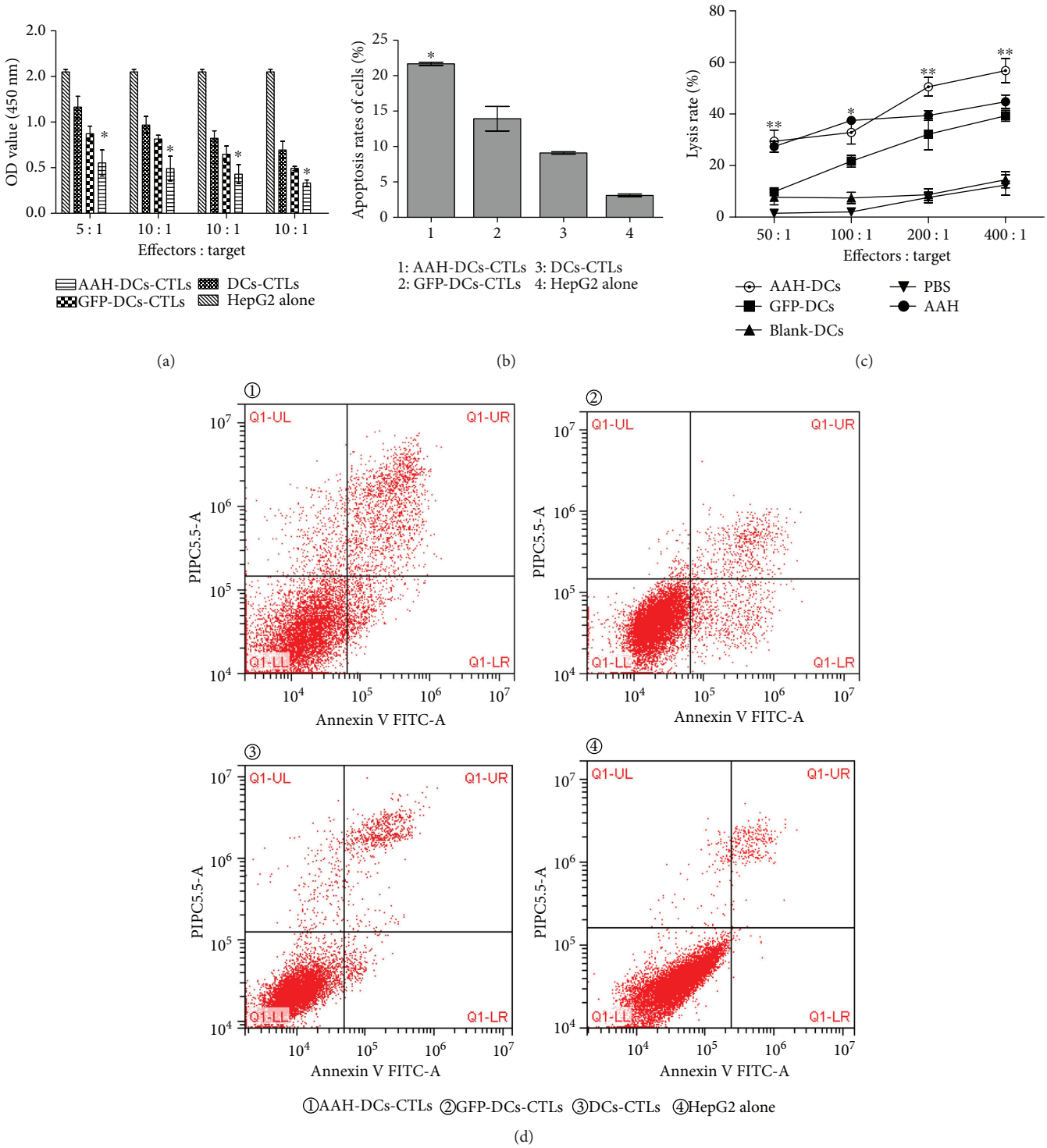

Figure 5: CTL activity. T cells cocultured with AAH-DCs, GFP-DCs, or blank DCs for 72 h were regarded as effector cells, respectively. HepG2 cells were used as target cells. On the other hand, AAH-DCs, GFP-DCs, and blank DCs were applied as vaccines to immunize C57BL/6 mice, respectively. The experiments were performed in triplicate, and the bars represent the mean ± SD. (a) The effect of T cells cocultured with DCs on the proliferation of HepG2 cells by CCK-8 analysis. $^{*}P < 0.05$, when compared with other groups. (b) The proapoptosis effect of T cells cocultured with DCs on HepG2 cells by FCM. $^{*}P < 0.05$, when compared with the control groups. (c) The lysis effect of CTLs derived from immunized mice against HepG2 cells. $^{*}P < 0.05$, $^{**}P < 0.01$ when compared with other groups except the AAH group. According to our results, although there was no statistical differences between the AAH-DCs group and the AAH group, the lysis effect of the AAH-DC vaccine against HepG2 cells was stronger than that of the AAH vaccine. (d) The picture of apoptosis of target cells by FCM.

mechanism of DC-based vaccine is that DCs could induce both $CD4^+$ T helper cells and $CD8^+$ CTLs resulting in activating apoptosis signal pathways in tumor cells [27]. In the current study, we observed that AAH-DCs cocultured with T lymphocytes had a stronger cell-killing effect against HepG2 cells than the control groups in vitro. We also found that the AAH-DC vaccine could induce more effective cellular immune responses in vivo when compared with the control groups. Although our study was limited in HCC cell lines, the results supplied us with a theory and practice basis for exploring the antitumor function of CTL immune response in animal models. A report by Wu et al. [28] has shown that DCs loaded with Ad vector carrying human papillomavirus-16 E6/E7 (HPV-16 E6/E7) fusion gene cocultured with isogenous T cells induced CTL response resulting in a remarkably lethal effect on cervical cancer cell CaSki in vitro. Fu et al. [29] also reported the significant inhibition function of CTLs elicited by HPV E6/E7-loaded DCs against tumor-bearing nude mice. The above data support the hypothesis that Ad vector harboring antigen plays a role in constructing DC-mediated tumor vaccine.

5. Conclusions

In conclusion, the current study identified that the gateway recombinant cloning technology is a powerful and efficient method of constructing recombinant adenovirus. The destination product, Ad-AAH-IRES2-EGFP, combining with DCs could significantly kill HepG2 cells in vitro. We propose that the AAH-DC vaccine may be a potential candidate for immunotreatment of HCC and other types of malignancies expressing AAH.

Data Availability

The data used to support the findings of this study are available from the corresponding author upon request.

Conflicts of Interest

The authors declare that there is no conflict of interest regarding the publication of this paper.

Authors' Contributions

Yujiao Zhou, Feifei Liu, and Chengmin Li share co-first authorship.

Acknowledgments

This work was supported by the National Natural Science Foundation of China (Grant no. 30972587).

References

[1] A. Villanueva, V. Hernandez-Gea, and J. M. Llovet, "Medical therapies for hepatocellular carcinoma: a critical view of the evidence," *Nature Reviews Gastroenterology & Hepatology*, vol. 10, no. 1, pp. 34–42, 2013.

[2] C. Armengol, M. R. Sarrias, and M. Sala, "Hepatocellular carcinoma: present and future," *Medicina Clínica*, vol. 150, no. 10, pp. 390–397, 2018.

[3] J. K. Heimbach, L. M. Kulik, R. S. Finn et al., "AASLD guidelines for the treatment of hepatocellular carcinoma," *Hepatology*, vol. 67, no. 1, pp. 358–380, 2018.

[4] H. Yang, K. Song, T. Xue et al., "The distribution and expression profiles of human aspartyl/asparaginyl beta-hydroxylase in tumor cell lines and human tissues," *Oncology Reports*, vol. 24, no. 5, pp. 1257–1264, 2010.

[5] E. Revskaya, Z. Jiang, A. Morgenstern et al., "A radiolabeled fully human antibody to human aspartyl (asparaginyl) β-hydroxylase is a promising agent for imaging and therapy of metastatic breast cancer," *Cancer Biotherapy & Radiopharmaceuticals*, vol. 32, no. 2, pp. 57–65, 2017.

[6] X. Dong, Q. Lin, A. Aihara et al., "Aspartate β-hydroxylase expression promotes a malignant pancreatic cellular phenotype," *Oncotarget*, vol. 6, no. 2, pp. 1231–1248, 2015.

[7] M. Luu, E. Sabo, S. M. de la Monte et al., "Prognostic value of aspartyl (asparaginyl)-β-hydroxylase/humbug expression in non–small cell lung carcinoma," *Human Pathology*, vol. 40, no. 5, pp. 639–644, 2009.

[8] S. M. d. l. Monte, S. Tamaki, M. C. Cantarini et al., "Aspartyl-(asparaginyl)-β-hydroxylase regulates hepatocellular carcinoma invasiveness," *Hepatology*, vol. 44, no. 5, pp. 971–983, 2006.

[9] Z. H. Xian, S. H. Zhang, W. M. Cong, H. X. Yan, K. Wang, and M. C. Wu, "Expression of aspartyl beta-hydroxylase and Its clinicopathological significance in hepatocellular carcinoma," *Modern Pathology*, vol. 19, no. 2, pp. 280–286, 2006.

[10] K. Wang, J. Liu, Z. L. Yan et al., "Overexpression of aspartyl-(asparaginyl)-β-hydroxylase in hepatocellular carcinoma is associated with worse surgical outcome," *Hepatology*, vol. 52, no. 1, pp. 164–173, 2010.

[11] A. Aihara, C. K. Huang, M. J. Olsen et al., "A cell-surface β-hydroxylase is a biomarker and therapeutic target for hepatocellular carcinoma," *Hepatology*, vol. 60, no. 4, pp. 1302–1313, 2014.

[12] K. Palucka and J. Banchereau, "Cancer immunotherapy via dendritic cells," *Nature Reviews Cancer*, vol. 12, no. 4, pp. 265–277, 2012.

[13] H. T. Su, B. Li, L. Zheng, H. Wang, and L. Zhang, "Immunotherapy based on dendritic cells pulsed with CTPFoxM1 fusion protein protects against the development of hepatocellular carcinoma," *Oncotarget*, vol. 7, no. 30, pp. 48401–48411, 2016.

[14] H. Bendz, S. C. Ruhland, M. J. Pandya et al., "Human heat shock protein 70 enhances tumor antigen presentation through complex formation and intracellular antigen delivery without innate immune signaling," *Journal of Biological Chemistry*, vol. 282, no. 43, pp. 31688–31702, 2007.

[15] B. Hu, A. Tai, and P. Wang, "Immunization delivered by lentiviral vectors for cancer and infectious diseases," *Immunological Reviews*, vol. 239, no. 1, pp. 45–61, 2011.

[16] W. Zhang and A. Ehrhardt, "Getting genetic access to natural adenovirus genomes to explore vector diversity," *Virus Genes*, vol. 53, no. 5, pp. 675–683, 2017.

[17] S. Naryzhny, V. Zgoda, A. Kopylov, E. Petrenko, O. Kleist, and A. Archakov, "Variety and dynamics of proteoforms in the human proteome: aspects of markers for hepatocellular carcinoma," *Proteomes*, vol. 5, no. 4, p. 33, 2017.

[18] N. Mukaida and Y. Nakamoto, "Emergence of immunotherapy as a novel way to treat hepatocellular carcinoma," *World Journal of Gastroenterology*, vol. 24, no. 17, pp. 1839–1858, 2018.

[19] T. Noda, M. Shimoda, V. Ortiz, A. E. Sirica, and J. R. Wands, "Immunization with aspartate-β-hydroxylase–loaded dendritic cells produces antitumor effects in a rat model of intrahepatic cholangiocarcinoma," *Hepatology*, vol. 55, no. 1, pp. 86–97, 2012.

[20] M. Shimoda, Y. Tomimaru, K. P. Charpentier, H. Safran, R. I. Carlson, and J. Wands, "Tumor progression-related transmembrane protein aspartate-β-hydroxylase is a target for immunotherapy of hepatocellular carcinoma," *Journal of Hepatology*, vol. 56, no. 5, pp. 1129–1135, 2012.

[21] Y. Tomimaru, S. Mishra, H. Safran et al., "Aspartate-β-hydroxylase induces epitope-specific T cell responses in hepatocellular carcinoma," *Vaccine*, vol. 33, no. 10, pp. 1256–1266, 2015.

[22] E.-W. Choi, D.-S. Seen, Y. B. Song et al., "AdHTS: a high-throughput system for generating recombinant adenoviruses," *Journal of Biotechnology*, vol. 162, no. 2-3, pp. 246–252, 2012.

[23] R. G. Crystal, "Adenovirus: the first effective in vivo gene delivery vector," *Human Gene Therapy*, vol. 25, no. 1, pp. 3–11, 2014.

[24] G. F. Wang, B. Qi, L. L. Tu, L. Liu, G. C. Yu, and J. X. Zhong, "Construction of adenovirus vectors encoding the lumican gene by gateway recombinant cloning technology," *International Journal of Ophthalmology*, vol. 9, no. 9, pp. 1271–1275, 2016.

[25] P. Bernard, "New *ccdB* positive-selection cloning vectors with kanamycin or chloramphenicol selectable markers," *Gene*, vol. 162, no. 1, pp. 159-160, 1995.

[26] M. Oey, I. L. Ross, and B. Hankamer, "Gateway-assisted vector construction to facilitate expression of foreign proteins in the chloroplast of single celled algae," *PLoS One*, vol. 9, no. 2, article e86841, 2014.

[27] A. Ballestrero, D. Boy, E. Moran, G. Cirmena, P. Brossart, and A. Nencioni, "Immunotherapy with dendritic cells for cancer," *Advanced Drug Delivery Reviews*, vol. 60, no. 2, pp. 173–183, 2008.

[28] X. M. Wu, X. Liu, Q. F. Jiao et al., "Cytotoxic T lymphocytes elicited by dendritic cell-targeted delivery of human papillomavirus type-16 E6/E7 fusion gene exert lethal effects on CaSki cells," *Asian Pacific Journal of Cancer Prevention*, vol. 15, no. 6, pp. 2447–2451, 2014.

[29] S. Fu, Q. Jiao, Q. Huang, X. Liu, F. Yi, and F. Song, "Antitumor effects of dendritic cell vaccine carrying HPV-16 E6/E7 gene on the transplantable tumor of human cervical cancer in nude mice," *Journal of Chongqing Medical University*, vol. 38, no. 5, pp. 521–516, 2013.

Hindawi
Journal of Immunology Research
Volume 2018, Article ID 3753081, 12 pages
https://doi.org/10.1155/2018/3753081

Research Article

The Imbalance between Foxp3$^+$Tregs and Th1/Th17/Th22 Cells in Patients with Newly Diagnosed Autoimmune Hepatitis

Ma Liang,[1] Zhang Liwen,[2] Zhuang Yun,[1] Ding Yanbo,[1] and Chen Jianping[1]

[1]*Department of Digestive Disease, The First People's Hospital of Changzhou, The Third Affiliated Hospital of Soochow University, Changzhou, Jiangsu, China*
[2]*Department of Pediatrics, The Second People's Hospital of Changzhou, Affiliate Hospital of Nanjing Medical University, Changzhou, Jiangsu, China*

Correspondence should be addressed to Chen Jianping; chenjianping123abc@163.com

Received 15 March 2018; Accepted 20 May 2018; Published 27 June 2018

Academic Editor: Dechun Feng

This study is aimed at examining the potential role of regulatory T- (Treg-) Th1-Th17-Th22 cells in the pathogenic process of autoimmune hepatitis (AIH). The numbers of Foxp3$^+$Tregs and Th1, Th17, and Th22 cells were measured in 32 AIH patients using flow cytometry. Moreover, a murine model of experimental autoimmune hepatitis (EAH) was also established and used to investigate the function of Treg-Th1-Th17-Th22 cells in disease progression. AIH patients undergoing an active state had significantly decreased numbers of $CD3^+CD4^+CD25^+Foxp3^+$Tregs and increased numbers of $CD3^+CD4^+CD25^-Foxp3^+$T, $CD3^+CD4^+$IFN-γ^+Th1, $CD3^+CD4^+$IL-17^+Th17, and $CD3^+CD4^+$IL-2^+Th22 cells as well as higher levels of Th1/Th17/Th22-type cytokines compared to AIH patients in remission and HC. Additionally, the numbers of $CD3^+CD4^+CD25^+Foxp3^+$Tregs were negatively correlated with the numbers of Th1-Th17-Th22 cells. Also, the serum levels of IL-17A and IL-22 were correlated positively with liver injury (ALT/AST), whereas the serum levels of IL-10 were correlated negatively with hypergammaglobulinaemia (IgG, IgM) in AIH patients. Interestingly, the percentages of spleen Tregs, expression of Foxp3 mRNA, and liver IL-10 levels decreased, whereas the percentages of spleen Th1-Th17-Th22 cells, expression of T-bet/AHR/RORγt mRNA, and liver IFN-γ, IL-17, and IL-22 levels increased in the murine model of EAH. Our findings demonstrated that an imbalance between Tregs and Th1-Th17-Th22 cells might contribute to the pathogenic process of AIH.

1. Introduction

Autoimmune hepatitis (AIH) is a type of autoimmune inflammatory liver disease characterized by hypergammaglobulinaemia, circulating autoantibodies, and the liver injury with elevated levels of serum liver enzymes [1]. While genetic and environmental factors contribute to the pathogenic process of AIH [2], dysfunctional immune responses are also crucial for the development and progression of AIH [3]. However, the precise process of autoimmune responses remains obscure. Furthermore, although most patients respond well to immunosuppressive therapy, progression and end-stage liver disease occur in 10%–20% of cases and liver transplantation may be necessary [4]. Hence, further illustration of the mechanism underlying the breakdown of self-tolerance and leading to the development of AIH is of great importance in the management of patients with AIH.

It is generally believed that autoreactive T cells play a central role in the initiation and progression of AIH [5]. For example, numerous studies have revealed a transient and moderate increase in the production of Th1 cytokines, including interleukin-2 (IL-2), interferon-γ (IFN-γ), and tumor necrosis factor α (TNF-α) in AIH patients [6, 7]. In addition, recent studies also suggested that Th17 cells and further released cytokine IL-17 may induce accumulation of proinflammatory cells [8, 9], which contributed to the occurrence of AIH. In addition to well-characterized Th1 and Th17 lymphocytes, a new IL-22-producing T cell, termed Th22 cell, has been described as expressing its key cytokine IL-22, which can activate signal transduction and transcription 3 (STAT3) [10]. Recent studies have reported

that the Th22 cell has hepatoprotective and antifibrotic functions in acute liver injury models of HBV [11]. Furthermore, Th22 cells are associated with inflammatory conditions and numerous autoimmune diseases, such as rheumatoid arthritis (RA) and systemic lupus erythematosus (SLE) [12, 13]. However, little is known about the role of Th22 cells in the pathogenesis of AIH. We believe that Th22 cells may partially contribute to the pathogenesis of AIH, and their expressions are likely time-dependent.

Regulatory T cells (Tregs) are important regulators of immune tolerance to self-antigens [14, 15], and their impairment has been associated with the development of autoimmune diseases [16, 17]. Human Tregs are $CD4^+CD25^+$, and their development and function depend on forkhead box protein 3 (FoxP3) expression [14, 15]. Previous studies in animal models have shown that a decreased number of $CD4^+CD25^+FoxP3^+$T cells was detected [18], and function impairment was associated with the inflammatory activity of the liver [18, 19]. This reason is possible in that Tregs can actively suppress proinflammatory T cell responses [20]. At present, it is clear that Tregs can suppress Th1 and Th17 cell-mediated responses [20–22]. However, the relationship between Tregs and Th22 cells remains unclear. Moreover, recent studies have reported that FoxP3 is also expressed in some $CD25^-$ T cells, which may be induced peripherally by environmental antigens [23–25]. While some studies have shown that $CD4^+CD25^-FoxP3^+$T cells lacked inhibitory function [24], others indicated that $CD4^+$-$CD25^-FoxP3^+$T cells inhibited inflammation [25]. However, little is known about the expression of $CD4^+CD25^-FoxP3^+$T cells in AIH patients and whether or not these cells are associated with disease development.

In the current study, we examined the numbers of circulating $Foxp3^+$Tregs and Th1-Th17-Th22 cells, and the concentration of serum inflammatory cytokines in AIH patients, and used the mouse model of EAH to investigate the biological importance of Tregs and Th1/Th17/Th22 cells in the pathogenesis of AIH. The results of this experiment indicated a decreased Treg level and increased Th1, Th17, and Th22 cell levels, and all these cells contributed to the development of AIH. More importantly, a significantly negative correlation between Tregs and Th22 cells was noted in our experiment. These data indicated that Tregs and Th22 cells, in addition to classically described Th1 and Th17 cells, are involved in the process of AIH.

2. Material and Methods

2.1. Subjects. A total of 32 patients with newly onset AIH were recruited sequentially at the inpatient clinic of the Department of Digestive Disease, the First People's Hospital of Changzhou, the Third Affiliated Hospital of Soochow University, China. All patients were analyzed in an active disease state, as defined by ALT values or AST values above 50 U/mL. 23 patients were treated with prednisolone alone at a median dose of 100 mg at the time of acute presentation. 9 patients received prednisolone in combination with azathioprine at a median dose of 100 mg. Another 20 age-, gender-, and ethnicity-matched healthy controls (HCs) were recruited from the Department of Medical Examination Center of our hospital during the same period, and they had no history of any chronic inflammatory disease. Individual patients with AIH were diagnosed, according to the international criteria for the definitive diagnosis of AIH type I [4]. Patients with any other autoimmune diseases, connective tissue diseases (CTDs), chronic inflammatory diseases, recent infection, or a history of hepatitis virus infection or those who had received immunosuppressive therapies or glucocorticoid therapies within the past 6 months were excluded from the study. All subjects signed an informed consent form prior to the initiation of the study, and the study was approved by the Ethical Committee of the First People's Hospital of Changzhou.

2.2. Clinical Examination. The clinical data of each subject was collected from the hospital records. These data included age, sex, and laboratory tests. Individual subjects were subjected to routine laboratory tests for full blood cell counts and the concentrations of serum alanine transaminase (ALT) and aspartate aminotransferase (AST), antinuclear and smooth muscle antibody (ANA/SMA), IgG, IgM, and IgA by a biochemistry automatic analyzer (Roche Diagnostics, Branchburg, USA) and scattered turbidimetry on a Siemens special protein analysis instrument (Siemens Healthcare Diagnostics Products GmbH, Germany).

2.3. Animals. Adult C57BL/6 female mice were purchased from Nanjing Medical University (Jiangsu, China), and they were housed at controlled temperature with light-dark cycles, with free access to food and water. The experiments had been approved by the animal experimentation committee, and guidelines for human care for laboratory animals were observed. Each experiment was performed with five animals per group and repeated at least three times.

2.4. Induction of Experimental Autoimmune Hepatitis (EAH). Induction of experimental autoimmune hepatitis (EAH) was performed through intraperitoneal injection of the mice with freshly prepared S-100 antigen at a dose of 0.5 to 2 mg/mL in 0.5 mL phosphate-buffered saline (PBS) emulsified in an equal volume of complete Freund's adjuvant (CFA) on day 0. A poster dose was given on day 7 as well [26]. Disease severity was assessed histologically on day 28 at the peak of disease activity. Disease severity was graded on a scale of 0 to 3 by an observer blinded to the identity of the samples.

2.5. Histological Evaluation. Liver tissues from sacrificed animals were fixed with 4% (*v*/*v*) PFA, dehydrated through a graded series of sucrose, frozen in an optimal cutting temperature (OCT) compound (Tissue TCK, Miles Elkhart, IN, USA), and stored at −80°C. 5 μm cryostat sections were stained with hematoxylin and eosin (HE) to reveal and estimate the degree of inflammatory cell infiltration. Liver histology of EAH mice was scored using light microscopy and a modified Scheuer scoring scale, assigning scores for lobular inflammation (0, none; 1, mild-scattered foci of lobular-infiltrating lymphocytes; 2, moderate-numerous foci of lobular-infiltrating lymphocytes; and 3, severe-extensive pan–lobular-infiltrating lymphocytes).

2.6. Flow Cytometric Analysis of Intracellular Cytokine Staining. Freshly isolated peripheral blood mononuclear cells (PBMCs) of AIH patients and spleen mononuclear cells (SMNCs) of EAH mice were stimulated in duplicate with 50 ng/mL of phorbol myristate acetate (PMA) and 1.0 mg/mL of ionomycin (Sigma, St. Louis, MO, USA) in RPMI 1640 medium at room temperature in a humidified incubator with 95% air and 5% carbon dioxide for 2 hours and then cultured for another 4 hours in the presence of 0.5 mg/mL of brefeldin A (BFA, Sigma). The numbers of $CD3^+CD4^+$IFN-γ^+Th1, $CD3^+CD4^+$IL-17^+Th17, $CD3^+CD4^+$IL-22^+Th22, and $CD3^+CD4^+CD25^+Foxp3^+$Tregs in individual samples and the frequency of $CD3^+CD8^-IFN\gamma^{+-}$ Th1, $CD3^+CD8^-IL17^+$Th17, $CD3^+CD8^-IL22^+$Th22, and $CD4^+CD25^+FoxP3^+$Tregs in EAH mice were determined by flow cytometry following intracellular staining with anticytokine antibodies.

2.7. Enzyme-Linked Immunosorbent Assay for IL-10, IFN-γ, IL-17, and IL-22. The cytokine levels in the serum (human) and in the supernatant of normalized hepatic tissue weight (mice) were collected and allowed to clot at 4°C for 2 hours. The clots were removed by centrifuging at 7000 rpm for 30 min in a refrigerated centrifuge. Serum/supernatant was obtained from all subjects by centrifugation and stored at −80°C for determination of cytokine levels. The levels of cytokines in the serum/supernatant were measured by enzyme-linked immunosorbent assay (ELISA) using commercially available IL-10, IFN-γ, IL-17, and IL-22 ELISA kits (Boster, Wuhan, China) according to the manufacturer's instructions.

2.8. RT-PCR. Total RNA was acquired from the hepatic tissue at each time point from EAH mice. The expressions of transcriptional repressors Foxp3, T-bet, RORγt, and AHR were then measured through real-time quantitative RT-PCR. Total RNA was extracted from hepatic tissue using the acid guanidinium thiocyanate-phenol-chloroform method. Total RNA of 2 μg was reverse transcribed with hexamer and M-MuLV reverse transcriptase (New England Biolabs, Ipswich, MA) according to the manufacturer's instructions. cDNA corresponding to 25 ng of total RNA was subjected to quantitative PCR (qPCR) using primer sets and TaqMan probes corresponding to murine Foxp3, T-bet, AHR, RORγt, and GAPDH with qPCR Master Mix. All estimated mRNA values were normalized to GAPDH mRNA levels. The sizes of the PCR amplicons were as follows: Foxp3, 172 bp; T-bet, 86 bp; RORγt, 112 bp; and AHR, 98 bp. Promoter-specific primers were used for amplification: FOXP3 (forward: *5′-AGGAGAAAGCGGATACCA-′3* and reverse: *5′-TGTGAGGACTACCGAGCC-′3*), T-bet (forward: *5′-TCTTACTGGCTGGGAACACC-′3* and reverse: *5′-GCAG AGGGTAGGAATGTGGG-′3*), AHR (forward: *5′-AGAATC CCACATCCGCATGATT-′3* and reverse: *5′-CATTGGACT GGACCCACCTC-′3*), RORγt (forward: *5′-CCAGCTACC AGAGGAAGTCAA-′3* and reverse: *5′-TCCATGAAGCC TGAAAGCCG-′3*), and GAPDH forward: *5′-TGTGTCCGT CGTGGATCTGA-′3* and reverse: *5′-TTGCTGTTGAAGTC GCAGGAG-′3*).

Table 1: The demographic and clinical characteristics of subjects.

Parameters	AIH	HC
Number	32	20
Age (years)	48 (37–76)	51 (41–74)
Gender: female/male	24/8	14/6
ALT (U/L)	125.9 ± 108.3*	27.2 ± 8.2
AST (U/L)	101.1 ± 53.7*	22.7 ± 5.7
γ-GT (U/L)	89.1 ± 30.3*	25.1 ± 7.4
ALP (U/L)	133.4 ± 37.1*	89.5 ± 23.6
Anti-ANA (+)	23/32 (71.8%)*	0/20 (0%)
Anti-ANA titer	1 : 640 (1 : 80–1 : 10000)	—
Anti-SMA (+)	2/30 (6.25%)	0/20 (0%)
Anti-SMA titer	1 : 1000 (1 : 160–1 : 3200)	—
IgG (g/L)	15.9 ± 3.7*	7.8 ± 2.3
IgM (g/L)	6.9 ± 1.9*	2.64 ± 0.87
IgA (g/L)	4.07 ± 2.3*	1.6 ± 1.1
WBC ($\times 10^9$/L)	7.93 (5.6–11.2)*	5.08 (3.9–9.2)

Data shown are the real case number or mean ± SD. Normal values: ALT: <40 IU/L; AST: <40 IU/L. Normal values: ANA: <1 : 80; SNA: <1 : 80. IgG (normal range: 7–16 g/L); IgM (normal range: 0.7–4.6 g/L); and IgA (normal range: 0.4–2.3 g/L). HC: healthy control; AIH: autoimmune hepatitis. *$p < 0.05$ versus HC.

Table 2: Effect of treatment on the values of clinical measures in follow-up AIH patients.

Parameters	Before treatment	After treatment
Number	19	19
Age (years)	42 (37–76)	42 (37–76)
Gender: female/male	16/3	16/3
ALT (U/L)	184.6 ± 105.3*	37.2 ± 10.4
AST (U/L)	126.4 ± 54.8*	43.6 ± 11.5
γ-GT (U/L)	105.6 ± 26.1*	76.1 ± 24.9
ALP (U/L)	152.5 ± 33.3*	93.7 ± 23.2
IgG (g/L)	17.7 ± 3.1*	8.7 ± 2.9
IgM (g/L)	7.8 ± 1.6*	4.5 ± 2.3
IgA (g/L)	3.9 ± 1.7*	2.6 ± 1.1

Data shown are the real case number or mean ± SD. Normal values: ALT: <40 IU/L; AST: <40 IU/L. IgG (normal range: 7–16 g/L); IgM (normal range: 0.7–4.6 g/L); IgA (normal range: 0.4–2.3 g/L). HC: healthy control; AIH: autoimmune hepatitis. *$p < 0.05$ versus posttreatment.

2.9. Statistical Analysis. The differences between the groups were analyzed by Mann–Whitney U test and Wilcoxon signed-rank test using SPSS 18.0 software for unpaired and paired comparisons, respectively. The relationship between variables was evaluated using the Spearman rank correlation test. A two-sided p value < 0.05 was considered statistically significant.

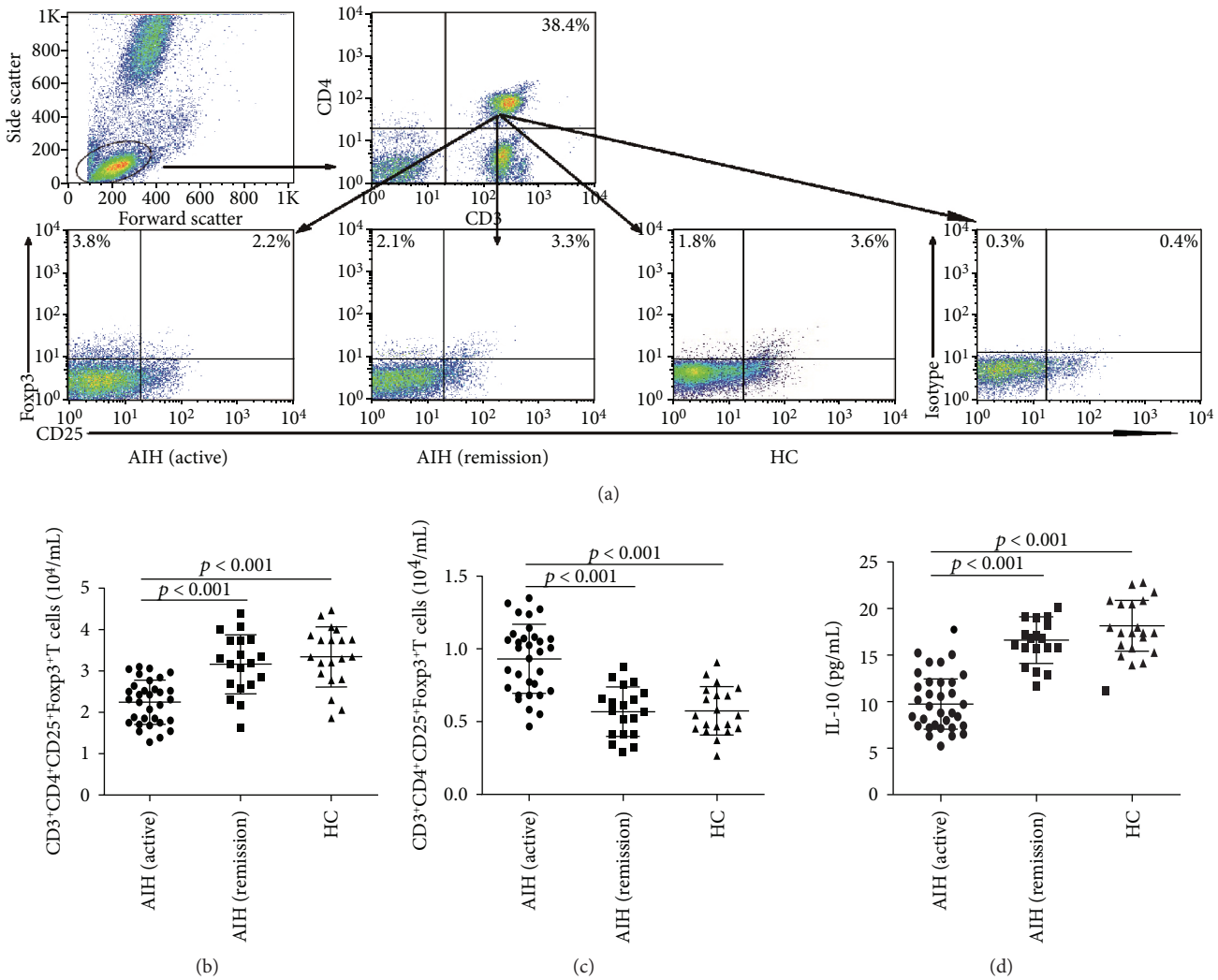

Figure 1: FACS analysis of the numbers of different subsets of circulating $CD3^+CD4^+$T cells and ELISA analysis of serum IL-10 in AIH patients. PBMCs were isolated from individual subjects, and PBMCs $5*10^5$/tube were stained in duplicate with FITC-anti-CD3, PE-Cy7-anti-CD25, and PerCP-anti-CD4 or isotype controls, fixed, and permeabilized, followed by intracellular staining with PE-anti-Foxp3. The frequency of $CD3^+CD4^+CD25^-Foxp3^+$ and $CD3^+CD4^+$ $CD25^+Foxp3^+$T cells was determined by flow cytometry analysis. The cells were gated on living lymphocytes and then gated on $CD3^+CD4^+$ cells, and at least about 30,000 events were analyzed for each sample. The numbers of each type of $CD3^+CD4^+Foxp3^+$T cells were calculated, according to the total numbers of PBMCs and the frequency of different types of $CD3^+CD4^+Foxp3^+$T cells. The concentrations of serum IL-10 in individual subjects were determined by ELISA. (a) Flow cytometry analysis; (b) the numbers of $CD3^+CD4^+CD25^+Foxp3^+$T cells; (c) the numbers of $CD3^+CD^{4+}CD25^-Foxp3^+$T cells; (d) serum levels of IL-10. Data shown are representative FACS charts or the mean numbers of each type of cells per mL of peripheral blood and the mean levels of serum IL-10 in individual subjects from two separate experiments. The horizontal lines indicate the median values for each group. Data shown are representative charts of different subsets of $CD3^+CD4^+$T cells and serum IL-10 from individual groups of subjects ($n = 20$ for the HC, $n = 32$ for the patients at 0 week, and $n = 19$ for the patients at 8 weeks posttreatment).

3. Results

3.1. Demographic and Clinical Characteristics of Study Subjects. The baseline (before treatment) demographic characteristics of AIH patients and HC are summarized in Table 1. As expected, the concentrations of serum ALT, AST, γ-GGT, and ALP in the patients were significantly higher than those in the HC. Furthermore, 23 of 32 patients with new-onset AIH were positive for anti-ANA antibodies, while two were positive for anti-SMA antibodies. In addition, abnormally higher levels of serum IgG, IgM, and IgA were detected in the patients, as compared with those in the HC in this population. Furthermore, we analyzed the values of clinical parameters and in 19 AIH patients 8 weeks posttreatment. We found that the serum levels of ALT, AST, γ-GGT, and ALP were significantly descending compared to per-treatment values. Similarly, the titers IgG, IgM, and IgA were significantly decreased compared to the pretreatment levels (Table 2).

3.2. Altered Numbers of $CD3^+CD4^+FoxP3^+$T Cells and Changed Levels of Serum IL-10 in AIH Patients. We first

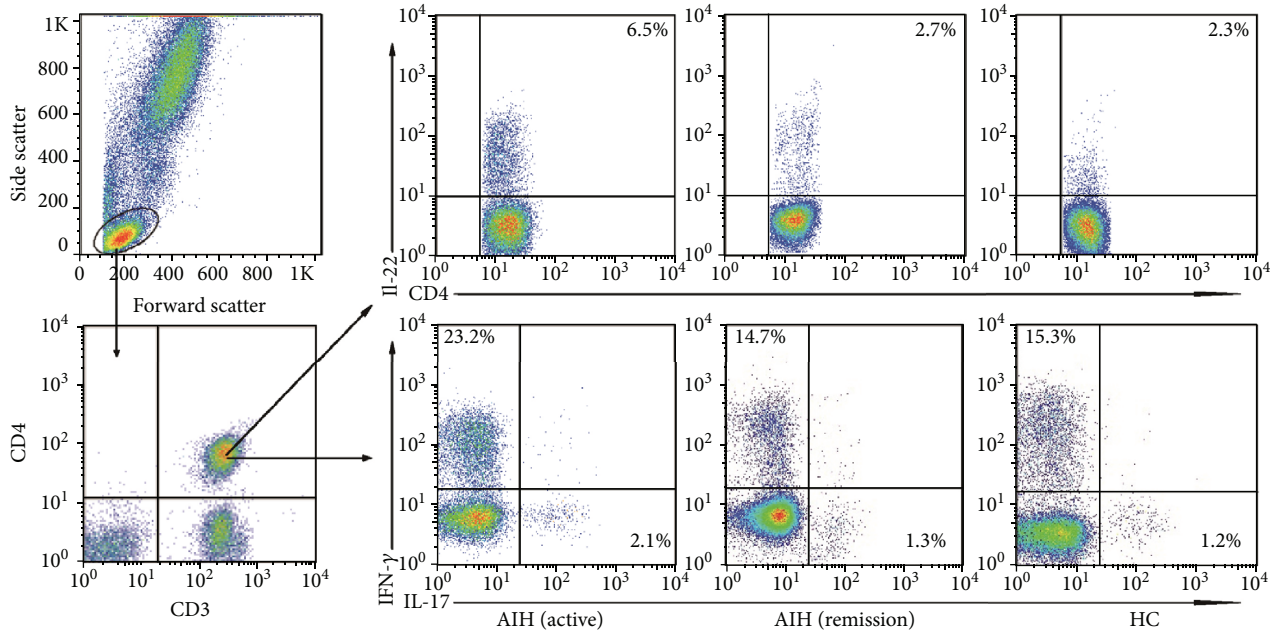

(a)

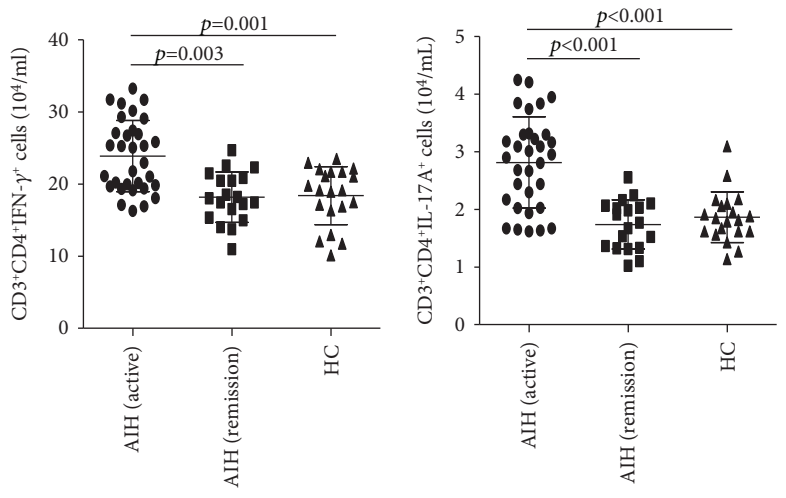

(b)

(c)

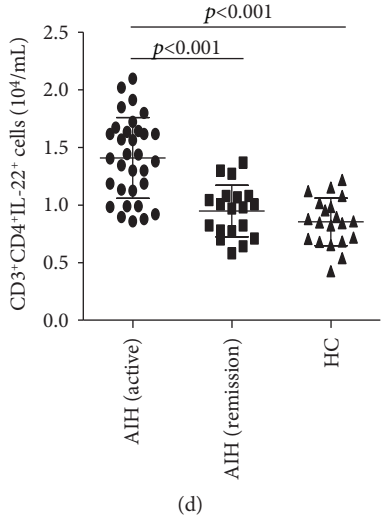

(d)

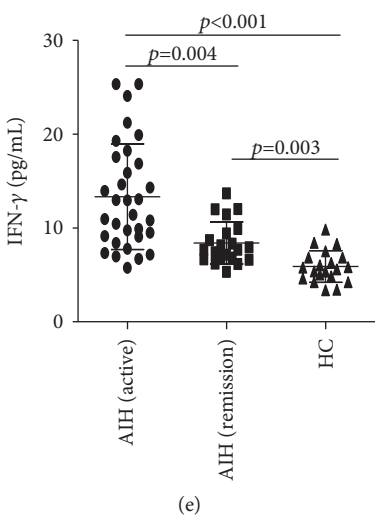

(e)

Figure 2: Continued.

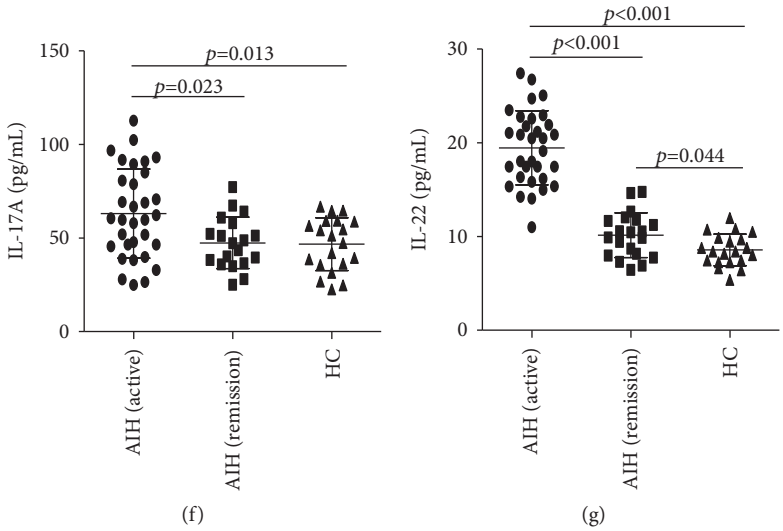

Figure 2: FACS analysis of the numbers of different subsets of circulating effector $CD3^+CD4^+$T cells and ELISA analysis of serum IFN-γ, IL-17, and IL-22 in AIH patients. PBMCs were isolated from individual subjects, and PBMCs $5 * 10^5$/tube were stained in duplicate with APC-anti-CD4 and PerCP-anti-CD3 or isotype controls, fixed, and permeabilized, followed by intracellular staining with FITC-anti-IL-17 and PE-Cy7-anti-IFN-γ and PE-anti-IL-22. The frequency of $CD3^+CD4^+$IFN-γ^+Th1, $CD3^+CD4^+$IL-17^+Th17, and $CD3^+CD4^+$IL-22^+Th22 cells was determined by flow cytometry analysis. The cells were gated on living lymphocytes and then gated on $CD3^+CD4^+$ cells, and at least about 30,000 events were analyzed for each sample. The numbers of each type of $CD3^+CD4^+$T cells were calculated, according to the total numbers of PBMCs and different types of $CD3^+CD4^+$T cells. (a) The flow cytometry analysis; (b–d) the numbers of $CD3^+CD4^+$IFN-γ^+Th1, $CD3^+CD4^+$IL-17^+Th17, and $CD3^+CD4^+$IL-22^+Th22 cells; (e–g) serum levels of IFN-γ, IL-17, and IL-22. Data shown are representative FACS charts or the mean numbers of each type of cells per mL of peripheral blood in individual subjects from two separate experiments. The horizontal lines indicate the median values for each group. Data shown are representative charts of different subsets of $CD3^+CD4^+$T cells and serum IL-10 from individual groups of subjects ($n = 20$ for the HC, $n = 32$ for the patients at 0 week, and $n = 19$ for the patients at 8 weeks posttreatment).

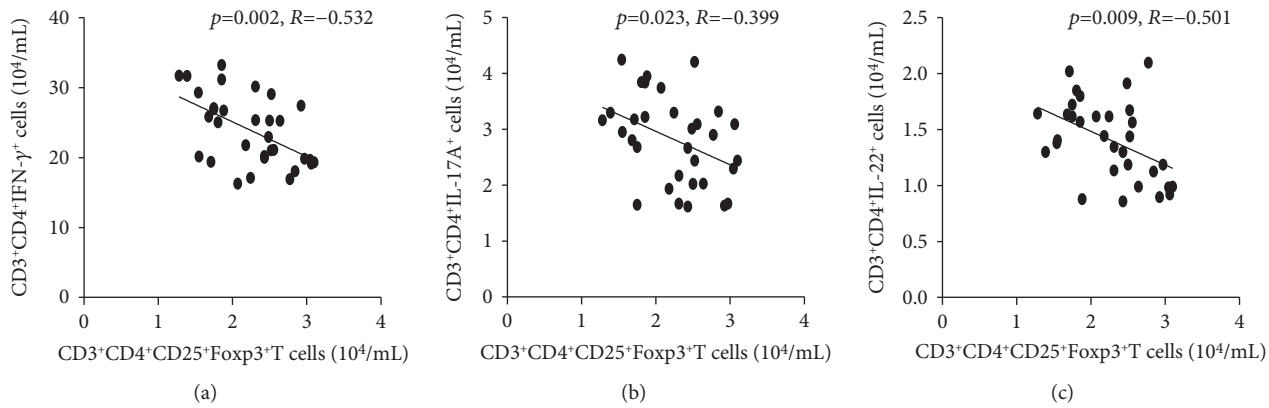

Figure 3: Correlation among the numbers of different subsets of circulating $CD3^+CD4^+$T cells in AIH patients. Correlation between the numbers of $CD3^+CD4^+CD25^+Foxp3^+$T cells and the numbers of $CD3^+CD4^+$IFN-γ^+Th1 (a), $CD3^+CD4^+$IL-17^+ Th17 (b), and $CD3^+CD4^+$IL-22^+Th22 cells (c) in AIH patients.

characterized the levels of different subsets of $CD3^+CD4^{+-}$ $FoxP3^+$T cells in PB of HC and AIH patients by flow cytometry analysis. As shown in Figure 1, AIH patients undergoing an active state had significantly decreased numbers of $CD3^{+-}$ $CD4^+CD25^+Foxp3^+$Tregs and increased numbers of $CD3^{+-}$ $CD4^+CD25^-Foxp3^+$T cells, compared to AIH patients in remission and HC. However, we did not find a significant difference in the numbers of $CD3^+CD4^+CD25^+Foxp3^+$Tregs and $CD3^+CD4^+CD25^-Foxp3^+$T cells between HC and AIH patients in remission.

Then, we further analyzed the levels of IL-10 in the serum of AIH patients and found a lower level of serum IL-10 in AIH patients undergoing an active state, compared to AIH patients in remission and HC (Figure 1(d)). However, we did not find a significant difference in the level of serum IL-10 between HC and AIH patients in remission. In addition, the concentrations of serum IL-10 were correlated positively with the numbers of $CD4^+CD25^+Foxp3^+$T cells ($r = 0.517$, $p = 0.002$), but not with the numbers of $CD4^+CD25^-Foxp3^{+-}$ T cells ($r = 0.381$, $p = 0.511$) in the patients.

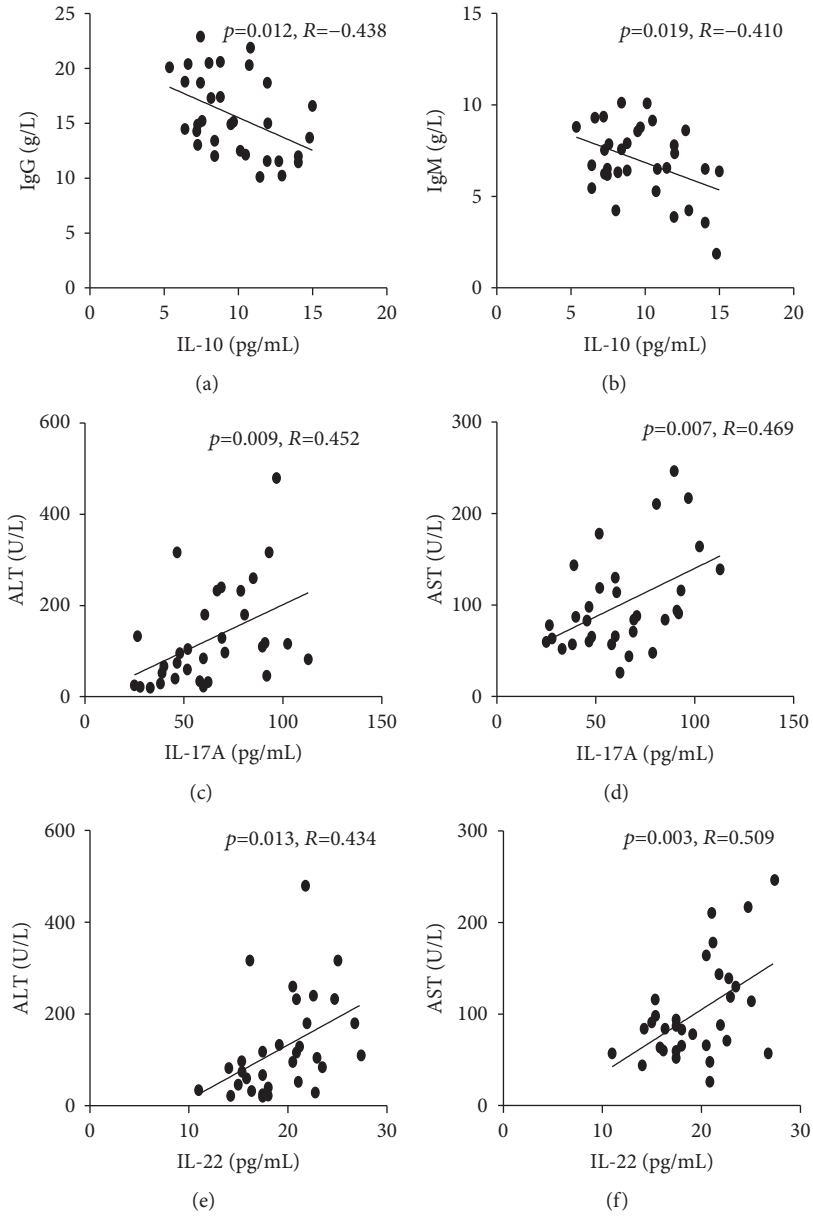

Figure 4: Correlation between serum levels of $CD3^+CD4^+$T cell-related cytokines and the values of clinical parameters in AIH patients. (a, b) Correlation between serum levels of IL-10 and titer IgG/IgM in AIH patients; (c, d) correlation between serum levels of IL-17A and ALT/AST in AIH patients; (e, f) correlation between serum levels of IL-22 and ALT/AST in AIH patients.

3.3. Increased Numbers of Th1/Th17/Th22 Cells and Related Cytokines in AIH Patients. Further comparison of different types of effector $CD3^+CD4^+$T cells found that AIH patients undergoing an active state had significantly increased numbers of $CD3^+CD4^+$IFN-γ^+Th1, $CD3^+CD4^+$IL-17^+Th17, and $CD3^+CD4^+$IL-22^+Th22 cells and higher levels of serum Th1 cytokine IFN-γ, Th17 cytokine IL-17A, and Th22 cytokine IL-22, compared to AIH patients in remission and HC (Figure 2). However, we did not find a significant difference in the numbers of Th1/Th17/Th22 cells and their related cytokines between HC and AIH patients in remission.

3.4. Negative Correlation between Tregs and Th1/Th17/Th22 Cells in AIH Patients. Tregs can suppress the proliferation and activation of other effector $CD3^+CD4^+$T cells [20–22]. In order to better characterize the role of Tregs in Th1/Th17/Th22 cells, correlation analysis was performed, and the results showed that decreased numbers of Tregs were significantly negatively correlated with the numbers of Th1 and Th17 cells in AIH patients undergoing an active state (Figures 3(a) and 3(b)). In addition, the numbers of Tregs also had a negative correlation with peripheral Th22 cell level with statistical significance in AIH patients undergoing an active state (Figure 3(c)). Moreover, further analysis indicated that decreased numbers of Tregs were negatively correlated with the concentrations of serum IFN-γ, IL-17, and IL-22 in AIH patients undergoing an active state (data not shown). However, we did not observe any significant

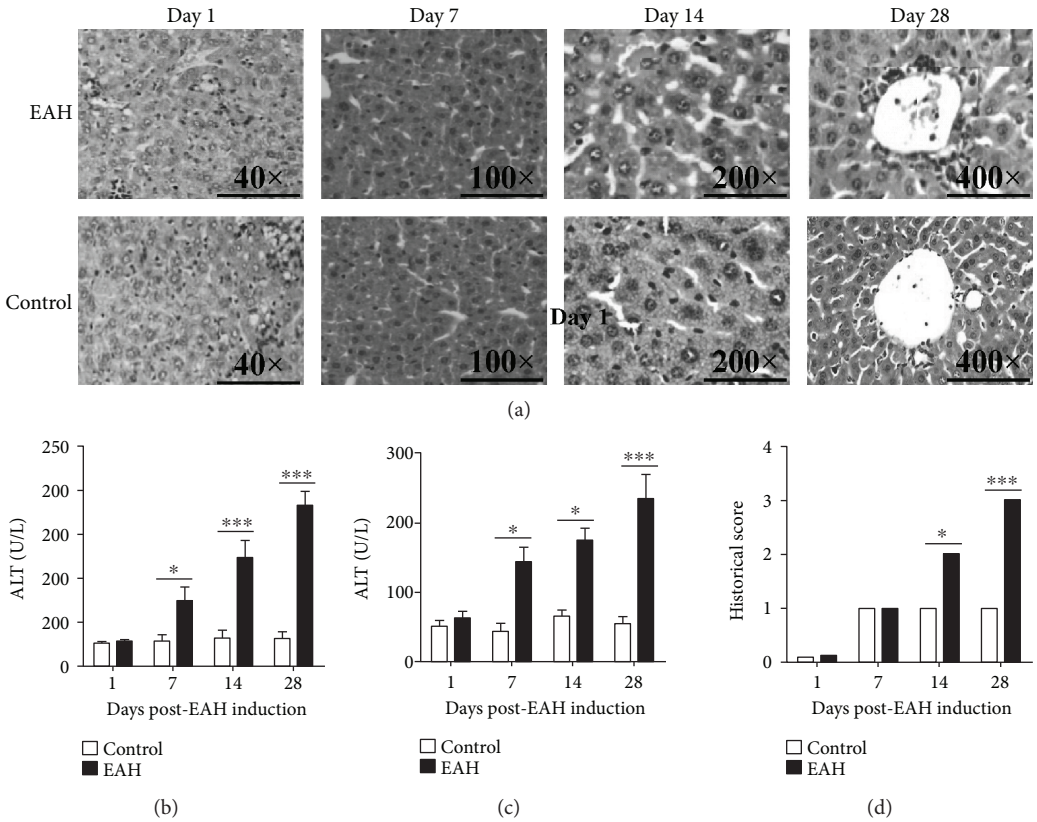

Figure 5: Biochemical and histological analyses in EAH mice. Ten mice (5 from the EAH group and 5 from the control group) were killed at each time point (7, 14, and 28 days). (a) Representative histological picture of liver lesions in animals after standard induction of EAH and controls (magnification, 40x, 100x, 200x, or 400x). (b) Serum ALT levels progressively upregulated from 1 to 28 days. (c) Serum AST levels progressively upregulated from 1 to 28 days. (d) Histological score of liver lesions in mice after standard induction of EAH. The horizontal lines indicate the mean values of the different groups. $^{*}p < 0.05$ and $^{***}p < 0.01$.

correlation among these cells in AIH patients in remission or HC. These data suggested that Tregs might also regulate Th22 cell-mediated responses, in addition to classically described Th1 and Th17 cells.

3.5. The Relationship between $CD3^+CD4^+$T Cell-Related Cytokines and Clinical Parameters in AIH Patients. To understand the importance of Tregs-Th1-Th17-Th22 cells, we analyzed the potential association of the levels of these $CD3^+CD4^+$T cell-related cytokines with the values of clinical parameters in AIH patients undergoing an active state. We found that the concentrations of serum IL-10 were correlated negatively with the concentrations of serum IgG and IgM, whereas the concentrations of serum IL-17 and IL-22 were positively correlated with the levels of ALT and AST (Figure 4). However, there was no other significant correlation between the levels of these $CD3^+CD4^+$T cell-related cytokines with any of the clinical parameters tested in this population (data not shown).

3.6. Statistical Increase in Th1/Th17/Th22 Cells and Decrease in Tregs in EAH Mice. To understand the effects of regulatory and effector T cells in vivo, we had successfully established the murine model of EAH. Compared with the control group, EAH mice had obvious liver injury evidenced by liver edema with a rising liver index and dramatically enhanced serum levels of AST and ALT (Figure 5). Splenocytes were collected from mice at each time point, and flow cytometry was performed to analyze the percentages of IFN-γ-producing Th1 cells, IL-17-producing Th17 cells, IL-22-producing Th22 cells, and $FoxP3^+$Tregs in EAH and control mice. We found that IFN-γ-producing $CD3^+CD8^-$ T cells (Th1 cells) and IL-17-producing $CD3^+CD8^-$ T cells (Th17 cells) in the experimental group significantly increased on the 7th, 14th, and 28th days of post-EAH induction, and IL-22-producing $CD3^+CD8^-$T cells (Th22 cells) obviously increased on the 14th and 28th days of post-EAH induction compared with those in the control group (Figures 6(a)–6(d)). Furthermore, our data also showed that the liver levels of IFN-γ, IL-17, and IL-22 on the 7th, 14th, and 28th days of post-EAH induction were statistically higher in the experimental group than in the control group (Figures 6(f)–6(h)). Moreover, $CD3^+CD4^+$-$CD25^+FoxP3^+$Tregs and liver levels of IL-10 obviously decreased on the 7th, 14th, and 28th days of post-EAH induction compared with those in the control group (Figures 6(e) and 6(i)).

3.7. Marked Changes of Hallmark Transcription Factor of Treg/Th1/Th17/Th22 Cells in EAH Mice. The transcriptional repressors FoxP3, T-bet, RORγt, and AHR were the hallmark transcription factors of Tregs, Th1 cells, Th17 cells, and Th22 cells, respectively. Immunohistochemistry and real-time

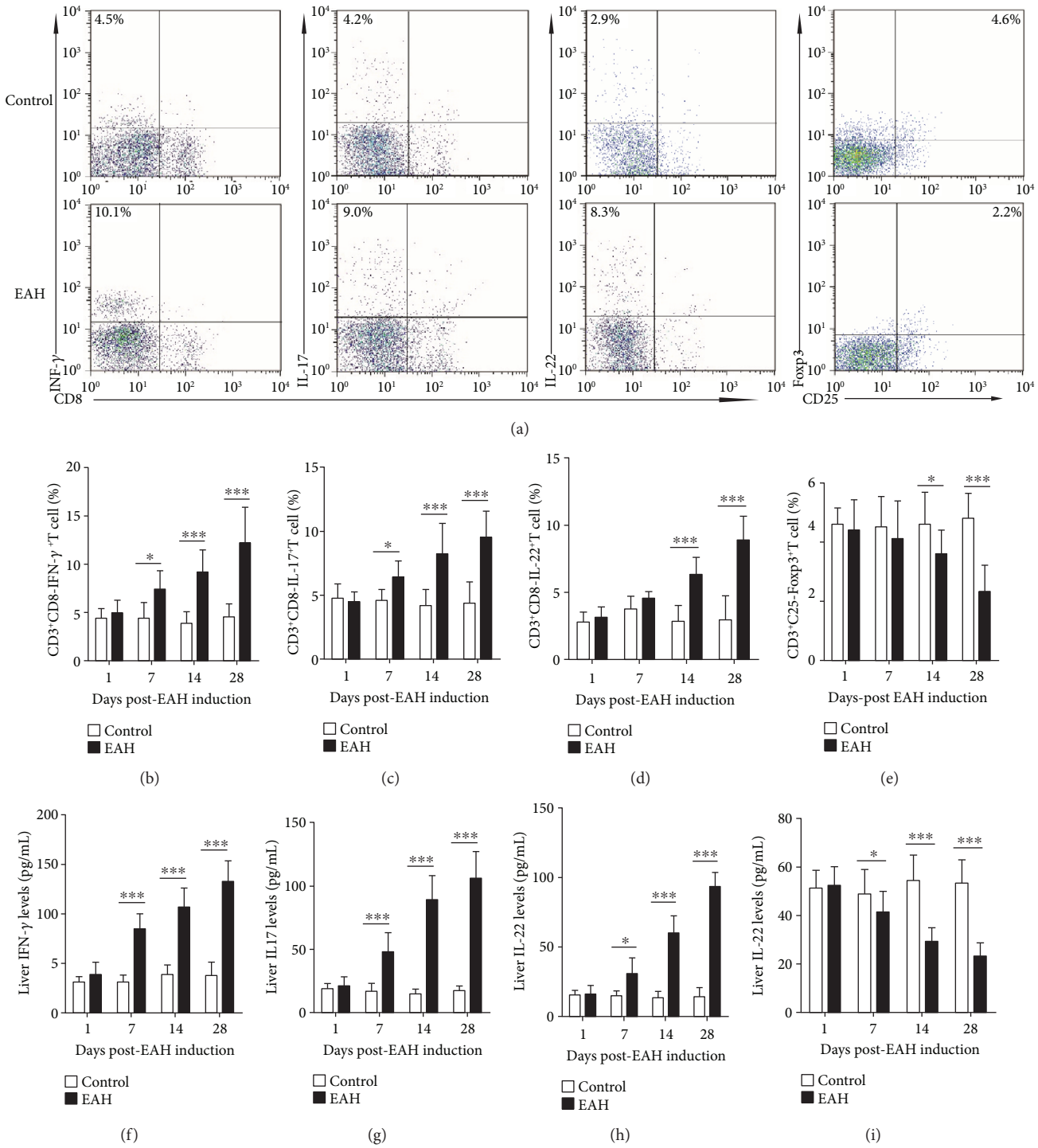

Figure 6: Flow cytometry of Treg/Th1/Th17/Th22 cells in SMNCs and ELISA analysis of hepatic levels of IL-10, IFN-γ, IL-17A, and IL-22 in EAH mice. Ten mice (5 from the EAH group and 5 from the control group) were killed at each time point (1, 7, 14, and 28 days). (a) Flow cytometry analysis of Tregs and Th1, Th17, and Th22 cells from the spleen on the 14th day. (b–e) Percentages of Tregs and Th1, Th17, and Th22 cells at each time point from EAH and control mice were analyzed by FACS. (f–i) Liver IL-10, IFN-γ, IL-17A, and IL-22 levels at each time point from EAH and control mice were used for ELISA. The horizontal lines indicate the mean values of the different groups. $^{*}p < 0.05$ and $^{***}p < 0.01$.

PCR were employed to further ascertain in detail whether Tregs and Th1, Th17, and Th22 cells had the potential of local changes in the process of EAH induction. The results found that the mRNA expression levels of T-bet, RORγt, and AHR in experimental mice increased remarkably 7, 14, and 28 days post-EAH induction compared with those in the control group, whereas the messenger RNA (mRNA) encoding Foxp3 was expressed in different ways (Figure 7).

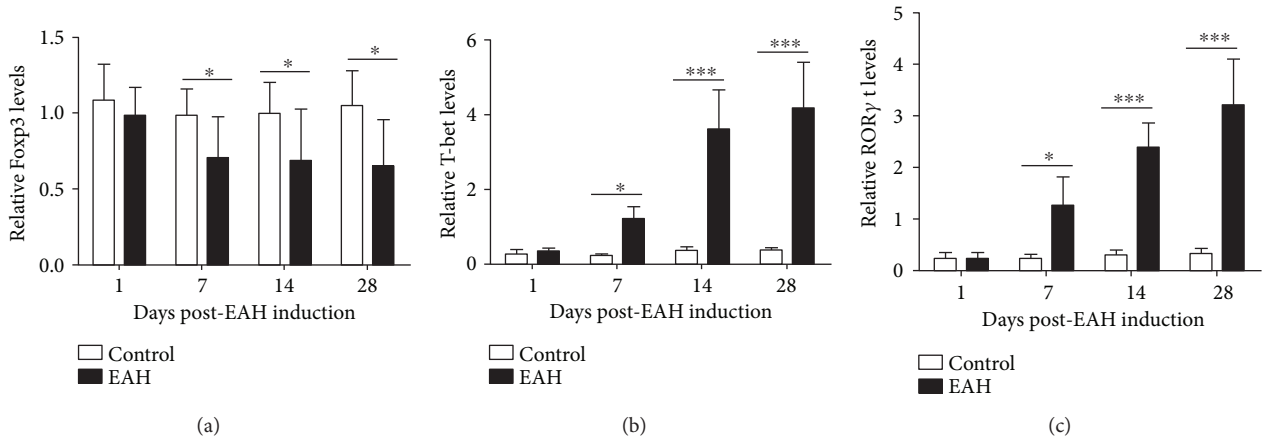

Figure 7: Foxp3, T-bet, RORγt, and AHR expressions in the hepatic tissue of EAH mice. Ten mice (5 from the EAH group and 5 from the control group) were killed at each time point (1, 7, 14, and 28 days). (a–d) The changes of Foxp3, T-bet, RORγt, and AHR expressions in the hepatic tissue of EAH mice, respectively. $^{*}p < 0.05$ and $^{***}p < 0.001$.

4. Discussion

Although dysregulated activation of effector $CD4^{+}$T helpers (Th) has been associated with the pathogenic process of autoimmune hepatitis [3, 5–7], this specific mechanism is still contradictory. In this study, we found a strong Th1 and Th17 proinflammatory response with increased levels of serum/liver Th1-type (IFN-γ) and Th17-type (IL-17A) cytokines in AIH patients undergoing an active state and EAH mice, indicating that Th1 and Th17 cells have critical functions in the pathogenic process of AIH, which were consistent with previous studies [6–9]. The significantly changed Th1 and Th17 cells may stem from the inflammatory environment, which preferably activates naive helper T cells towards Th1 and Th17 directions. In addition to Th1 and Th17 cells, Th22 cells expressing aryl hydrocarbon receptor (AHR) play a critical role in the development of immune and inflammatory diseases by producing proinflammatory cytokine IL-22 [10–12, 27, 28]. However, the possible mechanisms of Th22 cells and IL-22 in the development of AIH remain unknown. Notably, our data showed also a high expression level of Th22 cells and serum/liver Th22 type (IL-22) in AIH patients undergoing an active state and EAH mice. On the other hand, consistent with changes in Th1 and Th17 cells, the levels of Th22 cells and IL-22 decreased significantly after immunosuppressive drug treatment. These results suggested that Th22 cells, like Th1 and Th17 cells, also have major functions in the pathogenesis of AIH. More importantly, the levels of Th17/Th22-type (IL-17A, IL-22) cytokines were correlated positively with the levels of serum ALT/AST, which are a hallmark of liver injury, suggesting that Th22 and Th17 cells contribute to the progression of liver damage and fibrosis [6, 7, 11, 28]. Furthermore, our data showed a sustained replication of Th1/Th17/Th22-related mRNA (T-bet, RORγt, and AHR) in a time-dependent manner in EAH mice, which might be the direct cause of the gradual elevation of Th1/Th17/Th22 cells [29–31].

In addition to effector T cells, Tregs are important regulators of immune tolerance and inflammation response. In this study, we found lower levels of Tregs in AIH patients and in EAH mice in a time-dependent manner, which were consistent with previous studies [18, 32, 33] but were different from another report [19]. Conflicting results may be due to differences in methodology, or detection markers of the definition of Tregs, because Moritz et al. considered $CD4^{+}CD25^{high}CD127^{low}FoxP3^{+}$T cells as Tregs in their study. Moreover, these inconsistencies are partly due to enrollment of patients regardless of the phase of their disease. More importantly, we found that the concentrations of serum IL-10 were significantly higher and correlated positively with the numbers of Tregs and correlated negatively with the levels of serum immunoglobulins in AIH patients undergoing an active state, which might interfere with plasma B cell differentiation and inhibit immunoglobulin production, contributing to the pathogenic process of AIH [34]. These results suggested that deficient Tregs might contribute to the breakdown in tolerance in the development of AIH. Recent studies have reported that $CD4^{+}CD25^{-}$T cells can be induced for FoxP3 expression [23]. Functionally, some studies showed that $CD4^{+}CD25^{-}FoxP3^{+}$T cells have no inhibitory function; others indicated that these cells can inhibit inflammation in immune rejection and autoimmune diseases [24, 25]. In this study, our data showed increased numbers of $CD3^{+}CD4^{+}CD25^{-}FoxP3^{+}$T cells in AIH patients undergoing an active state. On the other hand, the numbers of $CD3^{+}CD4^{+}CD25^{-}FoxP3^{+}$T cells decreased after immunosuppressive drug treatment. However, there was no correlation between these cells and the clinical indicators. Hence, these new findings suggested that $CD3^{+}CD4^{+}CD25^{-}FoxP3^{+}$T cells may not be inhibitory Tregs. However, the role of these changes needs more studies to investigate.

Given that Tregs have the ability to inhibit the proliferation and activation of autoreactive Th1 and Th17 cells [20–22], we further set out to analyze the correlation between Tregs and Th1-Th17 cells in AIH patients. Our data demonstrated that Tregs were negatively correlated

with Th1 and Th17 cells as well as with Th1-type (IFN-γ) and Th17-type (IL-17A) cytokines, which were consistent with previous research that showed suppression of Th1 cell-mediated and Th17 cell-mediated responses by Tregs through inhibition of monocyte-derived TGF-β or IL-10 or IL-6 [21, 22]. These results indicated that the imbalance of Treg-to-Th1 and Treg-to-Th17 ratios might favor the pathogenesis of AIH. Furthermore, we further examined the association between Tregs and Th22 cells and found that Tregs were also negatively correlated with Th22 cells and IL-22 in the circulating levels of AIH patients, suggesting that deficient Tregs also enhanced Th22-mediated immune responses. This process might be due to the secretion of particular cytokines by Tregs. However, the specific mechanisms of Treg-regulated Th22 cell activation and differentiation need to be further explored in the process of AIH.

In conclusion, our data showed significantly reduced numbers of Tregs and serum IL-10 levels and increased numbers of Th1, Th17, and Th22 cells as well as higher levels of Th1-Th17-Th22-type cytokines in AIH patients and EAH mice. Additionally, the numbers of Tregs were negatively correlated with the numbers of Th1-Th17-Th22 cells and levels of IFN-γ, IL-17A, and IL-22. More importantly, serum IL-17A and IL-22 levels were positively correlated with the liver damage, whereas serum IL-10 levels were negatively correlated with hypergammaglobulinaemia. These novel findings suggested that effector Th1/Th17/Th22-cell-mediated immune response might be controlled by Tregs and the imbalance between Tregs and the Th1/Th17/Th22 axis might contribute to the process of AIH. We recognized that our study had limitations, such as the lack of functional study of Treg-regulated Th22 cells in the pathogenic process of AIH. Therefore, further studies on the molecular mechanisms are needed further to be carried out.

Data Availability

The data used to support the findings of this study are available from the corresponding author upon request.

Conflicts of Interest

All authors declare there were no conflicts of interest involved.

Authors' Contributions

Ma Liang and Zhang Liwen contributed equally to this work.

Acknowledgments

This study was supported by grants from the National Natural Science Foundation of China (no. 81700500); the Applied Basic Research Programs of Science, Technology Department of Changzhou City (CJ20160031); the Research Project of Jiangsu Provincial Commission of Health and Family Planning (no. H201547); the Major Scientific and Technological Project of Changzhou City Commission of Health and Family Planning (no. ZD201612); and the Scientific and Technological Project of Nanjing Medical University (no. 2017NJMU042). The authors thank Medjaden Bioscience Limited for assisting in the preparation of this manuscript.

References

[1] M. A. Heneghan, A. D. Yeoman, S. Verma, A. D. Smith, and M. S. Longhi, "Autoimmune hepatitis," *Lancet*, vol. 382, no. 9902, pp. 1433–1444, 2013.

[2] A. Podhorzer, N. Paladino, M. L. Cuarterolo et al., "The early onset of type 1 autoimmune hepatitis has a strong genetic influence: role of HLA and KIR genes," *Genes and Immunity*, vol. 17, no. 3, pp. 187–192, 2016.

[3] L. Ma, J. Qin, H. Ji, P. Zhao, and Y. Jiang, "Tfh and plasma cells are correlated with hypergammaglobulinaemia in patients with autoimmune hepatitis," *Liver International*, vol. 34, no. 3, pp. 405–415, 2014.

[4] A. J. Czaja, "Diagnosis and management of autoimmune hepatitis: current status and future directions," *Gut and Liver*, vol. 10, no. 2, pp. 177–203, 2016.

[5] Y. Ichiki, C. A. Aoki, C. L. Bowlus, S. Shimoda, H. Ishibashi, and M. E. Gershwin, "T cell immunity in autoimmune hepatitis," *Autoimmunity Reviews*, vol. 4, no. 5, pp. 315–321, 2005.

[6] T. Akkoc, "Re: the role of Th1/Th2 cells and associated cytokines in autoimmune hepatitis," *The Turkish Journal of Gastroenterology*, vol. 28, no. 2, pp. 115-116, 2017.

[7] A. Murthy, Y. W. Shao, V. Defamie, C. Wedeles, D. Smookler, and R. Khokha, "Stromal TIMP3 regulates liver lymphocyte populations and provides protection against Th1 T cell-driven autoimmune hepatitis," *Journal of Immunology*, vol. 188, no. 6, pp. 2876–2883, 2012.

[8] C. R. Grant, R. Liberal, B. S. Holder et al., "Dysfunctional CD39(POS) regulatory T cells and aberrant control of T-helper type 17 cells in autoimmune hepatitis," *Hepatology*, vol. 59, no. 3, pp. 1007–1015, 2014.

[9] M. S. Longhi, R. Liberal, B. Holder et al., "Inhibition of interleukin-17 promotes differentiation of $CD25^{-}$ cells into stable T regulatory cells in patients with autoimmune hepatitis," *Gastroenterology*, vol. 142, no. 7, pp. 1526–1535.e6, 2012.

[10] D. Sun, Y. Lin, J. Hong et al., "Th22 cells control colon tumorigenesis through STAT3 and polycomb repression complex 2 signaling," *Oncoimmunology*, vol. 5, no. 8, article e1082704, 2016.

[11] J. Zhao, Z. Zhang, Y. Luan et al., "Pathological functions of interleukin-22 in chronic liver inflammation and fibrosis with hepatitis B virus infection by promoting T helper 17 cell recruitment," *Hepatology*, vol. 59, no. 4, pp. 1331–1342, 2014.

[12] L. Zhao, H. Ma, Z. Jiang, Y. Jiang, and N. Ma, "Immunoregulation therapy changes the frequency of interleukin (IL)-$22^{+}CD4^{+}$ T cells in systemic lupus erythematosus patients," *Clinical & Experimental Immunology*, vol. 177, no. 1, pp. 212–218, 2014.

[13] S. Li, H. Yin, K. Zhang et al., "Effector T helper cell populations are elevated in the bone marrow of rheumatoid arthritis patients and correlate with disease severity," *Scientific Reports*, vol. 7, no. 1, p. 4776, 2017.

[14] R. Bommireddy and T. Doetschman, "TGFβ1 and T_{reg} cells: alliance for tolerance," *Trends in Molecular Medicine*, vol. 13, no. 11, pp. 492–501, 2007.

[15] L. S. K. Walker, "Treg and CTLA-4: two intertwining pathways to immune tolerance," *Journal of Autoimmunity*, vol. 45, pp. 49–57, 2013.

[16] J. Koreth, K. Matsuoka, H. T. Kim et al., "Interleukin-2 and regulatory T cells in graft-versus-host disease," *The New England Journal of Medicine*, vol. 365, no. 22, pp. 2055–2066, 2011.

[17] M. Kleinewietfeld and D. A. Hafler, "The plasticity of human Treg and Th17 cells and its role in autoimmunity," *Seminars in Immunology*, vol. 25, no. 4, pp. 305–312, 2013.

[18] P. Lapierre, K. Béland, C. Martin, F. Alvarez Jr, and F. Alvarez, "Forkhead box $p3^+$ regulatory T cell underlies male resistance to experimental type 2 autoimmune hepatitis," *Hepatology*, vol. 51, no. 5, pp. 1789–1798, 2010.

[19] M. Peiseler, M. Sebode, B. Franke et al., "FOXP3+ regulatory T cells in autoimmune hepatitis are fully functional and not reduced in frequency," *Journal of Hepatology*, vol. 57, no. 1, pp. 125–132, 2012.

[20] S. Shrestha, K. Yang, C. Guy, P. Vogel, G. Neale, and H. Chi, "T_{reg} cells require the phosphatase PTEN to restrain T_H1 and T_{FH} cell responses," *Nature Immunology*, vol. 16, no. 2, pp. 178–187, 2015.

[21] N. Joller, E. Lozano, P. R. Burkett et al., "Treg cells expressing the coinhibitory molecule TIGIT selectively inhibit proinflammatory Th1 and Th17 cell responses," *Immunity*, vol. 40, no. 4, pp. 569–581, 2014.

[22] J. L. McGovern, D. X. Nguyen, C. A. Notley, C. Mauri, D. A. Isenberg, and M. R. Ehrenstein, "Th17 cells are restrained by Treg cells via the inhibition of interleukin-6 in patients with rheumatoid arthritis responding to anti-tumor necrosis factor antibody therapy," *Arthritis and Rheumatism*, vol. 64, no. 10, pp. 3129–3138, 2012.

[23] M. Bonelli, A. Savitskaya, C. W. Steiner, E. Rath, J. S. Smolen, and C. Scheinecker, "Phenotypic and functional analysis of $CD4^+CD25^-Foxp3^+$ T cells in patients with systemic lupus erythematosus," *The Journal of Immunology*, vol. 182, no. 3, pp. 1689–1695, 2009.

[24] L. Ma, P. Zhao, Z. Jiang, Y. Shan, and Y. Jiang, "Imbalance of different types of $CD4^+$ forkhead box protein 3 $(FoxP3)^+$ T cells in patients with new-onset systemic lupus erythematosus," *Clinical and Experimental Immunology*, vol. 174, no. 3, pp. 345–355, 2013.

[25] K. Wen, G. Li, X. Yang et al., "$CD4^+$ $CD25^-$ $FoxP3^+$ regulatory cells are the predominant responding regulatory T cells after human rotavirus infection or vaccination in gnotobiotic pigs," *Immunology*, vol. 137, no. 2, pp. 160–171, 2012.

[26] X. Liu, X. Jiang, R. Liu et al., "B cells expressing CD11b effectively inhibit CD4+ T-cell responses and ameliorate experimental autoimmune hepatitis in mice," *Hepatology*, vol. 62, no. 5, pp. 1563–1575, 2015.

[27] M. Wang, P. Chen, Y. Jia et al., "Elevated Th22 as well as Th17 cells associated with therapeutic outcome and clinical stage are potential targets in patients with multiple myeloma," *Oncotarget*, vol. 6, no. 20, pp. 17958–17967, 2015.

[28] R. Lai, X. Xiang, R. Mo et al., "Protective effect of Th22 cells and intrahepatic IL-22 in drug induced hepatocellular injury," *Journal of Hepatology*, vol. 63, no. 1, pp. 148–155, 2015.

[29] A. Nosko, et al.M. A. Kluger, P. Diefenhardt et al., "T-bet enhances regulatory T cell fitness and directs control of Th1 responses in crescentic GN," *Journal of the American Society of Nephrology*, vol. 28, no. 1, pp. 185–196, 2017.

[30] Z. He, F. Wang, J. Ma et al., "Ubiquitination of RORγt at lysine 446 limits Th17 differentiation by controlling coactivator recruitment," *Journal of Immunology*, vol. 197, no. 4, pp. 1148–1158, 2016.

[31] P. M. Cochez, C. Michiels, E. Hendrickx et al., "AhR modulates the IL-22-producing cell proliferation/recruitment in imiquimod induced psoriasis mouse model," *European Journal of Immunology*, vol. 46, no. 6, pp. 1449–1459, 2016.

[32] I. An Haack, K. Derkow, M. Riehn et al., "The role of regulatory CD4 T cells in maintaining tolerance in a mouse model of autoimmune hepatitis," *PLoS One*, vol. 10, no. 11, article e0143715, 2015.

[33] S. Ferri, M. S. Longhi, C. de Molo et al., "A multifaceted imbalance of T cells with regulatory function characterizes type 1 autoimmune hepatitis," *Hepatology*, vol. 52, no. 3, pp. 999–1007, 2010.

[34] R. Liberal, C. R. Grant, B. S. Holder et al., "In autoimmune hepatitis type 1 or the autoimmune hepatitis-sclerosing cholangitis variant defective regulatory T-cell responsiveness to IL-2 results in low IL-10 production and impaired suppression," *Hepatology*, vol. 62, no. 3, pp. 863–875, 2015.